

**Removal of metaldehyde in aqueous solutions by
heterogeneous photocatalysis and adsorption processes**

A thesis submitted to University College London

for the degree of Doctor of Philosophy

by

Zhuojun Li

Department of Civil, Environmental & Geomatic Engineering

University College London

January 2020

Declaration

I, Zhuojun Li confirm that the work presented in this thesis is my own. Where information has been derived from other sources, I confirm that this has been indicated in the thesis.

Name: Zhuojun Li

Signature:

Date:

Abstract

Metaldehyde has been detected in surface water and drinking water in the UK, exceeding the EU and UK standard of $0.1 \mu\text{g L}^{-1}$. Conventional water treatment methods are not effective due to the physicochemical properties of metaldehyde while newly proposed methods are under research and cannot be applied at an industrial scale. This thesis investigated the removal of metaldehyde from aqueous solutions by heterogeneous photocatalysis using nanoparticle photocatalysts and adsorption processes using carbon materials, aiming to provide a feasible solution to the problem. Powdered activated carbon (PAC) proved to be the most effective material to remove metaldehyde from water. It has a relatively large specific surface area of $962.4 \text{ m}^2 \text{ g}^{-1}$ and a pore size distribution in the micro-/meso-pores range that favours adsorption of metaldehyde. Adsorption of metaldehyde onto PAC was explained by the Langmuir isotherm model, with a highest maximum adsorption capacity (q_m) of 28.33 mg g^{-1} , and by the pseudo-second order kinetic model, with highest adsorption rate (k_2) of $0.16 \text{ g mg}^{-1} \text{ min}^{-1}$. Low initial concentration of metaldehyde solution led to lower q_m of PAC for metaldehyde due to low driving force for mass transfer and competition with water molecules. Humic acid, which represents natural organic matter in water, has little effect on adsorption of metaldehyde onto PAC. For water samples collected from various stages at Walton-on-Thames Water Treatment Works, the best treatment stage for dosing PAC to remove metaldehyde was apparently after the 'static flocculation' stage. Desorption of metaldehyde from used PAC was observed, suggesting that constant monitoring of metaldehyde is essential for adjusting dosage and recycling of PAC. Lastly, low temperature on-site regeneration of used PAC may be possible.

Impact Statement

This thesis contributes to the knowledge of effectively removing a micropollutant from aqueous solutions. The impacts of this thesis are discussed as following:

Inside academia:

- The modified method regarding the detection of metaldehyde by GC-MS described in Chapter 3 and the modified solid-phase extraction loading technique described in Chapter 5 can help other researchers set up their method to identify and quantify metaldehyde in aqueous solutions using GC-MS.
- Powdered activated carbon (PAC) used in this study can effectively and efficiently remove metaldehyde from water, regardless of the water quality, due to the distinctive pore size distribution of the PAC and the physicochemical properties of metaldehyde. It suggests that adsorption is the preferred removal mechanism for metaldehyde under the studied experimental condition. This discovery can provide insights to researchers that are interested in adsorption of other micropollutants which share similar properties with metaldehyde. And it is helpful for researchers that are interested in synthesizing adsorbents with customized pore size distribution to remove certain micropollutant, based on their properties.
- A slight increase in the percentage removal of metaldehyde was observed when UV-C light was applied in the adsorption system using PAC and granular activated carbon (GAC) under the studied experimental condition in Chapter 3. This suggests that the combination of possible adsorption and oxidation could enhance the removal of metaldehyde. This finding can help researchers further investigate

the possible adsorption-oxidation system in terms of removing micropollutants from water.

Outside academia:

- Dosing PAC as slurry in the water collected after 'static flocculation' at Walton-on-Thames Water Treatment Works achieved the highest removal of metaldehyde under the studied experimental condition in Chapter 5. This discovery can be beneficial to water utility companies and drinking water treatment plants that share similar water sources, treatment processes, and daily output with Walton-on-Thames Water Treatment Works.
- Desorption of metaldehyde from used PAC back to water was observed under the studied experimental condition in Chapter 5. This result is informative for water utility companies and drinking water treatment plants. It also points out the importance of constant monitoring of micropollutants during the treatment processes, which helps to identify the appropriate time frame needed for adjusting the treatment methods.
- Low temperature on-site regeneration of used PAC may be possible. This aspect can be further looked into by water utility companies and drinking water treatment plants to develop an energy-saving and waste-reducing method to recycle and regenerate the used PAC.

Acknowledgements

Undertaking this PhD has been a great experience and a spectacular journey for me. I am thankful for all the help and care I have received from the academic/research staff, family, friends, and strangers during my study.

Firstly, I would like to express my greatest appreciation to my supervisor, Dr Luiza Cintra Campos, for her patient guidance, vital encouragement, continuous support and feedback on the experimental designs, manuscript preparations, and thesis write-up. Luiza is passionate about research and truly cares for me, not only for my research but also my life as an international student in London. I am often inspired by her enthusiasm and creative ideas.

Many thanks to my second supervisor, Prof Zhengxiao Guo, and members of his research group, Dr Yuchen Yang, Juntao Li, Dr Jian Guo, and Dr Zhuangnan Li. With the guidance from them, I have gained a brand new perspective to my research. I also extremely appreciate that they have helped me with the material characterization techniques in this thesis and that I have had the opportunity to have access to the analytical instruments in the Chemistry Department at UCL. And thanks to Dr Steve Firth for his instructions on performing EDX analysis.

Special thanks to Dr Judith Zhou for her technical support with the analytical instruments in the Environmental Engineering Laboratory of the Department of Civil, Environmental, and Geomatic Engineering at UCL, and her feedbacks on my methodology.

My thanks extend to the laboratory technicians of the Environmental Engineering Laboratory, Dr Utku Solpuker, Mrs Catherine Unsworth, and Dr Francis O'Shea for helping me with experimental settings and demonstrating lab classes. Many thanks to Dr Suseeladevi Mayadevi, Dr Jong Kyu Kim, Dr Bharat Kale, Dr Ulises Jáuregui-Haza, Dr Jenny O'Reilly, and Dr Michael Chipps for their collaborations and advices on my research. I would like to thank Dr Melisa Canales and Dr Anna Bogush for their support of my research as well.

My appreciation also goes to my friends in London, especially Like Xu, Fan Huang, Yu Shen, Vega Wang, Yuting Huang, and Dr Dong Ding, for all your help and support when I needed it most. Also thanks to my friends in China and around the world, especially Wenting Huang, Yidong Chen, Wenjia Fan, Qimiao Shen, Xian Jiang, Junyan Li, Haoyang Sun, Xiafeng Xu, Yang Yang, Yang Li, Chen Su, Shida Wang, and Yifan Wang for the happy memories we created together.

I would like to give my greatest appreciation to my parents and grandparents for believing in me and for their unconditional support throughout my study. Lastly, I am grateful for the love and support of Petri and his family. Petri, you are the best thing that ever happened to me. Jag älskar dig så mycket.

List of Publications

The experimental investigations presented in this thesis have been published in the following peer-reviewed journals respectively:

- Li, Z., et al., *Degradation of metaldehyde in water by nanoparticle catalysts and powdered activated carbon*. Environmental Science and Pollution Research, 2017. **24**(21): p. 17861-17873.
- Li, Z., et al., *The impact of humic acid on metaldehyde adsorption onto powdered activated carbon in aqueous solution*. RSC Advances, 2019. **9**(1): p. 11-22.
- Li, Z., et al., *Investigation of metaldehyde removal by powdered activated carbon from different water samples*. Environmental Science: Water Research & Technology, 2020.

The researcher has co-authored the paper published in the following peer-reviewed journal:

- Ferino-Pérez, A., et al., *Explaining the interactions between metaldehyde and acidic surface groups of activated carbon under different pH conditions*. Journal of Molecular Graphics and Modelling, 2019. **90**: p. 94-103.

Table of Contents

Abstract	3
Impact Statement	4
Acknowledgements	6
List of Publications	8
Table of Contents	9
List of Tables	14
List of Figures	16
Nomenclature	20
Abbreviations	22
Chapter 1. Introduction	25
1.1 Research problem	25
1.2 Overview of heterogeneous photocatalysis and adsorption processes in water treatment researches	31
1.3 Aim and objectives of the thesis	32
1.4 Outline of the thesis	34
Chapter 2. Literature review	37
2.1 Introduction	37
2.2 Metaldehyde	38
2.2.1 Properties and environmental fate of metaldehyde	38
2.2.2 Toxicity of metaldehyde	41
2.2.3 Concentrations of metaldehyde in surface water bodies	43
2.3 Determination and monitoring of metaldehyde in water	45
2.3.1 Determination of metaldehyde in aqueous solutions	45
2.3.2 Monitoring of metaldehyde in water	48
2.4 Conventional and potential treatment methods for metaldehyde	49

2.4.1	Conventional methods: oxidation with ozone, AOPs (UV photolysis and hydrogen peroxide under UV irradiation), and adsorption (GAC filtration)	49
2.4.2	Potential methods: AOPs (heterogeneous photocatalysis) and adsorption (adsorbents with different characteristics).....	53
2.4.3	Combination of oxidation and adsorption.....	61
2.4.4	Development of water treatment methods for metaldehyde	62
2.5	Researcher's previous work on removal of metaldehyde from water	66
2.5.1	C-1.5.....	67
2.5.2	PAC	67
2.6	Approaches for removal of metaldehyde from water within the present study.....	68
2.6.1	Heterogeneous photocatalysis	68
2.6.2	Adsorption	70
2.6.3	Material characterization techniques	70
2.7	Summary.....	73
Chapter 3. Removal of metaldehyde from water by nanoparticle photocatalysts and carbon materials.....		77
3.1	Introduction	77
3.2	Materials and methods.....	79
3.2.1	Materials	80
3.2.2	Material characterization techniques	82
3.2.3	Preparation of metaldehyde solutions	83
3.2.4	Experimental methods.....	85
3.2.5	Analytical methods for determination of metaldehyde in water.....	92
3.2.6	Presentation and analysis of data.....	99
3.3	Results and discussion	99
3.3.1	Characterizations of PAC and GAC.....	99

3.3.2	Removal of metaldehyde from MilliQ water by nanoparticle photocatalysts and powdered and granular carbon materials	105
3.3.3	Effect of UV-C light on the removal of metaldehyde by PAC and GAC..	110
3.3.4	Adsorption kinetic study of PAC under UV-C light	114
3.4	Summary.....	121
Chapter 4. The impact of humic acid on metaldehyde adsorption onto PAC in aqueous solutions		
		123
4.1	Introduction	123
4.2	Materials and methods.....	126
4.2.1	Materials	126
4.2.2	Material characterization techniques	127
4.2.3	Preparation of metaldehyde and HA solutions.....	129
4.2.4	Adsorption experiments	131
4.2.5	Analytical method for determination of metaldehyde and HA in water	134
4.2.6	Presentation and analysis of data.....	137
4.3	Results and discussion	138
4.3.1	Characterizations of adsorbents and adsorbates	138
4.3.2	Removal of metaldehyde in the single adsorption system.....	149
4.3.3	Removal of HA in the single adsorption system	163
4.3.4	Removal of metaldehyde in the binary adsorption system (competitive adsorption)	171
4.3.5	Adsorption mechanisms of metaldehyde and HA onto PAC.....	175
4.4	Summary.....	178
Chapter 5. Investigation of metaldehyde removal from different water samples by PAC		
		180
5.1	Introduction	180
5.2	Materials and methods.....	181
5.2.1	Materials	181

5.2.2	Analysis of water characteristics.....	185
5.2.3	Material characterization techniques	186
5.2.4	Preparation of metaldehyde solutions	187
5.2.5	Adsorption experiments	188
5.2.6	Desorption and regeneration experiment	191
5.2.7	Validation of detection of metaldehyde by GC-MS using a modified SPE loading technique	192
5.2.8	Presentation and analysis of data.....	196
5.3	Results and discussion	196
5.3.1	Characteristics of different water samples	196
5.3.2	ATR-FTIR and SEM analyses for flocs, PAC-SF, and PAC-RP	198
5.3.3	Removal of metaldehyde from different water samples	201
5.3.4	Adsorption mechanisms of metaldehyde onto PAC regarding different initial concentrations of metaldehyde working solutions.....	218
5.3.5	Desorption of metaldehyde and regeneration of PAC	223
5.4	Summary.....	225
Chapter 6. Removal of metaldehyde from aqueous solutions: an overall discussion		227
6.1	Overview of the experimental investigations	227
6.2	Adsorption mechanisms of metaldehyde from aqueous solutions onto PAC.....	232
6.3	Potential industrial application of PAC regarding removal of metaldehyde	236
Chapter 7. Conclusions and future work		239
7.1	Findings and contributions of this thesis	239
7.2	Limitations and recommendations for future research	245
References.....		251
Appendix A.1 Supplementary information for Chapter 3		271
Appendix A.2 Supplementary information for Chapter 4		275

Appendix A.3 Supplementary information for Chapter 5 277

List of Tables

Table 2.1 Physicochemical properties of metaldehyde	39
Table 2.2 Comparisons of treatment methods targeting metaldehyde.....	75
Table 3.1 GC-MS method for detection and analysis of metaldehyde	95
Table 3.2 Calibration and recovery of 1 mg L ⁻¹ metaldehyde sample solutions	98
Table 3.3 Characterizations of PAC and GAC from BET SSA analysis	104
Table 3.4 Removal of metaldehyde by different treatments.....	106
Table 3.5 Removal of metaldehyde by UV-C, PAC, PAC/UV-C, GAC, and GAC/UV-C	111
Table 3.6 Comparison of PAC used in this study with other adsorbents to remove metaldehyde.....	120
Table 4.1 Calibration of 15 mg L ⁻¹ HA sample solutions	137
Table 4.2 Removal of metaldehyde by different PAC dosages.....	150
Table 4.3 Removal of metaldehyde by 2-h PAC treatment at different pH.....	153
Table 4.4 Results from the ANOVA single factor statistic tests comparing C_{t-2h} at different pH.....	154
Table 4.5 Statistical analysis of the suitability of the isotherm models using the AIC method	163
Table 4.6 Removal of HA by different PAC dosages	165
Table 4.7 Removal of metaldehyde and HA by PAC in the binary adsorption system	172
Table 4.8 Adsorption kinetic constants of metaldehyde and HA	177
Table 5.1 Recovery rates of metaldehyde prepared using the water collected from the Regent's Park lake	195
Table 5.2 Characteristics of different water samples	197
Table 5.3 Removal of metaldehyde from the water samples collected at different treatment stages	204
Table 5.4 Summary of parameters obtained from the metaldehyde adsorption isotherm study using the water collected after 'pre-ozone contactors' and 'static flocculation'	212
Table 5.5 Comparison of q_m and K_L regarding adsorption of metaldehyde onto PAC under different experimental conditions and using different water samples	218

Table 5.6 Parameters obtained from the metaldehyde adsorption isotherm study using MilliQ water	223
Table 5.7 Detection of metaldehyde after dosing used PAC into MilliQ water	224
Table 6.1 Adsorption kinetic and isotherm studies of the PAC used for removing metaldehyde.....	233
Table A.1.1 Multi-point selected for BET SSA analysis of the PAC used in Chapter 3	272
Table A.1.2 Multi-point selected for BET SSA analysis of the GAC used in Chapter 3	274
Table A.2.1 Multi-point selected for BET SSA analysis of the PAC used in Chapter 4	276
Table A.3.1 Characteristics of different water samples without spiking metaldehyde	278
Table A.3.2 Characteristics of different water samples spiked with 5 $\mu\text{g L}^{-1}$ metaldehyde without PAC treatment.....	279
Table A.3.3 Characteristics of different water samples spiked with 5 $\mu\text{g L}^{-1}$ metaldehyde after the 30-min PAC treatments	280

List of Figures

Figure 2.1 Overview of literature review	37
Figure 2.2 Metaldehyde and its two major metabolites.....	42
Figure 2.3 Direct and indirect photolysis of chloral hydrate under a low pressure UV light.....	51
Figure 2.4 Band gap theory	54
Figure 2.5 Semiconductors with different band gap energy.....	54
Figure 2.6 Heterogeneous photocatalysis by TiO ₂ /UV	55
Figure 2.7 Structure of graphene.....	58
Figure 2.8 Single-walled CNTs, double-walled CNTs, and multi-walled CNTs.....	59
Figure 3.1 Photoreactor.....	88
Figure 3.2 Schematic diagram of the photoreactor.....	89
Figure 3.3 Standard calibration curve for metaldehyde detection and calibration ...	97
Figure 3.4 SEM images of PAC and GAC at different magnifications	101
Figure 3.5 BET SSA analysis of PAC and GAC	103
Figure 3.6 Concentrations of metaldehyde solutions without treatment and after 2-h treatment using different materials	106
Figure 3.7 Concentrations of metaldehyde solutions without treatment and after 2-h treatment by UV-C, PAC, PAC/UV-C, GAC, and GAC/UV-C	110
Figure 3.8 The proposed adsorption-oxidation system in the treatment of applying activated carbon particles under UV-C light for removing metaldehyde	113
Figure 3.9 Removal of metaldehyde in the 2-h treatment using PAC under UV-C light	115
Figure 3.10 The pseudo-first order kinetic model	117
Figure 3.11 The pseudo-second order kinetic model	118
Figure 4.1 Model structure of HA.....	125
Figure 4.2 Calibration curve for the determination of HA.....	136
Figure 4.3 BET SSA analysis of PAC	139
Figure 4.4 SEM images of virgin PAC at different magnifications	140
Figure 4.5 SEM images of metaldehyde loaded PAC and HA loaded PAC at different magnifications.	142

Figure 4.6 EDX spectra of virgin PAC, metaldehyde loaded PAC, and HA loaded PAC	143
Figure 4.7 ATR-FTIR spectra of virgin PAC, metaldehyde, HA, metaldehyde loaded PAC, and HA loaded PAC	145
Figure 4.8 XPS spectra and element analyses of virgin PAC, metaldehyde, metaldehyde loaded PAC, HA, and HA loaded PAC.....	146
Figure 4.9 pH_{PZC} of PAC.....	148
Figure 4.10 Concentrations of metaldehyde solutions without and after 2-h treatment by different PAC dosages in the single adsorption system.....	149
Figure 4.11 Effect of time on metaldehyde removal by PAC in the single adsorption system.....	151
Figure 4.12 Concentrations of metaldehyde solutions without and after 2-h treatment using 0.05 g PAC under different pH environments in the single adsorption system	152
Figure 4.13 The pseudo-first order kinetic model fitting of 1 mg L ⁻¹ metaldehyde solution (500 mL) with 0.05 g PAC in the 2-h treatment time	155
Figure 4.14 Data fitted to the pseudo-first order kinetic with two gradients	156
Figure 4.15 The pseudo-second order kinetic model fitting of 1 mg L ⁻¹ metaldehyde solution (500 mL) with 0.05 g PAC in the 2-h treatment time	157
Figure 4.16 Metaldehyde adsorption equilibrium curve	159
Figure 4.17 The Freundlich isotherm model fitting	160
Figure 4.18 The Langmuir isotherm model fitting	161
Figure 4.19 Concentrations of HA solutions without and after 2-h treatment using PAC with different dosages in the single adsorption system	164
Figure 4.20 Effect of time on HA removal by PAC in the single adsorption system	166
Figure 4.21 Comparison of adsorption of metaldehyde and HA onto PAC in 2 h in the single adsorption systems	167
Figure 4.22 The pseudo-second order kinetic fitting of 30 mg L ⁻¹ metaldehyde with 0.25 g PAC in the 2-h treatment time	169
Figure 4.23 Concentrations of metaldehyde and HA in the binary adsorption system without and after PAC treatment with different initial concentrations of HA.....	172
Figure 4.24 Effect of time on adsorption of metaldehyde in the single and binary adsorption systems	173

Figure 4.25 The pseudo-first order kinetic model fitting for metaldehyde adsorption onto PAC in the binary adsorption system	174
Figure 4.26 The pseudo-second order kinetic model fitting for metaldehyde adsorption onto PAC in the binary adsorption system	175
Figure 5.1 Location of Walton-on-Thames Water Treatment Works.....	182
Figure 5.2 Illustration of the six main treatment stages at WTWTW	183
Figure 5.3 Location of the Regent’s Park lake.....	185
Figure 5.4 Two calibration curves.....	194
Figure 5.5 ATR-FTIR spectra of PAC-SF, PAC-RP, flocs, and metaldehyde	198
Figure 5.6 SEM images of flocs, PAC-SF, and PAC-RP	200
Figure 5.7 Effect of different PAC dosing concentrations on removal of 600 mL of 5 $\mu\text{g L}^{-1}$ metaldehyde working solution prepared using the water collected after ‘pre-ozone contactors’ from WTWTW	202
Figure 5.8 Concentrations of metaldehyde solutions without and after 30 mg PAC treatment in the 600 mL water samples collected from different treatment stages at WTWTW.....	204
Figure 5.9 Percentage removal and concentration of metaldehyde ($C_{t-30min}$) in the water collected after ‘pre-ozone contactors’ and after ‘static flocculation’ with different PAC dosing concentrations	206
Figure 5.10 Metaldehyde adsorption equilibrium curve fitted to the Freundlich and the Langmuir isotherm models using the water collected after ‘pre-ozone contactors’ and after ‘static flocculation’ at WTWTW.....	208
Figure 5.11 The Freundlich isotherm model fitting for the water collected after ‘pre-ozone contactors’ at WTWTW.....	209
Figure 5.12 The Langmuir isotherm model fitting for the water collected after ‘pre-ozone contactors’ at WTWTW.....	209
Figure 5.13 The Freundlich isotherm model fitting for the water collected after ‘static flocculation’ at WTWTW	210
Figure 5.14 The Langmuir isotherm model fitting for the water collected after ‘static flocculation’ at WTWTW	211
Figure 5.15 Comparison of water characteristics for different water samples without and after PAC treatment.....	215
Figure 5.16 Effect of initial concentration on metaldehyde removal by PAC in the single adsorption system.....	219

Figure 5.17 Metaldehyde adsorption equilibrium curve fitted to the Freundlich and the Langmuir isotherm models using MilliQ water.....	220
Figure 5.18 The Freundlich isotherm model fitting for MilliQ water.....	221
Figure 5.19 The Langmuir isotherm model fitting for MilliQ water	222
Figure 6.1 Overview of the thesis	227
Figure A.1.1 Data from the BET SSA analysis of the PAC used in Chapter 3.....	271
Figure A.1.2 Data from the BET SSA analysis of the GAC used in Chapter 3	273
Figure A.2.1 Data from the BET SSA analysis of the PAC used in Chapter 4.....	275

Nomenclature

Symbol	Description	Unit
$1/n$	= heterogeneity factor	dimensionless
C_0	= concentration of adsorbate in solution without treatment	$\mu\text{g L}^{-1}$ or mg L^{-1}
C_e	= concentration of adsorbate in solution after treatment at equilibrium	$\mu\text{g L}^{-1}$ or mg L^{-1}
C_t	= concentration of adsorbate in solution after treatment at a specific time	$\mu\text{g L}^{-1}$ or mg L^{-1}
k_1	= the pseudo-first order kinetic rate constant	min^{-1} or h^{-1}
k_2	= the pseudo-second order kinetic rate constant	$\text{g mg}^{-1} \text{min}^{-1}$
K_F	= the Freundlich constant	$(\text{mg g}^{-1})/(\text{mg L}^{-1})^{1/n}$ or $(\mu\text{g mg}^{-1})/(\mu\text{g L}^{-1})^{1/n}$
K_L	= the Langmuir constant	$\text{L } \mu\text{g}^{-1}$ or L mg^{-1}
K_{oc}	= the organic-carbon/water partition coefficient	dimensionless
K_{ow}	= the octanol/water partition coefficient	dimensionless
m	= mass of adsorbent	mg or g
M	= number of parameters in the isotherm models	dimensionless
N	= number of data points	dimensionless
q_e	= amount of adsorbate adsorbed on adsorbent at equilibrium	$\mu\text{g mg}^{-1}$ or mg g^{-1}
$q_{exp,i}$	= q_e from experimental data	$\mu\text{g mg}^{-1}$ or mg g^{-1}
q_m	= maximum adsorption capacity of adsorbent	$\mu\text{g mg}^{-1}$ or mg g^{-1}
q_t	= amount of adsorbate adsorbed on adsorbent at a specific time	$\mu\text{g mg}^{-1}$ or mg g^{-1}
$q_{the,i}$	= theoretical q_e calculated from isotherm models	$\mu\text{g mg}^{-1}$ or mg g^{-1}

R^2	= coefficient of determination	dimensionless
t	= time	min or h
V	= volume of solution	mL or L

Abbreviations

AC	= activated carbon
ACF	= activated carbon fibre
ADI	= acceptable daily intake
AIC	= Akaike information criterion
ANOVA	= analysis of variance
AOPs	= advanced oxidation processes
ATR-FTIR	= attenuated total reflection Fourier transform infrared
BAC	= biological activated carbon
BDH	= British Drug Houses
BET	= Brunauer-Emmett-Teller
C-1.5	= cetyl trimethyl ammonium bromide modified carbon doped TiO ₂ nanoparticle photocatalyst with 1.5% carbon, 98.5% TiO ₂
C-40	= cetyl trimethyl ammonium bromide modified carbon doped TiO ₂ nanoparticle photocatalyst with 40% carbon, 60% TiO ₂
C-80	= cetyl trimethyl ammonium bromide modified carbon doped TiO ₂ nanoparticle photocatalyst with 80% carbon, 20% TiO ₂
CCD	= the water collected after 'counter-current dissolved air flotation units' at Walton-on-Thames Water Treatment Works
C-MET	= Centre for Materials for Electronics Technology
CNTs	= carbon nanotubes
CoCoDAF	= counter-current dissolved air flotation
COD	= chemical oxygen demand
CPA	= carbon powder from sugar cane leaves agro-waste
CPAA	= activated carbon powder from sugar cane leaves agro-waste
CTAB	= cetyl trimethyl ammonium bromide
DAF	= dissolved air flotation

DCM	= dichloromethane
DO	= dissolved oxygen
DOC	= dissolved organic carbon
EDX	= energy-dispersive X-ray spectroscopy
EU	= European Union
GAC	= granular activated carbon
GC	= gas chromatography
GC-MS	= gas chromatography with mass spectrometry
HA	= humic acid
HPLC	= high performance liquid chromatography
IR	= infrared
LC	= liquid chromatography
LC-MS	= liquid chromatography with mass spectrometry
LOD	= limit of detection
LOQ	= limit of quantification
MO	= the water collected after 'main ozone contactors' at Walton-on-Thames Water Treatment Works
MS	= mass spectrometry
MW	= MilliQ water
MWHA	= MilliQ water with humic acid
NCL	= National Chemical Laboratory
NOM	= natural organic matters
NPOC	= non-purgeable organic carbon
P25	= nanoparticle Degussa TiO ₂
PAC	= powdered activated carbon
PAC-SF	= powdered activated carbon sample dosed in metaldehyde working solution prepared using the water collected after 'static flocculation' at Walton-on-Thames Water Treatment Works

PAC-RP	= powdered activated carbon sample dosed in metaldehyde working solution prepared using the water collected from the Regent's Park lake
PSD	= pore size distribution
PZC	= point of zero charge
RP	= the water collected from the Regent's Park lake
RSD	= relative standard deviation
RSS	= residual sum of squares
SD	= standard deviation
SEM	= scanning electron microscope
SF	= the water collected after 'static flocculation' at Walton-on-Thames Water Treatment Works
SLGO	= single-layer graphene oxide
SPE	= solid-phase extraction
SSA	= specific surface area
TAML	= tetra-amido macrocyclic ligands
TDS	= total dissolved solids
TiO ₂ -G	= TiO ₂ doped graphene
TOC	= Total Organic Carbon
UCL	= University College London
UK	= United Kingdom
UPLC	= ultra performance liquid chromatography
UV	= ultraviolet
UV ₂₅₄	= absorbance at 254 nm wavelength
WTWTW	= Walton-on-Thames Water Treatment Works
XPS	= X-ray photoemission spectroscopy
ZnO-G	= ZnO doped graphene

Chapter 1. Introduction

1.1 Research problem

With the development of science and technology, people's living standards and conditions have improved significantly over the last few decades. Pesticides, fertilizers, pharmaceuticals and personal care products have dramatically improved the quality of people's life. Nevertheless, the by-coming toxic materials and chemicals from these modern products can enter natural water bodies, including surface water, as micropollutants. Stamm *et al.* defined micropollutants as anthropogenic chemical compounds occurring in the aquatic environment, with low concentrations (up to the ' $\mu\text{g L}^{-1}$ ' range) but above their potential natural background levels due to human activities [1]. For example, the United Kingdom (UK) Department of Environment, Food and Rural Affairs reported that in 2007, pesticides including isoproturon, simazine, and diuron were detected in more than 6% of surface water samples in England and Wales; and they exceeded the standard common pesticide limit ($0.1 \mu\text{g L}^{-1}$ for individual pesticide) set by the European Commission Drinking Water Directive [2]. Pharmaceuticals can also enter water bodies from sewage (human drugs) and soil (veterinary drugs). For instance, it was reported by the World Health Organization that in 2006, the concentration of paracetamol detected in surface water in the UK was 555 ng L^{-1} [3]. Currently, the World Health Organization has no regulations regarding pharmaceuticals in drinking water because the potential health effects from low concentration life-long exposure to them is uncertain [4]. However, many researchers suggested that pharmaceuticals in drinking water need to be regulated. For example, Kümmerer proposed that the limit of pharmaceuticals in drinking water should be set as the limit of quantification [5]. On the other hand, Kumar *et al.* and Leung *et al.*

argued that the provisional safety levels for the amount of pharmaceuticals in drinking water should be derived from a health-based limit such as acceptable daily intake (ADI), which is the level of a chemical that can be consumed daily for a lifetime without risk to health [4, 6].

Micropollutants can enter surface water which is one of the main sources of drinking water; and their presence may be harmful to living species and human health. Therefore, to minimize their effects on drinking water quality and public health, it is essential to establish appropriate treatment methods for removing them from water. Many water treatment methods including coagulation/flocculation and filtration are effective for removing organic pollutants and particulates from water. For example, according to the research of Jiang, coagulation/flocculation are effective for removing dissolved organic carbon (DOC), chemical oxygen demand (COD), and biological oxygen demand (BOD) from water [7]. However, these methods are ineffective for removing micropollutants such as metaldehyde and paracetamol, since they occur in the environment at trace levels, up to the ' $\mu\text{g L}^{-1}$ ' range [8, 9].

The micropollutant investigated in this study is metaldehyde, an organic compound used as a selective pesticide. It targets slugs which is considered one of the most serious pests, especially for crops that grow in no-tillage systems [10]. Metaldehyde is widely used in the UK for agricultural purpose and gardening. The UK Environment Agency reported that in 2009, more than 8% of the crops were associated with the use of metaldehyde, especially potatoes, wheat, and oil-seed rape; and metaldehyde has been detected in surface water at high levels (up to $8 \mu\text{g L}^{-1}$) [11]. There have been growing concerns of the presence of metaldehyde in the environment at relatively high concentrations, due to its extensive usage and persistence in the environment. In fact,

according to the Water UK, metaldehyde has occasionally been detected in treated drinking water with the highest concentration of $1 \mu\text{g L}^{-1}$ [8]. The concentrations of metaldehyde found in surface water (up to $8 \mu\text{g L}^{-1}$) and in drinking water (up to $1 \mu\text{g L}^{-1}$) were above the European Union (EU)'s regulatory drinking water standards and the legal standards in the UK for individual pesticide ($0.1 \mu\text{g L}^{-1}$) and total pesticides ($0.5 \mu\text{g L}^{-1}$) [8, 11, 12]. Apart from this, in 2010, metaldehyde in water bodies was assessed by the European Food Safety Authority to be harmful to aquatic organisms including gastropods [13]. Additionally, metaldehyde also presents high risks to mammals; for example, it is stated by Gupta that acute poisoning from oral ingestion of metaldehyde is common in dogs, birds, and wild animals [14]. Therefore, it is significant to remove metaldehyde from water to meet the EU and UK standard and to protect the environment.

Oxidation and adsorption are two common principles of water treatment methods for removing organic pollutants in water treatment [15, 16]. Traditional water treatment methods such as chemical oxidation with ozone - to break down the compound into harmless components - and adsorption using granular activated carbon (GAC) - to adsorb the pollutants onto the pores and surface of GAC - are commonly used for removing organic pollutants from water. For example, ozone is often applied in wastewater treatment and drinking water treatment to break down pollutants with high molecular weight. Wu *et al.* and Camel *et al.* argued that ozone is also applied to remove colour, COD, and total organic carbon (TOC) via direct reactions between pollutants and ozone molecules, and indirect reactions with oxidants after the decomposition of ozone [17, 18]. On the other hand, GAC is widely used for removing synthetic organic compounds such as pharmaceutical products and pesticides, natural organic compounds (NOM) such as humic substances, and compounds that are

causing taste and odour in the water via adsorption processes; its abundant surface area and surface functional groups contribute to the effective adsorption of organic compounds [19, 20]. However, these commonly used treatment methods turned out to be ineffective in removing metaldehyde from water. It is explained by the Water UK and Castle *et al.* that due to its physicochemical properties, metaldehyde cannot easily be broken down into benign components by common chemical oxidation methods such as chlorine and ozone [8]; and the high polarity of metaldehyde would not allow it to be sufficiently adsorbed onto activated carbon (AC) [12].

However, there are many emerging water treatment methods that apply the same principles (oxidation and adsorption) but with different approaches. For instance, heterogeneous photocatalysis, one of the most efficient advanced oxidation processes (AOPs), is characterized by a series of oxidation processes initiated by the generation of hydroxyl radicals from the interaction between a light source and a catalyst [21, 22]. Hydroxyl radicals are non-selective and would react rapidly with organic pollutants with high reaction rate constants such as 10^8 to $10^{10} \text{ M}^{-1}\text{s}^{-1}$, leading to the degradation or mineralization of organic pollutants [23]. According to the research of Pereira *et al.*, Vogna *et al.*, and Klavarioti *et al.*, heterogeneous photocatalysis is considered very effective for removing micropollutants such as pharmaceuticals including carbamazepine and paracetamol from water [24-26]. Therefore, as a micropollutant, metaldehyde may potentially be degraded via heterogeneous photocatalysis with the aid of appropriate photocatalysts and catalysis methods.

In addition, removing pollutants from water by adsorption processes using different adsorbents such as AC with different characteristics is another approach. Powdered activated carbon (PAC), which has a larger surface area, higher porosity, and different

pore size distribution, compared with GAC, is considered to be effective for removing a wide range of pollutants [15]. For example, Serrano *et al.* argued that the addition of PAC in a membrane bioreactor led to the highest removal of pharmaceuticals including trimethoprim; and it also enhanced the removal efficiency of COD to 95% [27]. Moreover, AC can be modified using different methods such as acidic/base treatments and impregnations of chemicals to remove target pollutants from water [20]. Surface modifications of AC change its characteristics including the porosity, surface area, and different surface functional groups, which may enhance the removal of pollutants from water, compared to commercial AC [20]. For example, Chen *et al.* stated that the adsorption capacity of iron modified AC for arsenic was found to be significantly improved with more than 200 times longer bed time, compared with non-treated AC [28]. Hence, PAC and modified AC may be more effective regarding the removal of metaldehyde, compared to GAC.

Since heterogeneous photocatalysis and adsorption processes have shown potential in removing other micropollutants from water, novel treatment methods using these two approaches for removing metaldehyde from water have been studied. These treatment methods include AOPs by heterogeneous photocatalysis using TiO_2 as the photocatalyst under ultraviolet (UV) irradiation [29], adsorption processes using phenolic resin-derived carbon as the adsorbent [30], electrochemical treatment using novel adsorbents [31], and a dual-stage treatment using different adsorbents and ion-exchange resin [32]. However, these treatment methods are either time/energy-consuming or costly, suggesting that they are not suitable for industrial use at the current stage of research. Moreover, it is argued by many researchers that the presence of NOM in water could affect the effectiveness of many treatment methods. For example, Autin *et al.* and Matsui *et al.* argued that NOM molecules can block the

active sites on photocatalysts and reduce the adsorption capacity of adsorbents for organic micropollutants [29, 33]. Moreover, Yoon *et al.* stated that the presence of NOM in water has reduced the removal of estrogenic compounds by adsorption onto PAC [34]. In fact, metaldehyde as a pesticide often enters surface water bodies via soil and runoff. It is highly likely for metaldehyde to be associated with NOM. Therefore, the effect of NOM on the removal of metaldehyde is a significant aspect to consider when developing the appropriate treatment method.

Hence, the research problem addressed by this thesis is summarised as: (1) metaldehyde exists in surface and drinking water in the UK at levels that are higher than the EU and UK standard; (2) traditional water treatment methods are not effective for removing metaldehyde; and (3) newly-developed treatment methods for removing metaldehyde are either not cost-effective or still under research; therefore, they cannot be widely applied at an industrial scale.

Lastly, it is essential to note that the usage of metaldehyde in the UK remains controversial. In November 2015, at the beginning of this research, metaldehyde was considered as one of the emerging micropollutants that challenges the water treatment industry, as discussed in this section. However, towards the end of this research, there have been ongoing debates as to whether the usage of metaldehyde should be banned. On 19th December 2018, the Environment Secretary announced a ban on the outdoor usage of metaldehyde in the UK from spring 2020, due to the high risk it presents to wildlife [35]. However, on 30th July 2019, the High Court decided to lift the ban with immediate effect after a legal challenge from Chiltern Farm Chemicals, one of the UK's largest suppliers of metaldehyde [36]. While the usage of metaldehyde remains debatable, it is important to consider that there may be a risk of contamination

of water supply sources by metaldehyde or any other pesticides used in agriculture and gardening practices. Therefore, although the investigations included in this thesis were performed to address the metaldehyde problem listed above, the outcome of the thesis may be applied for removing other micropollutants such as acetaldehyde from water, which have similar properties to metaldehyde.

1.2 Overview of heterogeneous photocatalysis and adsorption processes in water treatment researches

This thesis followed the two common principles of water treatment methods, oxidation and adsorption, but with different approaches, including heterogeneous photocatalysis using different photocatalysts and adsorption processes using carbon materials.

Photocatalytic AOPs (photocatalysis) include homogeneous photocatalysis and heterogeneous photocatalysis. Ribeiro *et al.* described photocatalysis as the processes that hydroxyl radicals, produced from the interaction between a light source (artificial or natural) and a catalyst, such as ferric/ferrous irons ($\text{Fe}^{2+}/\text{Fe}^{3+}$) or titanium dioxide (TiO_2), break down pollutants to intermediate compounds and then further into carbon dioxide and water, achieving mineralization in the end [22]. According to Ribeiro *et al.*, if the catalyst (solid) and the pollutants/reactants (liquid) are not in the same phase, it is defined as heterogeneous photocatalysis; and if the catalyst (liquid) and the pollutants/reactants (liquid) are in the same phase, it is defined as homogeneous photocatalysis [22]. Heterogeneous photocatalysis has been studied extensively regarding its application in water treatment and has shown promising results regarding the degradation of organic compounds. For example, Calza *et al.*

found complete removal of buspirone (15 mg L^{-1}) from water at 30 min by incorporating artificial sunlight and suspended Degussa TiO_2 as the photocatalyst [37].

Apart from heterogeneous photocatalysis, development and applications of novel porous adsorbents is another approach for removing organic pollutants from water. Defined by Ali and Gupta, adsorption is a phenomenon taking place at the surface of materials, which describes the binding and adhesion of components to the surface of a material resulting in an increase of the concentration of a specific compound at the surface or inter-surface of the material; and the pollutant that binds to the surface is defined as an adsorbate while the material of which the surface it adheres to is defined as an adsorbent [38]. AC including PAC is argued to be one of the most widely used adsorbents; and it is considered to be very effective for removing organic pollutants [39]. For example, Joseph *et al.* found out that PAC achieved the highest removal of endocrine disrupting chemicals such as bisphenol-A and 17α -ethinyl estradiol from various water samples, compared with single-walled carbon nanotubes and multi-walled carbon nanotubes [40].

This thesis investigated the removal of metaldehyde in aqueous solutions by heterogeneous photocatalysis using different photocatalysts and adsorption processes using carbon materials. It discussed and compared both approaches and provided a potentially feasible, practical, and economical solution to the research problem.

1.3 Aim and objectives of the thesis

To solve the research problem listed in Section 1.1, the main aim of this thesis is to investigate the application of heterogeneous photocatalysis and adsorption processes

as potential methods for removing metaldehyde in drinking water treatment plants.

The specific objectives are:

(1) To assess the effectiveness of nanoparticle photocatalysts and carbon materials for removing metaldehyde by:

- Comparing the removal of metaldehyde using different photocatalysts under UV-C light and using carbon materials without UV-C light;
- Comparing the removal of metaldehyde by PAC and GAC with and without the application of UV-C light and investigating the potential synergistic adsorption-oxidation system;

(2) To determine the impact of humic acid (as a representative of NOM) on adsorption of metaldehyde from water onto PAC by:

- Comparing the removal of metaldehyde by PAC in the single adsorption system with the variation of PAC dosage, contact time, pH of metaldehyde solution,
- Comparing the removal of metaldehyde by PAC in the binary adsorption system with the variation of concentrations of humic acid;

(3) To verify the effect of water quality on adsorption of metaldehyde from different water samples by:

- Comparing the removal of metaldehyde by PAC from different water samples including synthetic water, surface water, and partially treated water collected from a drinking water treatment plant;
- Identifying the potential dosing stage of PAC for a drinking water treatment plant;

(4) To explain the adsorption mechanisms of removing metaldehyde from aqueous solutions onto PAC by:

- Understanding the characteristics of PAC that can influence the removal of metaldehyde;
- Determining the adsorption mechanisms by fitting experimental data to adsorption kinetic and isotherm models.

1.4 Outline of the thesis

Chapter 2 reviews the literature that are related to this research. Section 2.2 gives a description of the properties, environmental fate, and current situation of metaldehyde. Section 2.3 explains the analytical methods that determine metaldehyde in aqueous solutions. Section 2.4 discusses different water treatment methods including oxidation with ozone, AOPs by heterogeneous photocatalysis, application of different carbon materials as adsorbents, and the development of novel treatment methods targeting metaldehyde. Section 2.5 briefly discusses the previous findings from the researcher's MSc project since this thesis builds on the researcher's previous work [41]. Section 2.6 explains the techniques which the researcher used in this thesis to tackle the metaldehyde problem. And Section 2.7 summarises the main issues that are relevant to remove metaldehyde from water and explains the reasons why the two approaches of heterogeneous photocatalysis and adsorption processes are chosen.

Chapter 3 contains a description of an experimental investigation of applying different nanoparticle photocatalysts and carbon materials to remove metaldehyde from synthetic water. Section 3.2 describes the materials involved in this chapter concluding different nanoparticle photocatalysts and carbon materials, the experimental methods used in this chapter including the preparation of metaldehyde solutions and batch experiments, and the analytical methods used in this chapter including the detection

of metaldehyde by gas chromatography with mass spectrometry (GC-MS). Section 3.3 processes the data from the experiment, including fitting data to different kinetic models, delivering Objective (1) and Objective (4). This experimental investigation is summarised in Section 3.4 showing that PAC was highly effective in removing metaldehyde from MilliQ water on its own and PAC treatment may be a potentially less time/energy-consuming treatment method than photocatalysis.

Chapter 4 describes an experimental investigation of adsorption of metaldehyde from synthetic water onto PAC with the presence of humic acid (HA), a representative compound of background organic matter. PAC was initially found effective in removing metaldehyde from MilliQ water in Chapter 3 and the presence of NOM can potentially affect the adsorption capacity of many adsorbents for the target pollutant, as discussed in Section 1.1. This chapter hence investigated the impact of HA on the removal of metaldehyde by adsorption onto PAC. Section 4.2 presents the materials used in this chapter, material characterization techniques used for analysing the relationship between the adsorbates and PAC, the experimental and analytical methods used in this chapter including batch experiments of the single (metaldehyde) and binary (metaldehyde and HA) adsorption systems, and determination of metaldehyde and HA in aqueous solutions. Data are presented and fitted to different kinetic and isotherm models with discussions and comparisons to literature in Section 4.3, delivering Objective (2) and Objective (4). Section 4.4 summarises the adsorption mechanisms of metaldehyde from aqueous solutions onto PAC in the single and binary adsorption systems.

Chapter 5 describes an experimental investigation of adsorption of metaldehyde onto PAC from different water samples. Based on the findings in Chapter 4 that adsorption

of metaldehyde onto PAC was not affected by HA, this chapter then studied the potential application of PAC in a practical scenario. Section 5.2 contains a description of the characteristics of different water samples including synthetic water, natural surface water, and water collected at different treatment stages from a water treatment plant, together with descriptions of the water treatment plant and the site where surface water samples were collected. Section 5.2 also explains the materials, experimental and analytical methods involved in this chapter, followed by analyses of the data including fitting data to different isotherm models in Section 5.3, delivering Objective (3) and Objective (4). A description of a small experimental investigation of desorption of metaldehyde from used PAC back to water and regeneration of used PAC is included in Section 5.3.5. Section 5.4 summarises this chapter.

Chapter 6 contains an overall discussion of the thesis. Section 6.1 gives an overview of the described experimental investigations in this thesis. Section 6.2 discusses the adsorption mechanisms of metaldehyde from aqueous solutions onto PAC. Section 6.3 discusses the potential application of the proposed method in drinking water treatment plants.

Chapter 7 presents the conclusions and recommendations for future research. Section 7.1 summarises the main findings and achievements of this thesis and explains the novelty of this research. Section 7.2 explains the limitations in this research and gives recommendations for future work.

Chapter 2. Literature review

2.1 Introduction

This literature review describes the properties of metaldehyde, the analytical method of determining metaldehyde in aqueous solution and monitoring of metaldehyde, and conventional and potential treatment methods of removing it from water (Figure 2.1).

The researcher's previous work and the researcher's approaches in this thesis on removal of metaldehyde are included in this chapter as well.

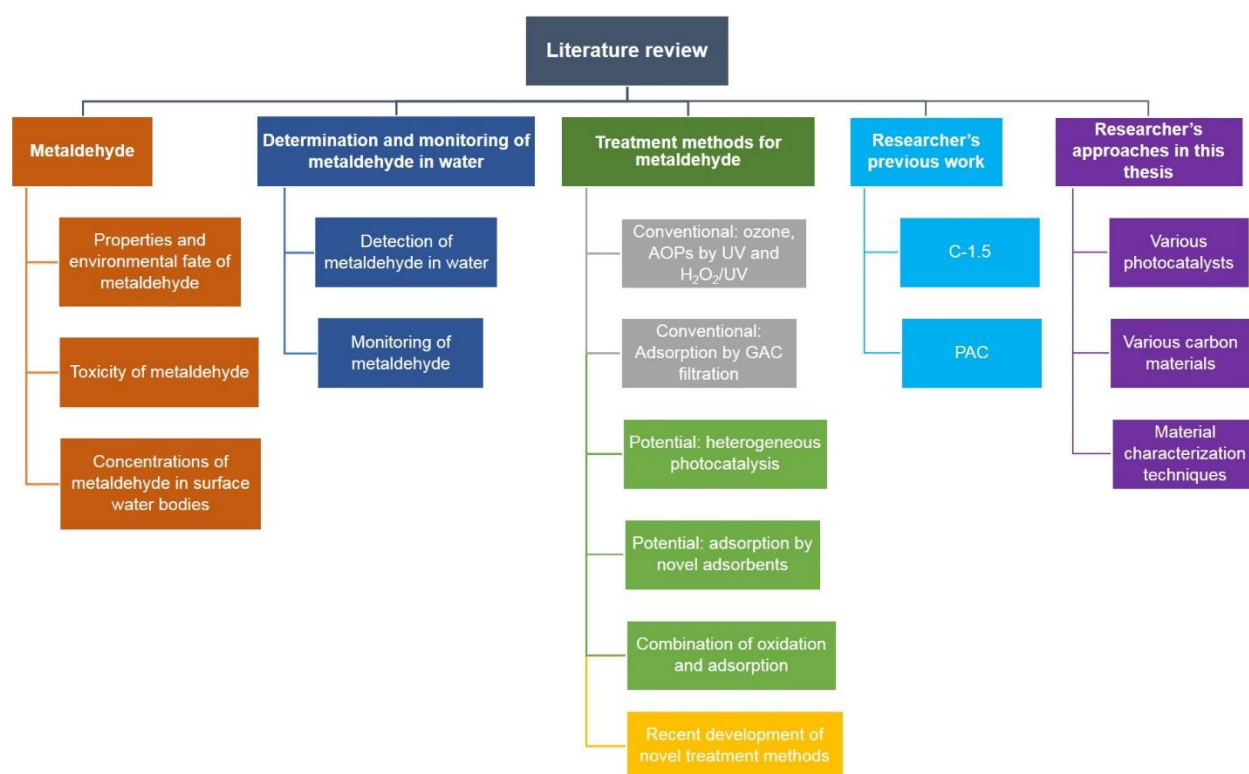


Figure 2.1 Overview of literature review

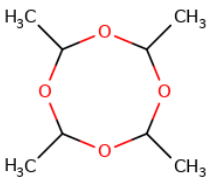
2.2 Metaldehyde

2.2.1 Properties and environmental fate of metaldehyde

Metaldehyde is a selective pesticide that has been widely used since the 1940's for agricultural and gardening purposes [12, 42]. It is the active ingredient in 80% of slug repellents in the world which targets at slugs and snails, and it is mostly applied during autumn and winter seasons to protect cereal and potato crops from an increasing number of molluscs under the wet weather conditions [12].

Metaldehyde ($C_8H_{16}O_4$) is a dry, white/colourless, crystalline, synthetic compound with a menthol odour [43]. It is a cyclic tetramer of acetaldehyde (CH_3CHO) and can be obtained by treating acetaldehyde with acid catalyst [12]; it is considered as an extremely polar organic compound (Table 2.1).

Table 2.1 Physicochemical properties of metaldehyde [12, 43, 44]

Chemical structure	
Molar mass (g mol⁻¹)	176.21
CASRN ^I	108-62-3
IUPAC ^{II} name	2,4,6,8-Tetramethyl-1,3,5,7-tetroxocane
Water solubility ^{III} (mg L⁻¹)	188
Methanol solubility ^{IV} (mg L⁻¹)	1730
Boiling point (°C)	115 (sublimes)
Melting point (°C)	246.2 (closed capillary)
Flash point (°C)	36 (closed cup)
Density (g cm⁻³)	1.27
log K_{ow} ^V	0.12
log K_{oc} ^{VI}	0.18-0.37

The properties of metaldehyde, such as the log K_{ow} and log K_{oc} values, have significant impacts on its fate in the environment. K_{ow} is the octanol/water partition coefficient, which is defined as the ratio of a chemical compound's concentration in the octanol-rich phase to the water-rich phase, indicating the tendency of the compound to move from the aqueous phase into lipids, i.e. the lipophilicity of the compound [45]. The value

^I CASRN = Chemical Abstract Service Registry Number

^{II} IUPAC = International Union of Pure and Applied Chemistry

^{III} In water, at 20 °C

^{IV} In methanol, at 20 °C

^V K_{ow} = the octanol/water partition coefficient, at 20 °C

^{VI} K_{oc} = the organic-carbon/water partition coefficient

of K_{ow} is usually expressed as $\log K_{ow}$, which is used for predicting the absorption of micropollutants on soil. This is because lipids can accumulate in soil and they constitute up to 30% of the soil organic carbon [46]. In this case, since Luo *et al.* argued that $\log K_{ow} < 2.5$ suggests low sorption potential [47], the low $\log K_{ow}$ of metaldehyde (0.12) therefore indicates that metaldehyde is not lipophilic and does not absorb into soil. Similarly, K_{oc} is the organic-carbon/water partition coefficient, which is the ratio of a chemical compound's concentration absorbed per unit mass soil to its concentration in water [48]. K_{oc} value is often used for describing the mobility of pesticides and low $\log K_{oc}$ value indicates high mobility in the environment. In this case, the low $\log K_{oc}$ value of metaldehyde (0.18-0.37) suggests that metaldehyde prefers to stay in the water and it can easily move around in the soil moisture (the water present in the space between soil particles). [12, 49, 50].

Metaldehyde can enter drains, surface water, and disperse in the water cycle via soil and direct application. When applied on crops, metaldehyde can enter soil; and while in soil, it can degrade to acetaldehyde and eventually to water and carbon dioxide with a half-life between 3.17 to 223 days [12]. As discussed, due to its properties, metaldehyde is extremely mobile in the soil moisture; therefore, it is frequently detected in water bodies, especially with high precipitation and heavy rainwater runoff [12]. Metaldehyde can also enter the water cycle directly. For example, at point sources, metaldehyde can be spilled on the ground and subsequently be washed into drains with rainfall. It can be directly applied to water bodies that are located near crops by accident as well [12, 49]. In the aquatic environment, metaldehyde has a solubility of approximately 200 mg L^{-1} at $17 \text{ }^\circ\text{C}$ and a slow degradation process; therefore, it is considered semi-persistent in water [12].

2.2.2 Toxicity of metaldehyde

2.2.2.1 Effects of metaldehyde on animals and the environment

In 2009, the World Health Organization classified metaldehyde as a moderately hazardous (class II) pesticide [51], and the United State Environmental Protection Agency classified metaldehyde as a 'restricted use pesticide' due to its potential short-term (in the range of months) and long-term (life-long) health effect on wildlife [12, 52]. Metaldehyde is toxic to all animals, by dermal absorption (slightly toxic), ingestion (moderately toxic), and inhalation (highly toxic) [14]. In fact, metaldehyde is palatable and can therefore easily be digested by animals [53]. For example, oral ingestion is the most common exposure of metaldehyde, with poisoning incidents frequently reported in pets and birds. This is because the baits formulated in metaldehyde pellets resemble dog food and they are flavoured with bran to attract snails; however, dogs and other pets are unfortunately attracted as well [14]. Oral ingestion of metaldehyde by these animals can cause dysfunctions of organs including liver, kidney, lungs and central nerve system [14]. These poisoning effects come from acetaldehyde, which is the degraded product of metaldehyde after ingestion effects [54]. Metaldehyde can undergo hydrolysis under acidic condition, forming acetaldehyde which can later be oxidized to acetic acid, and then eventually to carbon dioxide and water (Figure 2.2) [14]. Poisoning of metaldehyde is also acute in domestic animals and wildlife since a very small amount of metaldehyde can cause organ failures and death [14]. For instance, the concentration of metaldehyde in commercial slug pellets is normally at 1.5, 3, or 4% by weight [12]; however, 4% pelleted metaldehyde is toxic to wildlife [52], since it is a rapid acting and fatal pesticide for most mammals when consumed [55, 56].

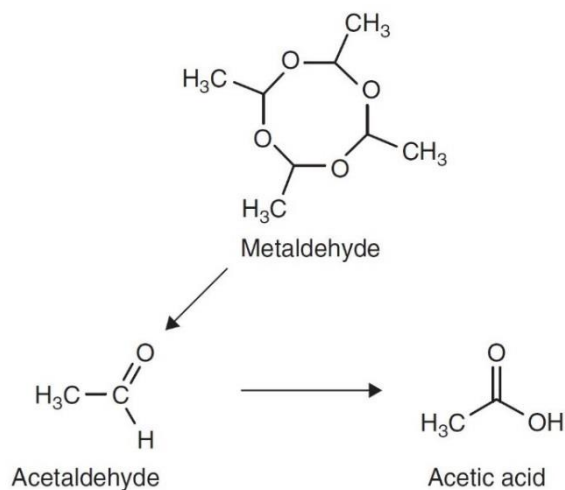


Figure 2.2 Metaldehyde and its two major metabolites (figure reproduced with permission of the rights holder, Elsevier) [14]

In addition, the presence of metaldehyde at high levels in the aquatic environment presents a risk to the ecosystem. Horgan *et al.* stated that high levels of metaldehyde in the environment can lead to the depletion of beneficial aquatic fauna, especially beneficial snails; they also mentioned that the extensive usage of metaldehyde created pests that are resistant to slug repellents, which increased damages of rice crops [57]. Furthermore, metaldehyde in surface water was assessed to be harmful to aquatic organisms including gastropods [13]. For example, Moreau *et al.* stated that metaldehyde may be toxic to oysters; and they suggested to further investigate the effect of metaldehyde on aquatic invertebrates, especially the ones that have significant economic impacts [58].

2.2.2.2 Effects of metaldehyde on human health

Dermal contact with metaldehyde can cause skin irritations for humans; for example, repeated skin exposure to metaldehyde may cause dermatitis, and repeated eye exposure can cause conjunctivitis [52]. Moreover, as mentioned in Section 1.1, up to

1 $\mu\text{g L}^{-1}$ of metaldehyde has been detected in drinking water in the UK [8], which may have effects on human health. However, to discuss this, it is essential to consider the ADI of metaldehyde. According to the European Commission, the ADI of metaldehyde is 0.02 mg per kg by weight per day [59]. Therefore, to exceed the ADI of metaldehyde, a person with a body weight of 50 kg would need to drink approximately 1000 L of water every day, even if the drinking water contains the highest detected concentration of metaldehyde at 1 $\mu\text{g L}^{-1}$ [8]. Based on this, it is argued that there is no risk to health if people occasionally consume water that contains trace amount of metaldehyde [8]. Additionally, the Water UK and the Drinking Water Inspectorate explained that the standard for individual pesticide (0.1 $\mu\text{g L}^{-1}$) in drinking water was not set on the basis of health effect; in 1980, the European Commission set this standard to reflect the detection limit of the analytical methodology at that time and to generally limit pesticides as an environmental policy [8, 60].

Although the current level of metaldehyde in water presents no risk to human health, the accumulative life-long effect on human health of consuming drinking water that contains metaldehyde higher than 0.1 $\mu\text{g L}^{-1}$ is still unknown. For example, Saad *et al.* argued that metaldehyde can bioaccumulate over time, which may have effects on certain organs [61]. Therefore, it is of great significance to remove metaldehyde from water to improve the quality of drinking water, and to protect the ecosystem, aquatic environment, birds and mammals [13].

2.2.3 Concentrations of metaldehyde in surface water bodies

As a result of extensive usage, metaldehyde has been detected in surface water with the highest concentration of 8 $\mu\text{g L}^{-1}$ in the UK [11]. For example, concentrations of

metoldehyde were found as high as $8 \mu\text{g L}^{-1}$ in the River Thames from August to October in 2012. According to the Drinking Water Inspectorate, in 2015, concentrations of metoldehyde exceeded the EU and UK standard of $0.1 \mu\text{g L}^{-1}$ at water sampling locations of water companies including Anglian Water and Thames Water, in England and Wales [12, 62]. The presence of relatively high concentrations of metoldehyde in surface water bodies therefore raised concerns.

In the UK, to protect the surface water bodies that are used as sources for potable water, the concept of Drinking Water Protected Areas was introduced [12]. According to the UK Environment Agency, Drinking Water Protected Areas, within the Water Framework Directive, are protected areas where raw water is extracted from reservoirs, rivers, and the ground [63]. This is to ensure that these areas are not polluted with additional substances such as pesticides, which can lead to additional water treatment processes [63, 64]. Within the Drinking Water Protected Areas, Safeguard Zones are identified by the UK Environment Agency and water companies as drinking water sources that are 'at risk' and need additional treatment, due to the pollution of raw water by land use [63, 64]. It is reported that in 2014, more than 100 Drinking Water Protected Areas were considered to be 'at risk' in England, due to concentrations of pesticides in raw water exceeding the EU and UK standard, with metoldehyde being the most significant active chemical compound [12]. Safeguard Zones were therefore set up at the upstream of these water sources; for example, there are 96 Safeguard Zones in England for surface water because of pesticide contamination [12, 65].

Currently, water companies including Thames Water are aiming to improve water quality by catchment management to reduce the concentration of metoldehyde at its sources, supporting alternative slug repellents such as iron phosphate at highly-

affected catchments, and considering developing new treatment methods that target at removing metaldehyde [8, 66].

2.3 Determination and monitoring of metaldehyde in water

2.3.1 Determination of metaldehyde in aqueous solutions

Since metaldehyde has been detected in the environment in the range of 1 to 8 $\mu\text{g L}^{-1}$ [11], exceeding the EU and UK standard of 0.1 $\mu\text{g L}^{-1}$, it is significant to develop sensitive and quantitative analytical methods. This is to ensure that metaldehyde in aqueous solutions can be determined at concentrations lower than the standard [8, 11, 12]. Two instrumental techniques are commonly used, gas chromatography with mass spectrometry (GC-MS) and liquid chromatography with mass spectrometry (LC-MS). These two techniques are normally used together with pre-concentration and phase extraction processes such as solid-phase extraction (SPE) [12]. For example, in 2009, the UK Environment Agency published a guidance, proposing several GC-MS and LC-MS methods to determine metaldehyde in different water types including raw waters, processed waters, ground waters, and potable waters [11].

GC-MS is a technique used for identifying and quantifying trace organic compounds in a bulk sample. Components of the sample mixture are separated in a gas chromatography (GC) and then detected in a mass spectrometer (MS), based on the retention times and elution patterns of the components [67, 68]. Sample mixture is flash vaporized at the heated induction point of GC and enters the column inside the oven; components of the sample mixture are then carried by a carrier gas (mobile phase), usually helium, through the column and are separated on the column based on their affinity to the coating material of the column and the carrier gas [67]. Columns

are coated with different materials (stationary phase) to enhance the separation processes according to the compounds of interest [67]. After column effluent enters MS, components are ionized and fragmented. Since the fragments of the components carry the characteristics of their molecular structure [67], the fragments can be used for detecting and measuring the components of interest.

GC-MS has become a widely used analytical technique for analysing metaldehyde, since its methodology is relatively fast and simple. A non-polar column is used which allows metaldehyde to have a short retention time (usually less than 8 min), with a high oven temperature (150 to 300 °C) which elutes all analytes that can be present [12]. The detection limits of GC-MS for metaldehyde using the methods provided by the UK Environment Agency are between 0.004 and 0.006 $\mu\text{g L}^{-1}$ [11]. Other detection limits have also been reported at 0.01 and 5 $\mu\text{g L}^{-1}$ using different methods [31, 69]. However, metaldehyde in water needs to be extracted to the organic phase before being injected into the column and analysed by GC-MS. Extraction processes, such as SPE, are costly and time-consuming, but they also allow large volumes of water samples (250 to 1000 mL) to be extracted into 1 to 2 mL of eluate [12]. Therefore, the extraction/pre-concentration processes can lower the detection limit of GC-MS for metaldehyde. Many researches have used GC-MS for determining metaldehyde in aqueous solutions. For example, Autin *et al.* studied the degradation of metaldehyde by AOPs; they applied one of the methods proposed by the UK Environment Agency, which is suitable for analysing metaldehyde in laboratory grade water and surface water by GC-MS [29]. Similarly, Salvestrini *et al.* adapted the same method to analyse metaldehyde in laboratory grade water after sorption by GAC [70].

LC-MS is an analytical technique that combines liquid chromatography (LC), which can separate components from a mixture, with MS which can detect and determine each component [71]. The most commonly used LC is high performance liquid chromatography (HPLC), due to its sensitivity and high efficiency [72]. Sample mixture is injected into the column of LC; components of the sample mixture are separated on the column, based on their affinity to the mobile and stationary phase of LC [72]. Molecular and fragment ion peaks can be observed according to the mass to charge ratio, as a small portion of the sample is introduced into the MS [72].

LC-MS allows water samples containing metaldehyde to be directly injected, and it is highly sensitive, with detection limits in low 'ng L⁻¹' range, if using modern instruments [12]. Triple quadrupole (LC-MS-MS) detection systems are used for most methods for their better specificity [12]. To analyse metaldehyde in water, a non-polar stationary phase is used with a polar mobile phase, and sometimes a buffer is added into the mobile phase [12]. Although it can overcome some of the disadvantages of GC-MS, LC-MS is more expensive to purchase in comparison. In addition, the noisy measurements (with standard deviations of 10-20%) makes it difficult to pinpoint the detected compound; and the relationship between MS signal and the concentration of compound depends quite strongly on the structure of the compound [73]. Many researches have used LC-MS or LC-MS-MS for analysing metaldehyde in water. For example, Rolph *et al.* reported a detection limit of 0.5 µg L⁻¹ by LC-MS-MS for metaldehyde, using water samples without any extraction/pre-concentration processes [74].

There are other methods to determine metaldehyde in water with similar principles. For example, Li *et al.* proposed a method which used ultra performance liquid

chromatography-electrospray tandem mass spectrometry (UPLC–MS–MS) for analysing metaldehyde in water; they stated a detection limit of 3 ng L⁻¹ and reached recoveries of 96.1-106.3% [75]. Although their method is sensitive and confirmatory, it involves the use of UPLC-MS-MS, which is much more expensive compared with GC-MS and LC-MS and requires extensive pre-treatments/sample preparation.

Considering the cost, time, instruments and equipment available in the Environmental Engineering Laboratory of the Department of Civil, Environmental, and Geomatic Engineering at University College London (UCL), GC-MS was selected for analysing metaldehyde in aqueous solutions.

2.3.2 Monitoring of metaldehyde in water

Monitoring the levels of metaldehyde in water helps identify the areas where water sources are affected by metaldehyde pollution; it is also informative for drinking water treatment plants to make adjustments to their water treatment processes such as increasing the dosage of oxidants or adsorbents [76].

Monitoring strategies of metaldehyde in water are developing over time. For example, low volume (< 5 L) spot sampling (collected weekly or monthly) followed by GC-MS/LC-MS analysis is not considered effective, since concentrations of metaldehyde can fluctuate significantly over the sampling period, according to different weather conditions [12]. Automated water collection devices which collect water at programmed intervals (hourly or daily) may be more suitable, since the sampling period can be customized; however, it comes with a high capital cost for the equipment [76]. Alternatively, rapid on-line/on-site monitoring methods are convenient for catchment management [76]. GC-MS/LC-MS coupled with detectors at surface water

can provide rapid analysis of metaldehyde [12]. For example, in 2016, an online GC-MS system for metaldehyde detection, which can detect metaldehyde in raw water and different stages of treatment processes in 36 min, was trialled by Affinity Water in Hertfordshire [77]. This method is helpful for areas that are at high risk of metaldehyde pollution. Rapid detection of metaldehyde in these areas allows water companies to adjust their treatment methods accordingly. In addition, a passive sampling device is another method that can be deployed in sampling locations over a long period of time (days to months) [12]. Compounds in water are concentrated up in the devices with large volumes of water passing through [76]. Passive sampling devices are used for locating the major inputs of metaldehyde, which can provide information for catchment management [76]. For instance, river catchment monitoring programmes for metaldehyde can help convince major users of metaldehyde to reduce its usage; however, voluntary actions are limited due to practical and financial considerations [12].

2.4 Conventional and potential treatment methods for metaldehyde

2.4.1 Conventional methods: oxidation with ozone, AOPs (UV photolysis and hydrogen peroxide under UV irradiation), and adsorption (GAC filtration)

Oxidation with ozone is a common water treatment method used by many drinking water treatment plants. It is often installed at two locations, at the beginning of the main treatment line as a pre-treatment process (pre-ozone contactor), after sedimentation/before filtration as one of the main treatment processes (main ozone contactor), or at both locations [78]. Ozone is a powerful oxidant which can be used

for treating colour, odour, and pollutants in water; it can be used as a disinfectant as well [79]. When applied directly in water, it reacts rapidly with iron, manganese, cyanide, and hydrogen sulphide, with contact time between seconds to a few minutes [78]. Ozone can also be applied together with UV irradiation. For example, Andreozzi *et al.* argued that, oxidation reactions initiated by applying only ozone under UV light (wavelength at 254 nm) were even more active than the application of both ozone and hydrogen peroxide [80].

Compared to oxidation with ozone, AOPs are reactions that generate hydroxyl radicals in a large quantity, sufficient enough for water treatment; it was first proposed for potable water treatment by William H. Glaze in 1987 [81]. As discussed in Section 1.2, hydroxyl radicals can react with and break down organic compounds to oxidation products such as water and carbon dioxide [82]. UV photolysis and hydrogen peroxide under UV irradiation (H_2O_2/UV) are two examples of AOPs; and they often take place at the disinfection stage.

UV photolysis is defined as the decomposition/degradation of organic pollutants to intermediate substances and eventually to carbon dioxides, water, and salts, via photochemical reactions initiated by the application of UV light [83]. Sanches *et al.* stated that pesticides including alachlor, atrazine, diuron, pentachlorophenol, and chlorfenvinphos were efficiently degraded by direct photolysis under a low pressure UV light which has a high fluence of 1500 mJ cm^{-2} [84]. In fact, UV photolysis involves direct and indirect photolysis. For example, Gan *et al.* suggested that under a low pressure UV light, chloral hydrate can directly be broken down to carbon dioxide and chloride ion; it can also react with hydroxyl radicals, generated by the interaction

between the UV light and water, and degrade to carbon dioxide and chloride ion in the end (Figure 2.3) [85].

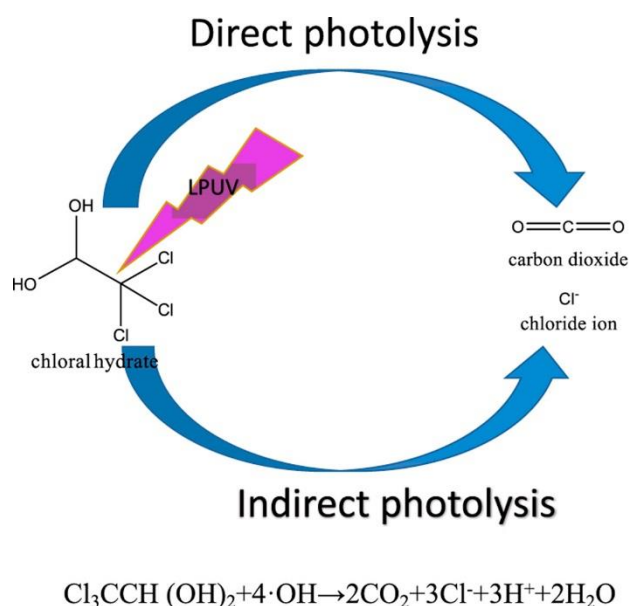


Figure 2.3 Direct and indirect photolysis of chloral hydrate under a low pressure UV light (LP = low pressure) (figure reproduced with permission of the rights holder, Elsevier) [85]

$\text{H}_2\text{O}_2/\text{UV}$ is another example of AOPs. H_2O_2 can form hydroxyl radicals rapidly under UV irradiation. For example, H_2O_2 irradiated with UV light (wavelength smaller than 280 nm) will undergo homolytic cleavage and form hydroxyl radicals (Equation 2.1), which will attack organic pollutants [80]. It is suggested that the application of $\text{H}_2\text{O}_2/\text{UV}$ can degrade metaldehyde in surface water [29], and alachlor in groundwater [86].



Although these oxidation methods are effective for degrading organic pollutants, they have some drawbacks. For example, current ozone treatments installed in drinking water treatment plants cannot degrade metaldehyde and meet the EU and UK standard [8]. This may be explained by one of the main downsides of oxidation,

competition for oxidation reactions due to the presence of scavengers such as carbonate species, NOM, sulphide, and nitrates in water [86]. These scavengers would compete for oxidation reactions with organic pollutants, in this case, metaldehyde. In addition, high energy consumption is a disadvantage of the AOPs that involve the application of UV light. Autin *et al.* argued that H₂O₂/UV can effectively degrade metaldehyde in water; however, they stated that due to the application of UV light, further researches are needed to reduce the energy input before potential application of this method at an industrial scale [29].

Application of adsorbents for removing organic pollutants via adsorption processes is another common water treatment method. Adsorption processes usually take place at the filtration stage in the filter adsorber or after filtration in the post-filter [87]. GAC is the most commonly used adsorbent in water treatment processes [16]. It is produced from charcoal, coconut, wood, or lignite and activated by physical/thermal activation using steam or carbon dioxide in the furnace with a temperature from 850 to 1000 °C [87]. Therefore, GAC has a porous structure and large surface area, which allows pollutants to be adsorbed onto the pores of GAC. GAC has pores with different sizes, such as macropores, mesopores, and micropores, for adsorbing pollutants that have different sizes. GAC is effective for removing organic pollutants such as pesticides, humic acids, and disinfection by-products [87]. In drinking water treatment plants, GAC is often used as a filtration medium in the filtration process, which follows the pre-ozone contactor and/or the main ozone contactor [78]. The particle size of GAC usually ranges from 100 µm to several mm in diameter [88].

Nevertheless, as discussed in Section 1.1, metaldehyde, the target pollutant studied in this thesis, is not responsive to these conventional water treatment methods. Its

concentration in water cannot be lowered to meet the standard of $0.1 \mu\text{g L}^{-1}$ by oxidation with ozone and GAC filtration [8]. Apart from the physicochemical properties of metaldehyde, which makes it difficult to be degraded by oxidation with ozone, the presence of NOM such as humic substances in water can affect the removal of metaldehyde as well. NOM molecules can be degraded by oxidation prior to metaldehyde. They can also block the pores of GAC and compete with metaldehyde for adsorption sites on GAC [34, 86]. Additionally, application of GAC can be expensive; this is because a large amount of waste may be produced without the recycling of GAC, while energy consumption may be high if recycled GAC is regenerated at high temperatures [89].

2.4.2 Potential methods: AOPs (heterogeneous photocatalysis) and adsorption (adsorbents with different characteristics)

Heterogeneous photocatalysis is one of the AOPs which requires the presence of a photocatalyst in the system, for example, TiO_2 or zinc oxide (ZnO), together with a light source (natural or artificial). It is determined as heterogeneous photocatalysis because the catalyst (solid) and the reactant (liquid) are not in the same phase. The principle of heterogeneous photocatalysis is to initiate the oxidation reactions to attack organic contaminants by generating hydroxyl radicals; and hydroxyl radicals are produced from the interaction between the photocatalyst and the light source [22]. Photocatalysts used in heterogeneous photocatalysis are often semiconductors; and each semiconductor has its own band gap. The band gap of the semiconductor defines the energy required to initiate the reactions that generate hydroxyl radicals during the photocatalytic process [90]. A semiconductor with a big band gap requires higher energy to initiate the reactions, compared with a semiconductor with a small band gap.

Figure 2.4 [90] demonstrates the band gap theory and Figure 2.5 [91] illustrates semiconductors with different band gap energy.

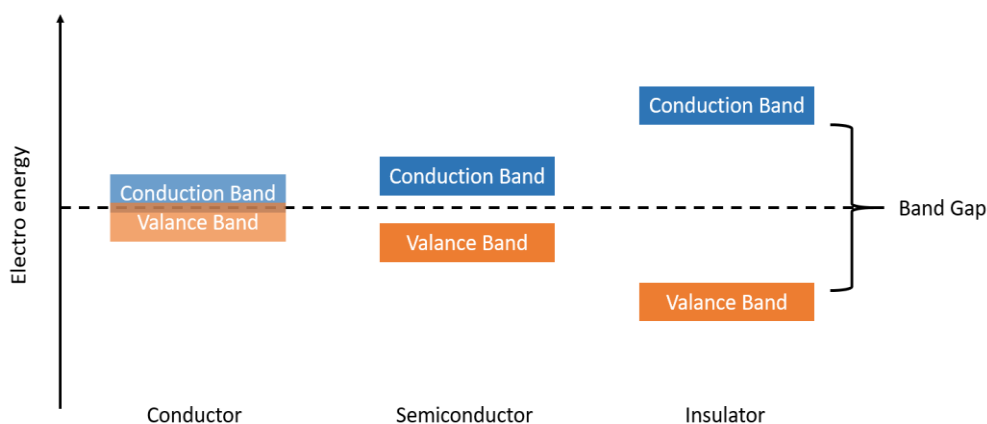


Figure 2.4 Band gap theory [90]

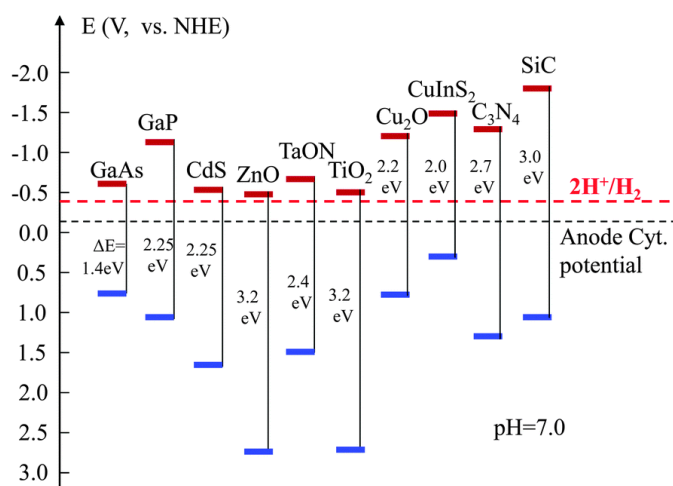


Figure 2.5 Semiconductors with different band gap energy (figure reproduced with permission of the rights holder, Royal Society of Chemistry) [91]

The process of heterogeneous photocatalysis is explained here using the treatment method of TiO_2 under UV irradiation (TiO_2/UV) as an example (Figure 2.6) [92]. When the photocatalyst (TiO_2 particle) is illuminated by the UV light which provides energy higher than its band gap energy (3.2 eV), electrons of the valence band are excited and jump to the conduction band, therefore initiating possible reactions of the electron-

hole pairs (Equation 2.2). This means that the surface of the photocatalyst has enough energy to form a positive hole in the valence band and an electron in the conduction band. Holes and electrons transfer to the surface of the photocatalyst. The hole oxidizes organic contaminants or produces hydroxyl radicals which act as oxidants in the system (Equation 2.3). The electron reduces oxygen which is then adsorbed on the surface of the photocatalyst and produces superoxide radicals and later hydroxyl radicals (Equation 2.4) [22].

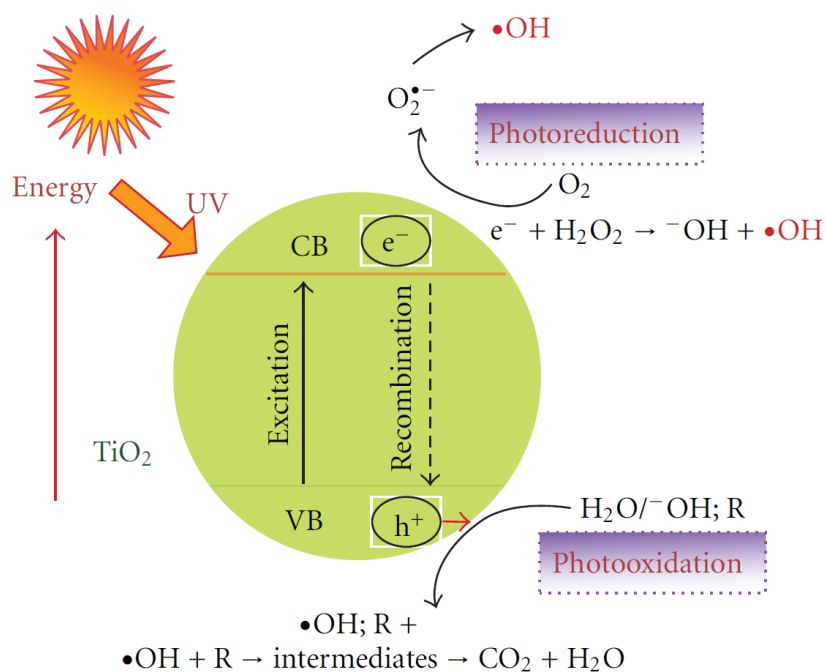


Figure 2.6 Heterogeneous photocatalysis by TiO_2/UV (CB = conduction band; VB = valence band) [92]

Many researchers suggested that heterogeneous photocatalysis is a promising treatment method to degrade organic pollutants, especially using nanoparticle photocatalysts with large surface area. For example, Kim *et al.* found that the application of nano-sized ZnO/laponite composite (20 g L^{-1}) under UV-C light with a reaction time of 60 min can successfully degrade humic acid (30 mg L^{-1}) by 90% [93]. And Doria *et al.* argued that the same composite (50 g L^{-1}) under UV-C light with a reaction time of 18 min can degrade metaldehyde (0.45 mg L^{-1}) by 20% [94]. Furthermore, Khraisheh *et al.* stated that 98% of carbamazepine (10 mg L^{-1}) was removed by TiO_2 -coconut shell powder composite (120 g L^{-1}) under UV-C light with a reaction time of 40 min [95]. In addition, heterogeneous photocatalysis may be applied at the disinfection stage in drinking water treatment plants since it can potentially treat pathogens in water as well [96].

There are many other prominent advantages of heterogeneous photocatalysis such as no addition of other chemical compounds and the stability of photocatalysts such as TiO_2 under UV irradiation in water [97]; but it also has shortcomings. Since the energy of the light source required in heterogeneous photocatalysis is based on the band gap energy of the semiconductor, the energy consumption may be high. However, it is argued by Kim *et al.* that modifying photocatalysts and incorporating visible light to the process may reduce the cost greatly [98]. For instance, Bae *et al.* found out that the degradation of trichloroacetate and carbon tetrachloride under visible light was considerably enhanced by adding platinum particles on dye-sensitized TiO_2 ($\text{Pt/TiO}_2/\text{Ru}^{\text{II}}\text{L}^3$) [99].

Another downside of heterogeneous photocatalysis is the recombination of electron-hole pairs [80]. Under this situation, the excited electron from the valance band would

return to its original position, hence reducing the effectiveness of the photocatalytic process. To prevent the electron-hole recombination, it is suggested that substances including transition metals can be added to trap electrons. For example, Hsieh *et al.* stated that incorporating zero-valent iron with TiO₂ could improve degradation efficiency of azo dye Acid Black 24 in water, as well as lengthening the life of the photocatalyst [100]. There are other disadvantages of heterogeneous photocatalysis. For example, pre-treatments may be required for water to be transparent in a certain spectral region [97]. Since photocatalysts require different band gap energy to initiate the photocatalytic process, the light that passes through water and reaches the surface of the photocatalyst needs to be in the corresponding spectral region. Additionally, Li *et al.* argued that toxic intermediate products may form with the degradation of some pollutants [101].

Developing adsorbents with different characteristics is another approach to remove pollutants from water via adsorption processes. For example, compared with GAC, PAC has smaller particle sizes, larger surface area and pore spaces. Yoon *et al.* argued that PAC successfully removed 3 estrogenic compounds: bisphenol A, 17 β -estradiol, and 17 α -ethynyl estradiol from drinking water samples; their percentage removal ranged from 31 to 99%, depending on different PAC types, dosages, and water quality [34]. In addition, they mentioned that the percentage removal of these compounds was lower with the presence of NOM; and increasing the PAC dosage increased the percentage removal [34]. However, more suspended solids need to be separated from the treated water, due to a higher dosage of PAC. And this may affect the treatment stages that remove suspended solids, such as sand/GAC filtration.

Graphene (the 2-dimension allotrope of carbon) is an adsorbent that has been of interests to many researchers, thanks to its physicochemical properties. It has a unique structure; a single atomic layer of carbon is arranged in a honeycomb structure (Figure 2.7). It has large surface area, good thermal conductivity, and provides great mobility for charge carriers [102]. There are numerous studies suggesting that graphene demonstrates an extraordinary adsorption capacity regarding the removal of heavy metal ions such as lead and cadmium [103] and azo dyes including methyl blue [104]. Xu *et al.* argued that unlike AC which is non-selective, graphene favours the adsorption of pollutants that have aromatic structures with benzene rings; they stated that the maximum adsorption capacity of graphene for bisphenol A was found to be 182 mg g⁻¹ at 302.15 K [102].

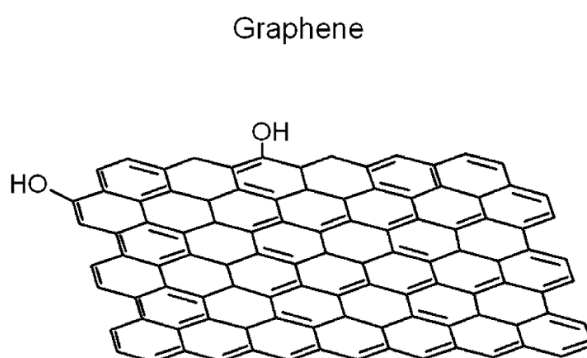


Figure 2.7 Structure of graphene: single atomic layer of carbon in honeycomb shape (reprinted with permission from Xu *et al.*. Copyright 2020 American Chemical Society) [102]

Although graphene presents some good characteristics that may be effective for removing pollutants from water, including the unique geometry and large surface area, it has disadvantages as well [105]. The structure of graphene is not absolutely stable, due to the strong interplanar interaction; and this suggests the atomic layers of graphene can restack to form graphite [105]. Moreover, the synthesis processes of

graphene composites are complex and costly, which make them difficult to be commercialised and applied for water treatment at an industrial scale.

In addition, carbon nanotubes (CNTs) are promising adsorbents that can potentially be applied to water treatment. The structure of CNTs is more stable, compared with graphene. CNTs are made by rolling graphene sheets into a cylinder shape. Defined by the number of concentric rings that the graphene sheets rolled up to form, there are single-walled, double-walled, and multi-walled CNTs (Figure 2.8) [106, 107]. Multi-walled CNTs were proven to remove heavy metal ions such as lead, copper, and cadmium from water effectively. Li *et al.* reported that the maximum adsorption capacities of multi-walled CNTs were 97.08 mg g^{-1} for lead, 24.49 mg g^{-1} for copper, and 10.86 mg g^{-1} for cadmium, which were three to four times larger than PAC and GAC [108]. Tofighy and Mohammadi suggested even higher adsorption capacities of CNTs for heavy metal ions, 118 mg g^{-1} for lead, 93 mg g^{-1} for cadmium, and 65 mg g^{-1} for copper, if the CNTs sheets have been oxidized with concentrated nitric acid [107].

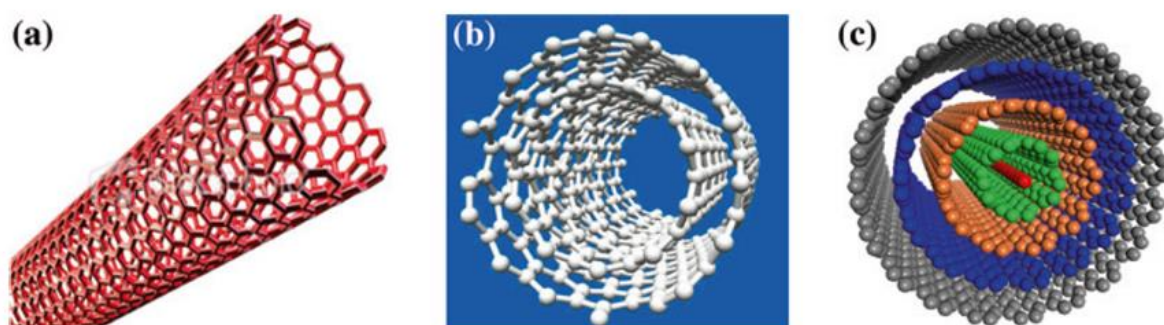


Figure 2.8 (a) Single-walled CNTs; (b) Double-walled CNTs; (c) Multi-walled CNTs (figure reproduced with permission of the rights holder, Springer) [106]

Similarly, CNTs have drawbacks as well. Since they are cylinders of rolled up graphene sheets, the synthesis processes of CNTs are complex and time-consuming

[109], which makes it difficult to be industrialised [110]. Moreover, both single-walled and double-walled CNTs are expensive, especially when they are used for synthesizing membranes in water treatment researches; therefore, large-scale and sustainable production of CNTs is challenging [110].

Activated carbon fibre (ACF) is another novel adsorbent that has drawn scientific attention. Compared with GAC and PAC, which have the ladder structure in terms of pore size distribution (micro-/meso-/macro-pores), ACF is a microporous material with low meso-porosity (sometimes even no macro-porosity); it has a fibre shape and well-defined porous structure [88]. The structure of AFC suggests that instead of passing through macropores, mesopores, and lastly reaching micropores, pollutants can directly be adsorbed onto micropores. This structure of ACF seems to be effective for removing pollutants that have small molecules. Lee *et al.* suggested that ACF has a high packing density, large surface area ($2000 \text{ m}^2 \text{ g}^{-1}$) and pore volume, and high-speed adsorption; they found the maximum adsorption capacity of ACF for p-nitrophenol was 247.85 mg g^{-1} , with 98.75% removal [111]. Despite having a larger surface area and larger breakthrough time, compared with GAC [112], ACF has its disadvantages when it comes to practical application in water treatment processes. For example, bacteria can adhere to the surface of ACF which has good biocompatibility; therefore, bacteria tend to breed on ACF, gradually turning it into pollutants [113]. Similarly, the utilisation of ACF can be difficult because of the high synthesis cost, compared with GAC and PAC [114]. In fact, Ma *et al.* argued that most ACFs are made from precursors based on the fossil fuels; they suggested that it is necessary to improve ACFs production, due to the shortage of the fossil fuel resources [115].

2.4.3 Combination of oxidation and adsorption

Adsorption is considered significant in the photocatalytic degradation process of pollutants [116]. Therefore, there are many studies that combined photocatalysts and adsorbents, trying to achieve further degradation of contaminants in water. Asha *et al.* argued that the combination of adsorption and photocatalytic property of GAC-TiO₂ demonstrated excellent efficiency and effectiveness in wastewater treatment; it can completely remove total volatile solids in 6 min and total solids in 9 min under UV light. [117]. They suggested that improved removal could result from: (1) pollutant molecules adsorbed onto GAC surface; (2) promoted formation of hydroxyl radicals due to scattered deposition of TiO₂ on GAC surface; and (3) enhanced oxidation reactions by hydroxyl radicals since pollutant molecules can be adsorbed to positions near TiO₂ loaded sites [117]. Additionally, Subramani *et al.* stated that TiO₂ impregnated AC, which was synthesized under mild hydrothermal conditions, can improve the photo-degradation of indigo carmine dye by more than 30%, compared with using AC alone [118].

The combination of photocatalysts and CNTs was studied as well. Yu *et al.* found that the adsorption and photocatalytic activity of TiO₂ for removing azo dyes were considerably enhanced by the addition of CNTs; they argued that compared with AC, CNTs can promote the adsorption of dyes onto TiO₂ under UV light [119]. CNTs can also facilitate the photocatalytic activities of TiO₂ for degrading dyes, since the electron-hole recombination can be prevented: (1) CNTs receive free migrating electrons from the conduction band, due to its special structure and electron-storage capacity (one electron for 32 carbon atoms) [116, 119]; and (2) oxygen adsorbed onto CNTs can accept electrons and form superoxide radicals, which later form hydroxyl

radicals and assist further reactions [119]. Wang *et al.* indicated that phenol was successfully degraded by more than 95% using multi-walled CNTs-TiO₂ composites under visible light, while pure TiO₂ only achieved 41% degradation [120].

From the studies above, the combination of photocatalysts and adsorbents seems to be a promising treatment method to remove organic pollutants such as metaldehyde. Nevertheless, the application of these methods in water treatment processes may be challenging, considering the main shortcomings of both oxidation by heterogeneous photocatalysis and adsorption by different adsorbents, as discussed in Section 2.4.2.

2.4.4 Development of water treatment methods for metaldehyde

To solve the metaldehyde problem, many approaches have been proposed. Autin *et al.* discussed that after the treatment of 8 mM H₂O₂ under UV irradiation of 600 mJ cm⁻², 95% of metaldehyde was degraded in laboratory grade water; complete degradation of metaldehyde was achieved by the treatment of 0.3 mM TiO₂ under UV irradiation of 600 mJ cm⁻² [29]. They also argued that the presence of NOM could affect the effectiveness of the adsorption system more than oxidation: under the same level of UV irradiation (1200 mJ cm⁻²), the treatment of H₂O₂/UV (92% degradation) was much more effective for degrading metaldehyde in surface water, compared with the treatment of TiO₂/UV (7% degradation) [29]. Although the treatment method proposed by Autin *et al.* is effective for removing metaldehyde, the energy consumption is considered high, since four 30 W low pressure mercury lamps were used for treating 250 mL of metaldehyde solution.

Busquets *et al.* stated that a tailored phenolic carbon was tested to be effective in removing metaldehyde [30]. They found the maximum adsorption capacity of this

adsorbent for metaldehyde was 76 mg g^{-1} , while the same of commercial GAC was 13 mg g^{-1} ; and the adsorption efficiency of metaldehyde can be maintained, with the presence of background organic matter [30]. They also argued that the adsorption of metaldehyde is independent of the specific surface area (SSA) and favours carbon materials that have high micro-porosity, narrow pore size distribution, and abundant mesopores; these characteristics allow efficient diffusive transport of metaldehyde molecules [30]. Therefore, as a promising adsorbent, further investigations of this newly developed adsorbent is needed, especially to test whether its adsorption ability is selective for metaldehyde. Moreover, since it is a tailored phenolic carbon, its synthesis process may be complex and costly. It is essential to consider the feasibility of applying this adsorbent at an industrial scale.

In addition, Nabeerasool *et al.* proposed another method to remove metaldehyde by adsorption processes using a new adsorbent (NyexTM), combined with an electrochemical destruction technique [31]. A treatment cycle included a 15-min mixing phase of NyexTM and metaldehyde solution, a 10-min settling phase, and finally a 15-min regeneration phase with an electrical current of 0.5 A (10 mA/cm^2) passing through the adsorbent bed to decompose metaldehyde; and after seven treatment cycles, the concentration of metaldehyde ($11 \text{ } \mu\text{g L}^{-1}$) was lowered to meet the standard of $0.1 \text{ } \mu\text{g L}^{-1}$ [31]. The advantage of this method is that the removal of metaldehyde is effective and no waste adsorbent is produced, since NyexTM can be regenerated and used for the next adsorption cycle. However, the energy consumption is very high and the whole process (seven cycles of treatment) is long.

Tang *et al.* suggested another method, using the treatment of tetra-amido macrocyclic ligands (TAML)/ H_2O_2 as an alternative to the treatment of $\text{H}_2\text{O}_2/\text{UV}$. This treatment

method turned out to be a relatively long process, during which metaldehyde decomposed to acetaldehyde and acetic acid. This method degraded metaldehyde slowly but steadily over many hours; initiation of degradation took 5 h with 5% degradation and then 60 h with 31% degradation [121]. Despite the advantage of being effective and economic, this method is slow, regarding the degradation process. Moreover, the safety of applying TAML in water treatment is still under study. Therefore, this method is not ready to be applied at drinking water treatment plants.

Tao and Fletcher proposed a dual-stage treatment method for removing metaldehyde using Macronet and ion-exchange resin. Macronet is a non-functionalised hyper-cross-linked polymer, which is a microporous material and works as a catalyst [32]. Water passed through the first column packed with 1g Macronet, while metaldehyde was decomposed into acetaldehyde; water then passed through the second column packed with 1 g ion-exchange resin, while acetaldehyde was removed by the amine functionalised ion-exchange resin [32]. They argued that no metaldehyde was detected in the first column and 40% of acetaldehyde was detected in the second column after running the process for 10 days [32]. However, the presence of inorganic ions such as calcium ions could decrease the catalytic performance of Macronet, due to the different working mechanisms of Macronet for metaldehyde (catalytic reaction) and for inorganic ions (adsorption): (1) inorganic ions will be adsorbed by Macronet via ion-exchange and metaldehyde will be degraded at the same time; and (2) then the bed will be saturated with inorganic ions and stop adsorbing them, while metaldehyde will still be degraded at a slower reaction rate [32]. Hence, further investigations of this method in terms of the impacts of other organic and inorganic pollutants are needed before this treatment method can be applied at a larger scale.

Nguyen *et al.* investigated the degradation of metaldehyde in water by modified Fenton's reactions; they applied single-layer graphene oxide (SLGO) with high hydrophilic characteristics in the treatment method [122]. Using this method, more than 92% of metaldehyde (50 mg L^{-1}) was removed in natural water samples which have a large amount of background organic matter and dissolved salt [122]. The advantage of this method is that the reaction is pH insensitive, which can be beneficial for treating different water samples. However, during this treatment process, instead of being completely degraded to water and carbon dioxide, metaldehyde was degraded into hydroxyl acetic acid (glycolic acid) and carbon dioxide [122]. Moreover, the catalytic performance of SLGO could gradually decrease over time [122]. Hence, methods need to be established for regeneration of SLGO before its potential application in water treatment industry.

Rolph *et al.* reported the removal of metaldehyde from water by adsorption onto different filtration media, including clean sand (without biofilm), active sand (with biofilm), and biological activated carbon (BAC) [74]. It was stated that the additional biosorption or biodegradation processes enhanced the adsorption of metaldehyde onto active sand due to its active biofilm [74]. BAC was found to be the most effective adsorbent for removing metaldehyde ($2.5 \text{ } \mu\text{g L}^{-1}$) from water (94% removal), while active sand, as a bio-adsorbent, removed 41% of metaldehyde [74]. Nevertheless, desorption of metaldehyde from used BAC back to water is common, and increased regeneration of BAC is required to maintain its adsorption capacity for metaldehyde [74]. Therefore, there are limitations, such as the cost of regeneration, regarding the potential application of these filtration media in the water treatment industry.

In summary, many treatment methods have been proposed to remove metaldehyde from water. However they all have drawbacks, especially regarding their practical application at an industrial scale and competition from other compounds in water. For example, the energy consumption of the treatment method proposed by Autin *et al.* is high (four 30 W low pressure mercury lamps were used) [29]. Busquets *et al.* used new adsorbent which was even effective for removing metaldehyde in surface water [30]. Nevertheless, the cost of using new adsorbent in drinking water treatment plants could be high. Nabeerasool *et al.* and Tang *et al.* both used novel oxidants or adsorbents, and both treatment processes were slow [31, 121]. Therefore, they would not be cost-effective and efficient. Tao and Fletcher used a dual-stage treatment method and new adsorbents; however, the presence of other compounds could decrease the effectiveness [32]. Nguyen *et al.* used modified Fenton's reactions with the application of SLGO; and this method needs to account for the cost and energy consumption for regeneration of SLGO [122]. Rolph *et al.* used active sand and BAC, but desorption of metaldehyde and increased regeneration of BAC must be considered [74]. Therefore, the underlying research gap is to find a feasible method to remove metaldehyde from water, with consideration of practical application at drinking water treatment plants.

2.5 Researcher's previous work on removal of metaldehyde from water

Since this thesis built on the research topic of the researcher's MSc project [41], the findings of the MSc project are briefly discussed in this section. The MSc project investigated the removal of metaldehyde from water under UV-C light, using cetyl trimethyl ammonium bromide (CTAB) modified carbon doped TiO₂ nanoparticle

photocatalyst with 1.5% carbon and 98.5% TiO₂ (C-1.5), provided by the National Chemical Laboratory (NCL) in Pune, India; commercially available PAC was investigated as well, to compare with C-1.5 [41]. Part of the findings from the researcher's MSc project [41] was published in the study of Li *et al.* [69].

2.5.1 C-1.5

The removal of metaldehyde from water using C-1.5 under UV-C light was not significant, compared with the findings of Autin *et al.*, which found complete degradation of 1 mg L⁻¹ of metaldehyde using 0.3 mM of TiO₂ under the UV irradiation of 600 mJ cm² [29]. The study of Li *et al.* suggested that C-1.5 (0.1 g) cannot effectively remove metaldehyde (1 mg L⁻¹) from water (500 mL) [69]. As discussed in Section 2.4.2, one of the problems of heterogeneous photocatalysis is the electron-hole recombination, which affects the generation of hydroxyl radicals. In addition, the energy provided by the 11 W UV-C light may not be sufficient, compared with the study of Autin *et al.* which used four 30 W low pressure mercury lamps [29]. Moreover, the dosing concentration of C-1.5 could be increased to observe whether the degradation efficiency could be improved. Furthermore, the carbon content of C-1.5 could be increased to improve the removal of metaldehyde, since 1.5% of carbon may be low for the adsorbent-catalyst system to work synergistically.

2.5.2 PAC

PAC (charcoal, decolorizing powder activated) used in this work was Darco G60, manufactured by British Drug Houses (BDH) laboratory supplies. Adsorption isotherms of PAC were analysed by varying the initial concentrations of metaldehyde solutions, with the incorporation of UV-C light. Experimental data fitted well with the

Langmuir isotherm model (R^2 ^{VII} = 0.98). It was found that the maximum adsorption capacity (q_m) of PAC for metaldehyde was 32.26 mg g⁻¹ and the Langmuir constant (K_L) was 2.01 L mg⁻¹ [69], which are larger than the q_m of 12.71 mg g⁻¹ and K_L of 0.02 L mg⁻¹, from the study of Radjenovic and Medunic [123]. These values confirmed the effective removal of metaldehyde by PAC. However, an in-depth study on adsorption of metaldehyde onto PAC is required to confirm the results from the researcher's MSc project [41].

2.6 Approaches for removal of metaldehyde from water within the present study

After reviewing the researches (Section 2.4 and Section 2.5) that studied potential treatment methods for metaldehyde, this thesis took the approaches of heterogeneous photocatalysis and adsorption processes to remove metaldehyde from water, while considering the feasibility of the treatment methods. This thesis also investigated the relationships among the studied adsorbates (metaldehyde and HA) and the adsorbent (PAC) by using a number of material characterization techniques.

2.6.1 Heterogeneous photocatalysis

As discussed in Section 2.4.2, the application of TiO₂ nanoparticle photocatalysts under UV-C light is the most common treatment method using the technique of heterogeneous photocatalysis. In this thesis, the experimental investigation, that studied the removal of metaldehyde by heterogeneous photocatalysis, applied two types of photocatalysts:

^{VII} R^2 = the coefficient of determination

(1) Carbon modified TiO₂ nanoparticle photocatalysts (containing at least 38% higher carbon content than C-1.5)^{VIII}, with exposure to UV-C light;

(2) TiO₂ modified graphene and ZnO modified graphene^{IX}, with exposure to visible light.

As mentioned in Section 2.4.4, Autin *et al.* found effective removal of metaldehyde by TiO₂/UV [29]. Bae and Choi stated effective degradation of trichloroacetate using modified TiO₂ under visible light [99]. Therefore, in this thesis, applying these photocatalysts under UV-C light and visible light may be effective in removing metaldehyde.

In fact, the photocatalysts used in this thesis were modified by either adding adsorbents on the photocatalyst or adding photocatalysts on the adsorbent. Modifications on these photocatalysts may enhance the removal of metaldehyde, due to the possible combination of oxidation and adsorption, as described in Section 2.4.3 [117]. In the proposed adsorbent-catalyst system: (1) adsorption of metaldehyde onto the adsorbents may be possible; (2) oxidation reactions may be promoted, since adsorbed metaldehyde molecules could be positioned closer to the photocatalysts; and (3) the adsorbents in the system can potentially remove scavengers from water, such as humic substances and inorganic compounds, as discussed in Section 2.4.1.

In addition, the application of these photocatalysts are considered more practical, relative to the researches discussed in Section 2.4.4. This is because (1) the carbon used in synthesizing the modified TiO₂ nanoparticle photocatalysts was made from

^{VIII} Developed and provided by NCL in Pune, India.

^{IX} Developed and provided by Centre for Materials for Electronics Technology (C-MET) in Pune, India.

cheap agro-waste; (2) the application of TiO₂ modified graphene and ZnO modified graphene, with exposure to visible light, would consume less energy than UV-C light; and (3) the dosing concentration of all photocatalysts was small (0.2 g L⁻¹), which potentially lowered the cost.

2.6.2 Adsorption

As explained in Section 2.4.2 and Section 2.5.2, Yoon *et al.* argued that three estrogenic compounds can be removed by PAC [34]; in addition, PAC was very effective in removing metaldehyde in the researcher's previous work [41, 69]. Therefore, adsorbents with smaller particle size and higher SSA, compared with GAC, may be effective for removing metaldehyde. In this thesis, carbon materials including chemically activated carbon powder (made from agro-waste) and PAC were investigated for removing metaldehyde. In particular, the removal of metaldehyde by adsorption onto PAC was investigated in-depth with the experiments that varied PAC dosage, contact time, different pH, and different initial concentrations of metaldehyde solution. The effect of UV-C light on the removal of metaldehyde by PAC was also studied. In addition, PAC, as the most effective adsorbent studied in this thesis, was further investigated from the perspective of materials chemistry. The in-depth study of PAC endeavoured to tie the effective removal of metaldehyde to the characteristics of PAC, and to explain the adsorption mechanisms of metaldehyde onto PAC.

2.6.3 Material characterization techniques

Scanning electron microscopy (SEM) is a material characterization technique that determines the size, shape, and texture of particles at nanometre scale; a fine beam of electrons scans the sample and detects signals from the interactions between the

sample and electrons [124]. For example, Ma *et al.* included the SEM images of ACFs, demonstrating their fibrous and porous structure [115]. SEM analysis of PAC in this thesis demonstrates the surface morphology of PAC and present the pores of PAC visually.

Additionally, energy-dispersive X-ray spectroscopy (EDX), used in conjunction with SEM, can detect the elemental composition of the sample, by detecting the X-rays emitted at specific wavelengths from the atoms on the surface of the sample [125]. For instance, Amin *et al.* stated that EDX analysis confirmed there was adsorbed succinic acid on the surface of low carbon steel electrodes [126]. Therefore, EDX analysis in this thesis may provide evidence of metaldehyde being adsorbed on the surface of PAC.

Similarly, X-ray photoemission spectroscopy (XPS) can measure the elemental composition of the surface of the sample quantitatively, by analysing the energy emitted when the surface of the sample is bombarded with X-rays in vacuum [127]. For example, Zhang *et al.* suggested that XPS analysis demonstrated adsorption of arsenate on magnetite-modified ACFs [128]. Therefore, XPS analysis may be helpful to present quantitative evidence of metaldehyde being adsorbed on PAC.

In addition, attenuated total reflection Fourier transform infrared (ATR-FTIR) is a technique for detecting functional groups, providing covalent bonding information, and identifying chemicals on the surface of the sample [129]. The sample is exposed to infrared (IR) radiation, with different wavelengths through a crystal (often diamond); the energy of IR radiation is absorbed differently at each wavelength, due to the characteristic vibrations of molecules on the surface of the sample; the absorption can

be measured to produce the specific IR spectra of the sample, demonstrating its characteristic surface chemistry [130, 131]. For instance, Ahmed *et al.* stated that glycine was adsorbed and bound onto the surface of diamond-like carbon [132]. In this thesis, comparing the ATR-FTIR spectra of different PAC samples (such as virgin PAC^x and the PAC that has been used for adsorption tests) may provide possible bonding information, regarding the adsorption of metaldehyde onto PAC.

Apart from EDX, XPS, and ATR-FTIR, which analyse the surface chemistry of the sample, Brunauer-Emmett-Teller (BET) SSA analysis is a material characterization technique that can be used to analyse the structure of the sample. BET SSA analysis can provide structural information of porous materials such as PAC, including the SSA, pore size distribution, and total pore volume [133]. The most commonly used method of BET SSA analysis is the nitrogen adsorption method; the adsorption capacity of the sample for nitrogen is dependent on the relative pressure (P/P_0); P is the partial pressure of nitrogen and P_0 is the saturated vapour pressure of nitrogen [134]. The pore structure of the sample can be determined by plotting the volume of nitrogen at standard temperature and pressure against P/P_0 ; this is because nitrogen condenses in micropores, with P/P_0 larger than 0.4; and the SSA of the sample can be determined using the BET equations, with P/P_0 from 0.05 to 0.35 [134]. For instance, Wu *et al.* compared the adsorption performance of different ACs for different chemicals including phenol, based on the pore properties and SSA of these ACs, which were determined by the nitrogen adsorption method [135]. Therefore, BET SSA analysis may be helpful to tie the effective adsorption of metaldehyde to the specific characteristics of PAC, such as pore size distribution.

^x Virgin PAC = the PAC that was unused for adsorption tests.

Lastly, the analysis of point of zero charge (PZC) of the sample is an experimental technique. It determines the pH at which the surface charge of the sample is zero [136]. For example, Carrales-Alvarado *et al.* suggested that the adsorption of metronidazole by ACFs, multi-walled CNTs, and AC were affected by the PZC of these materials; since the surface of these materials carried different charges, under different pH conditions [137]. In this thesis, determination of the PZC of PAC can indicate the pH conditions where the surface of PAC bears different charges; and different charges on the surface of PAC may enhance or prohibit the adsorption of metaldehyde. Subsequently, it can help determine if adjusting the pH of the water samples is beneficial for removing metaldehyde.

2.7 Summary

Chapter 2 started by introducing the properties and environmental fate of metaldehyde, toxicity of metaldehyde, and the current situation of metaldehyde being detected in surface water in Section 2.2. Understanding the properties of metaldehyde is essential for this study since they determine the effectiveness of treatment methods. For example, the ring structure of the metaldehyde molecule (Table 2.1) is very stable, which makes it difficult for metaldehyde molecules to be broken down by oxidation with ozone. The low log K_{ow} value of metaldehyde (0.12 at 20°C) suggests that metaldehyde is not responsive to GAC filtration, due to its low sorption potential [47]. The properties of metaldehyde are closely related to its fate in the environment. Being highly mobile in soil and soluble in water at environmentally relevant temperatures, metaldehyde can be washed into water bodies by rainwater runoff. The toxicity of metaldehyde and relatively high concentration of metaldehyde (up to 8 $\mu\text{g L}^{-1}$) [11]

detected in surface water in the UK raised concerns. Altogether, it is important to be aware of the metaldehyde problem and develop a feasible solution.

Section 2.3 discussed common and newly developed analytical methods to determine metaldehyde in water, including GC-MS, LC-MS, and UPLC-MS-MS. After reviewing these methods and considering the cost, process, and the availability of instruments, GC-MS was selected to be used for determining the concentration of metaldehyde in water in this thesis. Monitoring metaldehyde in surface water is also significant, because treatment methods can be adjusted according to the detected concentration of metaldehyde.

Section 2.4 briefly introduced conventional water treatment methods including oxidation with ozone, AOPs by UV photolysis and $\text{H}_2\text{O}_2/\text{UV}$, and adsorption by GAC filtration for organic pollutants. This section explained why they are not effective for removing metaldehyde. Then treatment methods that may potentially be applied for removing metaldehyde were reviewed, including heterogeneous photocatalysis, adsorption by adsorbents with different characteristics, and the combination of both. Their advantages and shortcomings were discussed as well. In addition, newly developed treatment methods for removing metaldehyde were reviewed (summarised in Table 2.2). After this, the research gap of this thesis was drawn.

Table 2.2 Comparisons of treatment methods targeting metaldehyde

Researches	Materials	Methods	Comments
Autin <i>et al.</i> [29]	P25 TiO ₂ and H ₂ O ₂	Use P25 TiO ₂ and H ₂ O ₂ under UV-C irradiation	Effective but energy consumption of UV-C light could be high
Busquets <i>et al.</i> [30]	Phenolic resin derived carbon	Incubate carbon in metaldehyde solution	Effective even with the presence of organic matter but the cost could be high since the carbon is tailored
Nabeerasool <i>et al.</i> [31]	Nyex™	Adsorption and electrochemical destruction by Nyex™ with electric current	Method is effective and no waste is produced but energy consumption is high
Tang <i>et al.</i> [121]	TAML and H ₂ O ₂	H ₂ O ₂ catalysed by TAML under ambient conditions	The safety of TAML process for water treatment needs to be studied
Tao and Fletcher [32]	Macronet and ion-exchange resin	Depolymerizing metaldehyde into aldehyde by Macronet and adsorption by ion-exchange resin	Effective but reaction rate and capacity are affected by the presence of inorganic ions
Nguyen <i>et al.</i> [122]	SLGO	Modified Fenton's reactions induced by SLGO	Effective method but left degraded product in water
Rolph <i>et al.</i> [74]	Sand with active biofilm and BAC	Batch experiments	BAC is the most effective adsorbents but desorption occurred

Section 2.5 discussed the findings from the researcher's MSc project, regarding the removal of metaldehyde using C-1.5 and PAC [41]. These findings suggested that more experiments were required to observe whether the degradation of metaldehyde could be improved by using carbon modified TiO₂ nanoparticle photocatalyst; and a more in-depth study of adsorption of metaldehyde onto PAC was required as well.

Based on the literature and researches reviewed in previous sections (Section 2.2 to Section 2.5), Section 2.6 explained the techniques used in this thesis for tackling the metaldehyde problem. As discussed in Section 2.4.2 and Section 2.4.4, high cost is one of the disadvantages of heterogeneous photocatalysis. In this thesis, carbon modified TiO₂ nanoparticle photocatalysts, developed by NCL, incorporated cheap carbon (made from sugar cane leaves agro-waste) with nanoparticle TiO₂ photocatalyst. This significantly reduced the cost of synthesizing the photocatalysts. Furthermore, increased carbon content of the modified photocatalysts may potentially promote the removal of metaldehyde; the proposed adsorbent-catalyst system may lower the impacts of scavengers in surface water on the removal of metaldehyde [86]. In addition, TiO₂ modified graphene and ZnO modified graphene, developed by C-MET, were tested for removing metaldehyde as well. It was suggested by C-MET that the dosage required for initiating the photocatalytic process was very small; and the oxidation process could be induced under visible light. This could reduce the cost and energy consumption of the treatment method as well. Finally, PAC is a widely available adsorbent and it does not require a synthesis process, compared with other adsorbents, such as graphene and CNTs, which also have high SSA. Adsorption of metaldehyde onto PAC, which showed promising results in the researcher's MSc project [41] was studied in-depth in this thesis, especially from the perspective of material chemistry. Material characterization techniques, including SEM, EDX, FTIR-ATR, XPS, BET SSA analysis and PZC analysis of PAC, were performed in this thesis, aiming to explain the adsorption mechanisms of metaldehyde and link the effective adsorption of metaldehyde to the specific characteristics of PAC.

Chapter 3. Removal of metaldehyde from water by nanoparticle photocatalysts and carbon materials

3.1 Introduction

Heterogeneous photocatalysis, which applies nanoparticle photocatalysts such as TiO_2 under UV irradiation to produce hydroxyl radicals and attack organic molecules [22, 92-94], may be effective for removing metaldehyde from water. TiO_2 , as a widely studied photocatalyst, has shown promising results for removing organic pollutants from water. For instance, Chung and Chen found that azo dye Reactive Violet 5 was successfully removed using TiO_2 as photocatalyst [138]; Lin *et al.* studied the degradation of benzylparaben by TiO_2/UV [139]. Another approach for removing metaldehyde could be adsorption processes using different carbon materials. The reason why GAC cannot effectively remove metaldehyde from water may be that the characteristics of GAC are not suitable for removing metaldehyde, such as the particle size, SSA, and pore size distribution. In fact, Busquets *et al.* mentioned that pore size distribution of the adsorbent is important for removing metaldehyde, since metaldehyde prefer adsorbing onto micropores and mesopores [30]. Therefore, adsorbents, which have smaller particle sizes, larger SSA, and abundant micro-/mesopores may be effective in removing metaldehyde from water by providing more adsorption sites.

This chapter investigated the effectiveness of a number of nanoparticle photocatalysts, including carbon modified TiO_2 nanoparticle photocatalysts with carbon contents of 40% and 80% (C-40 and C-80, provided by NCL), TiO_2 modified graphene and ZnO modified graphene ($\text{TiO}_2\text{-G}$ and Zn-G, provided by C-MET), for removing metaldehyde

from aqueous solutions. The effectiveness of different carbon materials, including carbon powder made from agro-waste (CPA, provided by NCL) and activated CPA (activated in the Environmental Engineering Laboratory at UCL), for removing metaldehyde was also investigated.

The photocatalytic activity of TiO_2 for degradation of pollutants is known to be enhanced by the addition of small amounts of absorbents; for example, AC and zeolites [140]. As described in Section 2.5.1, the researcher's previous work found that C-1.5 cannot effectively remove metaldehyde; one of the explanations is that 1.5% of carbon may be low for the adsorbent-catalyst system to work synergistically. In fact, in the proposed adsorbent-catalyst system, increasing the carbon content of C-1.5 may lead to a better performance regarding the removal of metaldehyde; C-40 and C-80, developed by NCL, were therefore tested for removing metaldehyde in this chapter. In addition, CPA is a cheap adsorbent, which was made from sugar cane leaves agro-waste at NCL; after being activated, it may be effective for removing metaldehyde from water by adsorption processes. Moreover, C-MET developed TiO_2 -G and Zn-G as photocatalysts, which can be applied under visible light and hence reduce the energy input. It is noted that only a preliminary test for TiO_2 -G and Zn-G were performed in this thesis because C-MET only provided a very limited amount. The effectiveness of these novel materials for removing metaldehyde from water was compared with commercially available materials including nanoparticle TiO_2 (Degussa P25), PAC, and GAC.

The experimental investigation described in this chapter aimed to find out the most suitable material and the corresponding treatment method for removing metaldehyde. It provided data for the next stage research, which focused on investigating the most

effective material for removing metaldehyde from water in-depth. The objectives of this experimental investigation are: (1) to find out the effectiveness of all materials for removing metaldehyde - provide data to identify the most effective material; (2) to investigate the effect of UV-C light on metaldehyde removal - provide information to determine if the application of UV-C light is necessary; and (3) to further study the most effective material and treatment method regarding metaldehyde removal – provide information to the designs of experiments in the next stage.

3.2 Materials and methods

In this chapter, all the experiments and analyses were conducted in the Environmental Engineering Laboratory at UCL, unless stated otherwise. In the researches that studied the removal of metaldehyde from water, such as Busquets *et al.*, Tao and Fletcher, and the work already carried out by the author, the concentration of metaldehyde was in the 'mg L⁻¹' range, the volume of metaldehyde solution was in the 'L' range, and the dosage of adsorbent was in the 'g' range [30, 41, 69, 141]. In fact, these scales and units are widely used for investigating the removal of organic pollutants from water at a laboratorial scale. For example, the same scales and units were used in the researches of Kumar *et al.* for removing acrylonitrile from water using GAC [142], and Asha *et al.* for removing BOD from wastewater using GAC, TiO₂/UV, GAC/UV, and GAC supported TiO₂/UV system [117]. Therefore, to compare this study with these researches, the concentration of metaldehyde was studied in the 'mg L⁻¹' range (using the unit of 'mg L⁻¹'), while the material dosage was studied in the 'g' range (using the unit of 'g') in this chapter.

3.2.1 Materials

The following novel materials were developed and provided by NCL to be evaluated for their ability to remove metaldehyde from water:

- **C-40**: cetyl trimethyl ammonium bromide (CTAB) modified carbon doped titanium dioxide (C-doped TiO₂) nanoparticle photocatalyst with 40% carbon, 60% TiO₂;
- **C-80**: CTAB modified C-doped TiO₂ nanoparticle photocatalyst with 80% carbon, 20% TiO₂;
- **CPA**: carbon powder from sugar cane leaves agro-waste;
- **CPAA**: activated carbon powder from sugar cane leaves agro-waste, activated in the Environmental Engineering Laboratory at UCL.

The synthesis processes of C-40 and C-80 were the same as C-1.5, which has been previously tested for removing metaldehyde from water in the researcher's MSc project and in the study of Li *et al.*, but with different amounts of CPA and titanium butoxide [41, 69]: 7.372 g titanium butoxide and 33.818 g isopropanol were added together and stirred for 0.5 h, 5 g CTAB was added to 7 mL of laboratory grade water and isopropanol and mixed well; after that, 0.5 g urea was dissolved in the mixture and then 0.03 g CPA was added; this mixture was added into the previous butoxide solution and stirred for 24 h at room temperature; then the mixture was dried at 80 °C for 5 h and lastly calcined at 300 °C for 3 h [69].

CPA was made at NCL using the agro-waste produced by burning sugar cane leaves. CPAA was activated by treating CPA using the method suggested by NCL (the activation procedure was performed in a fume cupboard): 2.85 mL of hydrochloric acid (HCl, 32% in concentration) was measured by a 5 mL Gilson pipette (uncertainty of ±

0.05 mL) and transferred into a plastic beaker (100 mL); the HCl in the beaker was then diluted to 25 mL by adding 22.15 mL of laboratory grade ultrapure water (MilliQ water); 20 mL of MilliQ water was measured by a 50 mL graduated glass cylinder (uncertainty of ± 0.5 mL) and added to the beaker and 2.15 mL of MilliQ water was measured by a 5 mL Gilson pipette (uncertainty of ± 0.05 mL) and added to the beaker; 2 g of CPA was weighed by a scale (uncertainty of ± 0.1 mg) and added to a glass Petri dish; the diluted 25 mL HCl was added to the Petri dish as well; then the Petri dish was placed on a hot plate and the carbon-HCl mixture (in the form of a slurry) was stirred by a magnetic stirrer, until the mixture was completely dry; the dried mixture was scraped off from the bottom of the Petri dish by a glass rod, returning to a powder form; the dried powder was transferred to another glass Petri dish and it was covered by foil. The Petri dish containing the dried powder was transferred from the fume cupboard to a counter; and it was then left there for 24 h at room temperature to cool down; after 24 h, the dried powder was collected from the Petri dish and stored in a glass container.

C-MET provided newly developed modified graphene as photocatalysts to be tested for the ability to remove metaldehyde from water, including:

- **TiO₂-G**: nanoparticle TiO₂ doped graphene;
- **ZnO-G**: nanoparticle ZnO doped graphene.

These novel materials were compared with the following commercially available materials:

- **P25**: nanoparticle TiO₂, Degussa P25;
- **PAC**: powdered activated carbon;

- **GAC:** granular activated carbon.

Commercial nanoparticle TiO₂ used in this chapter was Degussa P25, a mixture of anatase and rutile in a ratio of 3:1 [143], purchased from Sigma-Aldrich. Commercial PAC used in this chapter was DARCO[®] G60, purchased from BDH laboratory supplies. Commercial GAC used in this chapter was DARCO[®], 20-40 mesh size, activated charcoal, purchased from Sigma-Aldrich.

Other materials used in this chapter include 1 g of solid metaldehyde PESTANAL (analytical grade, purchased from Sigma-Aldrich), methanol and dichloromethane (both HPLC grade, purchased from Fisher Scientific). These were used for preparing metaldehyde stock solution and calibration stock solution. Laboratory grade ultrapure MilliQ water was used, dispensed from the ultrapure water filter/dispenser, manufactured by Purolite Corporation (dispensed at room temperature). Styrene divinyl benzene polymer disposable extraction column cartridges with 200 mg solvent per column (Baker SDB 1) were purchased from Fisher Scientific. And GC-MS vials (2 mL in volume) were purchased from Perkin Elmer.

3.2.2 Material characterization techniques

The following material characterization analyses were carried out in the Chemistry Department at UCL, unless stated otherwise.

SEM images of PAC were captured with an accelerating voltage of 20 kV under secondary electron imaging mode in Korea (provided by Dr Jong Kyu Kim). SEM images of GAC were taken by JSM-6701F Field Emission Scanning Electron Microscope at 10 kV under secondary electron imaging mode.

The procedure of BET SSA analysis of PAC and GAC was performed by Dr Yuchen Yang using Autosorb-iQ2 automated gas sorption analyser (Quantachrome Instruments) via adsorption and desorption of nitrogen gas at 77 K, after PAC and GAC being degassed at 180 °C for 24 h.

3.2.3 Preparation of metaldehyde solutions

Preparation of metaldehyde stock solutions and stock calibration solutions followed the guidance of the UK Environment Agency with slight modifications; all procedures were performed in a fume cupboard and glassware was used [11].

0.1 g of metaldehyde PESTANAL was weighed by a scale (uncertainty of ± 0.1 mg) and added into a 100 mL volumetric flask (uncertainty of ± 0.1 mL). 100 mL of HPLC grade methanol was then added into the flask to make 100 mL of metaldehyde stock solution at 1000 mg L⁻¹. The flask was well shaken and left in a fridge at 5 °C for at least 24 h before use, to ensure metaldehyde was dissolved completely in methanol. The stock solution can be stored between 1-10 °C up to one year [11].

In this chapter, metaldehyde working solutions at different concentrations were diluted from the stock solution using MilliQ water. This chapter aimed to select the most effective material for removing metaldehyde from water and find out the favourable removal mechanisms of metaldehyde. Therefore, it is better to eliminate other interfering compounds in natural water that may affect the treatment processes. For example, organic compounds in natural water may react with hydroxyl radicals that are produced by the photocatalytic reactions or compete with metaldehyde for adsorption sites on the adsorbents. Here, a concentration of metaldehyde working solution at 5 mg L⁻¹ was selected to study the effectiveness of the materials including

C-40, C-80, CPA, CPAA, P25, PAC, and GAC. This is to compare with the effectiveness of C-1.5 for removing metaldehyde at 5 mg L^{-1} from water, tested in the researcher's MSc project and in the study of Li *et al.* [41, 69]. The concentration of metaldehyde working solution was lowered from 5 mg L^{-1} to 1 mg L^{-1} to study the effectiveness of TiO₂-G and ZnO-G for removing metaldehyde, due to the limited amount of TiO₂-G and ZnO-G.

Before preparing metaldehyde working solutions, metaldehyde stock solution was brought to room temperature by removing it from the fridge for 20 min, to eliminate the effect of low temperature on measuring the volume of methanol. The stock solution was also covered with foil to avoid any light. Different volumes of metaldehyde stock solution were measured and diluted by MilliQ water to prepare metaldehyde working solutions at different concentrations. For example, 5 mL of metaldehyde stock solution was measured by a 10 mL graduated glass cylinder (uncertainty of $\pm 0.1 \text{ mL}$) and added to a 1000 mL volumetric flask (uncertainty of $\pm 0.4 \text{ mL}$); MilliQ water was then added to the flask to make 1000 mL of metaldehyde working solution at 5 mg L^{-1} . And 1 mL of metaldehyde stock solution was measured by a 2 mL graduated glass pipette (uncertainty of $\pm 0.01 \text{ mL}$) with an electrical pipette controller and added to a 1000 mL volumetric flask (uncertainty of $\pm 0.4 \text{ mL}$); MilliQ water was then added to the flask to make 1000 mL of metaldehyde working solution at 1 mg L^{-1} .

Metaldehyde in water samples (aqueous phase) was extracted into dichloromethane (organic phase) via SPE, as introduced in Section 2.3.1. Hence, it was essential to prepare a set of metaldehyde calibration solutions in dichloromethane (DCM) with different concentrations as external standards, to calibrate the concentrations of metaldehyde in water samples after SPE and analysis by GC-MS.

100 mL of metaldehyde stock calibration solution at 500 mg L⁻¹ was prepared in a 100 mL volumetric flask (uncertainty of ± 0.1 mL), by dissolving 0.05 g of metaldehyde PESTANAL (weighed by a scale with the uncertainty of ± 0.1 mg) in 100 mL of DCM. It can be stored between 1-10 °C up to one year [11]. Similar to the preparation of metaldehyde working solutions, before preparing the external standards, metaldehyde stock calibration solution was brought to room temperature while being covered with foil to avoid any light. The external standards at different concentrations can be prepared by diluting the metaldehyde stock calibration solution using DCM. For example, 0.2 mL of metaldehyde stock calibration solution was measured by a 1 mL graduated glass pipette (uncertainty of ± 0.008 mL) with an electrical pipette controller and added to a glass container; 9.8 mL of DCM was measured by a 10 mL graduated glass cylinder (uncertainty of ± 0.1 mL) and added to the glass container to make 10 mL of the external standard at 10 mg L⁻¹. Subsequently, the external standards that were at lower concentrations than 10 mg L⁻¹ were diluted from the prepared 10 mL external standard at 10 mg L⁻¹ using DCM.

3.2.4 Experimental methods

All experiments described in this chapter were carried out in batch systems. The percentage removal of metaldehyde, and the adsorbed amount of metaldehyde onto PAC were calculated using the following equations [142, 144]:

$$\text{Percentage removal} = \frac{(C_0 - C_e)}{C_0} \times 100\% \quad \text{Equation 3.1}$$

$$\text{Adsorbed amount at time } (q_t) = \frac{(C_0 - C_t)V}{m} \quad \text{Equation 3.2}$$

$$\text{Adsorbed amount at equilibrium } (q_e) = \frac{(C_0 - C_e)V}{m} \quad \text{Equation 3.3}$$

Equation 3.1 describes the percentage removal of metaldehyde where C_0 is the concentration of metaldehyde solution without treatment and C_e is the final concentration of metaldehyde after treatment at equilibrium. Equation 3.2 describes the amount of metaldehyde adsorbed on PAC at a specific time (q_t), where C_t is the concentration of metaldehyde at a specific time, V is the volume of the solution containing metaldehyde, and m is the mass of PAC. Equation 3.3 is similar to Equation 3.2 where q_e is the amount of metaldehyde adsorbed on PAC at equilibrium.

3.2.4.1 Batch experiments in a photoreactor

All experiments that used C-40, C-80, CPA, CPAA, P25, PAC, and GAC to remove metaldehyde from water were performed in a batch photoreactor. The photoreactor is a rectangular box made from stainless steel with four valves installed at the bottom and top. Figure 3.1 shows a photo of the photoreactor and Figure 3.2 shows a schematic diagram of the photoreactor. In some tests, a UV lamp as the source of radiation was used. This UV lamp is a UV-C medium pressure mercury-vapour Philips lamp, of 11 W and 240 V, made in Holland. The light intensity of this lamp was 1890 lx, measured by a lux metre (Apogee, model MQ-100, serial number 1514, made in the USA). The light density of the lamp in the photoreactor was 26 mW cm⁻². The lamp was inserted vertically and mounted from the top of the reactor which enabled it to be in contact with the solution inside. The reactor was surrounded by a water-cooling jacket to prevent the sample solution from being heated by the UV-C lamp during the tests. The reactor was connected to an air source from the air tap to ensure that the material loaded into the reactor was well mixed and evenly distributed in the solution

from bottom to top inside of the reactor. Supplying air to the solution in the photoreactor may also promote oxidation reactions. The air supply was maintained at $1 \text{ cm}^3 \text{ min}^{-1}$ through an air flow metre manufactured by CT Platon. In addition, a magnetic stirrer was placed inside the reactor to stir the sample solution and ensure the material was in contact with the solution. For the experiments that used the photoreactor, the volume of metaldehyde working solution was 500 mL, the concentration of metaldehyde working solution was 5 mg L^{-1} , the material dosage was 0.1 g (i.e. the dosing concentration of material was 0.2 g L^{-1}), and the treatment time was 2 h. All sample solutions were prepared as triplicates and were filtered through MILLEX 0.22 μm syringe driven membrane filter units (manufactured by Millipore Express) at the end of the experiments, to remove the suspended solid materials in the solutions.

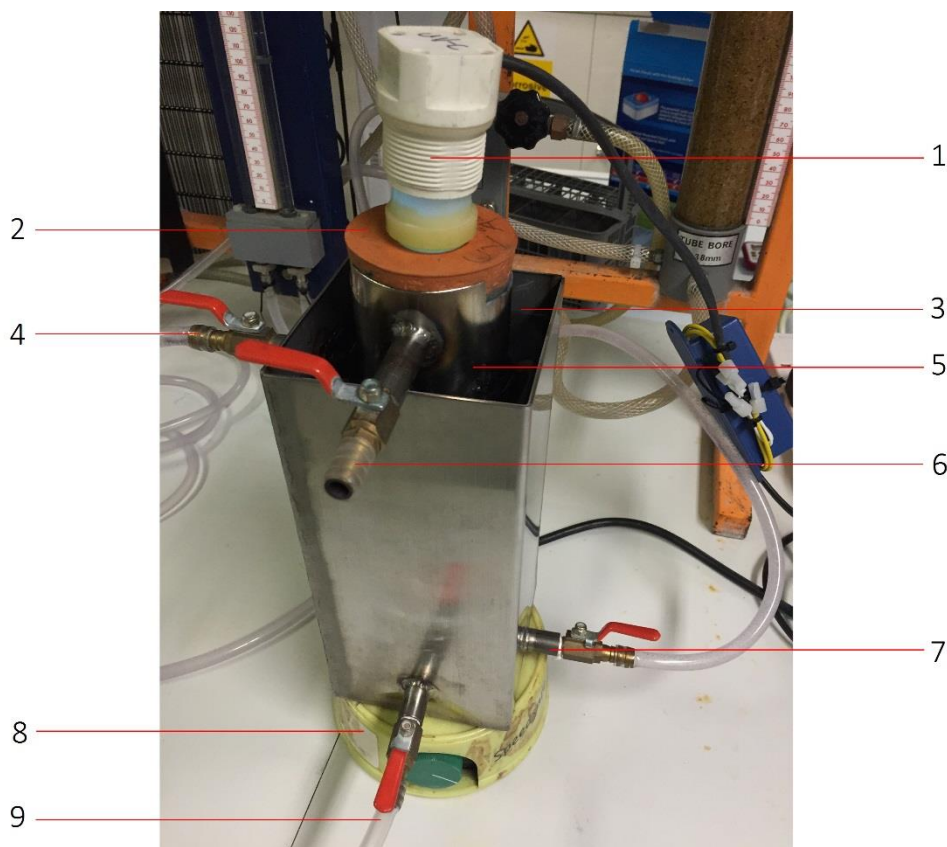


Figure 3.1 Photoreactor: 1. UV-C lamp in a quartz sleeve; 2. Rubber bung fitting at the top of the reactor, holding the UV-C lamp; 3. Water cooling jacket; 4. Opened valve on the side of the water cooling jacket connecting outflow of cooling water; 5. Central photoreactor; 6. Closed top valve connecting to the reactor; 7. Opened valve on the other side of the water cooling jacket connecting inflow of cooling water connecting from water tap; 8. Magnetic base controller; 9. Opened bottom valve connecting to air supply.

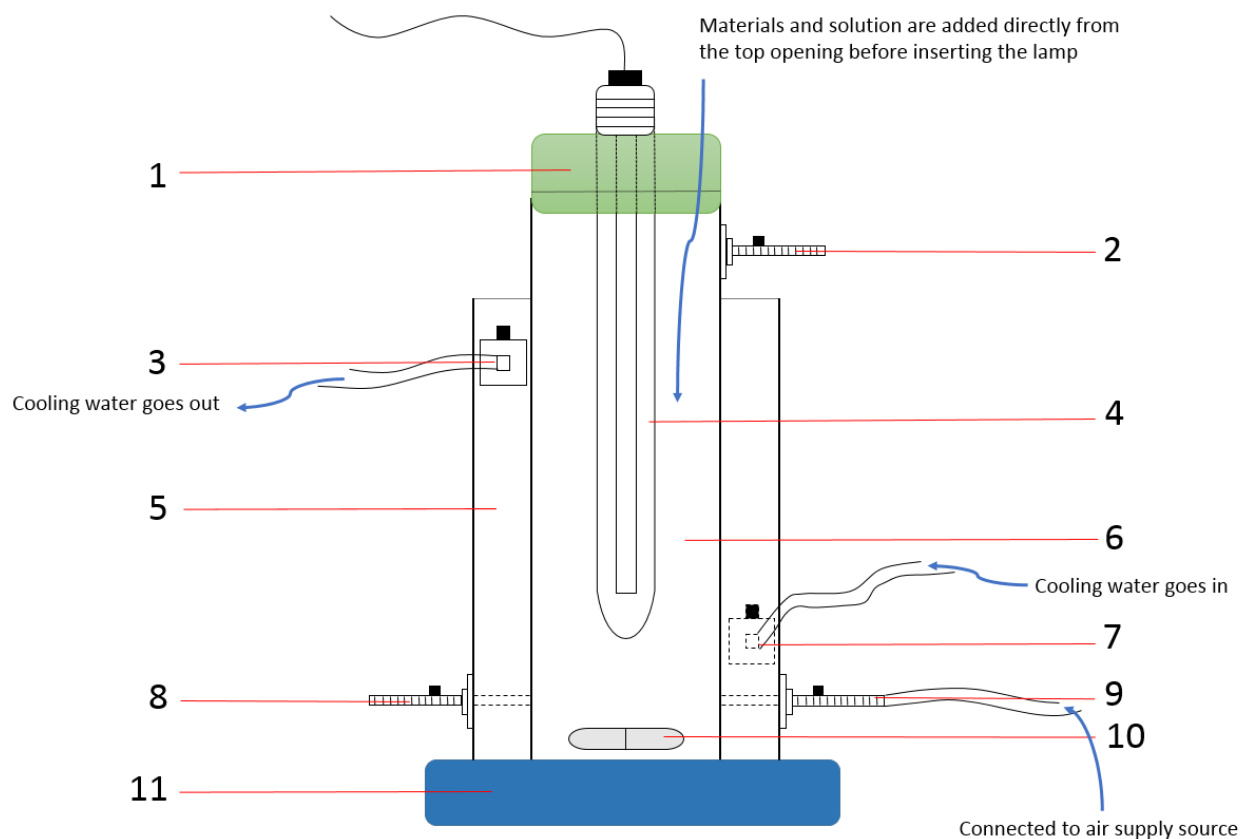


Figure 3.2 Schematic diagram of the photoreactor showing each component: 1. Rubber bung fitting at the top of the reactor, holding the UV-C lamp; 2. Closed top valve connecting to the reactor; 3. Opened valve on the side of the water cooling jacket connecting outflow of cooling water; 4. UV-C lamp in a quartz sleeve; 5. Water cooling jacket; 6. Central photoreactor; 7. Opened valve on the other side of the water cooling jacket connecting inflow of cooling water connecting from water tap; 8. Closed bottom valve connecting to the reactor; 9. Opened bottom valve connecting to air supply; 10. Magnetic stirrer; 11. Magnetic base controller.

Three sets of experiments were carried out using the photoreactor:

(1) To compare the effectiveness of C-40, C-80, CPA, CPAA, P25, PAC, and GAC for removing metaldehyde:

- UV-C light was applied in these treatments: C-40 under UV-C irradiation (C-40/UV-C), C-80 under UV-C irradiation (C-80/UV-C), P25 under UV-C irradiation (P25/UV-C); the UV-C light was applied as soon as the photocatalyst was dosed in the solution, i.e. the photocatalyst and the solution was exposed to the UV-C light for the whole treatment time;
- UV-C light was not applied in these treatments: CPA alone, CPAA alone, PAC alone, and GAC alone;
- For each treatment, the volume of metaldehyde working solution was 500 mL, the concentration of metaldehyde working solution was 5 mg L⁻¹, the material dosage was 0.1 g, and the treatment time was 2 h.

(2) To study the effect of UV-C light on the removal of metaldehyde using adsorbents including PAC and GAC:

- UV-C light was applied in all treatments: PAC under UV-C irradiation (PAC/UV-C) and GAC under UV-C irradiation (GAC/UV-C); the UV-C light was applied as soon as the adsorbent was dosed in the solution, i.e. the adsorbent and the solution was exposed to the UV-C light for the whole treatment time;
- For each treatment, the volume of metaldehyde working solution was 500 mL, the concentration of metaldehyde working solution was 5 mg L⁻¹, the material dosage was 0.1 g, and the treatment time was 2 h.

From these two experiments, the highest removal of metaldehyde was by PAC/UV-C. Therefore, the removal of metaldehyde by this treatment method was further investigated.

(3) To study the adsorption kinetics of metaldehyde in the treatment of PAC/UV-C (this adsorption kinetic study also supplemented the adsorption isotherm study in the researcher's MSc project [41]):

- For this experiment, the volume of metaldehyde working solution was 500 mL, the concentration of metaldehyde working solution was 5 mg L⁻¹, the PAC dosage was 0.1 g, and the treatment time was 2 h;
- UV-C light was applied as soon as PAC was dosed in the solution, i.e. the PAC and the solution was exposed to the UV-C light for the whole treatment time of 2 h;
- Samples were taken at 0, 5, 10, 15, 20, 30, 40, 50, 60, 90, and 120 min.

3.2.4.2 Preliminary test of removing metaldehyde from water under visible light using modified graphene

As mentioned in Section 3.2.3, the concentration of metaldehyde working solution was 1 mg L⁻¹ but a different experimental method was used for studying the effectiveness of TiO₂-G and ZnO-G for removing metaldehyde from water. This is because the amount of TiO₂-G and ZnO-G provided was very limited and they were shared among research groups in the Department of Civil, Environmental, and Geomatic Engineering. Therefore, metaldehyde working solutions at a lower concentration (1 mg L⁻¹) and a lower volume (80 mL) were prepared for this experiment in order to observe the possible removal of metaldehyde in water with a much smaller dosage of TiO₂-G and ZnO-G (16 mg), compared with other materials.

Two glass beakers (100 mL) were prepared. 80 mL of 1 mg L⁻¹ metaldehyde working solution was added to each beaker. 16 mg of TiO₂-G and 16 mg of ZnO-G were added to the two beakers respectively; and a magnetic stirrer was placed inside each beaker to help mix the solution. A visible light source (56 cm long, 18 W, 240 V General Electric white light, made in Hungary) was placed 30 cm above the surface of solutions. The visible light source has a light intensity of 14874 lx (measured by a lux metre: Apogee, model MQ-100, serial number 1514, made in the USA) and light density of 135 mW cm⁻². The treatment time was 2 h; and the visible light was applied as soon as TiO₂-G and ZnO-G were dosed in the solutions, i.e. the photocatalyst and the solution was exposed to the visible light for the whole treatment time of 2 h. It is noted that although the dosage of TiO₂-G and ZnO-G were smaller than other materials used in the experiments described in Section 3.2.4.1, the dosing concentration (0.2 g L⁻¹) was the same.

3.2.5 Analytical methods for determination of metaldehyde in water

3.2.5.1 Solid-phase extraction

In this thesis, the concentration of metaldehyde in water samples was analysed by GC-MS, as mentioned in Section 2.3.1. Therefore, solid-phase extraction (SPE), which is to extract metaldehyde from water (aqueous phase) and transfer it into DCM (organic phase), was performed for all samples prior to GC-MS analysis.

The SPE method used in this thesis followed the method used by Autin *et al.*; and it adapted the reference method proposed by the UK Environment Agency, which is suitable for using different water samples and volumes [11, 29]. J. T. Baker SPE 12G

vacuum manifold and Baker SDB 1 cartridges were used for this process. SPE was performed in a fume cupboard with the following procedures [69]:

- (1) Activation of the solvent in the cartridge: 10 mL of HPLC grade methanol (measured by a 10 mL graduated glass cylinder with the uncertainty of ± 0.1 mL) was used for washing the cartridge and the eluent was then discarded. The cartridge must not dry out during the process. It was noted that before activation, the solvent in the cartridge was dry and had a light orange colour, while after activation, the solvent in the cartridge was wet and had a dark greyish orange colour.
- (2) 2 mL of MilliQ water (measured by two 1 mL Gilson pipettes with the uncertainty of ± 0.01 mL) was added to the cartridge and the eluent was discarded. The cartridge must not dry out during the process.
- (3) 1 mL of sample solution (measured by a 1 mL Gilson pipette with the uncertainty of ± 0.01 mL) was loaded into the cartridge. The eluent was discarded.
- (4) Metaldehyde was absorbed by the solvent as soon as the sample solution was added. However, to ensure that metaldehyde was completely absorbed by the solvent, the cartridge was left for 15 min after the sample solution was added.
- (5) Another 2 mL of MilliQ water (measured by two 1 mL Gilson pipettes with the uncertainty of ± 0.01 mL) was added to the cartridge to ensure no sample solution was left on the inner wall of the cartridge. The eluent was discarded and the cartridge was dried by passing air through it via a vacuum pump. Drying the cartridge usually takes at least 45 min for the solvent to be completely dried and return to its original colour.
- (6) After the cartridge was dried, a 15 mL graduated glass vial (uncertainty of ± 0.1 mL) was placed inside the SPE vacuum manifold.

- (7) 3 mL of DCM (measured by a 10 mL graduated glass cylinder with the uncertainty of ± 0.1 mL) was added to the cartridge and the eluate was collect in the vial.
- (8) Possible residue in the cartridge was collected in the vial by passing air through the cartridge.
- (9) The vial was then removed from the SPE vacuum manifold and the eluate was reduced to 1 mL by evaporation with nitrogen gas.
- (10) Then, 1 mL of metaldehyde in DCM was obtained and transferred to a Perkin Elmer GC-MS vial by a glass micropipette and was ready to be analysed by GC-MS.

3.2.5.2 GC-MS method for determination of metaldehyde after SPE

GC-MS used in this thesis for analysing metaldehyde was Perkin Elmer precisely Clarus 500. It has an autosampler which makes injections to the chosen vials automatically, and a mass spectrometer with both a scanning mode and a selective ion monitoring mode. TurboMass is the software that controls the GC-MS. Analysed data and chromatograms can be demonstrated on a connected computer.

After SPE, the Perkin Elmer GC-MS vials containing the samples were placed into the vial holder slots, and the samples were then analysed by the GC-MS. The limit of detection (LOD) and limit of quantification (LOQ) for metaldehyde were $1.5 \mu\text{g L}^{-1}$ and $5 \mu\text{g L}^{-1}$, respectively; they were determined by analysing metaldehyde with known concentrations from $0.1 \mu\text{g L}^{-1}$ to 10mg L^{-1} , demonstrated by Li *et al.* [69, 145]. Each sample was injected and analysed three times by GC-MS to ensure constant repeatability of data. Prior to analysis of metaldehyde, DCM was injected five to ten times to ensure the analysis of consequent samples was not contaminated from any previous use of the GC-MS. The analysis conditions for detection of metaldehyde

using GC-MS in this thesis followed the method used by Salvestrini *et al.*; it was adapted from the method provided by the UK Environment Agency and was modified to optimization for the GC-MS in the Environmental Engineering Laboratory at UCL (Table 3.1) [11, 70]. The retention time of metaldehyde was 7.37 min using these conditions.

Table 3.1 GC-MS method for detection and analysis of metaldehyde

Parameters	Conditions
Carrier gas	Helium, 1 mL min ⁻¹
Column	Rxi-5ms, 30 m × 0.25 mm diameter, 1.0 µm film thickness
Injection volume	3 µL (pulsed split-less injection)
Injection temperature	180 °C
Temperature programme	Oven. Initial temperature 100 °C for 1 min, then 5 °C min ⁻¹ to 150 °C, and hold time for 1 min.
Ionization mode	Electron ionization
Selected ion recording of mass	45.0 (target) and 89.0 (qualifier)
Dwell time	0.2 s
Ionization energy	70 eV
Source temperature	200 °C

3.2.5.3 Calibration and validation of analysing metaldehyde by GC-MS

As introduced in Section 3.2.3, it is essential to calibrate the concentrations of metaldehyde in samples after SPE with a set of external standards, to validate the analytical method for detection of metaldehyde. This was done by preparing a batch

of metaldehyde sample solution in water with a known concentration and analysing this solution after SPE using GC-MS, together with the external standards.

1 mL of the metaldehyde stock solution was measured by a 2 mL graduated glass pipette (uncertainty of ± 0.01 mL) with an electrical pipette controller and added to a 1000 mL volumetric flask (uncertainty of ± 0.4 mL); MilliQ water was then added to the flask to make 1000 mL of metaldehyde sample solution at 1 mg L^{-1} . Then 1 mL of the metaldehyde sample solution at 1 mg L^{-1} was measured by a 1 mL Gilson pipette (uncertainty of ± 0.01 mL) and added into the SPE cartridge, then went through SPE, following the procedure described in Section 3.2.5.1. After SPE, metaldehyde was extracted from water into DCM. External standards were prepared with concentrations from $5 \text{ }\mu\text{g L}^{-1}$ to 10 mg L^{-1} , following the procedure described in Section 3.2.3; and 1 mL of each external standard was measured by 1 mL graduated glass pipettes (uncertainty of ± 0.008 mL) with an electrical pipette controller, and placed in the Perkin Elmer GC-MS vials. Triplicate samples were prepared to minimize performance errors and were analysed by GC-MS, together with the set of external standards. Each sample was injected and analysed by GC-MS three times to ensure constant repeatability of data.

Results from the GC-MS were presented by chromatograms and the area of integrated peaks of metaldehyde. The concentration of metaldehyde sample solution could be calculated and calibrated using the standard calibration curve (Figure 3.3). It was plotted with the concentrations of external standards on the x-axis and the integrated area of metaldehyde peaks of the corresponding external standards given by GC-MS on the y-axis. A best fit line was determined with an equation and R^2 value.

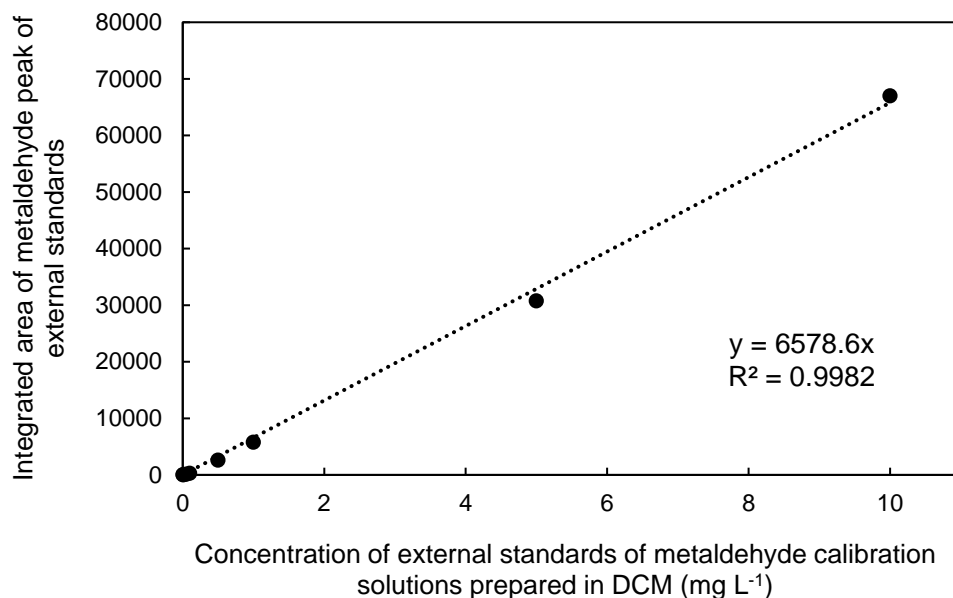


Figure 3.3 Standard calibration curve for metaldehyde detection and calibration

Based on the slope of the calibration curve (6578.6), the integrated area of metaldehyde peak of the prepared metaldehyde sample solution at 1 mg L⁻¹ after SPE can be calibrated to a corresponding concentration, demonstrated by Table 3.2. A recovery rate for the metaldehyde sample solution was calculated using Equation 3.4, [146] to determine the recovery of metaldehyde from aqueous phase to organic phase after SPE. Recovery rates are usually around 100%; they can be lower or higher because of sample loss or matrix interference during SPE and because of performance error and instrumental uncertainty. In general, the recovery rate is acceptable between 70 to 120% (average), with relative standard deviation (RSD) < 20% [147].

$$\text{Recovery rate} = \frac{\text{Measured concentration (after calibration)}}{\text{Theoretical concentration}} \times 100\% \quad \text{Equation 3.4}$$

In this case, the recovery rate of 1 mg L⁻¹ metaldehyde sample solution after SPE and GC-MS analysis was 103.4% (average) which is within the requirement of 70-120%,

with RSD of 8.7% which is also within the requirement of RSD < 20%. Hence, this analytical method for determining metaldehyde in water using GC-MS is valid.

Table 3.2 Calibration and recovery of 1 mg L⁻¹ metaldehyde sample solutions

Calibration equation	Slope	Integrated area of metaldehyde peaks of the triplicate samples			RSD of three parallel runs (%)	
$y = 6578.6x$ $R^2 = 0.9982$	6578.6	Sample 1	5429	6437	6757	9.1
		Sample 2	7026	7145	7783	4.5
		Sample 3	6870	6953	6796	0.9
Average area of nine runs				6799.56		
Measured concentration (mg L⁻¹)				1.03 ± 0.09		
Theoretical concentration (mg L⁻¹)				1		
Recovery rate (%)				103.4 ± 9		
RSD of nine runs (%)				8.7		

After validating this method, all sample solutions from the experiments (taken from the photoreactor and the beakers) were filtered using a MILLEX 0.22 µm syringe driven membrane filter unit (manufactured by Millipore Express) and went through SPE. After SPE, the samples were transferred into the Perkin Elmer GC-MS vials. The vials were then placed into the vial holder of the GC-MS and were ready to be injected by the autosampler. All samples were prepared in triplicate and each sample was injected three times by the autosampler to ensure repeatability and minimise instrumental error

(nine data points, $N = 9$). Before the injection of the samples, pure DCM was first injected five to ten times to ensure samples were not contaminated from the previous use of the GC-MS. All recovery rates of metaldehyde in this chapter were within the acceptable range of 70 to 120%, with RSD < 20%.

3.2.6 Presentation and analysis of data

All experimental data were analysed using Microsoft Excel, and they are presented with two digits after the decimal point. Percentages (%) are presented with one digit after the decimal point. Measurements after calibration are presented with standard deviation (SD) shown after the plus/minus symbol (\pm). SD is not presented if smaller than 0.01, unless stated otherwise. For regression analysis, R^2 values, slopes, and intercepts are presented with four digits after the decimal point.

3.3 Results and discussion

3.3.1 Characterizations of PAC and GAC

Characterizations of PAC and GAC were determined because they were effective in removing metaldehyde from MilliQ water. Figure 3.4 (A-D) presents the SEM images of PAC, illustrating that the average sizes of PAC particles are approximately 20-25 μm . These PAC particles are angular and their surface is flat, rough and porous. Figure 3.4 (A) gives an overview of the PAC particles with different sizes; (B) shows the angular shape of the PAC particles that have many edges; (C) demonstrates the edges of the PAC particle where adsorption processes can take place; and (D) shows the surface porous structure of the PAC particle.

Figure 3.4 (E-H) shows the SEM images of GAC, demonstrating the average sizes of the GAC particles are approximately 0.3-0.5 μm . Unlike the angular shape of PAC particles, GAC particles are more granular. Side view of a GAC particle shows a flaky, layered structure. The surface of GAC particles also shows visible macropores that have pore sizes between 50 nm and 100 μm [148]. Figure 3.4 (E) gives an overview of the GAC particles with different sizes; (F) shows the side view of a GAC particle with a layered structure, and the edges on the side of the GAC particle are potential adsorption sites; (G) demonstrates the porous surface structure of a GAC particle; and (H) shows that smaller pores are visible on a GAC particle.

Compared with the smooth and round shape of GAC, PAC has a more angular shape, which determines that it has more edges. In addition, the pore sizes of PAC are also generally smaller than GAC. And at these edges and small pores, the adsorption effects can be doubled by the van de Waals forces from both sides of the pore walls and edges [149].

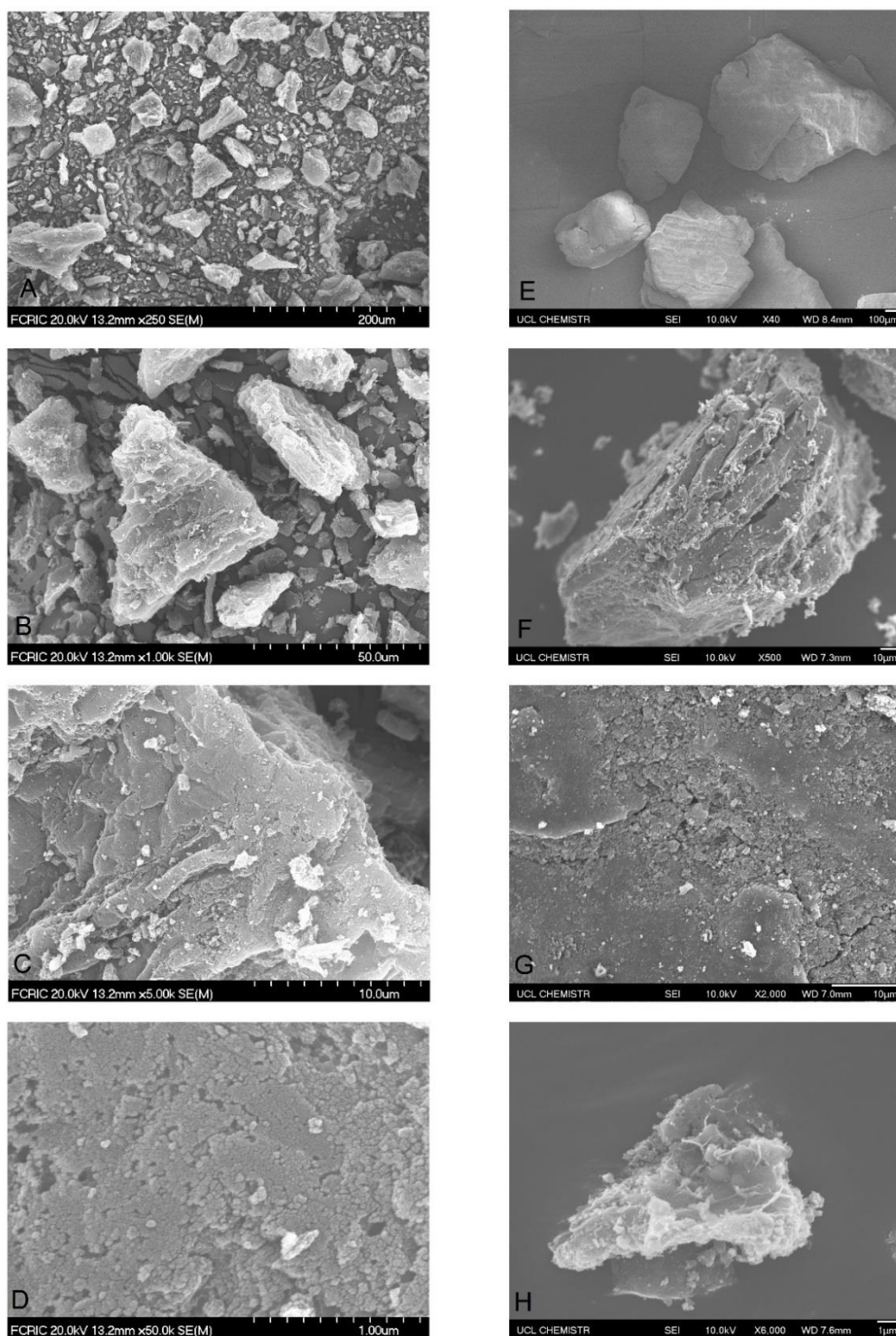


Figure 3.4 SEM images of PAC at different magnifications: (A) x 250 magnification; (B) x 1 000 magnification; (C) x 5 000 magnification; (D) x 50 000 magnification; and SEM images of GAC at different magnifications: (E) x 40 magnification; (F) x 500 magnification; (G) x 2 000 magnification; and (H) x 6 000 magnification. (SEI = secondary electron imaging mode)

BET SSA data were analysed by the software 'ASiQwin'. Figure 3.5 (A) and (B) demonstrate the nitrogen adsorption and desorption isotherms of PAC and GAC at 77 K, with relative pressure (P/P_0) on the x-axis and volume at standard temperature and pressure on the y-axis. Figure 3.5 (C) and (D) show the pore size distribution (PSD) of PAC and GAC, with pore width on the x-axis and $dV(d)$ value on the y-axis. PSD graphs demonstrate the volume increments of pores divided by the difference between the upper and lower pore size of each increment, hence showing the changes in pore volumes with variation of pore sizes [148]. PSD analysis of PAC and GAC was determined using the density functional theory methods in ASiQwin. Raw data from the BET SSA analysis of this PAC are presented in Figure A.1.1, Appendix A.1; and raw data from BET SSA analysis of this GAC are presented in Figure A.1.2, Appendix A.1.

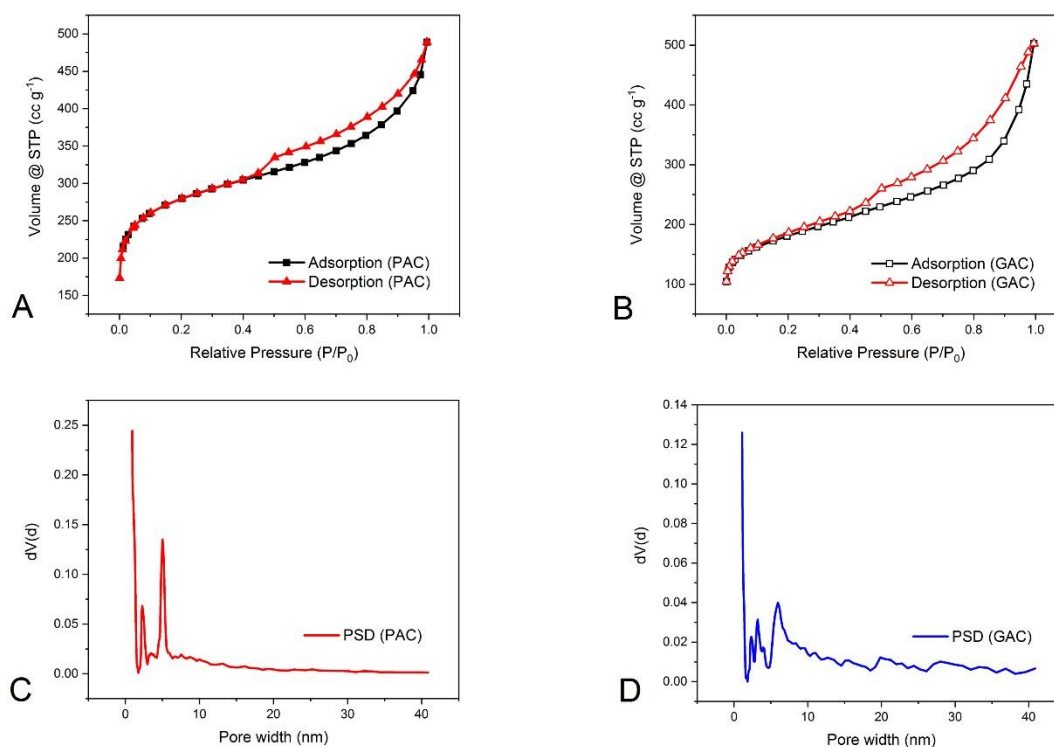


Figure 3.5 (A) Nitrogen adsorption and desorption isotherm of PAC at 77 K; (B) nitrogen adsorption and desorption isotherm of GAC at 77 K; (C) PSD of PAC; and (D) PSD of GAC (STP = standard temperature and pressure)

Table 3.3 shows the characterizations of PAC and GAC obtained from the analysis of ASiQwin. The SSA of PAC was determined by ASiQwin, using five points selected from relative pressure (P/P_0) ranging from 0.02 to 0.1 (details are included in Table A.1.1, Appendix A.1). As for GAC, the five points selected from relative pressure (P/P_0) ranging from 0.01 to 0.1 (details are included in Table A.1.2, Appendix A.1).

Table 3.3 Characterizations of PAC and GAC from BET SSA analysis

	PAC	GAC
SSA (m² g⁻¹)	1037.89 ^{XI}	649.78
Total pore volume (cm³ g⁻¹)	0.76 ^{XII}	0.77 ^{XIII}
Average pore size ^{XIV} (nm)	2.92	4.79

PAC and GAC are both dominated by micropores (< 2 nm) but PAC has a smaller average pore size. Mesopores (2 to 5 nm) are also abundant in PAC while larger mesopores (5 to 10 nm) are present in GAC. However, the amount of pores in PAC is much higher than that of GAC, which can be seen from the $dV(d)$ values in Figure 3.5 (C) and (D). The SSA of PAC is almost 1.6 times larger than that of GAC. Although PAC has more pores and a higher SSA, the total pore volume of PAC and GAC are almost the same. This is because PAC has more micropores and smaller mesopores, while GAC has more larger mesopores; these micropores and mesopores of PAC have smaller pore volume, while the larger mesopores of GAC have larger pore volume. Therefore, the total pore volume of PAC and GAC are similar.

^{XI} The PAC used in this chapter is the same as Li *et al.*, but its SSA was determined using with a different BET SSA analytical method. Li *et al.* used mercury, instead of nitrogen, for adsorption/desorption isotherm analysis, which resulted in the micropores in PAC being suppressed by mercury, hence giving a smaller SSA of 962 m² g⁻¹ [69].

^{XII} For pores smaller than 356.6 nm in diameter, determined at relative pressure 0.99460 (P/P₀)

^{XIII} For pores smaller than 358.4 nm in diameter, determined at relative pressure 0.99463 (P/P₀)

^{XIV} In diameter

3.3.2 Removal of metaldehyde from MilliQ water by nanoparticle photocatalysts and powdered and granular carbon materials

Figure 3.6 demonstrates the results of the experiments applying different treatments for removing metaldehyde under controlled conditions, including heterogeneous photocatalysis by the treatments of C-40/UV-C, C-80/UV-C, and P25/UV-C, and adsorption by the treatments of CPA alone, CPAA alone, PAC alone, and GAC alone. It is noted that the treatment of C-1.5 under UV-C irradiation (C-1.5/UV-C) and the treatment of applying UV-C light alone were tested for the removal of metaldehyde in the researcher's previous work, under the same experimental condition described in Section 3.2.4.1 [41]; these results are presented in this section as well, to compare with the results of the experiments described in Section 3.2.4.1. The prepared concentration of metaldehyde working solution (500 mL) was 5 mg L^{-1} before all treatments, while the material dosage was 0.1 g. C_0 (concentration of metaldehyde without treatment), C_{t-2h} (concentration of metaldehyde after the 2-h treatment), and percentage removal of metaldehyde are demonstrated by Table 3.4. It is essential to note that as discussed, due to the SPE process, the recovery rates of samples are acceptable within 70-120%. Hence, a treatment is considered to be effective when the percentage removal of metaldehyde is higher than 30%. Furthermore, the analysis of variance (ANOVA) single factor statistic tests were performed to determine if there were significant differences (p -values ≤ 0.05) without and after different treatments (Table 3.4).

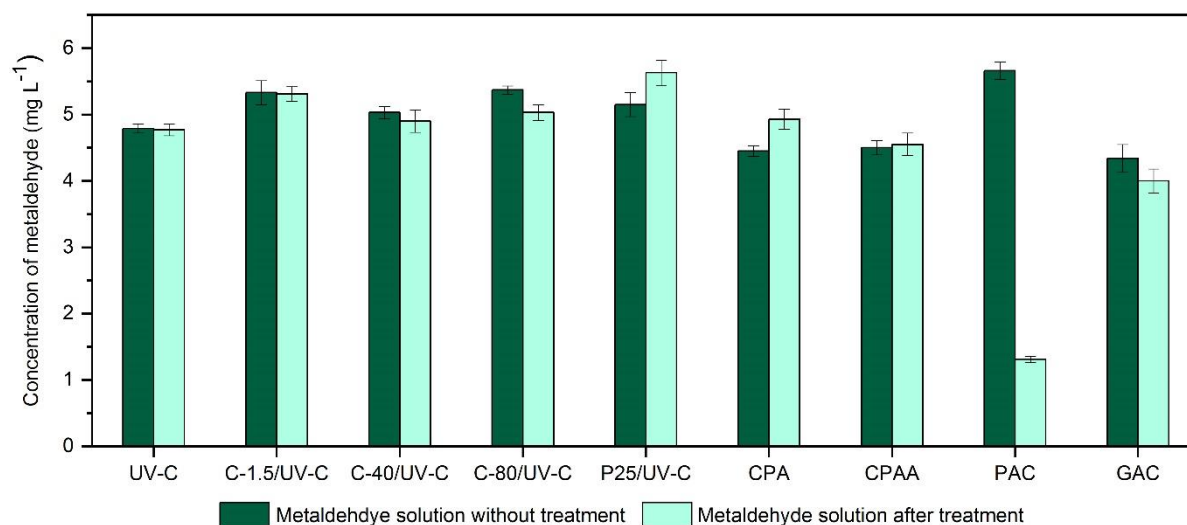


Figure 3.6 Concentrations of metaldehyde solutions without treatment and after 2-h treatment using different materials ($N = 9$, error bars showing SD)

Table 3.4 Removal of metaldehyde by different treatments ($N = 9$)

Treatment	C_0 (mg L ⁻¹)	C_{t-2h} (mg L ⁻¹)	Percentage removal of metaldehyde (%)	p -value
UV-C	4.79 ± 0.07	4.77 ± 0.09	2 ± 0.7	0.73
C-1.5/UV-C	5.33 ± 0.18	5.31 ± 0.11	3 ± 2.7	0.91
C-40/UV-C	5.03 ± 0.09	4.9 ± 0.17	5.9 ± 2.3	0.39
C-80/UV-C	5.37 ± 0.06	5.03 ± 0.12	6.4 ± 3.1	3.7E-03
P25/UV-C	5.15 ± 0.18	5.63 ± 0.19	0	N/A
CPA	4.45 ± 0.08	4.93 ± 0.15	0	N/A
CPAA	4.5 ± 0.11	4.55 ± 0.17	0	N/A
PAC	5.66 ± 0.13	1.31 ± 0.05	76.8 ± 0.9	5.15E-23
GAC	4.34 ± 0.21	4 ± 0.18	12.9 ± 4	2.85E-03

According to Figure 3.6 and Table 3.4, there were no effective removal of metaldehyde by all treatments except for PAC. The application of UV-C light alone under the studied experimental condition did not remove metaldehyde at all. Li *et al.* suggested that the 2-h treatment time and the intensity of this UV-C light may not be enough to initiate the photolytic process and degrade metaldehyde [69].

All treatments that applied photocatalysts under UV-C light showed either no removal of metaldehyde at all (C-1.5/UV-C, C-40/UV-C, and P25/UV-C) or slight removal of metaldehyde (C-80/UV-C). Similarly, this could be explained by the idea that the light intensity of the UV-C light in this experiment may not be high enough to activate these photocatalysts and initiate the photocatalytic process. In addition, the possible electron-hole recombination may prevent the generation of hydroxyl radicals. Moreover, according to the researcher's previous work and Li *et al.*, the percentage removal of metaldehyde by C-1.5/UV-C was slightly higher, when the initial concentrations of metaldehyde working solutions were higher, at 7.5 mg L⁻¹ (15.5%), 10 mg L⁻¹ (12.7%), and 12 mg L⁻¹ (6.9%) [41, 69]. However, they were still lower than 30%, which fell into the acceptable error range of recovery rate (analysis of metaldehyde by GC-MS via SPE), suggesting the removal of metaldehyde was not effective. This is because: (1) photocatalytic process is slow with low concentrations of contaminants and it may require longer treatment time than 2 h to remove contaminants effectively [150]; and (2) at high concentrations, the active sites on the surface of the nanoparticle photocatalyst could be gradually filled by metaldehyde molecules; therefore, removal of metaldehyde would be lower [69].

Increasing the carbon content of carbon modified TiO₂ nanoparticle photocatalysts from 1.5% (C-1.5) to 80% (C-80) only slightly increased the removal of metaldehyde

by less than 4% [69]. There are two possible explanations. Firstly, the carbon used in synthesizing C-1.5, C-40, and C-80 was CPA. Since CPA was not activated, it cannot contribute to significant adsorption of metaldehyde, due to the limitation of its SSA and pore volume. Secondly, since C-40 and C-80 have much higher carbon content, compared with C-1.5, quenching may occur in the system and it can inhibit the photocatalytic degradation of metaldehyde. For example, Zhong *et al.* argued the photocatalytic activity of carbon-deposited TiO₂ for removing azo dye Acid Orange 7 was affected by quenching [151]. Therefore, it is suggested by the researcher that incorporating activated carbon powder such as PAC in the synthesis of carbon modified TiO₂ nanoparticle photocatalysts may result in relatively higher removal of metaldehyde. Researches on the possible effects of quenchers in the system on removal of metaldehyde are recommended as well.

CPA and CPAA were not effective in removing metaldehyde. This could be because CPAA was chemically activated instead of being activated by steam or vapour like most commercially available AC. Therefore, the porosity, pore size distribution, and SSA of CPAA could be lower than PAC. In fact, different activation methods can significantly affect the characteristics of the AC. For instance, Chen *et al.* suggested that the SSA and microporous volume of AC (made from tobacco stem) activated by zinc chloride (ZnCl₂) is two times larger than those activated by potassium hydroxide (KOH) and potassium carbonate (K₂CO₃) [152]. Therefore, the activation method of CPAA described in Section 3.2.1 may not be suitable to produce the desired characteristics of the adsorbent that are favoured by adsorption of metaldehyde. And it is suggested by the researcher that CPA may be activated using other methods such as steam/vapour activation and BET SSA analysis should be performed for both CPA and CPAA to confirm this.

On the other hand, compared with the percentage removal of metaldehyde by GAC alone (12.9%), PAC alone removed metaldehyde by 76.8%. This suggests that adsorption by PAC is one of the favourable removal mechanisms for metaldehyde. It can be explained that the higher SSA of PAC ($1037.89 \text{ m}^2 \text{ g}^{-1}$), compared with GAC ($649.78 \text{ m}^2 \text{ g}^{-1}$), provided metaldehyde molecules with more adsorption sites. Moreover, the abundant micropores and mesopores in PAC, compared with GAC, can assist the transport of metaldehyde molecules to the active sites, promoting the adsorption of metaldehyde. Busquets *et al.* had similar findings with phenolic carbon, which demonstrated effective removal of metaldehyde with an adsorption capacity of 76 mg g^{-1} for metaldehyde solutions at 64 mg L^{-1} . Since PAC showed effective removal of metaldehyde, the treatment of PAC/UV-C was investigated for removing metaldehyde, to determine the effect of UV-C light on the removal of metaldehyde using PAC. Adsorption of metaldehyde by the treatment of GAC/UV-C was studied as well, to compare with PAC/UV-C.

As for the preliminary test of $\text{TiO}_2\text{-G}$ and ZnO-G , no removal of metaldehyde was observed at all. It is highly likely that the small amount of $\text{TiO}_2\text{-G}$ and ZnO-G applied in the system cannot remove metaldehyde. Unfortunately, the amount of $\text{TiO}_2\text{-G}$ and ZnO-G was limited to perform more tests. Therefore, if available, a higher dosage of $\text{TiO}_2\text{-G}$ and ZnO-G is recommended for removing metaldehyde. Additionally, although it was suggested by C-MET that the energy from visible light could be enough to initiate the photocatalytic process, light sources with higher energy may be required.

3.3.3 Effect of UV-C light on the removal of metaldehyde by PAC and GAC

Figure 3.7 presents the results of the experiments that incorporated UV-C light to remove metaldehyde from MilliQ water using adsorbents including PAC and GAC ^{XV}. The prepared concentration of metaldehyde working solutions (500 mL) for the experiments was 5 mg L⁻¹ before all treatments; the material dosage was 0.1 g; the treatment time was 2 h. In the treatment of PAC/UV-C and GAC/UV-C, UV-C light was applied as soon as the adsorbent was dosed into the solution; the adsorbent was exposed to the UV-C light for the whole treatment time. C_0 , $C_{t=2h}$, and percentage removal of metaldehyde are demonstrated by Table 3.5.

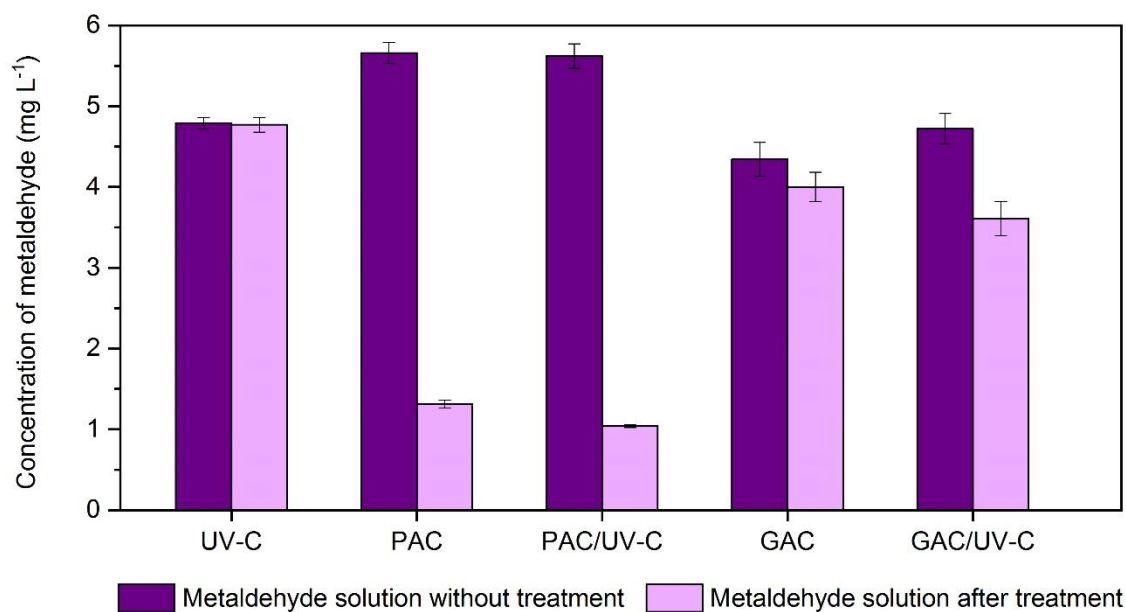


Figure 3.7 Concentrations of metaldehyde solutions without treatment and after 2-h treatment by UV-C, PAC, PAC/UV-C, GAC, and GAC/UV-C ($N=9$, error bars showing SD)

^{XV} The result of the experiment of applying UV-C light alone to remove metaldehyde, which was tested in the researcher's previous work [41], is included in Figure 3.7, to compare with the results of the experiments described in Section 3.2.4.1.

Table 3.5 Removal of metaldehyde by UV-C, PAC, PAC/UV-C, GAC, and GAC/UV-C ($N = 9$)

Treatment	C_0 (mg L ⁻¹)	C_{t-2h} (mg L ⁻¹)	Percentage removal of metaldehyde (%)	p -value
UV-C	4.79 ± 0.07	4.77 ± 0.09	2 ± 0.7	0.73
PAC	5.66 ± 0.13	1.31 ± 0.05	76.8 ± 0.9	5.15E-23
PAC/UV-C	5.62 ± 0.15	1.04 ± 0.02	81.4 ± 0.6	7.88E-23
GAC	4.34 ± 0.21	4 ± 0.18	12.9 ± 4	2.85E-03
GAC/UV-C	4.72 ± 0.19	3.61 ± 0.21	24.8 ± 4.9	2.96E-07

As discussed in Section 3.3.2, UV-C light alone cannot degrade metaldehyde under the studied experimental condition. This is possibly due to the 2-h treatment time not being long enough for photolysis to degrade metaldehyde; and the light intensity of the UV-C light used may not be high enough for initiating photolytic process. In fact, the light intensity may not even be high enough for activating the photocatalysts, including C-40 and C-80, as mentioned in Section 3.3.2. On the other hand, the removal mechanism of metaldehyde seems to favour adsorption more. As discussed in Section 3.3.2 and demonstrated in Table 3.5, 12.9% of metaldehyde was removed using GAC alone and 76.8% of metaldehyde was removed using PAC alone.

Higher removal of metaldehyde was observed in both PAC/UV-C and GAC/UV-C, compared to PAC alone and GAC alone. Although the improvement was not significant, it is suggested that the possible adsorption-oxidation system in the treatments of PAC/UV-C and GAC/UV-C may enhance the removal of metaldehyde. Interestingly, the removal of metaldehyde by PAC/UV-C was only slightly more effective (by 4.6%)

than PAC alone, while the removal of metaldehyde by GAC/UV-C increased by 11.9%, compared to GAC alone. Other researches showed similar findings; for example, Asha *et al.* reported that combining UV light with GAC treatment increased the removal efficiency of total solid concentration, total volatile solids, and BOD from wastewater by more than 50% [117]; and Velasco *et al.* argued that the photon-carbon interaction can reach the adsorbed phenol molecules in the pores of AC and promote degradation [153].

Based on the photochemical behaviour of AC under UV irradiation proposed by Velasco *et al.* [153], there are two possible explanations for the slightly higher removal of metaldehyde by PAC/UV-C and GAC/UV-C (possible adsorption-oxidation). Firstly, metaldehyde molecules are adsorbed onto the surface of PAC and GAC; and the concentration of metaldehyde becomes much higher on the surface of PAC and GAC. Photochemical reactions are then faster with a higher concentration of contaminants [150, 153]. Therefore, with a higher concentration of metaldehyde molecules adsorbed on the surface of PAC and GAC, the 2-h treatment time may be long enough for photolysis to degrade some of the adsorbed metaldehyde molecules.

Secondly, Velasco *et al.* stated that when AC is illuminated by UV irradiation, the interaction between photon and carbon occurring at the surface of the AC can promote the generation of charge carriers (electrons and holes); and the charge carriers can reach the adsorbed molecules inside the pores [153]. In this case, these charge carriers can migrate and reach the adsorbed metaldehyde molecules inside the pores of PAC and GAC. According to Velasco *et al.*, the photogenerated carriers have enough redox potential to directly degrade the adsorbed pollutant; and they can also generate hydroxyl radicals to break down the adsorbed pollutant, since water

molecules are also adsorbed/trapped in the pores of AC [153]. Therefore, in this case, adsorbed metaldehyde molecules on the pores of PAC and GAC can be degraded via the oxidation reactions induced by these charge carriers, as demonstrated by Figure 3.8.

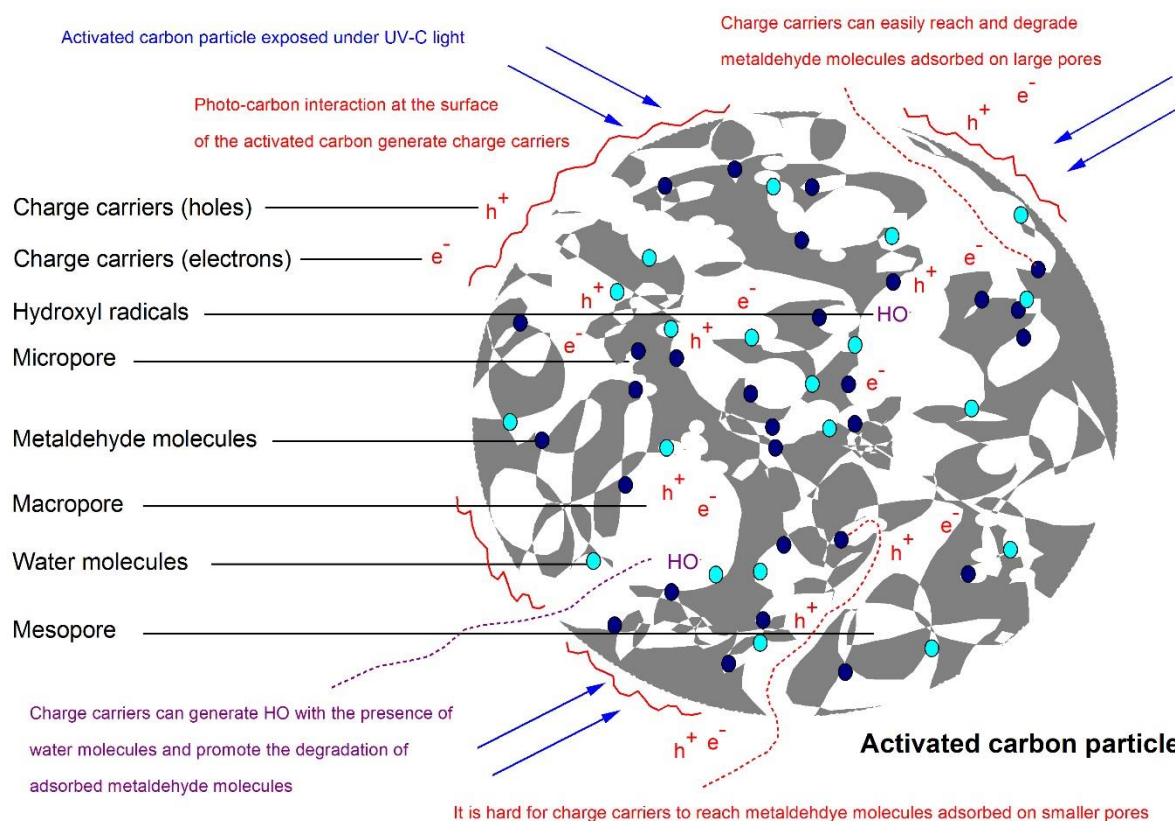


Figure 3.8 The proposed adsorption-oxidation system in the treatment of applying activated carbon particles under UV-C light for removing metaldehyde (navy dots = metaldehyde molecules; teal dots = water molecules)

In addition, the proposed adsorption-oxidation system can also explain the results in Table 3.5. The percentage removal of metaldehyde by GAC/UV-C increased by 11.9% compared with GAC alone, while the percentage removal of metaldehyde by PAC/UV-C increased only by 4.6% compared with PAC alone. Since the photogenerated carriers can reach the adsorbed metaldehyde molecules on the pores of PAC and GAC, they would have easy access to the outer surface and large pores (such as

macropores and large mesopores) of PAC and GAC, while the access to micropores is relatively less direct. Therefore, the adsorbed metaldehyde molecules on these large pores would be degraded, prior to the ones adsorbed on micropores. As discussed in Section 3.3.1, GAC has more large pores than PAC; therefore, the application of UV-C promoted the removal of metaldehyde in GAC/UV-C (11.9%) more than PAC/UV-C (4.6%).

Although the addition of UV-C light did not significantly improve the removal of metaldehyde by PAC, PAC/UV-C was still the most effective treatment to remove metaldehyde. Therefore, the adsorption kinetic of PAC/UV-C was further investigated. This adsorption kinetic study would also complete the adsorption isotherm study in the researcher's MSc project [41].

3.3.4 Adsorption kinetic study of PAC under UV-C light

PAC was effective for removing metaldehyde in Section 3.3.1 and Section 3.3.2; and it was the most effective material studied so far. 76.8% of metaldehyde was successfully removed by PAC alone. A set of experiments was further performed using 500 mL of 5 mg L⁻¹ metaldehyde working solution and 0.1 g PAC with a 2-h treatment time under UV-C light. UV-C light was applied as soon as PAC was dosed into the solution; PAC was exposed to the UV-C light for the whole time in the 2-h treatment time. Samples were taken at 0, 5, 10, 15, 20, 30, 40, 50, 60, 90, and 120 min. PAC dosage for this experiment was 0.1 g because after the 2-h treatment, metaldehyde needs to be detected by GC-MS, in order to complete the kinetic study. Figure 3.9 demonstrates the variation of metaldehyde concentration and the amount of metaldehyde adsorbed onto PAC under UV-C light (q_t) with time.

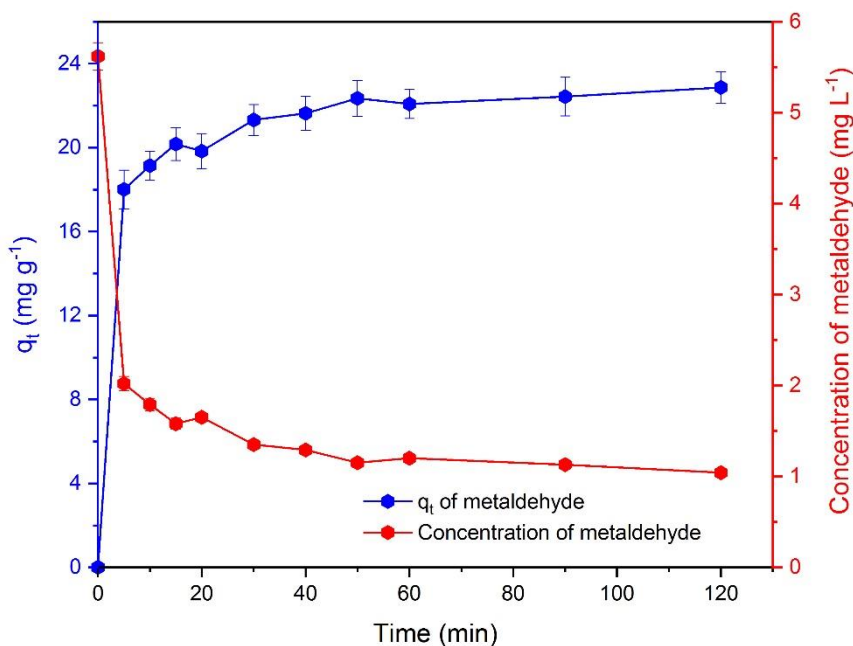


Figure 3.9 Removal of metaldehyde in the 2-h treatment using PAC under UV-C light ($N = 9$, error bars showing SD)

At 5 min, the removal of metaldehyde already achieved 64.1% with q_{t-5min} of 18.01 mg g⁻¹, indicating that at the very beginning of the reaction, the adsorption efficiency of PAC under UV-C light was at its highest. For a 2-h treatment time, the removal of metaldehyde plateaued from 30 to 120 min, with a total percentage removal of 81.4% and q_{t-2h} of 22.87 mg g⁻¹, suggesting PAC was being gradually saturated with metaldehyde and reached equilibrium ($q_{t-2h} = q_e = 22.87$ mg g⁻¹). q_e of 22.87 mg g⁻¹ in this experiment is higher than the q_{t-2h} of 21.75 mg g⁻¹ obtained from the experiment of using PAC alone in Section 3.3.3 (in which the concentration of metaldehyde decreased from $C_0 = 5.66$ mg L⁻¹ to $C_{t-2h} = 1.31$ mg L⁻¹). This suggests a slightly higher adsorption capacity of PAC for metaldehyde under UV-C light. This can be explained by the proposed adsorption-oxidation system in the treatment of PAC/UV-C. As discussed in Section 3.3.3, under UV-C light, the photo-carbon interaction generates charge carriers such as electrons and holes, which can migrate in the pores of PAC

[153]. These charge carriers will reach and degrade the adsorbed metaldehyde molecules on the pores of PAC. After this, the adsorption sites on the pores of PAC, which used to be occupied, will open up again for adsorbing more metaldehyde molecules in water. In this system, the adsorption and oxidation process take place simultaneously. Therefore, the adsorption capacity of PAC for metaldehyde under UV-C light was slightly higher, compared with PAC alone, benefiting from the degradation of adsorbed metaldehyde molecules by the photogenerated charge carriers.

To study the adsorption kinetic of PAC under UV-C light for removing metaldehyde, the pseudo-first order and pseudo-second order equations were used as they are the most common kinetic models for adsorption. The pseudo-first order model, according to Lagergren, assumes the adsorption rate is proportional to the difference of adsorbate adsorbed at equilibrium (q_e) and at time (q_t), shown by Equation 3.5; k_1 is the pseudo-first order kinetic rate constant and t is the time [154].

$$\frac{dq_t}{dt} = k_1(q_e - q_t) \quad \text{Equation 3.5}$$

Take the log value of each side, Equation 3.5 can be linearized into Equation 3.6:

$$\ln(q_e - q_t) = \ln q_e - k_1 t \quad \text{Equation 3.6}$$

To fit the experimental data in Figure 3.9 to Equation 3.6, $\ln(q_e - q_t)$ was plotted against time with a slope of $-k_1$ and intercept of $\ln q_e$ (Figure 3.10).

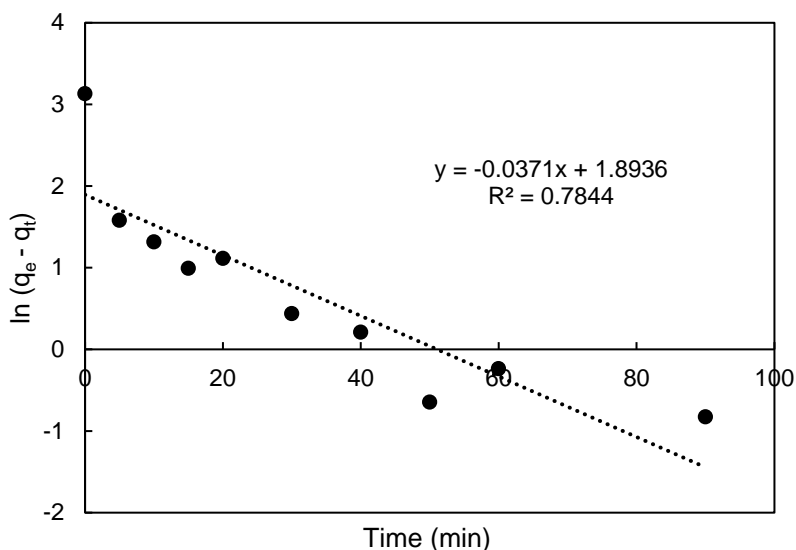


Figure 3.10 The pseudo-first order kinetic model

The R^2 value of 0.7844 suggests that the experimental data were not well fitted to the pseudo-first order model. The intercept of 1.8936 which represents $\ln q_e$ gives a theoretical q_e value of 6.64 mg g^{-1} . Nevertheless, this theoretical value cannot match to the experimental q_e value of 22.87 mg g^{-1} obtained from the experiment, which confirms that this model is not suitable. However, compared with the study of Salvestrini *et al.*, in which GAC has a k_1 value of 0.45 h^{-1} with a R^2 value of 0.87, the k_1 obtained in this section is $3.71 \times 10^{-2} \text{ min}^{-1}$, which is 2.23 h^{-1} , almost five times higher; this suggests PAC under UV-C light is more efficient than the GAC used by Salvestrini *et al.* regarding the removal of metaldehyde [70].

The experimental data were also fitted to the pseudo-second order model. According to Ho and McKay, the pseudo-second order model assumes the adsorption capacity is proportional to the number of active sites on the adsorbent that are occupied by the adsorbate [155]. It also assumes that the rate-limiting step in the system may be due to surface reactions that include chemisorption (such as valence forces) and physical interactions (such as van der Waals forces) [155, 156]. Therefore, in this case, the

important components of the reaction are the interactions between metaldehyde molecules and the surface of PAC. Equation 3.7 was given by Ho and McKay in a differential form, where k_2 is the pseudo-second order kinetic rate constant [155]:

$$\frac{dq_t}{dt} = k_2(q_e - q_t)^2 \quad \text{Equation 3.7}$$

And it can be integrated into Equation 3.8:

$$q_t = \frac{k_2 t q_e^2}{1 + k_2 t q_e} \quad \text{Equation 3.8}$$

Equation 3.8 can be transferred into Equation 3.9:

$$\frac{t}{q_t} = \frac{1}{k_2 q_e^2} + \left(\frac{1}{q_e}\right) t \quad \text{Equation 3.9}$$

To fit the data to Equation 3.9, t/q_t was plotted against time and from which a theoretical q_e and k_2 were calculated (Figure 3.11).

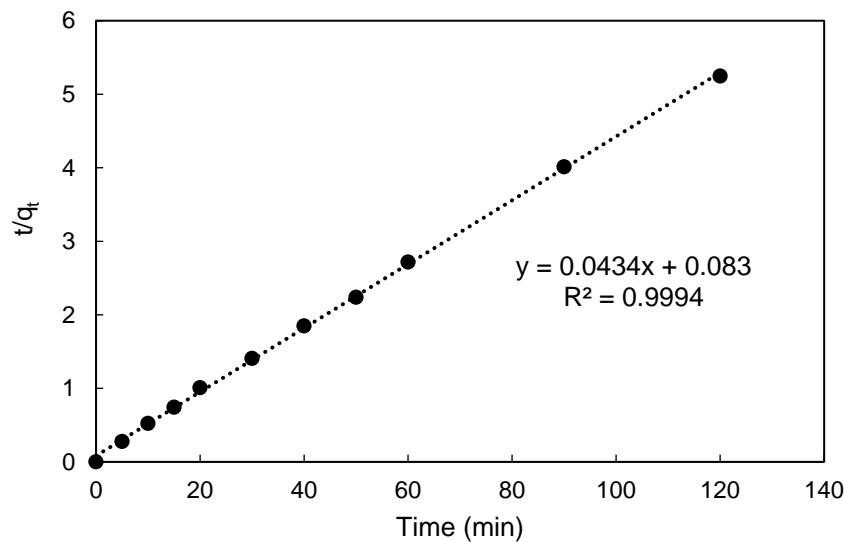


Figure 3.11 The pseudo-second order kinetic model

The R^2 value of 0.9994 suggests that the data were very well fitted to the pseudo-second order model. The slope of $1/q_e$ is 0.0434, giving the theoretical value of $q_e = 23.04 \text{ mg g}^{-1}$. This value is very close to the value obtained in the experiment, again, confirming that data were well fitted. From the intercept (0.083) and the slope (0.0434), the k_2 is determined as $0.02 \text{ g mg}^{-1} \text{ min}^{-1}$, using Equation 3.9. Compared to the k_2 value ($8 \times 10^{-5} \text{ g mg}^{-1} \text{ min}^{-1}$) of the GAC studied by Salvestrini *et al.*, the treatment of PAC/UV-C in this experiment was approximately 288 times more efficient than the GAC used by Salvestrini *et al.* for removing metaldehyde [70]. The relatively high reaction kinetic (k_2) can be explained by fast interactions between metaldehyde molecules and the surface of PAC. Metaldehyde can be adsorbed onto the micropores of PAC with abundant mesopores facilitating the transport, which speed up the adsorption kinetic [30]. It also benefits from the synergistic adsorption-oxidation system of PAC/UV-C, since oxidation process can take place at the same time as adsorption, prompting the reaction kinetic.

Table 3.6 compares the characteristics of the PAC used in this experiment and the experimental results in this chapter regarding the removal of metaldehyde with other studies.

Table 3.6 Comparison of PAC used in this study with other adsorbents to remove metaldehyde

Researches	Adsorbent	q_m (mg g ⁻¹)	SSA (m ² g ⁻¹)	k_1 (min ⁻¹) or k_2 (g mg ⁻¹ min ⁻¹)
This chapter	PAC	32.26 [69]	1037.89	$k_2 = 0.02$
Busquets <i>et al.</i> [30]	GAC	15	500	N/A
	Tailored phenolic resin-derived carbon	76	2000	N/A
Nabeerasool <i>et al.</i> [31]	Nyex™	0.018	N/A	N/A
Salvestrini <i>et al.</i> [70]	GAC	320	774	$k_2 = 8 \times 10^{-5}$
Tao and Fletcher [32, 141]	GAC	71	560	$k_2 = 5.8 \times 10^{-4}$
	Macronet	200	402	$k_1 = 11.6 \times 10^{-3}$
	Ion-exchange resin	441	N/A	$k_2 = 0.17$

Table 3.6 indicates that removal of metaldehyde by adsorption processes onto PAC is a complex mechanism, and the effectiveness and efficiency depend very much on the treatment material. For example, the study of Tao and Fletcher stated the GAC used has the adsorption capacity of 71 mg g⁻¹, which is almost 5 times higher than the 15 mg g⁻¹ capacity of the GAC used by Busquets *et al.*. However, the SSA of the two GAC do not differ that much (560 m² g⁻¹ and 500 m² g⁻¹ respectively) [30, 141]. This suggests that adsorption capacity of materials is not strictly relevant to their SSA; more factors such as PSD need to be taken into consideration.

Moreover, the adsorption capacity of PAC used in this chapter for metaldehyde was 32.26 mg g^{-1} , which is not as high as the GAC used by Tao and Fletcher, and Salvestrini *et al.*. However, this PAC was effective and much more efficient in removing metaldehyde, with a reaction rate 288 times higher than that of Salvestrini *et al.* and 40 times higher than that of Tao and Fletcher [69, 70, 141]. This implies that high adsorption capacity does not necessarily mean high adsorption rate. In addition, the adsorption rate of metaldehyde is not related to the SSA of the adsorbent as well. The GAC used by Salvestrini *et al.* has a high SSA of $774 \text{ m}^2 \text{ g}^{-1}$, but the adsorption rate is more than 7 times lower than the GAC used by Tao and Fletcher [70, 141]. Busquets *et al.* also suggested that regarding the removal of metaldehyde by adsorption processes, PSD of the adsorbent seems to affect the adsorption capacity more than SSA [30]. Therefore, it would be beneficial to investigate the adsorbent from the perspective of material chemistry. Material characterization techniques including BET SSA analysis are helpful for linking the characteristics of the adsorbent to the adsorption of metaldehyde, and explaining the adsorption mechanisms.

3.4 Summary

Among all the studied materials, PAC was the most effective material for removing metaldehyde in MilliQ water with the studied concentration of metaldehyde working solution (500 mL) at 5 mg L^{-1} , the dosage of PAC at 0.1 g, and the treatment time of 2 h, with and without UV-C light. This could be explained by its large SSA of $1037.89 \text{ m}^2 \text{ g}^{-1}$ which offers more adsorption sites for metaldehyde and its abundant micropores and mesopores could be favoured by metaldehyde adsorption. Data were very well fitted to the pseudo-second order kinetic model with a k_2 value of $0.02 \text{ g mg}^{-1} \text{ min}^{-1}$, indicating PAC can remove metaldehyde efficiently in a short period of time. PAC

alone removed 76.8% metaldehyde, while it can remove more than 81.4% under UV-C light.

Compared to PAC, C-40/UV-C, P25/UV-C, CPA, CPAA, and GAC showed no removal of metaldehyde while C-80/UV-C was not effective in removing metaldehyde (6.4%). The increased carbon content in C-40 and C-80, compared with C-1.5, only slightly promoted the removal of metaldehyde (less than 7%). GAC/UV-C increased removal of metaldehyde by 11.9%, compared to GAC alone.

To conclude, 76.8% of metaldehyde was removed by PAC alone, under the studied experimental condition in this chapter. Nevertheless, PAC would work slightly more effectively (by 4.6%) under UV-C light. However, considering the energy consumption, PAC alone is a cheaper and more effective solution than PAC/UV-C. Regarding the application of photocatalysts for removing metaldehyde from water via photocatalytic process, it is suggested that more parameters including the light intensity, the pH of metaldehyde working solution, the treatment time, and the material dosage need to be investigated further, to develop an effective treatment method.

This thesis chose to continue the investigation of removing metaldehyde from water by adsorption onto PAC without any additional light source, since PAC alone was effective and efficient for removing metaldehyde from water. Moreover, Suffet discussed that PAC costs even less than GAC and its application in drinking water treatment can be economically justified [157]. Therefore, compared with the photocatalysts used in this chapter, PAC may be more economically available and be applied at drinking water treatment plants, which is significant as it may be a potential feasible solution to the metaldehyde problem.

Chapter 4. The impact of humic acid on metaldehyde adsorption onto PAC in aqueous solutions

4.1 Introduction

Results from Chapter 3 showed that PAC alone can effectively and efficiently remove metaldehyde from MilliQ water, compared with the nanoparticle photocatalysts studied in Chapter 3. However, it is important to not only investigate the adsorption mechanisms of metaldehyde onto PAC, but also understand the effect of background organic matters on adsorption of metaldehyde onto PAC. In fact, according to Xia *et al.*, NOM is ubiquitous in drinking water sources such as surface water [158]. Therefore, since metaldehyde often enters surface water bodies via soil and runoff, it can be associated with NOM. NOM is a generic term for a heterogeneous mixture of organics, but the primary source of NOM in the environment are humic substances [159]. Humic substances, including humic acid (HA), fulvic acid, and humin, are mixtures of materials, formed via biochemical reactions from decay of plants and microbial remains; humic substances give the light brown colour to natural water [160, 161].

In fact, Radian and Mishael argued that interactions between pollutants and NOM such as HA are significant concerning the fate of pollutants in the environment and in water treatment processes [162]. NOM also affects adsorbents such as GAC and PAC regarding removal of organic micropollutants. For example, Zadaka *et al.* indicated that the removal of atrazine (the most commonly-used herbicide) from water by GAC was reduced by 20% with the presence of NOM [163]. Matsui *et al.* showed that the adsorption capacity of PAC could be significantly affected by the presence of NOM

[33]. Presence of NOM has negative effects on removal of metaldehyde as well. For example, Autin *et al.* claimed that NOM molecules would block the active sites of the photocatalyst, and subsequently inhibit the degradation process of metaldehyde; they argued that the presence of background organic matter would affect the adsorption even more than oxidation [29]. Moreover, Nabeerasool *et al.* stated that the removal efficiency of metaldehyde by electrochemical processes using novel adsorbents was reduced in peat water samples that contain high NOM, due to competition for active binding sites [31]. Hence, the presence of background organic matter may have impacts on adsorption processes of metaldehyde onto PAC.

This chapter investigated the adsorption of metaldehyde onto PAC with and without the presence of background organic matter, with a controlled study including adsorption of only organic matter onto PAC. Specifically, HA was selected to represent NOM in this study, since it is not only a significant component of NOM but also a common contaminant in surface water [162]. In the environment, HA accounts for 50-90% of organic matter in surface water and the typical concentration of HA is usually in the range of 0.1 to 20 mg L⁻¹ [144, 164]. Removal of HA in the water treatment processes is also significant because the residue of HA could lead to the formation of disinfection by-products, such as trihalomethanes; there have been evidences of close links between the exposure to disinfection by-products and cancers of organs in the human body [165]. For example, Morris *et al.* suggested there is a positive relationship between consuming water containing disinfection by-products and bladder and rectal cancer in the human body [166]; and Font-Ribera *et al.* specifically stated that exposure to trihalomethanes in drinking water is associated with an increased risk of bladder cancer in the human body [167].

HA is a distribution of coagulated organic macromolecules with an acidified strong-base extract [168]. HA mainly contains a number of functional groups including phenolic and carboxylic groups, but the chemical composition of HA can be different, depending on the geographic origin, climate, and biological conditions, with a variation of molar mass from 2000 to 1300 000 g mol⁻¹ [169]. Figure 4.1 demonstrates a hypothetical model structure of HA, including phenolic, carboxylic acid, enolic, quinone, and ether functional groups, sugars, and peptides [169].

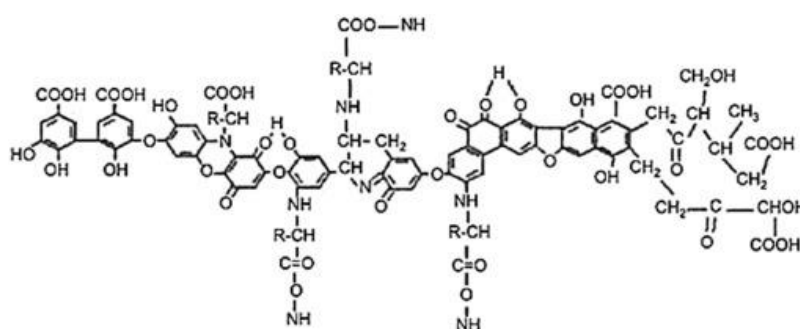


Figure 4.1 Model structure of HA (figure reproduced with permission of the rights holder, Elsevier) [169]

Since HA is an aggregation of molecules and its natural chemical composition can be different, it is argued by de Melo *et al.* that the precise characterization of HA in water is difficult [169]. Therefore, humic acid sodium salt (HA in its sodium salt form) is commonly used in researches that investigate HA. It has a molecular formula of C₉H₈Na₂O₄, a molecular weight of 226.14 g mol⁻¹, and its CASRN is 68131-04-4. Humic acid sodium salt is a commercially available chemical compound with a fixed chemical composition; therefore, it can be precisely characterized and analysed. For example, Kim *et al.* used humic acid sodium salt in their study of degradation of HA by photocatalytic reactions using nano-sized ZnO/laponite composite [93]. And Han *et al.* used humic acid sodium salt in their study of removing ibuprofen, boron, and

arsenic in the presence of HA using membrane distillation [170]. Hence, humic acid sodium salt was used in this thesis as well.

This chapter aimed to study closely the single and binary adsorption systems of metaldehyde and HA onto PAC, which contribute to the potential application of PAC in drinking water treatment plants. Mono-component solutions containing either only metaldehyde or only HA were used for the single adsorption system study. And multi-component solutions containing both metaldehyde and HA were used for the binary adsorption system study. The specific objectives of this chapter are: (1) to investigate the effect of PAC dosage, time, and pH on the adsorption of metaldehyde onto PAC in the single adsorption system; (2) to study the effect of PAC dosage and time on the adsorption of HA onto PAC in the single adsorption system; (3) to evaluate the adsorption of metaldehyde onto PAC in the binary adsorption system with the presence of HA, including varying the concentration of HA and adsorption time.

4.2 Materials and methods

In this chapter, all the experiments and analyses were conducted in the Environmental Engineering Laboratory at UCL, unless stated otherwise. As explained in Section 3.2, the concentrations of metaldehyde and HA were studied in the 'mg L⁻¹' range (using the unit of 'mg L⁻¹'), while PAC dosage was studied in the 'g' range (using the unit of 'g') in this chapter.

4.2.1 Materials

PAC used in this chapter was activated charcoal, DARCO® G60, 100 mesh particle size powder, purchased from Sigma-Aldrich. This PAC is different from the PAC used

in Chapter 3 because BDH laboratory supplies stopped supplying DARCO® G60. Therefore, PAC used in this chapter was purchased, since it bears the same trademark of DARCO® G60. Metaldehyde PESTANAL (analytical grade) and humic acid sodium salt (technical grade H16752) were also obtained from Sigma-Aldrich. HPLC grade methanol and HPLC grade DCM were purchased from Fisher Scientific. Laboratory grade ultrapure MilliQ water was used, dispensed from the ultrapure water filter/dispenser, manufactured by Purolite Corporation (dispensed at room temperature).

4.2.2 Material characterization techniques

The following material characterization analyses were carried out in the Chemistry Department at UCL, unless stated otherwise.

The procedure of BET SSA analysis of virgin PAC was performed by Dr Yuchen Yang using Autosorb-iQ2 automated gas sorption analyser (Quantachrome Instruments) via adsorption and desorption of nitrogen gas at 77K after virgin PAC degassed at a temperature of 180 °C for 24 h.

SEM images of virgin PAC, metaldehyde loaded PAC, and HA loaded PAC were acquired on JSM-6700F Field Emission Scanning Electron Microscope at 10 kV, under secondary electron imaging mode. EDX spectra of these samples were also acquired on JSM-6700F Field Emission Scanning Electron Microscope at 10 kV, under the signal type of energy dispersive spectroscopy, with times 20 000 magnification and an elevation angle of the EDX detector at 26 degrees.

ATR-FTIR spectra of virgin PAC, metaldehyde, HA, metaldehyde loaded PAC, and HA loaded PAC were measured on Platinum Attenuated Total Reflection (Bruker), which has a diamond crystal as the internal reflective component. Samples were measured in the wavenumber region of 4000 to 400 cm^{-1} (corresponding to wavelengths from 2.5 to 25 μm), with 128 scans and a spectral resolution of 2 cm^{-1} . The procedure of X-ray photoemission spectroscopy (XPS) measurements of these samples was performed by Dr Yuchen Yang using Thermo Scientific K-Alpha X-ray Photoelectron Spectrometer (Al-K- α). Survey scans of these samples were performed in the binding energy range of 135 to 1500 eV, under 12 kV with a monochromated X-ray spot size of 400 μm .

In addition, PZC of PAC (pH_{PZC}) was determined in the Environmental Engineering Laboratory at UCL. As explained in Section 2.6, pH_{PZC} determines the pH value where the electrical charge density on the surface of PAC is zero. It contributes to the understanding of the surface chemistry involving interactions between metaldehyde molecules and electrons on the surface of PAC.

The method of determining pH_{PZC} of PAC follows the acid-base titration method, using sodium chloride (NaCl) solution [142]: 5.844 g of NaCl was weighed by a scale (uncertainty of ± 0.1 mg). It was dissolved in 1000 mL of MilliQ water to make 1000 mL of 0.1 M NaCl solution in a 1000 mL volumetric flask (uncertainty of ± 0.4 mL). Seven 100 mL conical flasks with stoppers were prepared; 50 mL of the prepared 0.1 M NaCl solution was added into each flask. 100 mL of 0.1 M HCl was prepared by diluting 0.829 mL of HCl (37.5% in concentration, measured by a 1 mL Gilson pipette with the uncertainty of ± 0.01 mL) using MilliQ water in a 100 mL volumetric flask (uncertainty of ± 0.1 mL). 100 mL of 0.1 M sodium hydroxide (NaOH) was prepared

by dissolving 0.4 g of NaOH in 100 mL of MilliQ water in a 100 mL volumetric flask (uncertainty of ± 0.1 mL). For six of flasks, the initial pH values (pH_0) of the solutions were adjusted by adding drops of either 0.1 M HCl or 0.1 M NaOH to pH values of 2, 4, 6, 8, 10, and 12 (using 3 mL plastic pipettes)^{XVI}. And for one of them, pH_0 was not adjusted and kept as the original pH of the NaCl solution which was 6.27. After that, 0.06 g of PAC was added into each flask and mixed well with the NaCl solutions. These flasks were left to equilibrate for 48 h with intermittent manual mixing. Finally, the final pH values (pH_{48}) of the mixture were recorded. The differences between pH_0 and pH_{48} were calculated as ΔpH which were then plotted against pH_0 .

4.2.3 Preparation of metaldehyde and HA solutions

100 mL of metaldehyde stock solution at 1000 mg L⁻¹ and 100 mL of metaldehyde calibration stock solution at 500 mg L⁻¹ were prepared following the procedures described in Section 3.2.3.

Since de Melo *et al.* stated that the solubility of HA is reduced under acidic condition and precipitation can occur [169], HA stock solution was then prepared following the procedures proposed by Wang *et al.*: 0.5 g of humic acid sodium salt was weighed by a scale (uncertainty of ± 0.1 mg) and dissolved in 10 mL of 0.1 M NaOH (measured by a 10 mL Gilson pipette with the uncertainty of ± 0.1 mL) in a 500 mL glass beaker; the solution was then stirred by hand for 10 min using a glass rod. 200 mL MilliQ water was measured by a 500 mL graduated glass cylinder (uncertainty of ± 2.5 mL) and added to the beaker to dilute the solution, while the pH of the solution was adjusted to 7.0 by adding drops of 0.1 M HCl (using a 3 mL plastic pipette) [171]. After the pH has

^{XVI} pH of the solutions was measured by a pH meter (SevenMulti, Mettler Toledo).

been adjusted to 7.0, the solution was transferred into a 500 mL volumetric flask (uncertainty of ± 0.25 mL). MilliQ water with pH adjusted to 7.0 (by adding 0.1 M NaOH using a 3 mL plastic pipette) was then added into the flask to make 500 mL of HA stock solution at 1000 mg L^{-1} . After that the HA stock solution was transferred into another 500 mL glass beaker. It was stirred again using a magnetic stirrer for 5 min and filtered through $0.45 \text{ }\mu\text{m}$ Whatman cellulose nitrate membrane to remove any remaining suspended solids; then it was stored in a glass container in a fridge at $4 \text{ }^\circ\text{C}$ [93, 144, 171].

In this chapter, the studied concentration of metaldehyde working solution in the single adsorption system was 1 mg L^{-1} . This is to allow metaldehyde to be detected by GC-MS after PAC treatment. The studied concentration of HA working solution in the single adsorption system was 30 mg L^{-1} , which is higher than its common concentration range of 0.1 to 20 mg L^{-1} [164]. This concentration was selected to represent a high environmentally relevant concentration of HA, since Wang *et al.* stated that the concentration of HA can be around 30 mg L^{-1} for surface water from a terrestrial origin [144]. In the binary adsorption system, the studied concentration of metaldehyde working solution was fixed at 1 mg L^{-1} while the studied concentration range of HA solutions varied from 3 to 90 mg L^{-1} . This concentration range not only covered the common concentration range of HA but were even higher, in order to analyse the impact of different amounts of HA on the adsorption of metaldehyde onto PAC in the binary adsorption system.

As discussed in Section 3.2.3, metaldehyde stock solution can be diluted by MilliQ water to prepare metaldehyde working solutions. For example, 1 mL of metaldehyde stock solution was measured by a 2 mL graduated glass pipette (uncertainty of ± 0.01

mL) with an electrical pipette controller and added to a 1000 mL volumetric flask (uncertainty of ± 0.4 mL); MilliQ water was then added to the flask to make 1000 mL of metaldehyde working solution at 1 mg L^{-1} .

Similarly, different volumes of HA stock solution were measured and diluted by MilliQ water to prepare HA working solutions at different concentrations. For example, 30 mL of HA stock solution was measured by a 50 mL graduated glass cylinder (uncertainty of ± 0.5 mL) and added to a 1000 mL volumetric flask (uncertainty of ± 0.4 mL); MilliQ was then added into the flask to make 1000 mL of HA working solution at 30 mg L^{-1} .

Different amounts metaldehyde stock solutions and HA stock solutions were added together and diluted by MilliQ water to prepare multi-component solutions containing both metaldehyde and HA. For example, 1 mL of metaldehyde stock solution was measured by a 2 mL graduated glass pipette (uncertainty of ± 0.01 mL) with an electrical pipette controller and added to a 1000 mL volumetric flask (uncertainty of ± 0.4 mL); 30 mL of HA stock solution was measured by a 50 mL graduated glass cylinder (uncertainty of ± 0.5 mL) and added to the same flask as well; MilliQ water was then added to the flask to make 1000 mL of multi-component solution that contains metaldehyde at 1 mg L^{-1} and HA at 30 mg L^{-1} .

4.2.4 Adsorption experiments

To study the removal of metaldehyde from water using PAC with presence of HA, three main sets of experiments were carried out. All experiments were performed as batch tests, using mono-component metaldehyde solutions for the single adsorption system study, mono-component HA solutions for the single adsorption system study, and multi-component solutions containing both metaldehyde and HA for the binary

adsorption system study. PAC was added into the solutions and mixed by magnetic stirrers, to ensure PAC was in contact with the solutions. All samples were prepared as triplicates and filtered through 0.45 μm Whatman cellulose nitrate membrane to remove suspended PAC from the solution at the end of all experiments. The percentage removal of adsorbate (metaldehyde and HA) and the adsorbed amount of adsorbate (metaldehyde and HA) onto PAC were calculated using Equation 3.1, Equation 3.2, and Equation 3.3.

4.2.4.1 Batch experiments using mono-component metaldehyde solutions

Five 500 mL glass containers were wrapped with foil to prevent interference of light, which may cause decomposition of metaldehyde. In each container, 500 mL of 1 mg L^{-1} metaldehyde working solution was added. After that, 0.005, 0.01, 0.05, 0.1, and 0.5 g of PAC was added into these containers correspondingly. As soon as PAC was added, these solutions were stirred by magnetic stirrers to ensure PAC was in contact with the solutions. The contact time was 2 h, since metaldehyde was successfully removed by PAC within this time in Chapter 3.

After that, the same method was used for studying the effect of contact time on adsorption of metaldehyde. 0.05 g of PAC was added into 500 mL of 1 mg L^{-1} metaldehyde working solution for a 2-h contact time. Samples were taken at different time intervals at 0, 5, 10, 15, 20, 22.5, 25, 30, 40, 50, 60, 90, and 120 min. PAC dosage for this experiment was 0.05 g because after the 2-h treatment by PAC, metaldehyde needs to be detected by GC-MS to complete the study.

To study the effect of pH of metaldehyde solution on removing metaldehyde from water by adsorption onto PAC, 500 mL of 1 mg L^{-1} metaldehyde working solutions at

different pH (2 to 12) was added into six containers correspondingly. pH of the metaldehyde working solutions was adjusted by adding 0.1 M HCl and 0.1 M NaOH. 0.05 g of PAC was added into each of the six containers, with a contact time of 2 h. PAC dosage was selected as 0.05 g because after the 2-h treatment by PAC, metaldehyde needs to be detected by GC-MS to complete the study.

4.2.4.2 Batch experiments using mono-component HA solutions

Five 500 mL glass containers were prepared. In each container, 500 mL of 30 mg L⁻¹ HA working solution. After that, 0.05, 0.1, 0.25, 0.5, and 1 g of PAC was added into each container correspondingly. As soon as PAC was added, these solutions were stirred by magnetic stirrers to ensure PAC was in contact with the solutions. The contact time was 2 h.

Similarly, to study the effect of contact time on HA removal, 0.25 g of PAC was added into 500 mL of 30 mg L⁻¹ HA working solution for a 2-h contact time. Samples were taken at different time intervals at 0, 5, 10, 20, 30, 40, 50, 60, 90, and 120 min. However, since adsorption of HA onto PAC did not show signs of reaching equilibrium within 2 h, the experiment was then extended to 30 days. And samples were taken at 1, 2, 3, 4, 7, 10, 15, 25, and 30 days. PAC dosage of 0.25 g was selected for this experiment to ensure that HA can be detected even after 30 days of treatment.

4.2.4.3 Batch experiments using multi-component solutions containing metaldehyde and HA

The same dosage of PAC (0.05 g) was used in the binary adsorption system, so that the removal of metaldehyde in the binary system can be compared with the single

adsorption system. 0.05 g of PAC would also allow metaldehyde in the binary adsorption system to be detected after the 2-h treatment.

To study the impact of HA on metaldehyde removal in water, six containers were prepared. 500 mL multi-component solutions containing a fixed concentration of metaldehyde at 1 mg L⁻¹ and varied concentrations of HA at 3, 9, 15, 30, 60, and 90 mg L⁻¹ were prepared. They were added into the containers correspondingly. 0.05 g PAC was added into each container. The contact time was 2 h.

Another experiment was performed to analyse the effect of HA on the adsorption rate of metaldehyde onto PAC. 0.05 g PAC was added into the 500 mL multi-component solution that contains metaldehyde at 1 mg L⁻¹ and HA at 30 mg L⁻¹. The contact time was 2 h. Samples were taken at different time intervals at 0, 5, 10, 15, 20, 25, 30, 40, 50, 60, 90, and 120 min.

4.2.5 Analytical method for determination of metaldehyde and HA in water

Metaldehyde was analysed by GC-MS (Perkin Elmer precisely Clarus 500), following the method described in Section 3.2.5. Triplicate samples were prepared and each sample was injected three times at the autosampler of GC-MS. These would give nine data points ($N = 9$).

There are many techniques for analysing HA in water. For example, as discussed in Section 4.1, HA is a distribution of molecules, thus Kim *et al.* studied molecular weight fractionations from HA molecules, using HPLC coupled with a UV-Vis spectrophotometer [93]. Moreover, Helal *et al.* used nuclear magnetic resonance spectroscopy to study the chemical properties of HA [172]. However, due to the

availability of analytical instruments, these analyses of HA were not performed in this chapter; it is suggested by the researcher that if available, HA in water can be analysed using these techniques. In this chapter, determination of the concentration of HA in water followed the research of Wang *et al.*, which used a UV-Vis spectrophotometer for measuring the absorbance of sample solutions containing HA at 254 nm (wavelength), with MilliQ water as the blank measurement [144].

The UV-Vis spectrophotometer used in this chapter was CamSpec M550 Double Beam Scanning UV-Vis Spectrophotometer. Firstly, MilliQ water was added into two quartz cuvettes using a 3 mL plastic pipette. The quartz cuvettes were placed into the sample holders; and MilliQ water was measured by the UV-Vis spectrophotometer and the measurement was zeroed. One of the quartz cuvette containing MilliQ water was kept in the sample holder as the blank measurement. MilliQ water in the other quartz cuvette was discarded. Then sample solution containing HA was added into the empty quartz cuvette using a 3 mL plastic pipette. The quartz cuvette was then placed into the sample holder and measured by the UV-Vis spectrophotometer, with the MilliQ water as the blank measurement. Triplicate samples were analysed to ensure the constant repeatability of data (three data points, $N = 3$). Before and after each measurement, the quartz cuvette was washed and rinsed by MilliQ water to remove any residual solution that may remain on the wall of the cuvette, and to eliminate cross contamination of samples.

The results from the UV-Vis Spectrophotometer are given as the absorbance (cm^{-1}) of the solutions, regarding the presence of HA. A calibration method was needed to obtain the concentration of HA in the solutions. HA sample solution at 15 mg L^{-1} was prepared by diluting the HA stock solution using MilliQ water. A set of mono-

component HA solutions were prepared as external standards at 0.1, 0.5, 1, 5, 10, 30, 50, 100, and 200 mg L⁻¹ by diluting the HA stock solution using MilliQ water. HA sample solution and HA external standards were analysed by the UV-Vis Spectrophotometer at 254 nm (wavelength). The method of determining HA in water samples using UV-Vis spectrophotometer has a LOD of 0.03 mg L⁻¹ and a LOQ of 0.03 mg L⁻¹. A calibration curve was plotted with prepared HA standard solutions at different concentrations on the x-axis and the absorbance on the y-axis (Figure 4.2).

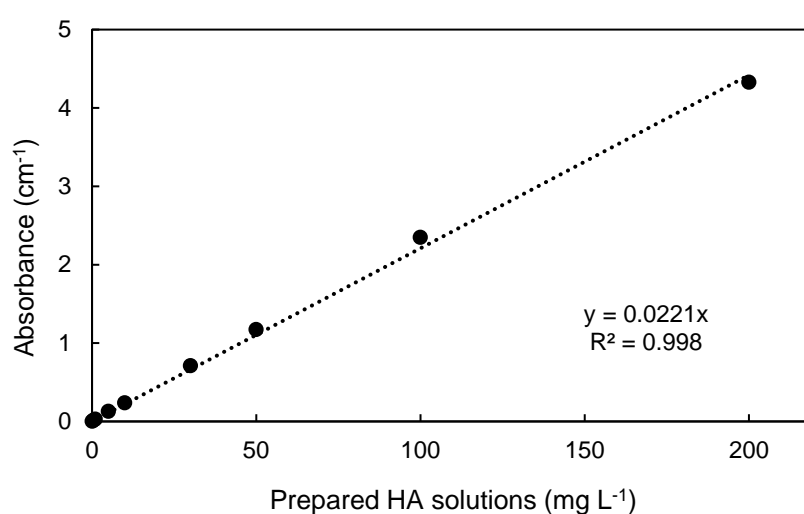


Figure 4.2 Calibration curve for the determination of HA

As shown in Figure 4.2, the R^2 value was 0.998, suggesting data were very well fitted. From the slope of the calibration curve (0.0221), the absorbance of HA (given by the UV-Vis spectrophotometer) of the prepared 15 mg L⁻¹ HA sample solution can be calibrated to the corresponding concentration, demonstrated by Table 4.1. A calibration rate for the prepared 15 mg L⁻¹ HA sample solution was calculated using the same equation for calculating recovery rate (Equation 3.4), to determine the accuracy of analysing HA by UV-Vis spectrophotometer. The calibration rates of HA solutions are usually around 100% and can be lower or higher because of instrumental uncertainty [173]. Due to the accuracy of UV-Vis spectrophotometer (instrumental

uncertainty of $\pm 0.06\%$) and performance error, the calibration rate of HA can be accepted within $100 \pm 20\%$, with RSD $< 20\%$ [174-176].

Table 4.1 Calibration of 15 mg L^{-1} HA sample solutions

Calibration equation	Slope	Absorbance of triplicate HA sample solutions (cm^{-1})			Average absorbance (cm^{-1})	Measured concentration (mg L^{-1})	Calibration rate (%)
$y=0.0221x$ $R^2=0.998$	0.0221	0.351	0.3509	0.351	0.35	15.88	105.9 (RSD $< 0.1\%$)

In this chapter, sample solutions from the binary adsorption system experiments, which contain both metaldehyde and HA, were analysed using both methods to determine the concentrations of metaldehyde and HA separately. The presence of HA does not affect the detection of metaldehyde in multi-component solutions and the presence of metaldehyde does not affect the detection of HA in multi-component solutions. All recovery rates of metaldehyde in this chapter were within the acceptable range of 70 to 120% with RSD $< 20\%$. All calibration rates of HA in this chapter were within the acceptable range of $100 \pm 20\%$, with RSD $< 20\%$.

4.2.6 Presentation and analysis of data

All data were analysed using Microsoft Excel, and they are presented with two digits after the decimal point. Percentages (%) are presented with one digit after the decimal point. Measurements after calibration are presented with standard deviation (SD) shown after the plus/minus symbol (\pm). SD is not presented if smaller than 0.01, unless

stated otherwise. For regression analysis, R^2 values, slopes, and intercepts are presented with four digits after the decimal point.

4.3 Results and discussion

4.3.1 Characterizations of adsorbents and adsorbates

4.3.1.1 BET SSA analysis of PAC

Figure 4.3 (A) shows the 77 K nitrogen adsorption and desorption isotherm of virgin PAC. The BET SSA of virgin PAC was determined to be $962.4 \text{ m}^2 \text{ g}^{-1}$ using five points selected from relative pressure (P/P_0) ranging from 0.02 to 0.1 (details are included in Table A.2.1, Appendix A.2), with a total pore volume of $0.79 \text{ cm}^3 \text{ g}^{-1}$ ^{XVII}. The isotherm presents a combination of Type I and IV isotherms with the hysteresis loop at relative pressure above 0.4, which indicates the combination of both micropores and mesopores. This phenomenon can be further evidenced by the PSD analysis using the density functional theory methods, as shown in Figure 4.3 (B). Raw data from the BET SSA analysis of this PAC are presented in Figure A.2.1, Appendix A.2.

^{XVII} For pores smaller than 315 nm in diameter, determined at 0.99388 relative pressure (P/P_0)

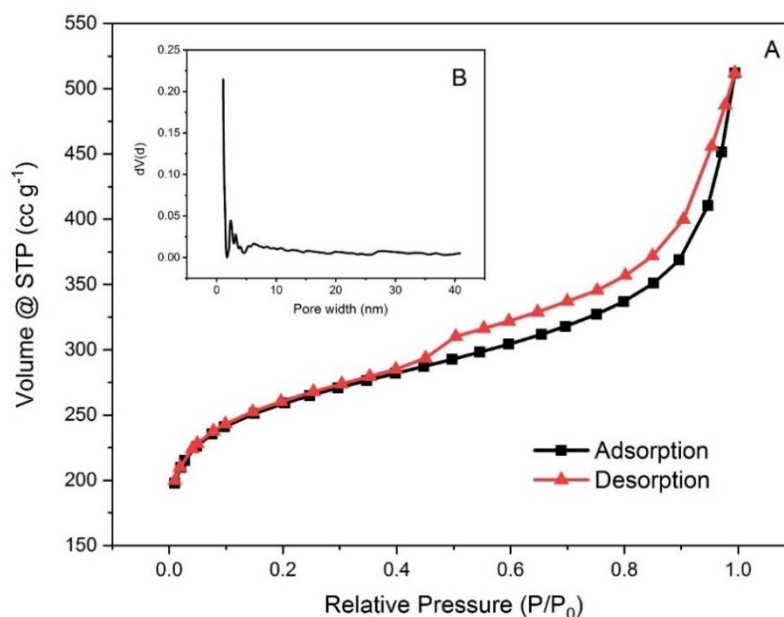


Figure 4.3 (A) Nitrogen adsorption and desorption isotherm of virgin PAC at 77 K; and (B) PSD of virgin PAC (STP = standard temperature and pressure)

Virgin PAC is dominated by micropores with pore width smaller than 2 nm. It also has abundant mesopores, especially the ones with pore width between 2 and 5 nm. Regarding PSD, as discussed in Chapter 3, virgin PAC is considered to be favourable for adsorption of compounds with small molecules such as metaldehyde, given the large numbers of micropores and mesopores of virgin PAC. However, for compounds which have large and complex structures, such as HA, adsorption onto this PAC may not be as effective.

4.3.1.2 SEM analysis

SEM analysis was done for three PAC samples including virgin PAC, metaldehyde loaded PAC, and HA loaded PAC. Metaldehyde loaded PAC and HA loaded PAC were collected after two 2-h adsorption tests of 0.1 g PAC with 500 mL of 10 mg L⁻¹

metaldehyde solution and 0.1 g PAC with 500 mL of 30 mg L⁻¹ HA solution, by filtering the PAC through 0.45 µm Whatman cellulose nitrate membranes.

Figure 4.4 illustrates the SEM images of virgin PAC which shows its structure and surface morphology. Virgin PAC particles are scattered around and their sizes vary from a few microns to 20 µm. The edges of the particles are angular while the surface is rough and porous. Visible pores can be seen on both edges and surface of virgin PAC particles.

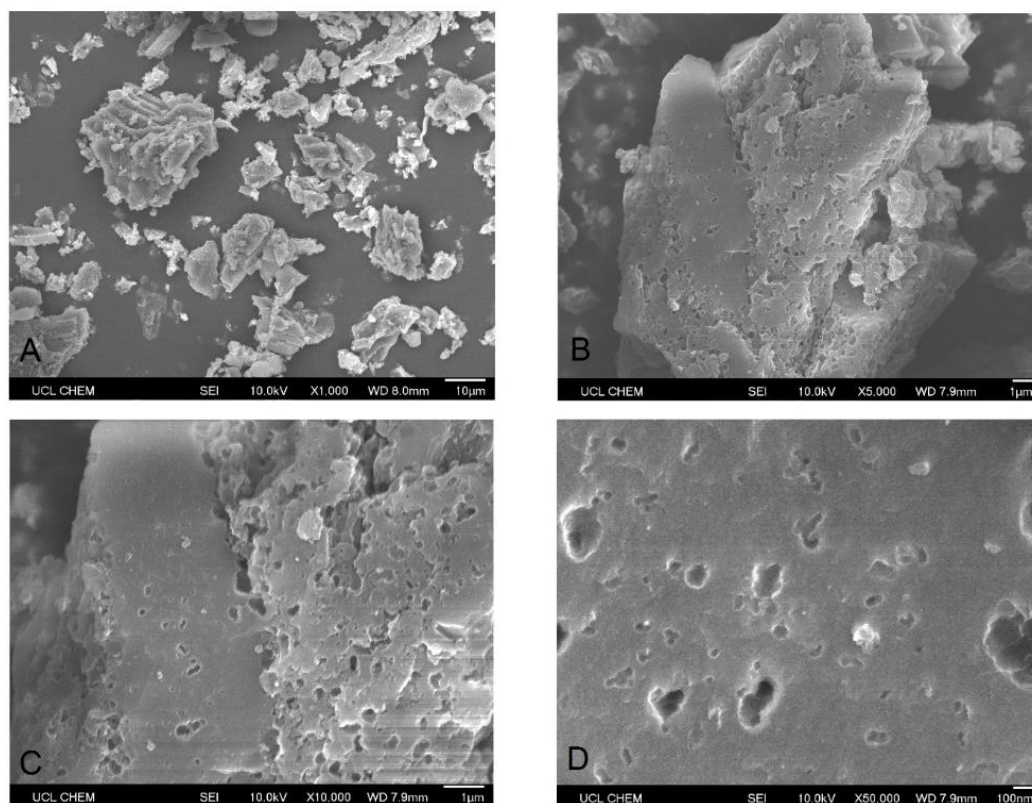


Figure 4.4 SEM images of virgin PAC at different magnifications: (A) ×1 000 magnification, an overview of PAC particles scattering around; (B) ×5 000 magnification, a PAC particle with visible pores on surface; (C) ×10 000 magnification, the edges and surface of the PAC particle which are potential adsorption sites; (D) ×50 000 magnification, macropores and some mesopores can be seen on the surface. (SEI = secondary electron imaging mode)

Figure 4.5 (A-C) shows the SEM images of metaldehyde loaded PAC at different magnifications. These images show no visible difference when compared with virgin PAC. Visible pores can be seen on the surface and edges of metaldehyde loaded PAC. Figure (D-F) shows the SEM images of HA loaded PAC at different magnifications. Similarly, these images show no visible difference when compared with virgin PAC. However, visible pores were more prominent on the surface of HA loaded PAC, compared with metaldehyde loaded PAC. This may be explained by the fact that pores of metaldehyde loaded PAC are occupied/blocked by adsorbed metaldehyde molecules due to effective removal on metaldehyde. Compared to metaldehyde, HA was not very effectively removed by PAC; hence the pores on HA loaded PAC are unblocked and visible pores are more prominent.

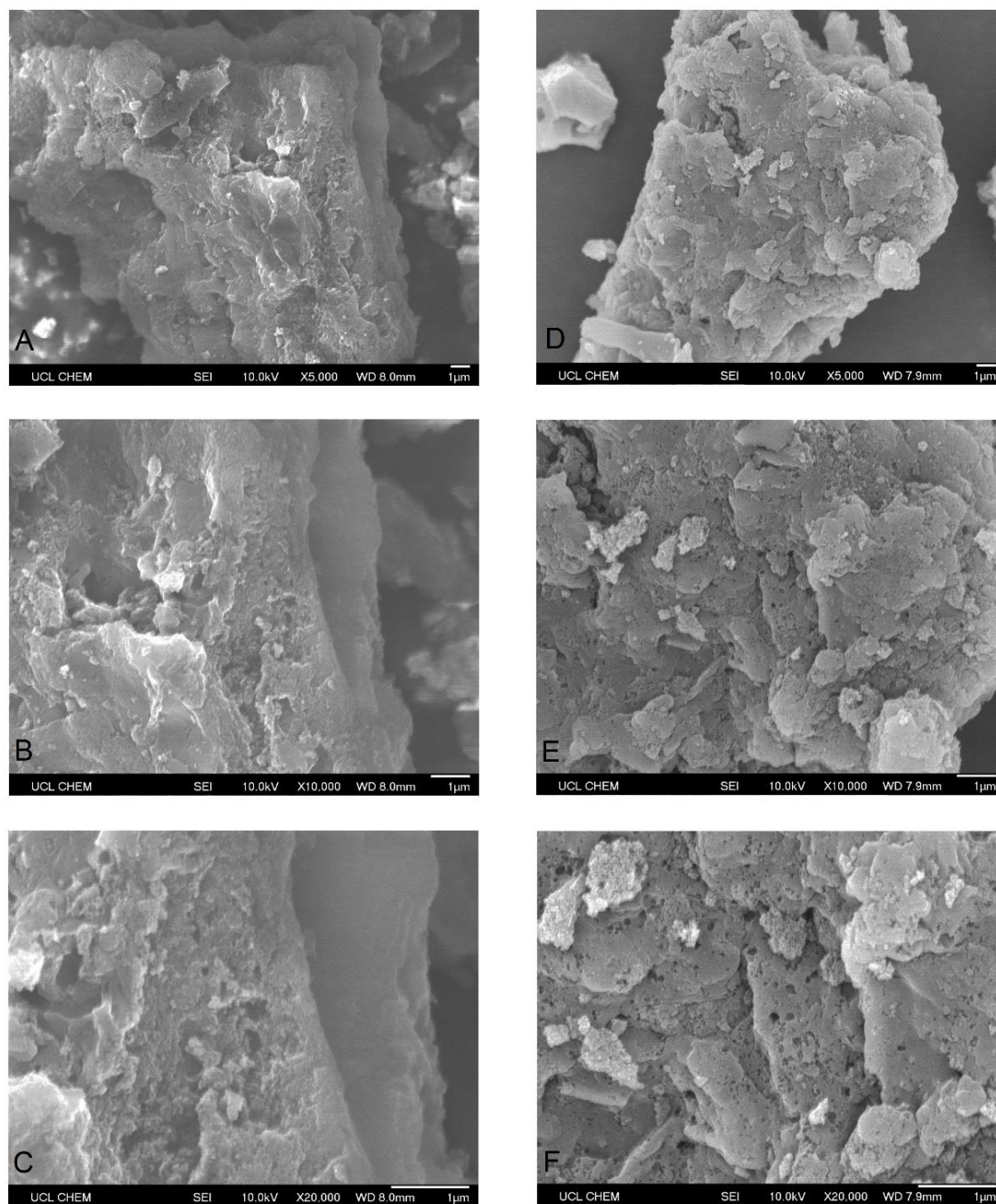


Figure 4.5 SEM images of metaldehyde loaded PAC at different magnifications: (A) x 5 000 magnification; (B) x 10 000 magnification; (C) x 20 000 magnification; and SEM images of HA loaded PAC at different magnifications: (D) x 5 000 magnification; (E) x 10 000 magnification; (F) x 20 000 magnification.

4.3.1.3 EDX analysis

EDX analysis of virgin PAC, metaldehyde loaded PAC, and HA loaded PAC was performed; however, the results were inconclusive. Figure 4.6 shows the spectra of the three PAC samples.

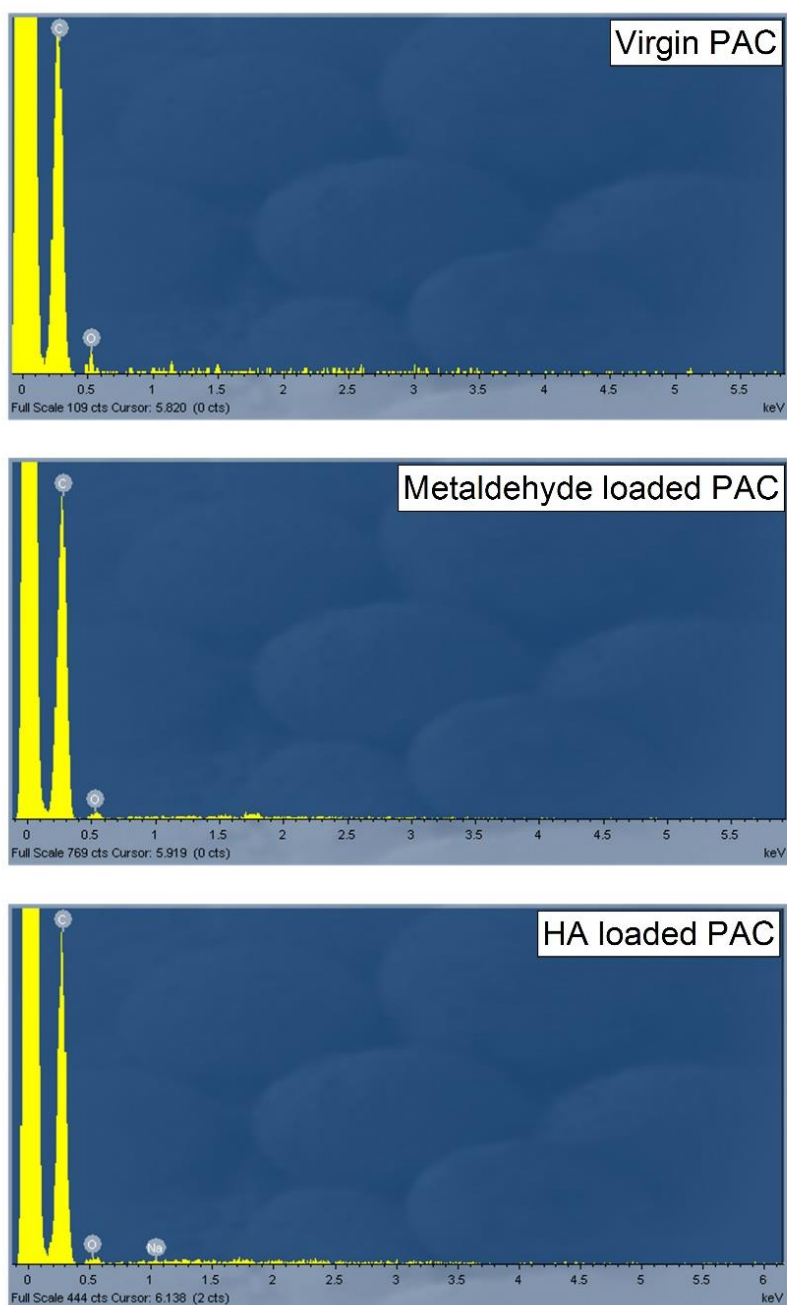


Figure 4.6 EDX spectra of virgin PAC, metaldehyde loaded PAC, and HA loaded PAC

Due to the limitation of X-ray spectroscopy, hydrogen cannot be detected [177]. Only carbon and oxygen are visible on the spectra of virgin PAC, metaldehyde loaded PAC, and HA loaded PAC. Sodium peak was expected to be seen on HA loaded PAC since HA (humic acid sodium salt, $C_9H_8Na_2O_4$) contains sodium, but there was none. A higher oxygen peak was expected to be seen on metaldehyde loaded PAC since metaldehyde ($C_8H_{16}O_4$) contains oxygen; however, it was not observed. These could be explained by the sample preparation process of SEM/EDX. An adhesive carbon tape needs to be used during the process. Since PAC is also made of carbon, the large quantity of carbon in the system would affect the detection of other elements, especially when the concentrations of other elements were small. For example, HA was not well adsorbed by PAC; therefore, the sodium content in HA loaded PAC was trace, compared to carbon. The inconclusive results could also be explained by the nature of EDX. The electrons in the system were travelling in a circular motion and could detect an area with a certain depth. The thickness of PAC samples that were on top of the carbon tape is much thinner than that of the carbon tape. Hence, the detection process would make PAC the minority in the system, let alone the possible compounds adsorbed onto it.

4.3.1.4 ATR-FTIR analysis

ATR-FTIR analysis of virgin PAC, metaldehyde, HA, metaldehyde loaded PAC, and HA loaded PAC was performed. The results are shown by Figure 4.7.

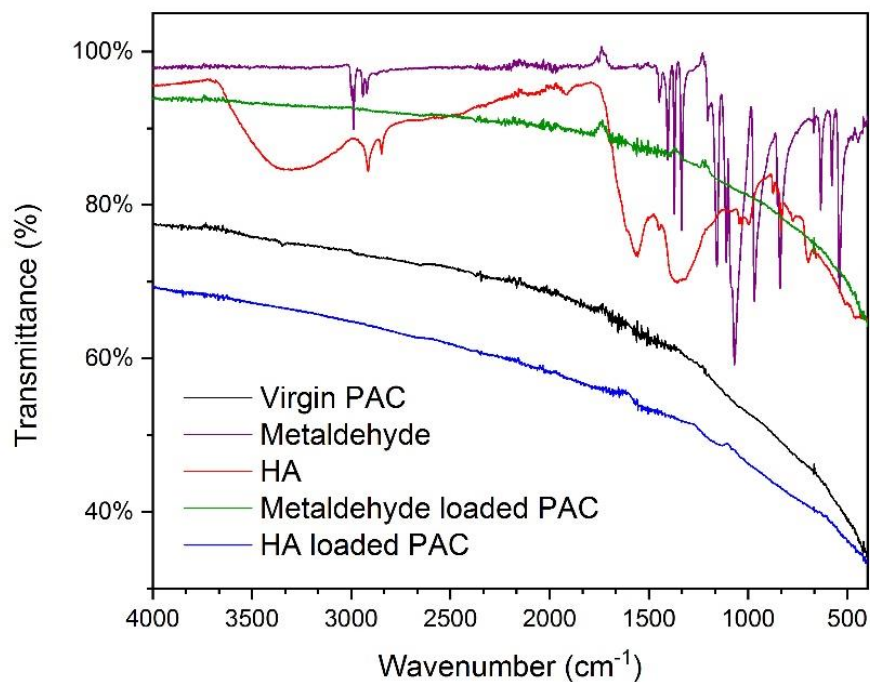


Figure 4.7 ATR-FTIR spectra of virgin PAC, metaldehyde, HA, metaldehyde loaded PAC, and HA loaded PAC

The result of ATR-FTIR analysis was also inconclusive because the spectral shifts cannot be observed. For example, the signature peak of metaldehyde at 1040 cm^{-1} (correspond to C-O bond) was not observed on metaldehyde loaded PAC; and the signature peak of HA at 1407 cm^{-1} (correspond to C-H bond) was not observed on HA loaded PAC. Since the signal from PAC is much stronger than metaldehyde and HA loaded onto it, considering the mass ratio of PAC, loaded metaldehyde and HA, the expected spectral shifts were not observed.

4.3.1.5 XPS analysis

Because of the inconclusive results from EDX and ATR-FTIR, XPS analysis was further performed. Figure 4.8 demonstrates the results.

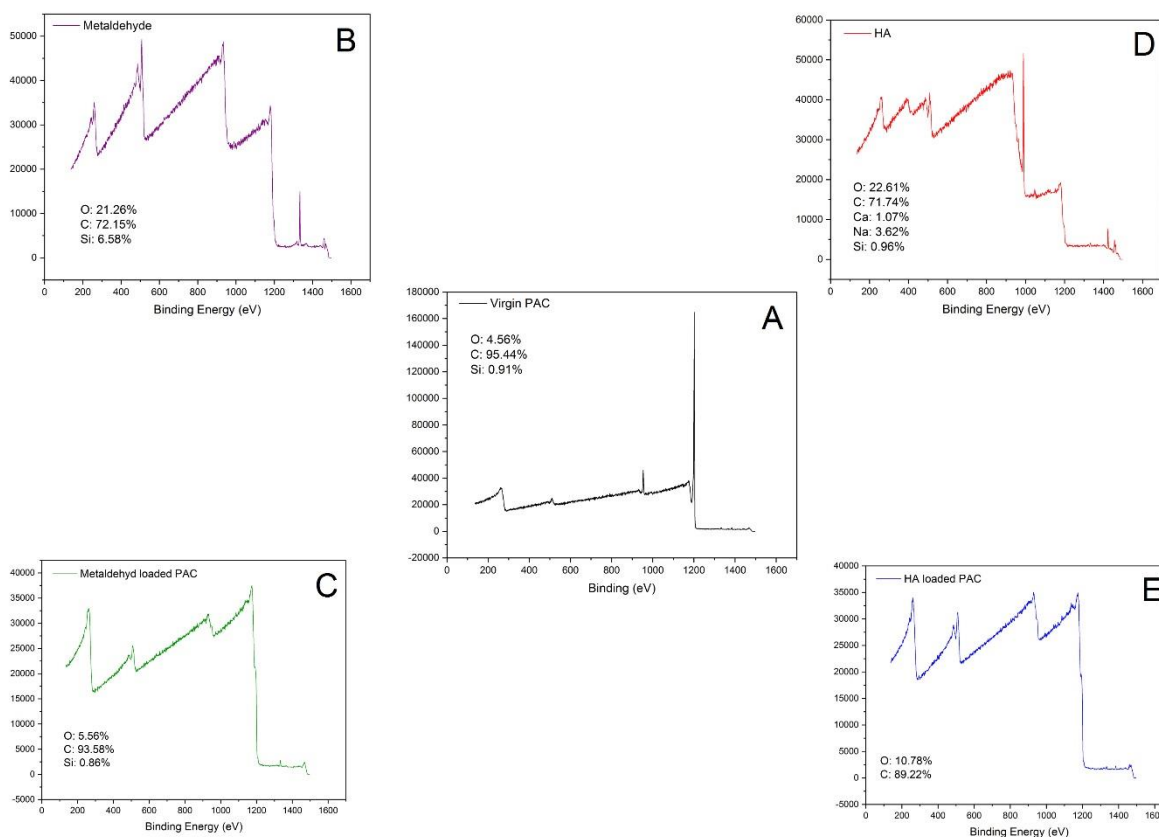


Figure 4.8 XPS spectra and element analyses: (A) virgin PAC; (B) metaldehyde; (C) metaldehyde loaded PAC; (D) HA; and (E) HA loaded PAC

As discussed in Section 4.3.1.3, hydrogen cannot be detected by X-ray spectroscopy; therefore, carbon and oxygen are the two main elements detected in all samples. From the elemental analysis, Figure 4.8 (A) shows that carbon is the most prominent element in PAC, as expected. Since PAC used in this study (activated charcoal, DARCO® G60) was manufactured from naturally occurring material, it contains crystalline silica (quartz) as impurity [178]; therefore, oxygen and silicon were detected in virgin PAC. In Figure 4.8 (E), it can be observed that there is an obvious increase of oxygen content where HA loaded PAC has more oxygen than the virgin PAC, suggesting the oxygen from HA (humic acid sodium salt, $C_9H_8Na_2O_4$) was adsorbed onto PAC. As for Figure 4.8 (C) metaldehyde loaded PAC, the increase of oxygen, which came from metaldehyde ($C_8H_{16}O_4$), was around 1%. Since the metaldehyde

content (5 mg) in mono-component metaldehyde solution was already smaller than that of the HA content (15 mg) in mono-component HA solution, it is possible that an expected increase of oxygen content in Figure 4.8 (C) is smaller. In addition, metaldehyde, as a quite volatile compound, has a melting point (closed capillary) of 246 °C and a boiling point (sublimes) of 115 °C. Therefore, there is a possibility that the extremely high vacuum in the XPS chamber could have removed most of the metaldehyde adsorbed onto the surface of PAC and left only those adsorbed on the inside of micropores.

4.3.1.6 PZC analysis of PAC (pH_{pzc})

Figure 4.9 shows that the pH_{pzc} of PAC is 7.35, i.e. the point where $\Delta\text{pH} = 0$. This suggests that the surface of PAC would be positively charged when the pH of the solution is lower than 7.35 (under a more acidic condition), while the surface of PAC would be negatively charged when the pH of the solution is higher than 7.35 (under a more alkaline condition).

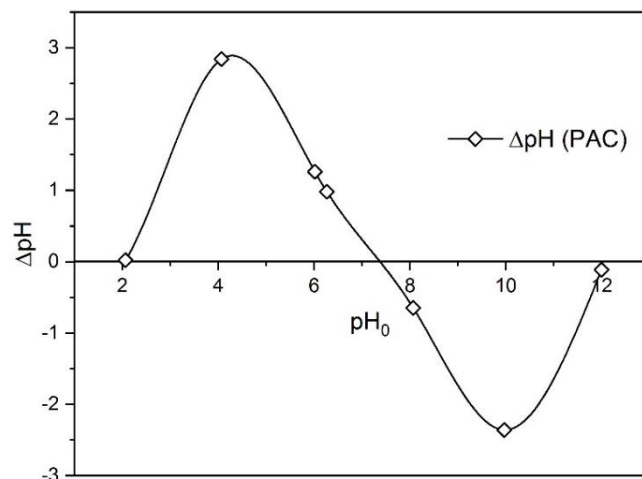


Figure 4.9 pH_{PZC} of PAC

Although metaldehyde molecules are polar, with oxygen atoms bearing negative charges and hydrogen atoms bearing positive charges, their chemical structure (as shown in Table 2.1) suggests that they are generally positively charged; negatively charged oxygen atoms of metaldehyde molecules are in the inner ring, while positively charged hydrogen atoms are on the outside. Zheng *et al.* argued that positively charged azo dye methylene blue molecules were strongly adsorbed by negatively charged GAC-supported TiO_2 under alkaline conditions [179]. Therefore, positively charged metaldehyde molecules may prefer adsorption onto a negatively charged surface. It is then expected that adsorption of metaldehyde onto PAC would be higher with the surface of PAC being negatively charged, when the pH of metaldehyde solution is higher than 7.35 (under a more alkaline condition).

BET SSA, SEM, EDX, ATR-FTIR, XPS, and PZC analyses of samples were performed in this section to present alternative evidences to the experimental results that metaldehyde and HA can adsorb onto PAC.

4.3.2 Removal of metaldehyde in the single adsorption system

4.3.2.1 Effect of PAC dosage

Figure 4.10 shows the concentrations of metaldehyde without and after treatment of PAC in the single adsorption system. It can be seen that metaldehyde was effectively removed, especially with higher PAC dosages. The ANOVA single factor statistic tests confirmed that there were significant differences (p -values ≤ 0.05) between the concentrations of metaldehyde without (C_0) and after (C_{t-2h}) the 2-h treatments that applied different PAC dosages (Table 4.2). Percentage removal of metaldehyde increased from 30.3 to 99.6% when PAC dosage increased from 0.005 to 0.05 g. When PAC dosage was higher than 0.05 g, metaldehyde could not be detected after the 2-h treatment, suggesting that its concentration was below the LOD of GC-MS for metaldehyde.

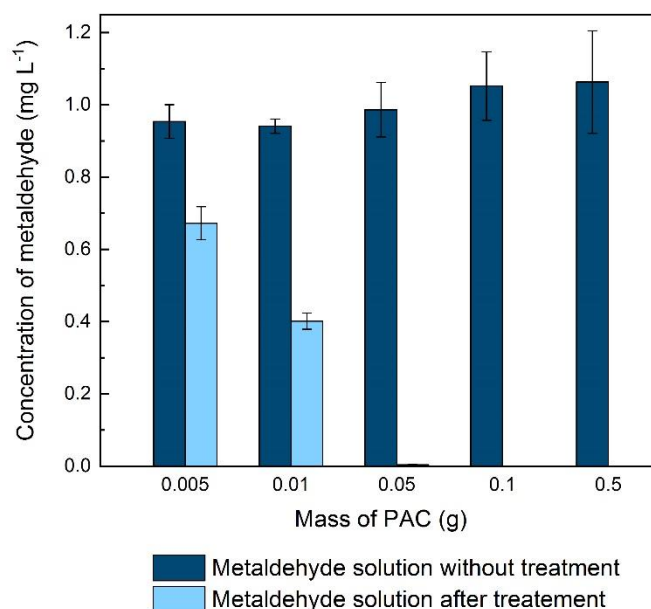


Figure 4.10 Concentrations of metaldehyde solutions without and after 2-h treatment by different PAC dosages in the single adsorption system ($N = 9$, error bars showing SD)

Table 4.2 Removal of metaldehyde by different PAC dosages ($N = 9$)

PAC dosage (g)	C_0 (mg L ⁻¹)	C_{t-2h} (mg L ⁻¹)	Percentage removal (%)	p -value
0.005	0.95 ± 0.05	0.67 ± 0.05	30.3 ± 5.3	2.28E-07
0.01	0.94 ± 0.02	0.4 ± 0.02	57.8 ± 1.9	1.07E-09
0.05	0.99 ± 0.08	0.004 ± 0.001 ^{XVIII}	99.6	4.07E-12
0.1	1.05 ± 0.09	< LOD	100	8.24E-16
0.5	1.06 ± 0.14	< LOD	100	1.45E-12

4.3.2.2 Effect of adsorption contact time

Figure 4.11 shows the concentration of metaldehyde solution and the amount of metaldehyde adsorbed onto PAC (q_t) over time. It can be seen that metaldehyde was rapidly adsorbed onto PAC in the first 5 to 10 min and gradually plateaued from 30 min, reaching equilibrium ($q_e = 9.93 \text{ mg g}^{-1}$) with 99.3% removal of metaldehyde in the end. The same trend was observed in Figure 3.9, Chapter 3.

^{XVIII} Three digits after the decimal point are presented here because the C_{t-2h} of metaldehyde after the 2-h treatment using 0.05 g PAC is low but still detectable by GC-MS.

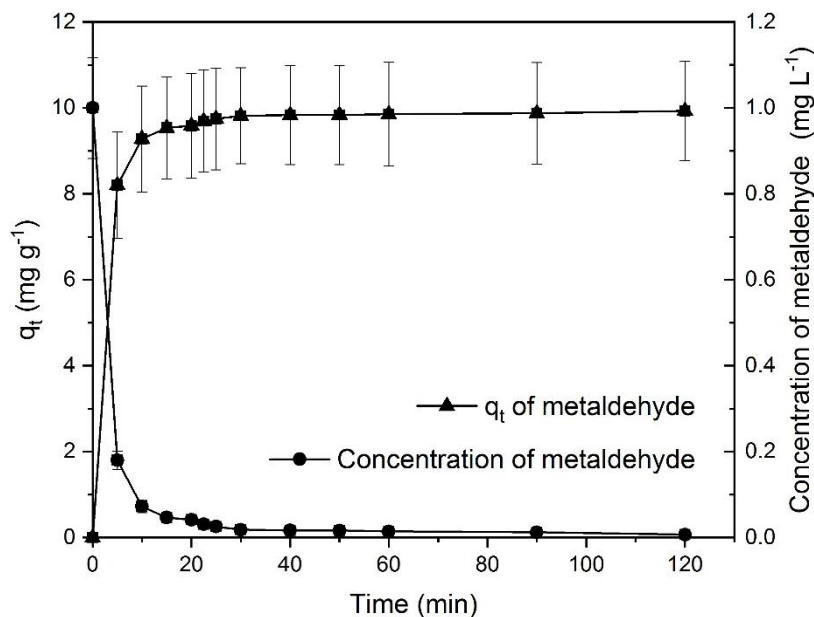


Figure 4.11 Effect of time on metaldehyde removal by PAC in the single adsorption system ($N = 9$, error bars showing SD)

4.3.2.3 Effect of pH of metaldehyde solution

Figure 4.12 presents the removal of metaldehyde under different pH conditions. Metaldehyde was effectively removed by PAC over the pH values tested. It is noted that under very acidic conditions such as pH 2, metaldehyde will undergo hydrolysis and decompose into acetaldehyde [180]. It was confirmed that after adjusting the pH of the prepared 1 mg L⁻¹ metaldehyde working solution to 2, the concentration of the metaldehyde working solution became 0.2 mg L⁻¹ without any treatment. Since this section presents the study of the effect of pH of metaldehyde solution on metaldehyde removal by PAC, data obtained from the metaldehyde working solution with an adjusted pH of 2 are excluded.

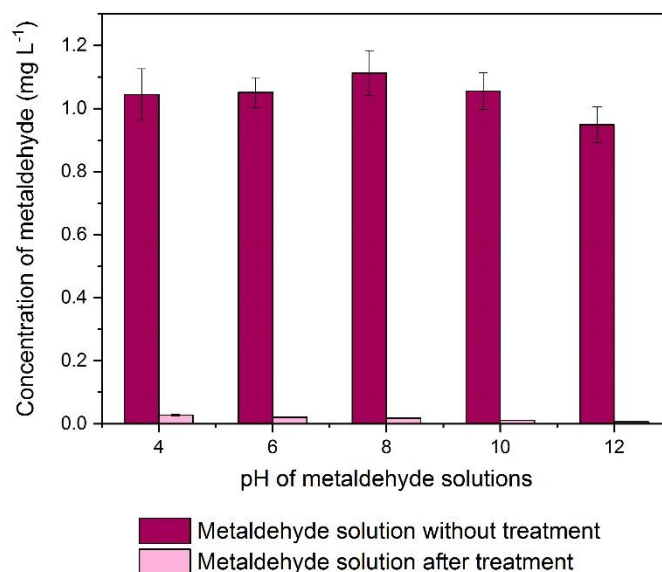


Figure 4.12 Concentrations of metaldehyde solutions without and after 2-h treatment using 0.05 g PAC under different pH environments in the single adsorption system ($N = 9$, error bars showing SD)

Table 4.3 demonstrates the removal of metaldehyde without (C_0) and after (C_{t-2h}) 0.05 g PAC treatment under each pH condition (pH = 4, 6, 8, 10, and 12). There were significant differences (p -values ≤ 0.05) between C_0 and C_{t-2h} under different pH conditions. Table 4.4 presents the p -values from the ANOVA single factor statistic tests which compared the concentrations of metaldehyde after (C_{t-2h}) 0.05 g PAC treatment between two different pH values. All p -values obtained were ≤ 0.05 , suggesting that there were significant differences between C_{t-2h} under different pH conditions, and that the pH of metaldehyde solutions indeed can affect metaldehyde removal. Removal of metaldehyde slightly increased from 97.4 to 99.3% as pH increased from 4 to 12. This suggests that adsorption of metaldehyde onto PAC is favoured under a more alkaline environment, which can be confirmed by the pH_{pzc} of PAC (7.35). The surface of PAC is negatively charged when the pH of the solution is higher than 7.35 and would interact with positively charged molecules [181]. As

discussed in Section 4.3.1.6, metaldehyde molecules in water are generally positively charged; therefore, it was expected that the removal of metaldehyde by PAC was slightly higher under a more alkaline environment.

Table 4.3 Removal of metaldehyde by 2-h PAC treatment at different pH values ($N = 9$)

pH	C_0 (mg L⁻¹)	C_{t-2h} (mg L⁻¹)	Percentage removal of metaldehyde (%)	p-value
4	1.04 ± 0.08	0.03	97.4 ± 0.3	1.4E-16
6	1.05 ± 0.05	0.02	98 ± 0.2	2.13E-20
8	1.11 ± 0.07	0.02	98.4 ± 0.2	4.43E-18
10	1.06 ± 0.06	0.01	98.9 ± 0.1	4.57E-19
12	0.95 ± 0.06	0.01	99.3 ± 0.1	1.51E-18

Table 4.4 Results from the ANOVA single factor statistic tests comparing C_{t-2h} at two different pH values

pH	C_{t-2h} (mg L⁻¹)	pH	C_{t-2h} (mg L⁻¹)	p-value
4	0.03	12	0.01	3.21E-13
6	0.02	12	0.01	1.48E-12
8	0.02	12	0.01	2.98E-11
10	0.01	12	0.01	1.13E-10
4	0.03	10	0.01	1.74E-11
6	0.02	10	0.01	6.68E-10
8	0.02	10	0.01	7.46E-08
4	0.03	8	0.02	4.32E-07
6	0.02	8	0.02	6.39E-03
4	0.03	6	0.02	5.81E-05

Although the removal of metaldehyde by PAC is indeed associated with the pH of metaldehyde solution, metaldehyde was effectively removed by PAC under all pH conditions with a small improvement (1.9%) by changing the pH to a more alkaline environment. Therefore, the necessity of adjusting the pH of the solution needs to be considered. In fact, in Section 4.3.2.1 and Section 4.3.2.2, the pH of metaldehyde solutions was 6.27 in situ (without adjusting the pH), and the removal of metaldehyde from both experiments was higher than 99%. Considering the potential application of PAC in drinking water treatment plants for removing metaldehyde, adjusting the pH of water before dosing PAC may increase the cost but only achieve a small improvement. Therefore, it is not recommended to change the pH of water for the sole purpose of enhancing the removal of metaldehyde by PAC in a practical scenario.

4.3.2.4 Adsorption kinetic studies of metaldehyde in the single adsorption system

Experimental data from Section 4.3.2.2 were analysed using the two most commonly used kinetic models, the pseudo-first order and the pseudo-second order kinetic models, the same as in Section 3.3.4.

The pseudo-first order model was proposed by Lagergren for a liquid-solid adsorption system that is based on solid capacity. It assumes that the adsorption rate is proportional to the difference of q_t and q_e [154, 182] and controlled by diffusion [183]. It also considers that only one active site of PAC is needed to adsorb one metaldehyde molecule [184, 185]. Data were fitted to the pseudo-first order kinetic model using Equation 3.6 (Figure 4.13).

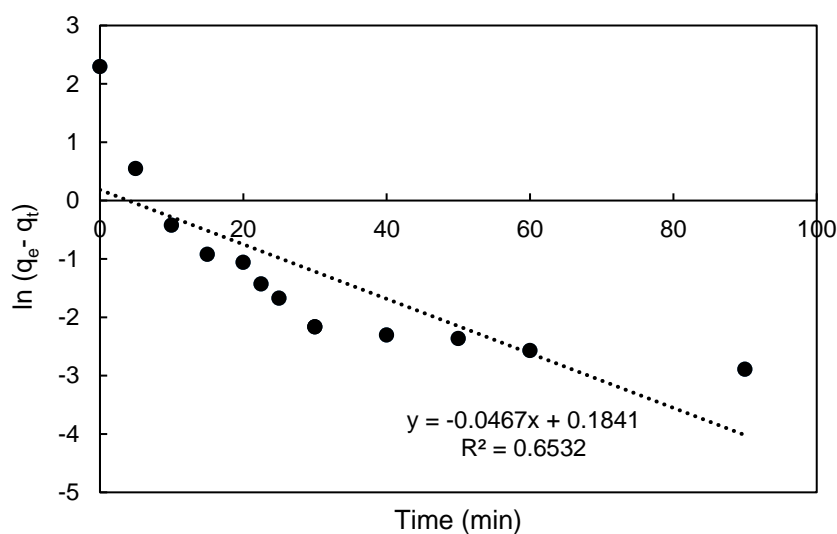


Figure 4.13 The pseudo-first order kinetic model fitting of 1 mg L⁻¹ metaldehyde solution (500 mL) with 0.05 g PAC in the 2-h treatment time

Experimental data were not well fitted to the pseudo-first order model with $R^2 = 0.6532$. The calculated theoretical value of q_e from this model is 1.2 mg g⁻¹ and k_1 is 0.05 min⁻¹

1. The value of q_e is clearly different from the experimental value of $q_e = 9.93 \text{ mg g}^{-1}$, confirming that this fitting is not very suitable.

Since the data were not fit well to the pseudo-first order model via a single linear fitting and the data were showing a two-stage trend, two linear fittings were plotted with two gradient stages from 0 to 30 min and from 30 to 120 min (Figure 4.14).

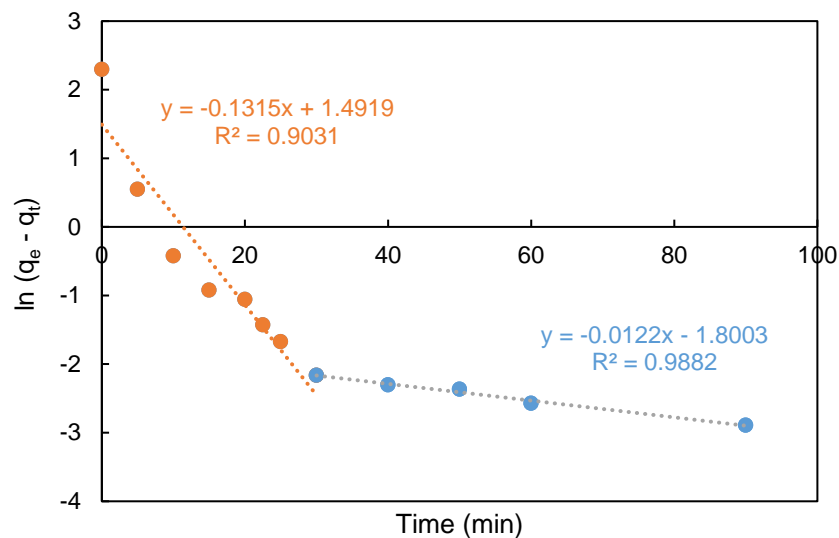


Figure 4.14 Data fitted to the pseudo-first order kinetic with two gradients

Data were better fitted with the two-stage plot ($R_{0-30\text{min}}^2 = 0.9031$, $R_{30-120\text{min}}^2 = 0.9882$). According to Li *et al.*, the two gradients in the pseudo-first order kinetic model have two interpretations: for a chemically-controlled model, two gradients suggest two chemically different adsorption sites; and for a diffusion-controlled model, two gradients imply different diffusion rates [183]. In this case, it is unlikely that PAC has two largely different adsorption sites, regarding the chemical composition; therefore, the two gradients can be explained as two different pore diffusion rates which determine the adsorption rate of metaldehyde onto PAC in the diffusion-controlled adsorption process [183]. The first rate ($k_1=0.13 \text{ min}^{-1}$) indicates a higher rate of diffusion via the easily accessed macropores; and the second rate ($k_1=1.22 \times 10^{-2} \text{ min}^{-1}$)

1) which is more than 10 times slower than the first one represents a slower rate of diffusion via mesopores and micropores [183].

The pseudo-second order kinetic model describes the adsorption rate as proportional to the difference of q_e and q_t squared as shown by Equations 3.7, Equation 3.8, and Equation 3.9. It can simulate well intraparticle diffusion process with plane and spherical adsorbent particles [186]. Moreover, the pseudo-second order model assumes that the adsorption rate of the process is controlled by surface reactions which can be chemisorption involving valence forces via exchanges of electrons between adsorbate and adsorbent, as well as interactions of physical nature such as van der Waals forces [155, 156, 187]. This model also assumes that two active sites of PAC are needed to adsorb one metaldehyde molecule [184, 185]. Figure 4.15 presents data fitted to the pseudo-second order kinetic model.

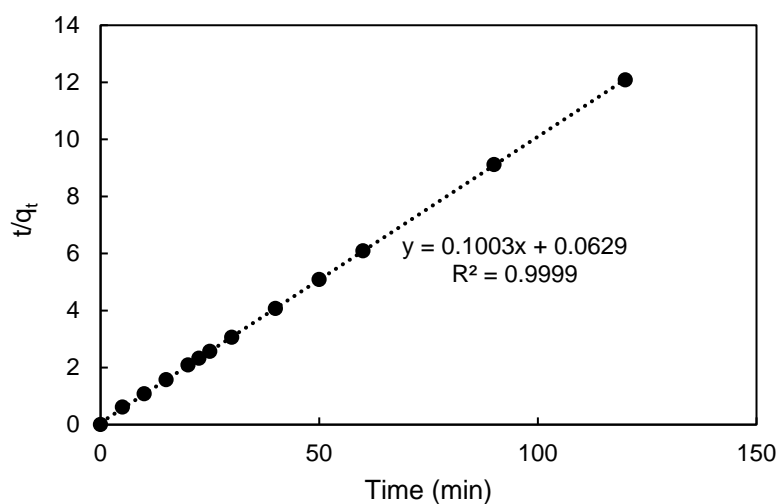


Figure 4.15 The pseudo-second order kinetic model fitting of 1 mg L⁻¹ metaldehyde solution (500 mL) with 0.05 g PAC in the 2-h treatment time

Data were very well fitted to the pseudo-second order kinetic model with $R^2 = 0.9999$. Calculated q_e from this model is 9.97 mg g⁻¹ which is very close to the experimental value of 9.93 mg g⁻¹. This confirms that the pseudo-second order kinetic model is more

suitable for analysing the data. The value of k_2 obtained is $0.16 \text{ g mg}^{-1} \text{ min}^{-1}$. It is much higher than the $k_2 = 8 \times 10^{-5} \text{ g mg}^{-1} \text{ min}^{-1}$ obtained by Salvestrini *et al.* using GAC, suggesting a very fast adsorption reaction rate of metaldehyde onto PAC [70], which benefits from the fast and direct surface adsorption. Good fitting to the pseudo-second order kinetic model implies that under the studied experimental condition, the process and mechanism of metaldehyde molecules adsorbing onto PAC is via intraparticle diffusion, while the fast adsorption reaction is due to direct surface adsorption [156].

4.3.2.5 Adsorption isotherm studies of metaldehyde in the single adsorption system

Taking into account the analysis in Section 4.3.2.4, the adsorption isotherm for metaldehyde onto PAC was determined to reach equilibrium at 120 min. The most commonly used adsorption isotherm models, the Freundlich isotherm model and the Langmuir isotherm model, were studied because these two models can give the maximum adsorption capacity of PAC for metaldehyde. Figure 4.16 shows the adsorption equilibrium curve of metaldehyde onto PAC fitted to these two models.

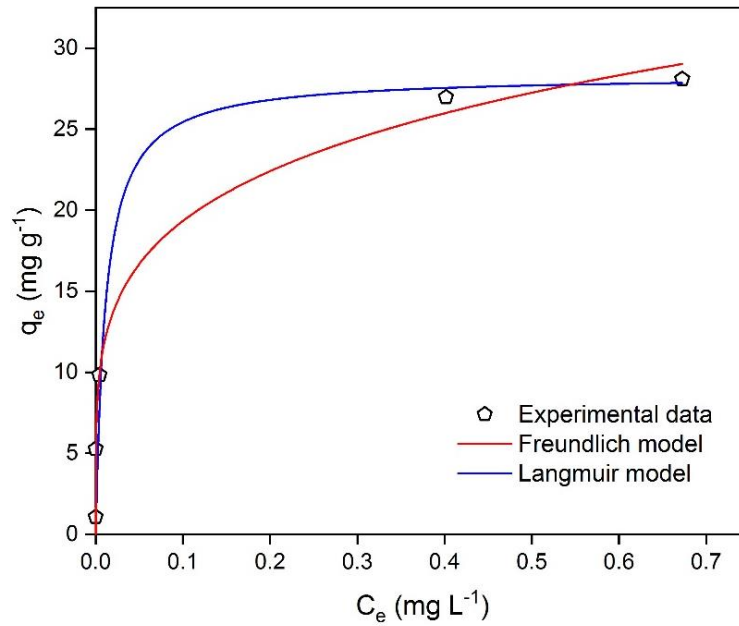


Figure 4.16 Metaldehyde adsorption equilibrium curve showing the experimental data and the Freundlich and Langmuir isotherm models in the single adsorption system

It is of great significance to select the best fitting isotherm model to correlate the experimental data, as shown in Figure 4.16. The Freundlich isotherm is generally used for heterogeneous surfaces and it assumes multilayer sorption [188]. It predicts that the adsorbate concentrations on the adsorbent will increase, given there is an increase of the adsorbate in the liquid. Equation 4.1 and Equation 4.2 describe the Freundlich isotherm model where $1/n$ is the heterogeneity factor (i.e. adsorption intensity) and K_F is the Freundlich constant (i.e. adsorption capacity) [142, 182]. Figure 4.17 shows data fitted to the Freundlich isotherm model using these two equations.

$$q_e = K_F C_e^{1/n} \quad \text{Equation 4.1}$$

$$\log q_e = \log K_F + \frac{1}{n} \log C_e \quad \text{Equation 4.2}$$

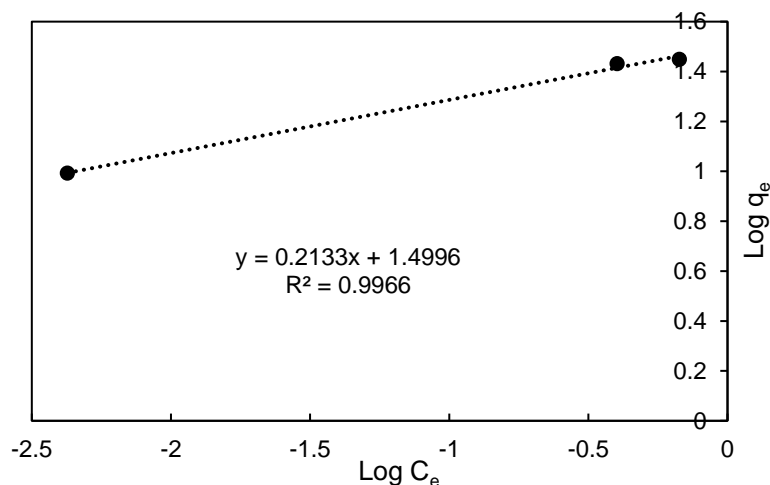


Figure 4.17 The Freundlich isotherm model fitting

Data were well fitted with $R^2 = 0.9966$ and the fitting gives $1/n$ value of 0.21 ($n = 4.73$) and the K_F value of $31.59 \text{ (mg g}^{-1}\text{)/(mg L}^{-1}\text{)}^{1/n}$. As Kumar *et al.* stated that $1/n$ indicates the relative distribution of energy sites; the higher the $1/n$, the higher the affinity is between adsorbate and adsorbent, and the adsorbent sites will be more heterogeneous [142]. Moreover, when $n > 1$, the adsorption is a physical process, and when $n < 1$, the adsorption is a chemical process [189]. In this case, the adsorption is considered as a physical. A low value of $1/n$ such as 0.21 suggests that the affinity between the PAC used in this study and metaldehyde is low and the heterogeneity of PAC sites is low. As an indicator of adsorption capacity, the K_F value obtained in this study is $31.59 \text{ (mg g}^{-1}\text{)/(mg L}^{-1}\text{)}^{1/n}$, more than 10 times higher than the one obtained by Kumar *et al.* around $2.5 \text{ (mg g}^{-1}\text{)/(mg L}^{-1}\text{)}^{1/n}$ [142]. Kumar *et al.* argued that their high K_F value suggests effective adsorption [142]; therefore, the high K_F value obtained here can confirm the effective removal of metaldehyde by PAC in the experiment (Section 4.3.2.1). In addition, fitting the data to the Freundlich isotherm model provided information on the adsorption of metaldehyde on PAC. For example, $n = 4.73$ suggests physical adsorption of metaldehyde onto PAC. However, on the

other hand, the low $1/n$ value suggests that the affinity between PAC and metaldehyde are low [142], while the experimental results of effective removal of metaldehyde suggest otherwise. Therefore, the Freundlich isotherm model is not completely suitable for fitting the experimental data, but nor can it be rejected.

The Langmuir isotherm is a commonly used model for adsorption studies that use adsorbents with homogeneous surfaces. It assumes the existence of monolayer coverage of the adsorbate at the surface of the adsorbent; therefore, the adsorbent has a maximum capacity for the adsorbate; and once a saturation is reached, there will be no more adsorption [182]. Equation 4.3 and Equation 4.4 describe the Langmuir isotherm model where K_L ($L\ mg^{-1}$) is the Langmuir constant and q_m ($mg\ g^{-1}$) is the saturation/maximum adsorption capacity. Figure 4.18 shows data fitted to the Langmuir isotherm model using these two equations.

$$q_e = \frac{K_L C_e q_m}{1 + K_L C_e} \quad \text{Equation 4.3}$$

$$\frac{C_e}{q_e} = \frac{1}{K_L q_m} + \frac{C_e}{q_m} \quad \text{Equation 4.4}$$

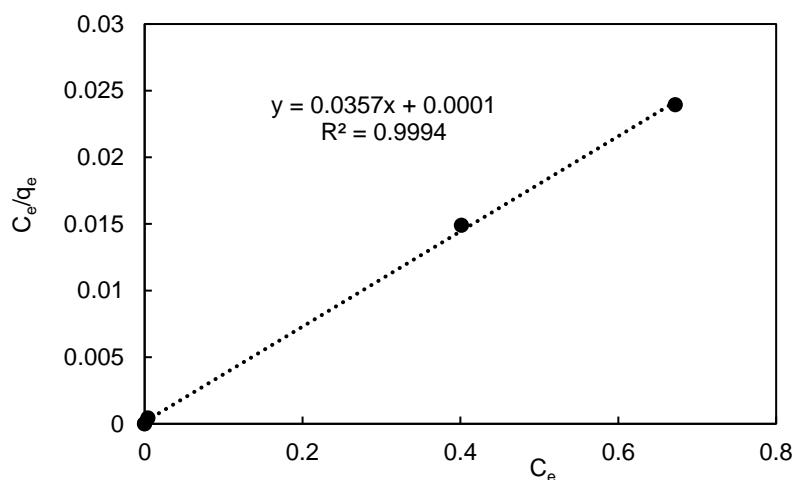


Figure 4.18 The Langmuir isotherm model fitting

Data were very well fitted with $R^2 = 0.9994$ and the fitting gives q_m of 28.33 mg g^{-1} and K_L of 88.25 L mg^{-1} . The maximum adsorption capacity q_m represents the saturation of one molecule thick metaldehyde on the surface of PAC at equilibrium. K_L correlates to the concentration where the amount of metaldehyde adsorbed onto PAC is equal to $q_m/2$. A high K_L value in this case indicates the high affinity of metaldehyde molecules to adsorb onto PAC, which can be confirmed by the effective removal of metaldehyde in the experiment (Section 4.3.2.1). All parameters obtained from fitting data to the Langmuir isotherm model agree with the experimental results of effective metaldehyde removal. Therefore, the Langmuir isotherm model may be more suitable for representing metaldehyde adsorption onto PAC, compared with the Freundlich isotherm model.

Therefore, the suitability of the two isotherm models was then analysed using a statistical method, the Akaike information criterion (AIC). AIC is a model selection criteria method and it estimates the probability of a model to predict future values, based on the fittings of data; the most suitable model is the one that has a minimum AIC value, among all other models [190]. AIC uses a non-linear regression algorithm [191], which considers the residual sum of squares (RSS) and the number of free parameters [192]. RSS and AIC values were calculated using Equation 4.5 and Equation 4.6, where h is the number of data points in the isotherm model fitting, $q_{exp,i}$ are the q_e from experimental data, $q_{the,i}$ are the theoretical q_e calculated from the Freundlich and Langmuir isotherm models, and M is the number of parameters in the isotherm models [191]. Statistical analysis of the suitability of the adsorption isotherm models using the AIC method is presented in Table 4.5.

$$RSS = \sum_{i=1}^h (q_{exp,i} - q_{the,i})^2 \quad \text{Equation 4.5}$$

$$AIC = h \times \ln\left(\frac{RSS}{h}\right) + 2 M \quad \text{Equation 4.6}$$

Table 4.5 Statistical analysis of the suitability of the isotherm models using the AIC method

	Langmuir isotherm model		Freundlich isotherm model	
	K_L (L mg ⁻¹)	q_m (mg g ⁻¹)	K_F (mg g ⁻¹)/(mg L ⁻¹) ^{1/n}	$1/n$
	88.25	28.33	31.59	0.21
RSS	33.6		30.6	
AIC	11.5		13.1	

Statistical analysis using the AIC method suggests that the Langmuir isotherm model is more suitable for analysing the experimental data, since it has a AIC value of 11.5 while the Freundlich isotherm model has an AIC value of 13.1 [191].

4.3.3 Removal of HA in the single adsorption system

4.3.3.1 Effect of PAC dosage

Figure 4.19 shows the concentrations of HA without (C_0) and after (C_{t-2h}) treatment by different PAC dosages. The ANOVA single factor statistic tests confirmed that there were significant differences (p -values ≤ 0.05) between the concentrations of HA without (C_0) and after (C_{t-2h}) treatment (Table 4.6). As explained in Section 4.2.5, the acceptable calibration rate of HA using UV-Vis spectrophotometer is from 80 to 120% (i.e. 24 mg L⁻¹ to 36 mg L⁻¹); therefore, any treatment that achieved percentage

removal of HA higher than 20% is considered effective. The removal of HA was moderately effective by adsorption onto PAC, with PAC dosages ≥ 0.25 g. The percentage removal of HA increased from 21.6 to 32%, with increasing PAC dosage from 0.25 to 1 g. Although the concentration of HA before treatment ($C_0 = 30 \text{ mg L}^{-1}$) was much higher than that of metaldehyde ($C_0 = 1 \text{ mg L}^{-1}$), a high dosage of PAC at 1 g can only remove 32% of HA in 2 h.

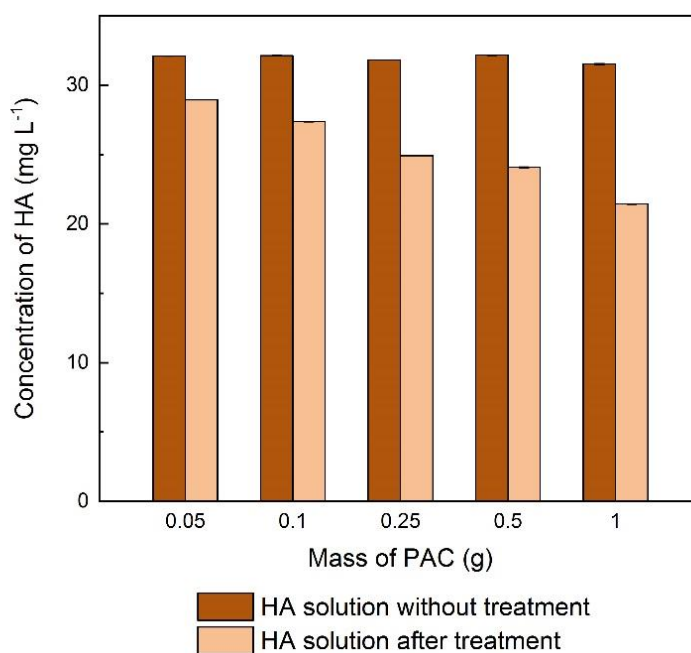


Figure 4.19 Concentrations of HA solutions without and after 2-h treatment using PAC with different dosages in the single adsorption system ($N = 3$, error bars showing SD)

Table 4.6 Removal of HA by different PAC dosages ($N = 3$)

PAC dosage (g)	C_0 (mg L ⁻¹)	C_{t-2h} (mg L ⁻¹)	Percentage removal of HA (%)	p -value
0.05	32.1 ± 0.01	28.94 ± 0.01	9.8 ± 0.1	8.5E-10
0.1	32.13 ± 0.01	27.37 ± 0.01	14.8	6.96E-11
0.25	31.8 ± 0.01	24.92	21.6	1.39E-12
0.5	32.16 ± 0.01	24.08 ± 0.02	25.1 ± 0.1	9.8E-11
1	31.52 ± 0.03	21.43	32	6.72E-11

4.3.3.2 Effect of adsorption contact time

PAC dosage was selected as 0.25 g in this experiment to remove HA ($C_0 = 30 \text{ mg L}^{-1}$) from 500 mL MilliQ water, aiming to identify the time required for the adsorption system to reach equilibrium. Figure 4.20 shows the adsorption of HA from 0 to 30 days. There is no clear sign that adsorption of HA would gradually plateau and reach equilibrium. At the end of the 30-day experiment, 50% of HA was removed. Based on this trend, it was highly possible that PAC would have continued removing HA even after the 30-day treatment.

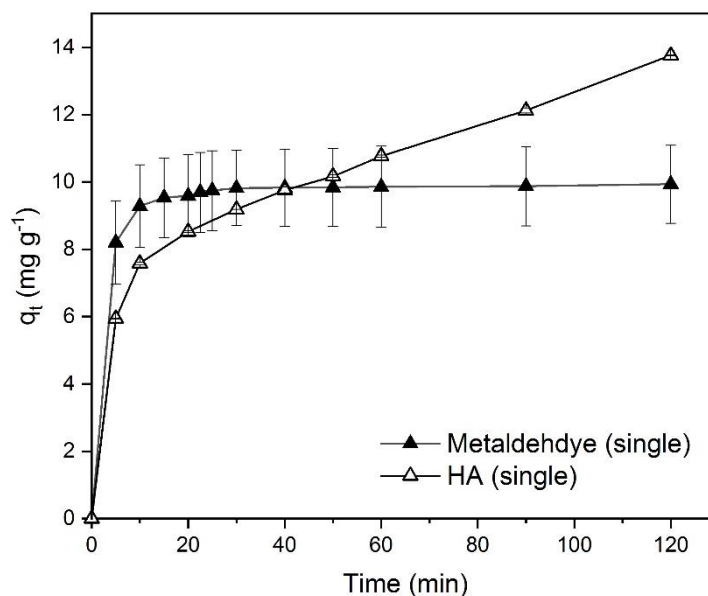


Figure 4.20 Effect of time on HA removal by PAC in the single adsorption systems ($N = 3$, error bars showing SD)

Due to the different behaviour of adsorption of HA and metaldehyde onto PAC over time, the first 120 min of the HA adsorption curve was compared with that of metaldehyde in the single adsorption system (Figure 4.21). In the first 5 min, both HA and metaldehyde were rapidly adsorbed onto PAC. However, after that, adsorption of metaldehyde slowed down significantly and trended towards equilibrium. Adsorption of HA was not as fast as metaldehyde over the first 5 min, but it kept increasing at a steady, slower rate. At the end of the 120 min, 21.6% of HA was removed. Interestingly, the trend of adsorption of HA onto PAC over the shorter timescale (from 0 to 120 min) was very similar to the trend over the longer timescale (from 0 to 30 days).

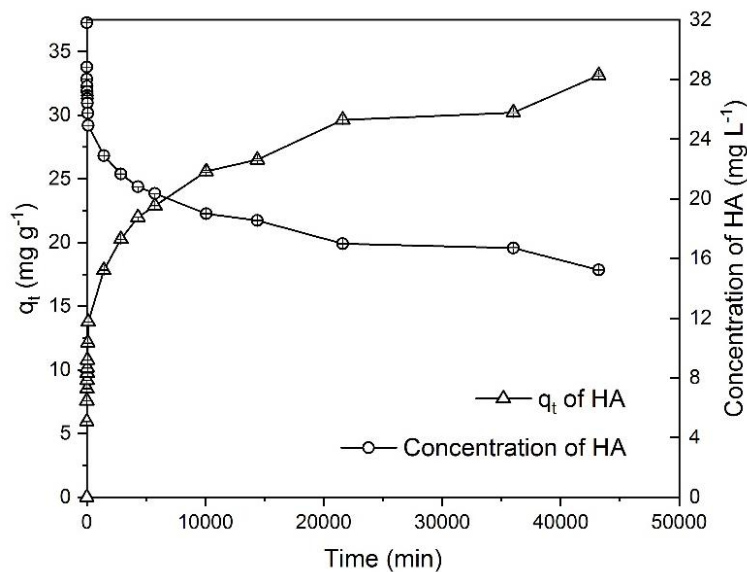


Figure 4.21 Comparison of adsorption of metaldehyde and HA onto PAC in 2 h in the single adsorption system ($N = 9$ for metaldehyde, $N = 3$ for HA, error bars showing SD)

Zhang *et al.* found similar behaviour of HA during the adsorption process onto modified aged refuse; they argued that the adsorption process of HA is via slow diffusion [193]. As discussed in Section 4.1, since HA is a distribution of molecules and it has a much larger chemical structure than metaldehyde [194], the diffusion process for HA onto PAC is therefore much slower, due to the PSD of the PAC used in this study. Compounds with small structures such as metaldehyde may prefer adsorption onto the abundant micropores on this PAC, while compounds with large structures such as HA may prefer adsorption onto less abundant macropores on this PAC. The adsorption of HA onto PAC may slow down after the easily accessed macropores on the surface of PAC are occupied; then HA molecules would continuously slowly diffuse from the surface to the inner pores of PAC [193]. Moreover, the slow adsorption of HA can also be explained by the low driving force for a low concentration gradient. Zhang *et al.* argued that the diffusion process may be further slowed down due to the gradual

decrease of HA concentration in the solution and gradual increase of HA concentration on the adsorbent surface [193].

4.3.3.3 Adsorption kinetic studies of HA in the single adsorption system

As discussed in Section 4.3.3.2, it was found that the adsorption of HA onto PAC did not reach equilibrium in 30 days. Therefore, the Freundlich and Langmuir adsorption isotherm models and the pseudo-first order kinetic model cannot be applied to the data since these models require the adsorption system to reach equilibrium and give the values of C_e and q_e . However, data from Section 4.3.3.2 could be fitted to the pseudo-second order kinetic model, which only requires the value of q_t and does not necessarily require the adsorption system to reach equilibrium; it can also reproduce the diffusion-driven adsorption process very well [186]. Figure 4.22 shows the data fitted to the pseudo-second order kinetic model.

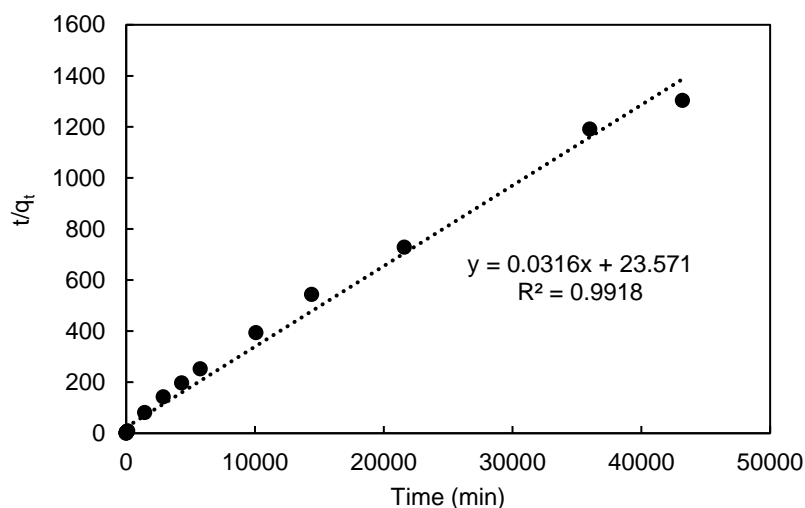


Figure 4.22 The pseudo-second order kinetic fitting of 30 mg L⁻¹ metaldehyde with 0.25 g PAC in the 2-h treatment time

Data were well fitted to the pseudo-second order kinetic model with $R^2 = 0.9918$, suggesting that adsorption mechanisms of HA onto the PAC used in this study could be explained as diffusion-driven. And it benefits from the relatively fast surface adsorption in the beginning. Calculated q_e is 31.65 mg g⁻¹ while q_t at the end of 30 days is 33.14 mg g⁻¹. This implies the system would have reached equilibrium with a q_e of 31.65 mg g⁻¹ in 30 days, if the system followed the pseudo-second order model completely. The value of k_2 is 4.23×10^{-5} g mg⁻¹ min⁻¹, indicating a very slow adsorption rate compared to that of metaldehyde.

The adsorption kinetic study of HA was compared with other studies. For example, Capasso *et al.* studied the adsorption of HA on zeolitic tuffs which are mineral-rich volcanic tuff, namely the phillipsite-/chabazite-rich Neapolitan Yellow Tuff and a clinoptilolite-rich tuff from Turkey [195]. Capasso *et al.* argued that there was fast adsorption of HA onto zeolitic tuffs at first, then it reached a pseudo steady-state in 4 days; however, the removal of HA increased again and reached equilibrium in 60 days

[195]. The trend reported by them and the trend of HA adsorbed onto the PAC in this study share some similarities. Figure 4.20 demonstrates that 29% of HA was removed in the first day and 50% of HA was removed at 30 days in this study, while Capasso *et al.* found 50% removal of HA on the first day and 96% removal of HA at the end of their experiment (60 days). They suggested that the absorption of HA has two routes; one of them occurs over 3 to 10 days, and the other occurs over 60 days [195]. This may explain the observed two-step behaviour regarding the adsorption of HA onto PAC. In addition, the two-step behaviour also resembles the diffusion-controlled adsorption model that has two pore diffusion rates, as discussed in Section 4.3.2.4.

Moreover, Kołodziej *et al.* used modified ACs with different pH_{pzc} for removing HA from water by adsorption; they suggested that adsorption of HA seems to favour adsorbents with relatively low or neutral pH_{pzc} [196]. Since HA is a mixture of molecules and it has different fractions, Kołodziej *et al.* analysed two fractions of HA, brown and gray HA [196]. According to Baigorri *et al.*, brown HA is soluble under alkaline conditions independent of ionic strength, while gray HA is soluble under alkaline condition and low ionic strength [197]. The research of Kołodziej *et al.* showed that the adsorption of brown HA and gray HA onto two types of ACs modified by ammonization (AC/N) and hydrogen treatment (AC/H) have reached equilibrium in 100 h. Figure 4.20 presents a similar trend to their research regarding the adsorption of brown HA and gray HA onto the modified ACs. In addition, adsorption of both fractions of HA reached equilibrium around 70 h by the mesoporous AC (AC0) without modification. In their study, AC/N and AC/H have pH_{pzc} of 7.5 and 8.5, respectively. These values are quite similar to the pH_{pzc} of the PAC used in this study (7.35). They all carry negative surface charges under a more alkaline condition. Nevertheless, AC0 has a pH_{pzc} of 6.7, which suggests that adsorption of HA indeed seems to favour adsorbents with relatively low

pH_{pzc}. In terms of kinetic analysis, Kołodziej *et al.* found q_e is 32.89 mg g⁻¹ for adsorption of brown HA onto AC/H using the pseudo-second order model, which is very similar to 31.65 mg g⁻¹ obtained in this study. However, their k_2 value is 9.57×10⁻³ g mg⁻¹ min⁻¹, much higher than the k_2 obtained in this study, because adsorption of HA reached equilibrium in a shorter time in their study [196].

4.3.4 Removal of metaldehyde in the binary adsorption system (competitive adsorption)

4.3.4.1 Effect of the initial concentrations of HA

To study the removal of metaldehyde in the binary adsorption system, the concentrations of HA were 3, 9, 15, 30, 60, and 90 mg L⁻¹, while the concentration of metaldehyde was fixed at 1 mg L⁻¹, in the multi-component solutions (500 mL); these concentrations correspond to the metaldehyde/HA molar ratios of 1/23, 1/70, 1/117, 1/233, 1/468, and 1/704, respectively. Figure 4.23 shows that metaldehyde was effectively removed in the binary adsorption system, with different initial concentrations of HA after PAC treatment (competitive adsorption). Table 4.7 presents the removal of metaldehyde and HA in the binary adsorption system. 90.2% of metaldehyde was removed, even with a very high initial concentration of HA (90 mg L⁻¹). This finding suggests that the presence of HA does not significantly affect the removal of metaldehyde by PAC in the binary adsorption system. The removal of metaldehyde decreased from 98.6 to 90.2%, with the concentration of HA increased from 3 to 90 mg L⁻¹. And the removal of HA was moderately effective in the binary adsorption system with $C_0 = 3$ mg L⁻¹, and there was no effective removal of HA with $C_0 > 3$ mg L⁻¹.

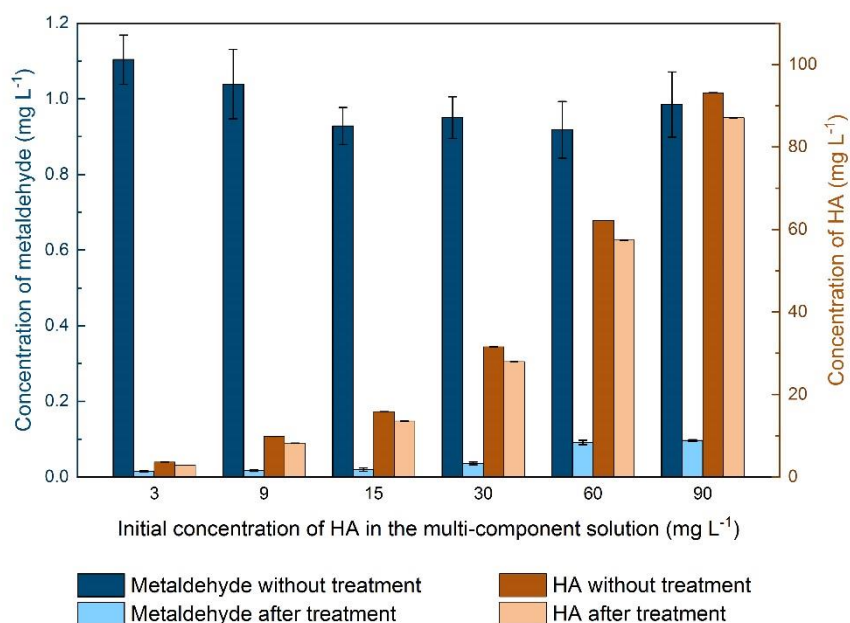


Figure 4.23 Concentrations of metaldehyde and HA in the binary adsorption system without and after PAC treatment, with different initial concentrations of HA while initial concentration of metaldehyde was fixed to be 1 mg L⁻¹ ($N = 9$ for metaldehyde, $N = 3$ for HA, error bars showing SD)

Table 4.7 Removal of metaldehyde and HA by PAC in the binary adsorption system ($N = 9$ for metaldehyde, $N = 3$ for HA)

Metaldehyde				HA			
C_0 (mg L ⁻¹)	C_{t-2h} (mg L ⁻¹)	Removal (%)	p -value	C_0 (mg L ⁻¹)	C_{t-2h} (mg L ⁻¹)	Removal (%)	p -value
1.1 ± 0.06	0.02	98.6 ± 0.2	1.24E-18	3.62 ± 0.01	2.88 ± 0.01	20.5 ± 0.4	1.98E-07
1.04 ± 0.09	0.02	98.4 ± 0.3	8.48E-16	9.82 ± 0.03	8.22	16.3 ± 0.3	2.71E-07
0.93 ± 0.05	0.02	97.8 ± 0.4	2.53E-18	15.88	13.53 ± 0.01	14.8	6.53E-11
0.95 ± 0.05	0.04	96.2 ± 0.5	1.37E-18	31.55 ± 0.01	27.98	11.3	1.11E-10
0.92 ± 0.07	0.09 ± 0.01	89.9 ± 1.3	9.76E-16	62.22 ± 0.01	57.42 ± 0.01	7.7	1.34E-10
0.99 ± 0.09	0.1	90.2 ± 0.9	1.31E-14	93.12 ± 0.02	87.08 ± 0.02	6.5	8.73E-10

4.3.4.2 Effect of adsorption contact time

Figure 4.24 compares the adsorption of metaldehyde (1 mg L^{-1}) using 0.05 g PAC in the single adsorption system (Section 4.3.2.2) and the adsorption of metaldehyde (1 mg L^{-1}) and HA (30 mg L^{-1}) using 0.05 g PAC in the binary adsorption system. Adsorption of metaldehyde in the binary adsorption system was only slightly lower and slower than in the single adsorption system. They both showed the same trend of fast adsorption in the first 5 min and quite slow adsorption after 5 min; the adsorption of metaldehyde in both systems plateaued at 30 min, approaching equilibrium with higher than 98% removal of metaldehyde in the end.

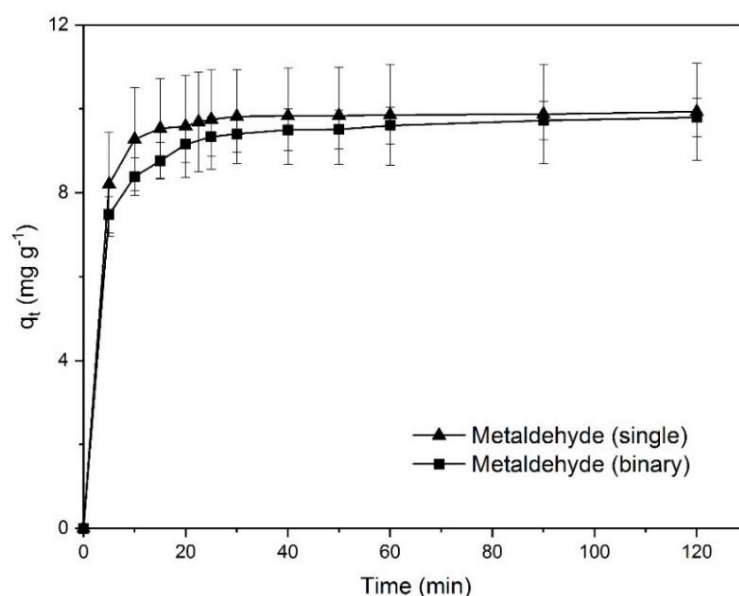


Figure 4.24 Effect of time on adsorption of metaldehyde (1 mg L^{-1}) with 0.05 g PAC in the single adsorption system and adsorption of metaldehyde (1 mg L^{-1}) and HA (30 mg L^{-1}) with 0.05 g PAC in the binary adsorption system ($N = 9$, error bars showing SD)

4.3.4.3 Adsorption kinetic studies of metaldehyde in the binary adsorption system

The pseudo-first order and the pseudo-second order kinetic models were applied to adsorption of metaldehyde onto PAC in the binary adsorption system. Figure 4.25 presents data fitted to the pseudo-first order model. Although data were not very well fitted ($R^2 = 0.8192$), this fitting is better than the pseudo-first order model fitting of metaldehyde in the single adsorption system, which has a R^2 value of 0.6532. Compared with Figure 4.13 in Section 4.3.2.4, the trend line in Figure 4.25 does not show a clear two-gradient trend. The intercept gives a theoretical q_e value of 2.49 mg g^{-1} and the slope gives k_1 value of 0.04 min^{-1} . The k_1 value is slightly lower than the one obtained in the single adsorption system (Section 4.3.2.4), due to the presence of HA.

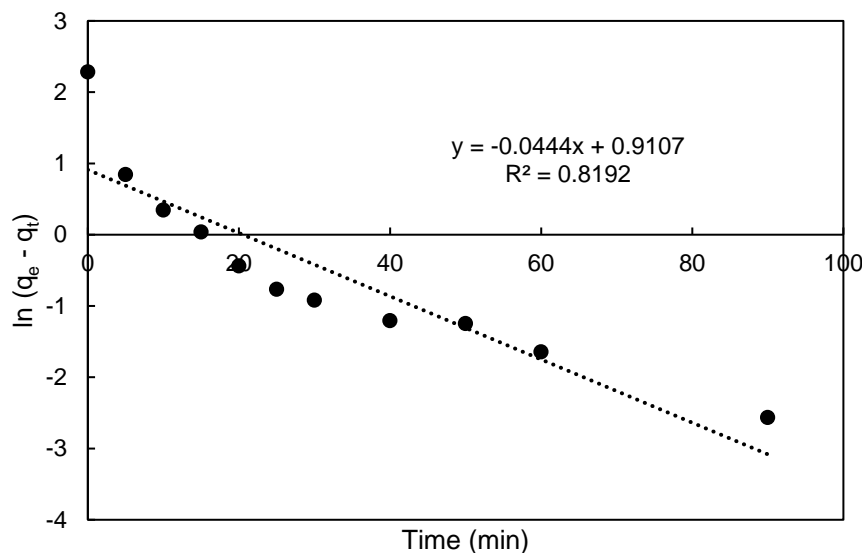


Figure 4.25 The pseudo-first order kinetic model fitting for metaldehyde adsorption onto PAC in the binary adsorption system of 1 mg L^{-1} metaldehyde and 30 mg L^{-1} HA with 0.05 g PAC in the 2-h treatment time

As shown in Figure 4.26, data were very well fitted to the pseudo-second order model ($R^2 = 0.9998$), with a calculated q_e of 9.88 mg g^{-1} which is very close to the experimental value of 9.8 mg g^{-1} . k_2 is $0.07 \text{ g mg}^{-1} \text{ min}^{-1}$ which is less than half of the k_2 obtained for metaldehyde in the single adsorption system. This confirmed that the adsorption rate of metaldehyde is slower in the binary adsorption system because of the presence of HA.

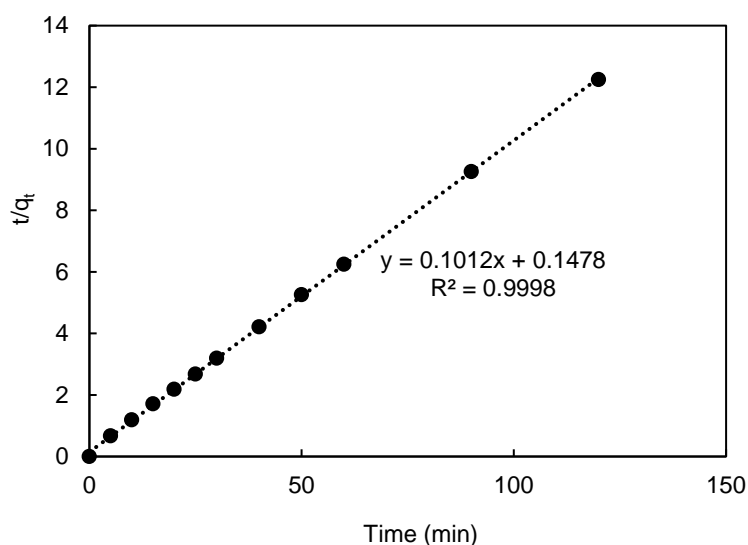


Figure 4.26 The pseudo-second order kinetic model fitting for metaldehyde adsorption onto PAC in the binary adsorption system of 1 mg L^{-1} metaldehyde and 30 mg L^{-1} HA with 0.05 g PAC in the 2-h treatment time

4.3.5 Adsorption mechanisms of metaldehyde and HA onto PAC

In general, the PAC used in this chapter was very effective to remove metaldehyde from aqueous solutions, especially in the single adsorption system. Combined with the BET SSA analysis, effective removal of metaldehyde could be explained by the characteristics of the PAC used in this chapter. The SSA of the PAC used is quite large ($962.4 \text{ m}^2 \text{ g}^{-1}$) and it is dominated by micropores with abundant mesopores present. According to Busquets *et al.*, adsorption of metaldehyde could be greatly

enhanced with carbon materials that are highly microporous with the presence of mesopores assisting diffusive transport [30].

In this chapter, the average removal of metaldehyde in the binary system of 500 mL of metaldehyde (1 mg L^{-1}) and HA (30 mg L^{-1}) was around 97.5% using 0.05 g PAC (dosing concentration of 100 mg L^{-1}), while Nguyen *et al.* found 94% average removal of 25 mg L^{-1} metaldehyde in surface water and tap water, via modified Fenton's process using 100 mg L^{-1} graphene oxide and 1% H_2O_2 . In both researches, the presence of HA only slightly affected the removal of metaldehyde [122]. Nguyen *et al.* argued that this is due to the limited adsorption capacity of graphene oxide for background organic matter or the oxidation process takes place very quickly before the active sites of graphene oxide become occupied [122]. In this chapter, compared to metaldehyde, HA was not effectively removed by the PAC used. Moreover, when increasing the proportion of HA in the binary system, the removal of metaldehyde was only slightly affected. This could be explained by the PSD of the PAC used. Micropores and mesopores are suitable for adsorbing small-sized compounds with a stable structure such as metaldehyde. On the other hand, HA is a large and complex compound which has a variety of molecules [198]; it may not fit in the micropores of this PAC. The average 10-20% removal of HA in the 2-h treatment time could be explained by the attachment of HA molecules to the surface and limited macropores of PAC. The continuous slow removal of HA in 30 days (Section 4.3.3.2) could result from the slow diffusion of HA molecules from macropores to mesopores. Hence, under the studied experimental conditions, HA is not considered as a competitive compound that would compete with metaldehyde for adsorption onto PAC.

Table 4.8 demonstrates the kinetic constants analysed for metaldehyde and HA in both systems. The adsorption rate (k_2) of 0.16 g mg⁻¹ min⁻¹ for metaldehyde in single system is much higher than the k_2 of GAC (8×10⁻⁵ g mg⁻¹ min⁻¹) used by Salvestrini *et al.*, and the k_2 of GAC (5.8×10⁻⁴ g mg⁻¹ min⁻¹) used by Tao and Fletcher [70, 141]. This suggests that under the studied experimental condition, adsorption of metaldehyde onto PAC in the single adsorption system is quite fast. Additionally, k_2 of 0.07 g mg⁻¹ min⁻¹ for metaldehyde in the binary adsorption system is lower, indicating HA moderately affects the adsorption rate of metaldehyde in the binary adsorption system, and it may prolong the time for the adsorption of metaldehyde onto PAC to reach equilibrium.

Table 4.8 Adsorption kinetic constants of metaldehyde and HA

	Kinetic constants	
	k_1 (min ⁻¹)	k_2 (g mg ⁻¹ min ⁻¹)
Metaldehyde (single)	0.05	0.16
HA (single)	N/A	4.23×10 ⁻⁵
Metaldehyde (binary)	0.04	0.07

Regarding the adsorption isotherm study of metaldehyde in the single adsorption system, the Langmuir isotherm model is relatively more suitable for fitting the experimental data. The maximum adsorption capacity of PAC for metaldehyde obtained from the Langmuir isotherm model is 28.33 mg g⁻¹, which is much higher than the 15 mg g⁻¹ of GAC used by Busquets *et al.* [30].

Additionally, the surface groups of PAC may contribute to the effective removal of metaldehyde as well. In fact, the mechanism regarding the interactions of pollutants with the surface groups of AC is complex. The interactions depend on the nature of the compound (such as metaldehyde) and the surface groups of the adsorbent (such as PAC); the state of their ionization and the pH of the medium are also important. For example, Ferino-Pérez *et al.* studied the interactions between metaldehyde and acidic surface groups of AC under different pH conditions via computational modelling [42]. Due to the limited timescale and scope of this thesis, it is suggested by the researcher to discuss this aspect further and confirm the conclusion of Ferino-Pérez *et al.* via experimental investigations [42].

4.4 Summary

Metaldehyde could be effectively removed from aqueous solutions by the PAC used in this chapter, with a maximum adsorption capacity (q_m) of 28.33 mg g⁻¹ in the single adsorption system. And it could reach equilibrium with an adsorption rate (k_2) of 0.16 g mg⁻¹ min⁻¹ under the studied experimental condition, in the single adsorption system as well. Adsorption of metaldehyde onto PAC, with a pH_{pzc} value of 7.35, was slightly more effective under alkaline conditions. HA could not be effectively removed by the PAC used in this chapter, with a maximum percentage removal of 50% in 30 days using 500 mL of 30 mg L⁻¹ HA solution and 0.25 g of PAC in the single adsorption system. Furthermore, it could take a very long time to reach equilibrium; presumably more than 30 days. The presence of HA in the binary adsorption system did not significantly affect the amount of metaldehyde adsorbed onto the PAC used in this chapter, but it slightly slowed down the adsorption. This could be explained by the fact that small metaldehyde molecules would prefer the abundant micropores and

mesopores of PAC, while large and complex HA molecules would only attach to the surface of PAC or adsorbed onto the relatively less common macropores of PAC. Adsorption of metaldehyde onto the PAC used in this chapter could be better described by the Langmuir isotherm model and the pseudo-second order kinetic model. This suggests that the adsorption process can be explained by the attachment of a single layer of metaldehyde molecules onto the surface of PAC; and it is promoted by fast surface reactions during the intraparticle diffusion process. Surface characteristics are significant for the effective removal of metaldehyde by PAC. For example, the fact that the PSD of the PAC used in this chapter is in the micro-/meso-pores range, this leads to the fast adsorption of metaldehyde onto PAC. This was confirmed by fitting the experimental data to the pseudo-second order kinetic model. Understanding the adsorption mechanisms of metaldehyde by PAC contributes to enhancing the potential application of PAC in drinking water treatment plants. For example, fast adsorption of metaldehyde by PAC suggests that the contact time required for PAC to remove metaldehyde from water may be within the industrial timescale of water treatment processes.

Since the presence of HA did not affect the removal of metaldehyde in the binary adsorption system by the PAC used in this study under the studied experimental condition, drinking water treatment plants may consider applying PAC for removing metaldehyde. For example, PAC can potentially be applied before flocculation, flotation, and filtration, depending on the configuration of the treatment plant. Therefore, the thesis further investigated the effect of water quality on the removal of metaldehyde by PAC, using the water samples collected from different water treatment stages at Walton-on-Thames Water Treatment Works.

Chapter 5. Investigation of metaldehyde removal from different water samples by PAC

5.1 Introduction

Results from Chapter 3 and Chapter 4 showed that PAC can remove metaldehyde from water effectively and efficiently, even with the presence of NOM; and it was more effective for removing metaldehyde, compared with the nanoparticle photocatalysts studied in Chapter 3 [69, 199]. Therefore, PAC has the potential of being applied in drinking water treatment plants. However, considering that it could be applied in any treatment stages between water intake and filtration, it is important to understand which treatment stage could be the best dosing position of PAC.

This chapter aimed to investigate the appropriate dosage of PAC for removing metaldehyde from the water samples collected from Walton-on-Thames Water Treatment Works (WTWTW) and identify the best treatment stage to dose PAC for removing metaldehyde at WTWTW. This chapter also illustrated the potential application of PAC in a real water treatment plant to remove metaldehyde, considering the possible regeneration of used PAC at a relatively low temperature of 60 °C. As there are NOM molecules present in natural water, background organic interference on the detection of metaldehyde by GC-MS was also analysed in this chapter. The specific objectives of this chapter are: (1) to study the effect of PAC dosage on the removal of metaldehyde in water at an environmentally relevant concentration; (2) to identify the best treatment stage at WTWTW to dose PAC for removal of metaldehyde; (3) to study the effect of water quality on the removal of metaldehyde by PAC; (4) to study the effect of initial concentrations regarding the adsorption mechanisms of

metaldehyde onto PAC; and (5) to study possible desorption of metaldehyde from used PAC back to water and possible regeneration of used PAC at a low temperature.

5.2 Materials and methods

In this chapter, all the experiments and analyses were conducted in the Environmental Engineering Laboratory at UCL, unless stated otherwise. Considering the potential application of PAC in drinking water treatment plants, the studied concentration of metaldehyde working solution was $5 \mu\text{g L}^{-1}$, since it is close to the detected value of $8 \mu\text{g L}^{-1}$ in surface water by the UK Environment Agency, and it can represent the concentration of metaldehyde in raw water during peak season of metaldehyde usage [11, 74]. Correspondingly, the dosing concentration of PAC for removing metaldehyde was lowered to the ' mg L^{-1} ' range due to the lower concentration of metaldehyde working solution used in this chapter. Therefore, the concentration of metaldehyde was studied in the ' $\mu\text{g L}^{-1}$ ' range (using the unit of ' $\mu\text{g L}^{-1}$ '), while the dosing concentration of PAC was studied in the ' mg L^{-1} ' range (using the unit of ' mg L^{-1} ') in this chapter.

5.2.1 Materials

Different water samples, including synthetic water (MilliQ water and MilliQ water with HA), water collected from different treatment stages at WTWTW, and surface water collected from the Regent's Park lake, were used for investigating the removal of metaldehyde by adsorption onto PAC. It is noted that metaldehyde was not present in the water samples collected from WTWTW and the Regent's Park lake. Metaldehyde PESTANAL (analytical grade), PAC and humic acid sodium salt (technical grade H16752) were purchased from Sigma-Aldrich. HPLC grade methanol and HPLC grade

DCM were purchased from Fisher Scientific. Laboratory grade ultrapure MilliQ water was used, dispensed from the ultrapure water filter/dispenser, manufactured by Purolite Corporation (dispensed at room temperature).

5.2.1.1 Description of site: Walton-on-Thames Water Treatment Works

Walton-on-Thames Water Treatment Works is located on Hurst Road, Surrey, KT12 2EG (Figure 5.1). The reservoir that stores water feeding WTWTW is derived from the River Thames. The output of treated water from WTWTW varies from 50 to 135 Million Litres per Day (MLD), depending on the season.



Figure 5.1 Location of Walton-on-Thames Water Treatment Works (Coordinates: 51.404292, -0.400001; obtained from Google satellite image)

There are six main treatment stages at WTWTW, Figure 5.2 illustrates the process of each treatment stage and its contact time: (1) 'pre-ozone contactors', which feed ozone to oxidize and break down organic pollutants; (2) 'static flocculation', which uses

chemical dosing with ferric sulphate and polyelectrolyte as coagulant aid to trap natural organic matters as flocs; (3) 'counter-current dissolved air flotation (CoCoDAF) units', with a bottom layer filter of 600 mm sand (effective size 0.7 mm) and 600 mm of anthracite, which feed air to removal flocs formed at the previous stage and small particles in the water; (4) 'main ozone contactors', which feed ozone to further break down any residual organic pollutants; (5) 'GAC adsorbers', which remove any small particles and pollutants that are difficult to be removed by oxidation; and (6) 'series of screens and a contact tank', which disinfect the water before entering the mains, including dosing sodium hypochlorite as disinfectant firstly, then adjusting chlorine residue by adding more sodium hypochlorite or sodium bisulphate, and dosing ammonium sulphate in the end.

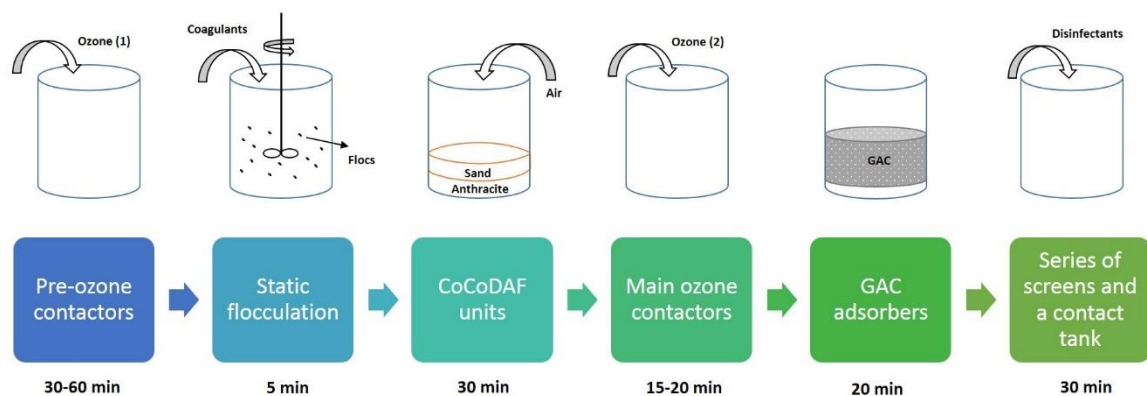


Figure 5.2 Illustration of the six main treatment stages at WTWTW and the approximated contact time of each stage

Water samples were collected at the end of each stage and securely sealed into 1 L plastic bottles by professional personnel from Thames Water. Water samples were then immediately transported to the Environmental Engineering Laboratory at UCL and stored in a fridge at 4 °C. All water samples were collected at WTWTW on 5th September 2018; and the overall treated water output was 50 million L on that day.

Considering the water treatment processes installed at WTWTW and the separation of PAC from the treated water (possibly towards the end of the treatment processes), PAC can potentially be applied after any treatment stage before 'GAC adsorbers'. Hence, this chapter did not consider the dosing of PAC after 'GAC adsorbers' since it would require additional installations to separate PAC from the treated water, leading to extra cost. Also, this chapter did not consider applying PAC before 'pre-ozone contactors' because Thames Water did not provide the raw water.

5.2.1.2 Description of site: the Regent's Park lake

The Regent's Park lake is located at Chester Road, London, NW1 4NR. It is a boating lake and is inhabited by aquatic animals including ducks and geese. Since the effect of water quality on the removal of metaldehyde by PAC is investigated in this chapter, water samples from the Regent's Park lake were collected to represent surface water. Figure 5.3 (A) shows the location of the Regent's Park lake and Figure 5.3 (B) shows the location where the water samples were collected. 8 L of water samples were collected on 3rd July 2018; they were immediately transported to the Environmental Engineering Laboratory at UCL and stored in a fridge at 4 °C.

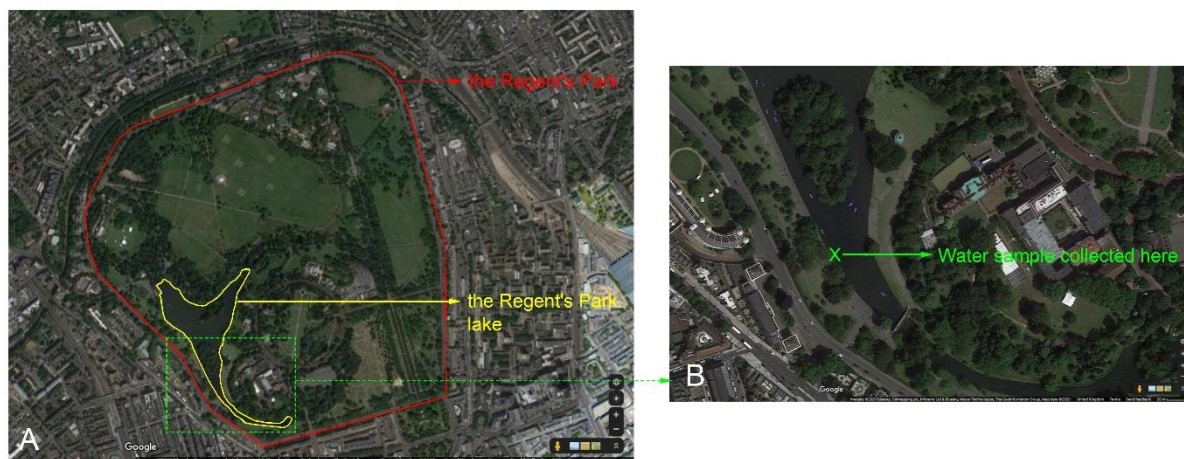


Figure 5.3 (A) The Regent's Park lake; and (B) the location where water samples were collected (Coordinates: 51.525510, -0.158351; obtained from Google satellite image)

5.2.2 Analysis of water characteristics

Water characteristics of different water samples, including DOC which was measured as non-purgeable organic carbon (NPOC), ions, dissolved oxygen (DO), pH, conductivity/ total dissolved solids (TDS), turbidity, and absorbance at 254 nm wavelength (UV_{254}), were analysed by Shimadzu total organic carbon analyser (TOC-L), Dionex ICS-1100, Jenway DO2 Meter 9200, pH/conductivity meter SevenMulti, Mettler Toledo, HACH 2100AN IS Turbidimeter (ISO method 7027), and Agilent Technologies Cary 60 UV-Vis, respectively. The concentration of HA in water was determined by Agilent Technologies Cary 60 UV-VIS spectrophotometer at 254 nm wavelength, following the same procedure described in Section 4.2.5. All calibration rates of HA in this chapter were within the acceptable range of $100 \pm 20\%$, with RSD $< 20\%$.

5.2.3 Material characterization techniques

In this chapter, ATR-FTIR and SEM analyses were performed for the following three samples in the Chemistry Department at UCL:

- (1) Floccs in the water collected after 'static flocculation';
- (2) 30 mg of the PAC sample (PAC-SF) which was dosed in 600 mL of 5 $\mu\text{g L}^{-1}$ metaldehyde working solution prepared using the water collected after 'static flocculation' for 30 min;
- (3) 30 mg of the PAC sample (PAC-RP) which was dosed into 600 mL of 5 $\mu\text{g L}^{-1}$ metaldehyde working solution prepared using the water collected from the Regent's Park lake for 30 min.

Flocs and PAC were filtered via 0.45 μm membrane and dried at room temperature for 24 h before analysis. These three specific samples were selected because there were suspended solids in the water collected from the Regent's Park lake and pre-existing floccs in the water collected after 'static flocculation'.

ATR-FTIR and SEM analyses could provide further insight into the relationships of floccs, PAC, and suspended solids in natural water. ATR-FTIR analysis was performed on Platinum Attenuated Total Reflection (Bruker), which has a diamond crystal as the internal reflective component. Samples were measured in the wavenumber region of 4000 to 400 cm^{-1} (correspond to wavelengths from 2.5 to 25 μm), with 128 scans and a spectral resolution of 2 cm^{-1} . And SEM analysis was performed on JSM-6701F Field Emission Scanning Electron Microscope at 10 kV under secondary electron imaging mode.

5.2.4 Preparation of metaldehyde solutions

100 mL of metaldehyde stock solution at 500 mg L⁻¹, 100 mL of metaldehyde calibration stock solution at 500 mg L⁻¹, and 500 mL of HA stock solution at 1000 mg L⁻¹ were prepared following the methods described in Section 3.2.3 and Section 4.2.3.

0.2 mL of metaldehyde stock solution was measured by a 2 mL graduated glass pipette (uncertainty of ± 0.01 mL) with an electrical pipette controller and added into a 100 mL volumetric flask (uncertainty of ± 0.1 mL); MilliQ water was added into the flask to make 100 mL of 1 mg L⁻¹ metaldehyde solution in MilliQ water. In this step, metaldehyde stock solution in methanol was diluted by MilliQ water to an intermediate concentration (1 mg L⁻¹). This was to minimize the effect of methanol (presence in the metaldehyde stock solution), as an organic compound, on the analyses of water characteristics (such as DOC) of water samples that were spiked with metaldehyde.

Different volumes of the metaldehyde solution in MilliQ water at 1 mg L⁻¹ were measured and diluted by different water samples to prepare metaldehyde working solutions at different concentrations. For example, 600 mL of metaldehyde working solution at 5 μ g L⁻¹ was prepared using the water collected after 'pre-ozone contactors', following this procedure: 600 mL of the water collected after 'pre-ozone contactors' was measured by two 500 mL graduated glass cylinders (uncertainty of ± 2.5 mL) and added into a 1 L glass beaker; 3 mL of the water sample was removed from the beaker by a 5 mL Gilson pipette (uncertainty of ± 0.05 mL) and discarded; then, 3 mL of the metaldehyde solution in MilliQ water at 1 mg L⁻¹ was measured by a 5 mL Gilson pipette (uncertainty of ± 0.05 mL) and added into the beaker; the solution was then mixed by hand using a glass rod for 30 s.

For experiments that studied the effect of initial concentrations of metaldehyde working solutions on the removal of metaldehyde by PAC, different volumes of the metaldehyde solution in MilliQ water at 1 mg L^{-1} were measured and diluted by MilliQ water to prepare metaldehyde working solutions at 1, 5, 10, and $50 \text{ } \mu\text{g L}^{-1}$. For example, 1 mL of the metaldehyde solution in MilliQ water at 1 mg L^{-1} was measured by a 1 mL Gilson pipette (uncertainty of $\pm 0.01 \text{ mL}$) and added to a 1000 mL volumetric flask (uncertainty of $\pm 0.4 \text{ mL}$); MilliQ water was added to the flask to make 1000 mL of $1 \text{ } \mu\text{g L}^{-1}$ metaldehyde working solution. And in the same study, different volumes of metaldehyde stock solution were measured and diluted by MilliQ water to prepare metaldehyde working solutions at 100 and $1000 \text{ } \mu\text{g L}^{-1}$. For example, 2 mL of metaldehyde stock solution was measured by a 2 mL graduated glass pipette (uncertainty of $\pm 0.01 \text{ mL}$) with an electrical pipette controller and added into a 1000 mL volumetric flask (uncertainty of $\pm 0.4 \text{ mL}$); MilliQ water was added to the flask to make 1000 mL of $1000 \text{ } \mu\text{g L}^{-1}$ metaldehyde working solution.

5.2.5 Adsorption experiments

All experiments were performed as batch tests using 1 L glass beakers and analyses were performed as triplicates (three data points, $N = 3$), unless stated otherwise. Considering the practical scenario of dosing PAC in drinking water treatment plants, PAC was added into metaldehyde solutions as slurry [200], which was different from Chapter 3 and Chapter 4. PAC slurry was prepared by adding 1.5 g of PAC into 50 mL of MilliQ water (30000 mg L^{-1}). Thus, there was 30 mg of PAC in 1 mL of PAC slurry. Prior to dosing PAC to metaldehyde working solutions, the PAC slurry was well shaken by hand for 20 s to ensure its uniformity and dosed into the metaldehyde working solutions immediately. As soon as PAC was dosed, the metaldehyde working

solution was continuously stirred by a magnetic stirrer for the whole treatment time. This is to ensure that PAC was well mixed and evenly distributed in the solution.

The contact time for all adsorption experiments in this chapter was 30 min. As discussed in Section 4.3.2.2, adsorption of metaldehyde by PAC was fast in the first 5 min and plateaued around 30 min, while approaching equilibrium. In addition, the 30-min contact time also suits the industrial timescale of water treatment stages and allows the removal of metaldehyde to approach equilibrium, as mentioned in Section 5.2.1.1 (Figure 5.2). At the end of 30 min, the solutions were filtered by 0.45 μm Whatman cellulose nitrate membrane to remove suspended PAC. 500 mL of the solutions was used for SPE and analysis of metaldehyde, while the remaining 100 mL was used for water characteristics analyses. The percentage removal of metaldehyde and the amount of metaldehyde adsorbed onto PAC was calculated using Equation 3.1, Equation 3.2, and Equation 3.3, respectively.

To investigate the removal of metaldehyde from different water samples, four sets of adsorption experiments were carried out:

(1) To identify the suitable PAC dosing concentration to remove metaldehyde from the first treatment stage, i.e. after 'pre-ozone contactors':

Different PAC dosing concentrations, 0.05, 0.25, 0.5, 5, 25, 50, 100, and 150 mg L^{-1} , were applied to 600 mL of 5 $\mu\text{g L}^{-1}$ metaldehyde working solutions prepared using the water collected after 'pre-ozone contactors' at WTWTW.

(2) To compare the removal of metaldehyde by PAC at different treatment stages and identify the best treatment stage to dose PAC, as well as to determine the maximum adsorption capacity (q_m) of PAC for metaldehyde at that stage:

- PAC (dosing concentration of 50 mg L^{-1}) was applied to 600 mL of $5 \text{ } \mu\text{g L}^{-1}$ metaldehyde working solutions prepared using the water samples collected after 'pre-ozone contactors', 'static flocculation', 'CoCoDAF units', and 'main ozone contactors' at WTWTW. After this experiment, the highest removal of metaldehyde was found by dosing PAC into the water collected after 'static flocculation'.
- To determine the q_m of PAC for metaldehyde in the water collected after 'static flocculation', different dosing concentrations of PAC, 5, 25, 50, 100, and 150 mg L^{-1} , were added into 600 mL of $5 \text{ } \mu\text{g L}^{-1}$ metaldehyde working solutions prepared using the water collected after 'static flocculation'.

(3) To compare the removal of metaldehyde by PAC from different water samples and to determine the effect of water quality on adsorption of metaldehyde onto PAC:

PAC (dosing concentration of 50 mg L^{-1}) was applied to 600 mL of $5 \text{ } \mu\text{g L}^{-1}$ metaldehyde working solutions prepared using MilliQ water, MilliQ water with HA, the water collected from the Regent's Park lake, after 'static flocculation', 'CoCoDAF units', and 'main ozone contactors' at WTWTW. All water samples without and after 30 min of PAC treatment were analysed for water characteristics including pH, conductivity, TDS, fluoride, chloride, nitrate, NPOC, UV_{254} , and concentration of metaldehyde.

(4) To study the adsorption mechanisms of metaldehyde onto PAC with different initial concentrations of metaldehyde working solutions:

PAC (dosing concentration of 50 mg L^{-1}) was applied to 600 mL of metaldehyde working solutions prepared using MilliQ water with different initial concentrations (1, 5, 10, 50, 100, and $1000 \text{ } \mu\text{g L}^{-1}$), to study the adsorption mechanisms of metaldehyde onto PAC in the single adsorption system.

5.2.6 Desorption and regeneration experiment

It is essential to investigate possible desorption of metaldehyde from used PAC back into the water, since it is helpful for the determination of how often PAC needs to be recycled. Moreover, since Rolph *et al.* discussed that metaldehyde can be thermally degraded at $60 \text{ }^\circ\text{C}$ [74], then the potential regeneration of used PAC at the same temperature may be possible.

A three-stage experiment was performed to study the possible desorption of metaldehyde from used PAC back to water and possible thermal regeneration of used PAC:

(1) A 30-min adsorption stage:

Two sets of 600 mL of metaldehyde working solutions at $1000 \text{ } \mu\text{g L}^{-1}$ were prepared using MilliQ water. PAC (dosing concentration of 50 mg L^{-1}) was applied to each set of the metaldehyde working solution for a 30-min contact time, with constant stirring by a magnetic stirrer to ensure PAC was well-mixed in the solution. After that, PAC was separated from the solution by filtering it through $0.45 \text{ } \mu\text{m}$ membrane and placed on a glass Petri dish. Meanwhile, the concentrations of the filtered metaldehyde solutions (600 mL) after PAC treatment were measured to calculate the amount of metaldehyde adsorbed onto the used PAC ($q_{t-30min}$).

(2) A 24-h regeneration stage:

One set of the used PAC was covered with foil and dried on the counter at room temperature for 24 h. The other set of used PAC was covered with foil and placed in the oven at 60 °C for 24 h.

(3) A 30-min desorption stage:

After both sets of PAC was dried for 24 h, each set of used PAC was added into 600 mL of MilliQ water with constant stirring for 30 min. After the 30-min contact time, PAC was separated from the solution by filtering through 0.45 µm membrane. The two sets of water samples were analysed for the presence of metaldehyde.

5.2.7 Validation of detection of metaldehyde by GC-MS using a modified SPE loading technique

Detection of metaldehyde followed the method described in Section 3.2.5 using GC-MS. Since the concentrations of metaldehyde working solutions were low in this chapter, a different SPE loading technique was used. Instead of 1 mL of metaldehyde sample solution mentioned in step (3) of the SPE process described in Section 3.2.5.1, 500 mL of metaldehyde sample solution was loaded into the SPE cartridge using Dionex AutoTrace 280 at a rate of 5 mL min⁻¹. The whole sample solution loading time was 100 min. Step (9) of the SPE process, described in Section 3.2.5.1, was used to evaporate the eluate to 1 mL using nitrogen gas; this means that the SPE process concentrated the metaldehyde solution 500 times. Using this SPE loading technique enables metaldehyde to be detected by GC-MS, when its concentrations are 500 times lower than 1.5 µg L⁻¹ (the LOD of GC-MS for metaldehyde without concentrating

metaldehyde solution via SPE). For instance, 500 mL of $5 \mu\text{g L}^{-1}$ metaldehyde working solution was loaded into the SPE cartridge; after SPE, 1 mL eluate was collected and analysed by GC-MS. The concentration of the 1 mL eluate would be 2.5 mg L^{-1} if the recovery rate was 100%. Hence, the concentration of metaldehyde solution after SPE and measured by GC-MS would be 500 times higher than its actual concentration. The data presented in this chapter are the actual concentrations of metaldehyde solutions after calibration.

It is essential to validate this modified SPE loading technique for the analysis of metaldehyde. A set of metaldehyde sample solutions, with concentrations at 1, 2, 5, 10, 20, and $50 \mu\text{g L}^{-1}$, were prepared using the water collected from the Regent's Park lake. This water sample was selected as it represents a natural water source and the aim of this chapter was to study the removal of metaldehyde from different water samples with different water quality. Using the modified SPE loading technique, the corresponding concentrations of this set of metaldehyde solutions after SPE would be 0.5, 1, 2.5, 5, 10, and 25 mg L^{-1} , assuming 100% recovery.

Since natural water was used, matrix effect on the detection of metaldehyde by GC-MS was investigated as well. 6 mL of matrix was extracted from 3 L of the water collected from the Regent's Park lake via SPE (without spiking metaldehyde), following the described SPE process in Section 3.2.5.1 and the modified SPE loading technique described in this section: 500 mL of the water sample was loaded into one SPE cartridge, which ended up with 1 mL of elute (the matrix) by the end of the SPE process. This was done six times and 6 mL of matrix was acquired.

Then the prepared set of metaldehyde sample solutions using the water collected from the Regent's Park lake (1 to 50 mg L^{-1}) went through SPE, and they were analysed by GC-MS, together with two sets of metaldehyde calibration solutions as external standards. One set of external standard was prepared by diluting the metaldehyde calibration stock solution (500 mg L^{-1}) using the matrix obtained; the other set was prepared by diluting the metaldehyde calibration stock solution using DCM. Due to the limited matrix available (6 mL), the concentrations of the external standards prepared using the matrix were 0.5 , 1 , 2.5 , 5 , 10 , and 25 mg L^{-1} , which were the same concentrations as the concentrations of the prepared set of metaldehyde sample solutions after SPE (assuming 100% recovery). Since the other set of external standards was prepared using DCM, which was largely available, the concentrations of this set were 0.1 , 0.5 , 1 , 5 , 10 , and 50 mg L^{-1} , which covered the concentration range of the external standards prepared using the matrix. Figure 5.4 presents the two calibration curves obtained.

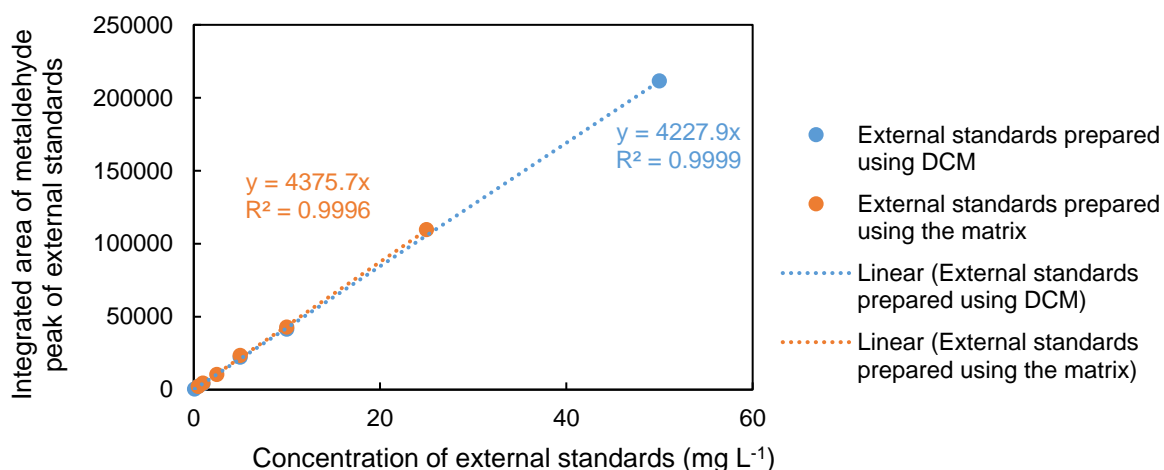


Figure 5.4 Two calibration curves obtained from two sets of external standards

Both calibration curves were very well fitted with the values of R^2 higher than 0.999. Table 5.1 shows the two sets of recovery rates of the metaldehyde solutions (1 to 50 $\mu\text{g L}^{-1}$) calibrated using these two curves.

Table 5.1 Recovery rates of metaldehyde prepared using the water collected from the Regent's Park lake (spiked with metaldehyde), calibrated by the two sets of external standards ($N = 3$)

Concentration ($\mu\text{g L}^{-1}$)	Recovery _{the matrix} (%)	Recovery _{DCM} (%)
1	79.0 \pm 6.4	81.8 \pm 6.7
2	88.0 \pm 8.7	91.1 \pm 9.1
5	104.6 \pm 0.9	108.2 \pm 0.9
10	108.7 \pm 4.3	112.5 \pm 4.4
20	101.5 \pm 1.7	105.1 \pm 1.7
50	110.9 \pm 5.4	114.8 \pm 5.6
<i>p</i> -value	0.65	

An ANOVA single factor statistic test was performed between the two groups of data, Recovery_{the matrix} and Recovery_{DCM}. There was no significant difference between them (p -value > 0.05). Therefore, the detection of metaldehyde by GC-MS was not affected by the matrix effect. Since Recovery_{DCM} at these concentrations were acceptable (within 70-120%) and the detection of metaldehyde was not affected by the matrix effect, external standards in this chapter were prepared using DCM, as described in Section 3.2.3. 5 $\mu\text{g L}^{-1}$ was selected as the working concentration of metaldehyde because: (1) good recovery rates of metaldehyde were found using this concentration; (2) 5 $\mu\text{g L}^{-1}$ is close to the detected concentration of metaldehyde in surface water;

and (3) this concentration is high enough for metaldehyde to be detected after PAC treatments. All recovery rates of metaldehyde in this chapter were within the acceptable range of 70 to 120%, with RSD < 20%.

5.2.8 Presentation and analysis of data

All data were analysed using Microsoft Excel, and they are presented with two digits after the decimal point. Percentages (%) are presented with one digit after the decimal point. Measurements after calibration are presented with standard deviation (SD) shown after the plus/minus symbol (\pm). SD is not presented if smaller than 0.01, unless stated otherwise. For regression analysis, R^2 values, slopes, and intercepts are presented with four digits after the decimal point.

5.3 Results and discussion

5.3.1 Characteristics of different water samples

Water characteristics analyses including pH, conductivity, TDS, negative ions (fluoride, chloride, nitrate), DOC (measured as NPOC), turbidity, DO, UV_{254} were performed for different water samples (without spiking metaldehyde), demonstrated by Table 5.2. Water samples were prepared as duplicates (two data points, $N = 2$). Raw data from the water characteristic analyses for these water samples are presented in Table A.3.1, Appendix A.3.

Table 5.2 Characteristics of different water samples without spiking metaldehyde ($N = 2$)

Water Samples	pH	Conductivity ($\mu\text{s cm}^{-1}$)	TDS (mg L^{-1})	Fluoride (mg L^{-1})	Chloride (mg L^{-1})	Nitrate (mg L^{-1})	NPOC (mg L^{-1})	Turbidity (NTU)	DO (mg L^{-1})	UV ₂₅₄ (cm^{-1})
The Regent's Park lake	8.75	1098	551	1.58	89.20 \pm 1.2	4.51	7.34	0.87	11.45	0.16
After 'pre-ozone contactors'	8.14	592	297	0.13	56.22 \pm 0.03	30.84 \pm 0.05	5.67 \pm 0.06	0.23	7.55	0.08
After 'static flocculation'	6.32	617	310	0.23 \pm 0.11	56.83 \pm 0.29	30.6 \pm 0.04	3.82 \pm 0.01	0.44	7.26	0.06
After 'CoCoDAF units'	7.67	592	298	0.13	56.94 \pm 0.52	31.15	4	0.11	7.28	0.05
After 'main ozone contactors'	7.64	592	298	0.14	56.89 \pm 0.26	31.21 \pm 0.04	3.62 \pm 0.11	0.08	7.95	0.04
After 'GAC adsorbers'	7.43	601	301	0.14	57.22 \pm 0.18	31.48 \pm 0.05	4.14 \pm 0.01	0.09	6.13	0.03
After 'series of screens and a contact tank'	7.39	607	305	0.13	58.1 \pm 0.15	31.57 \pm 0.07	3 \pm 0.05	0.1	6.80	0.03

5.3.2 ATR-FTIR and SEM analyses for flocs, PAC-SF, and PAC-RP

ATR-FTIR analysis was carried out for flocs, PAC-SF, and PAC-RP, based on other studies that showed attachments of adsorbates on the surface of adsorbents. For example, the spectra of chitosan before and after adsorption of dyes from synthetic wastewater presented evidence of the attachment of dyes on chitosan polymer [201]. Spectra of flocs, PAC-SF, and PAC-RP are shown in Figure 5.5. Signature peaks on the spectra of flocs at 3150 cm^{-1} (O-H), 1643 cm^{-1} (amide I: C=O) match the spectra of ferric sulphate which was the added coagulant in 'static flocculation' stage [202]. Spectra of PAC-SF and PAC-RP are similar due to the strong signal of carbon, suggesting that other peaks could be masked by the carbon and therefore less likely to be observed. However, there are a few weak dips around 3150 cm^{-1} and 1370 cm^{-1} on the spectra of PAC-SF, which may indicate the attachment of flocs onto PAC. Spectra of metaldehyde are added in Figure 5.5 for reference; but unfortunately as discussed in Section 4.3.1.4, the ATR-FTIR analysis of the adsorption of metaldehyde onto PAC-SF and PAC-RP was inconclusive.

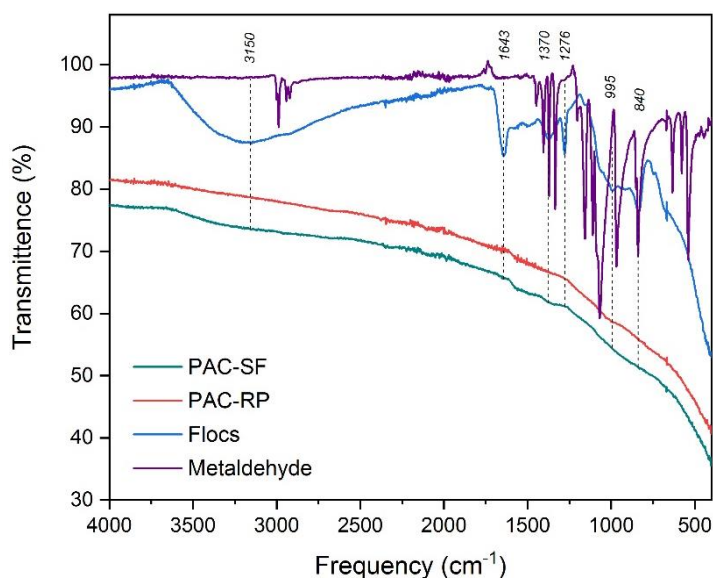


Figure 5.5 ATR-FTIR spectra of PAC-SF, PAC-RP, flocs, and metaldehyde

SEM images of flocs, PAC-SF, and PAC-RP are shown in Figure 5.6. The angular, fractured pattern of flocs in (A) can be seen on the surface of PAC-SF in (C), which suggests that flocs may be adsorbed onto the surface of PAC. Suspended solid which may be mineral, microplastic, plant fibre, or microorganism in the water collected from the Regent's Park lake can be seen in (F), with x10 000 magnification. These characterizations can be compared with the characterizations of virgin PAC, as discussed in Section 4.3.1.

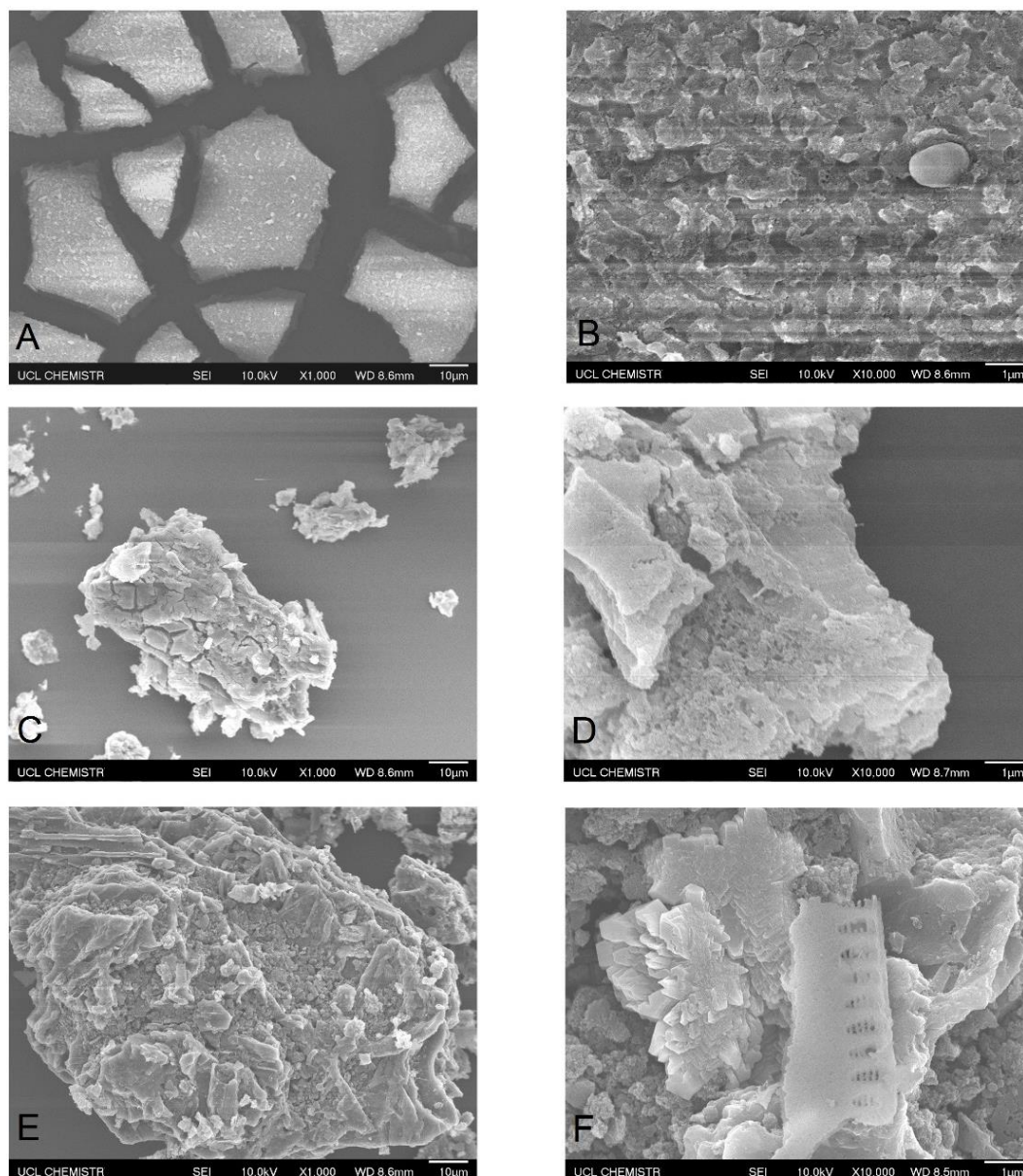


Figure 5.6 SEM images of flocs, PAC-SF, and PAC-RP: (A) $\times 1\,000$ magnification, flocs which have dried, fractured pattern morphology; (B) $\times 10\,000$ magnification, surface of flocs shown are more rounded; (C) $\times 1\,000$ magnification, PAC-SF particles are angular and have angular fractures; (D) $\times 10\,000$ magnification, PAC-SF has pores on the surfaces and edges; (E) $\times 1\,000$ magnification, PAC-RP shows angular PAC particles and impurities; and (F) $\times 10\,000$ magnification, impurities with systematic structure on the surface of PAC-RP, presumably in the Regent's Park lake water adsorbed onto the surface. (SEI = secondary electron imaging mode)

5.3.3 Removal of metaldehyde from different water samples

5.3.3.1 Removal of metaldehyde from the water collected after 'pre-ozone contactors' using different PAC dosing concentrations

Before identifying the best treatment stage at WTWTW to dose PAC for removing metaldehyde, it is essential to find out the appropriate PAC dosage to remove metaldehyde from the source water. This can provide information regarding the amount of PAC needed to remove metaldehyde in non-treated raw water, which may have low water quality. This is because the water quality would become better in later treatment stages, such as after 'main ozone contactors'; therefore less PAC may be required to remove metaldehyde at these stages. Since the source water from the reservoir supplying WTWTW was not available, the water sample available as the first treatment stage was the water collected after 'pre-ozone contactors'.

To find out the appropriate dosage of PAC to remove metaldehyde from the water collected after 'pre-ozone contactors', different PAC dosing concentrations (from 0.05 to 150 mg L⁻¹) were applied to 600 mL of 5 µg L⁻¹ metaldehyde working solutions prepared using this water sample, with a 30-min contact time. Figure 5.7 demonstrates the concentration of metaldehyde and the percentage removal of metaldehyde in water after PAC treatment.

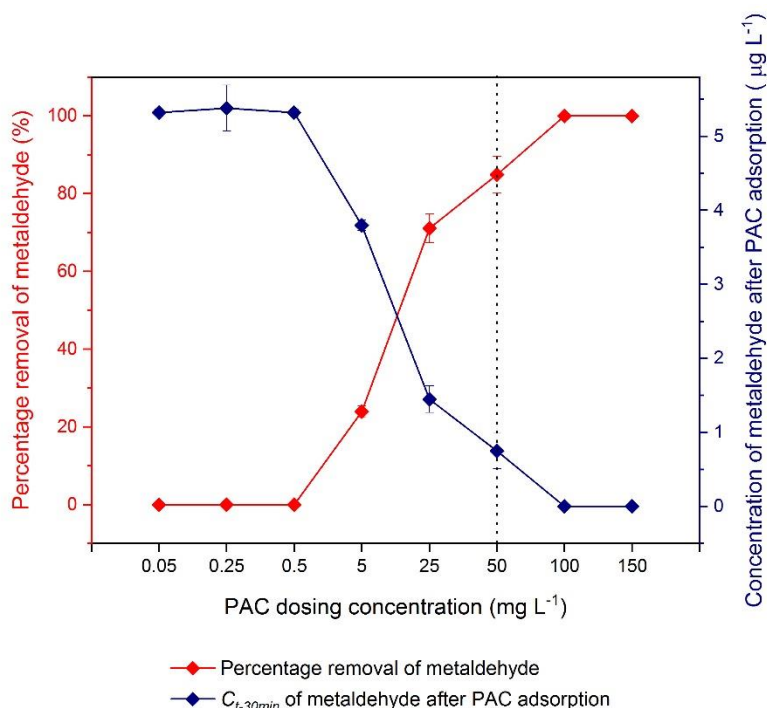


Figure 5.7 Effect of different PAC dosing concentrations on removal of 600 mL of 5 $\mu\text{g L}^{-1}$ metaldehyde working solution prepared using the water collected after ‘pre-ozone contactors’ from WTWTW with a dotted line indicating the selected working PAC dosing concentration for the next sets of experiments ($N = 3$, error bars showing SD)

Figure 5.7 shows that as PAC dosing concentration increased, the percentage removal of metaldehyde enhanced. And this agrees with the research of Anupam *et al.* which found higher removal of chromium (VI) from aqueous solutions with increasing dosage of PAC [203]. There was no removal of metaldehyde for PAC dosing concentration $\leq 0.5 \text{ mg L}^{-1}$ and metaldehyde could not be detected with PAC dosing concentration $\geq 100 \text{ mg L}^{-1}$. The modified SPE loading technique allows metaldehyde to be detected by GC-MS with a concentration 500 times lower than the LOD of $1.5 \mu\text{g L}^{-1}$, around $0.003 \mu\text{g L}^{-1}$. It indicates that PAC dosing concentration $\geq 100 \text{ mg L}^{-1}$ could ensure the concentration of metaldehyde is below $0.01 \mu\text{g L}^{-1}$ after

treatment, which would be within the EU and UK standard of $0.1 \mu\text{g L}^{-1}$. The dotted line marks the PAC dosing concentration of 50 mg L^{-1} , and it was selected as the PAC dosing concentration for the next set of experiments. This is because in order to analyse the experimental data, metaldehyde needs to be detected after PAC treatment.

5.3.3.2 Removal of metaldehyde from the water samples collected at different treatment stages

Removal of metaldehyde from the water samples collected at different treatment stages including after 'pre-ozone contactors', after 'static flocculation', after 'CoCoDAF units', and after 'main ozone contactors' were investigated by adding PAC (dosing concentration of 50 mg L^{-1}) into 600 mL of metaldehyde working solutions at $5 \mu\text{g L}^{-1}$ prepared using these water samples, with a 30-min contact time. Figure 5.8 shows the concentrations of metaldehyde solutions without and after 30-min PAC treatment and Table 5.3 presents the percentage removal of metaldehyde after PAC treatment, along with the p -values from the ANOVA single factor statistic tests.

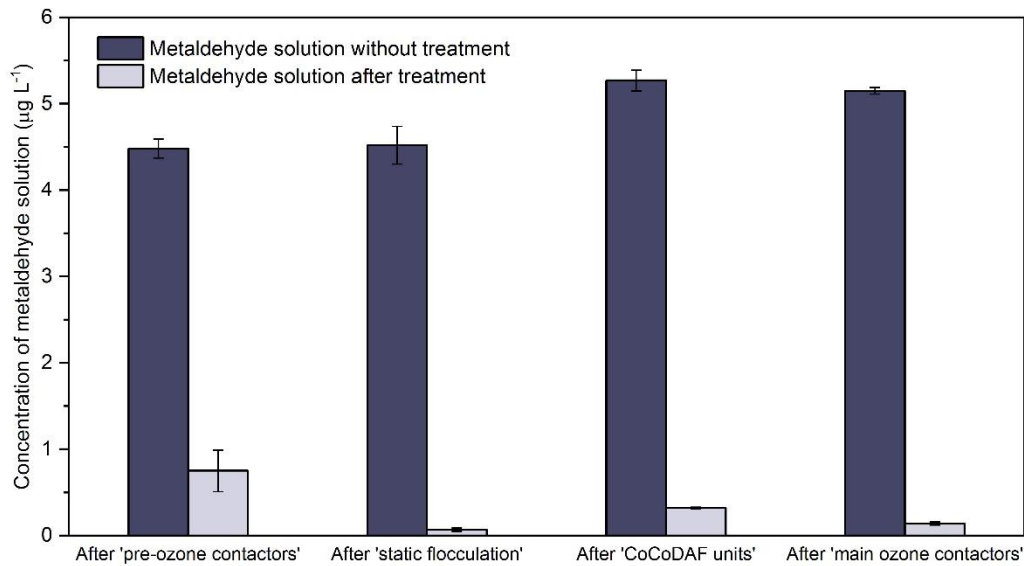


Figure 5.8 Concentrations of metaldehyde solutions without and after 30 mg PAC treatment in the 600 mL water samples collected from different treatment stages at WTWTW ($N = 3$, error bars showing SD)

Table 5.3 Removal of metaldehyde from the water samples collected at different treatment stages ($N = 3$)

Treatment stage	C_0 ($\mu\text{g L}^{-1}$)	$C_{t-30min}$ ($\mu\text{g L}^{-1}$)	Percentage removal (%)	p -value
After 'pre-ozone contactors'	4.48 ± 0.11	0.75 ± 0.24	82.9 ± 5.4	3.45E-04
After 'static flocculation'	4.52 ± 0.22	0.07 ± 0.02	98.4 ± 0.3	8.94E-06
After 'CoCoDAF units'	5.27 ± 0.12	0.32 ± 0.01	94.1 ± 0.3	1.39E-05
After 'main ozone contactors'	5.15 ± 0.04	0.14 ± 0.02	97.2 ± 0.5	8.87E-07

Metaldehyde was effectively removed from all water samples. However, the removal of metaldehyde was expected to be higher at later treatment stages such as after 'CoCoDAF units' and after 'main ozone contactors'. This is because the water quality of the water samples was expected to be better (i.e. with lower DOC, hence less competitive adsorption) at later treatment stages, compared to earlier treatment stages such as after 'static flocculation'. However, the highest removal of metaldehyde (98.4%) from all water samples was found using the water sample collected after 'static flocculation'. And 94.1% and 97.2% of metaldehyde were removed after 'CoCoDAF units' and after 'main ozone contactors', respectively. The existence of flocs in the water sample collected after 'static flocculation' distinguished it from all other water samples, hence suggesting that the flocs may be important in assisting the adsorption of metaldehyde from water onto PAC. In fact, Hami *et al.* stated that after flocculation, addition of PAC in the dissolved air flotation (DAF) tank would significantly increase the removal of BOD and COD [204]. And Serpa *et al.* suggested that the combination of PAC and flocs formed suspended PAC-flocs, which showed effective removal of methylene blue [205]. They suggested that the adsorption process was through rapid mass transfer to PAC-flocs and onto PAC itself at the same time [205]. These researches agree with the findings of Jiang *et al.*, which showed effective removal of salicylic acid, ibuprofen and diclofenac from water by super PAC with the presence of flocs, due to neutralization of charge and possible adsorption on the flocs [206]. In addition, Cook and Newcombe explained that flocs in the adsorption system of PAC may have an open structure, which enables the adsorbate to diffuse easily to the PAC particle [207].

Due to the fact that the removal of metaldehyde was the highest in the water collected after 'static flocculation', another set of experiments were performed to find the

maximum adsorption capacity (q_m) of PAC using the water collected after 'static flocculation'. Figure 5.9 compares the removal of metaldehyde between the most effective PAC dosing stage (after 'static flocculation') and the least effective PAC dosing stage (after 'pre-ozone contactors'), with PAC dosing concentrations ranging from 5 to 150 mg L⁻¹.

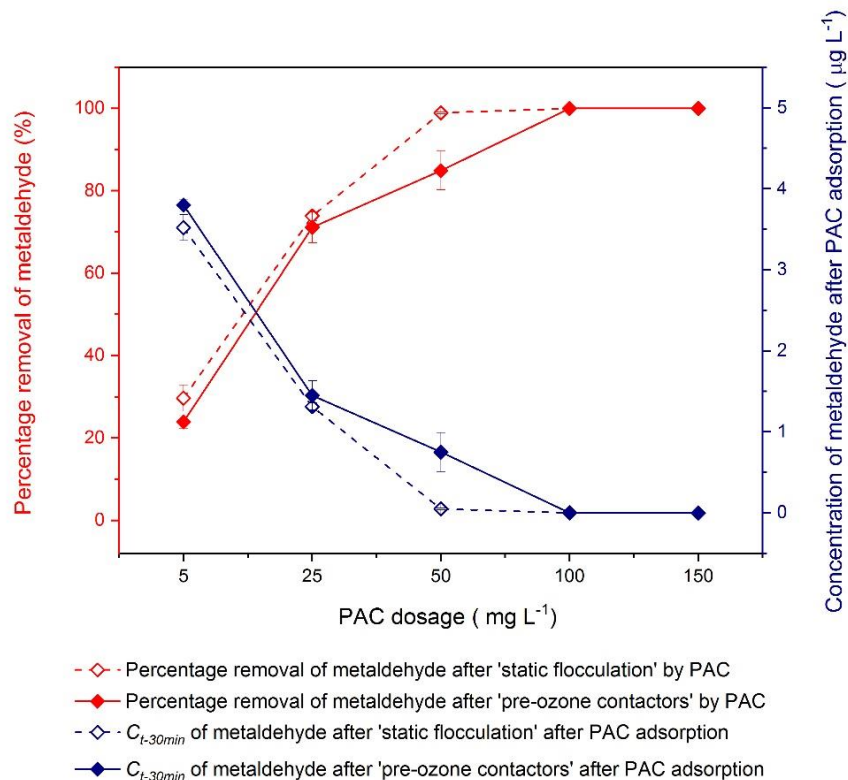


Figure 5.9 Percentage removal and concentration of metaldehyde ($C_{t-30min}$) in the water collected after 'pre-ozone contactors' and after 'static flocculation' with different PAC dosing concentrations ($N = 3$, error bars showing SD)

The removal of metaldehyde from the water collected after 'static flocculation' was slightly higher than the water collected after 'pre-ozone contactors' at all PAC dosing concentrations, but relatively more distinctive when the dosing concentrations were higher than 50 mg L⁻¹. The ANOVA single factor statistic tests were performed between $C_{t-30min}$ of two water samples at every PAC dosing concentration to determine

if there was a significant difference. For PAC dosing concentration of 5 and 25 mg L⁻¹, there was no significant difference in the percentage removal and $C_{t-30min}$ of these two water samples (p -value = 0.8 and 0.4, respectively). For PAC dosing concentration of 50 mg L⁻¹, there was a significant difference in the percentage removal and $C_{t-30min}$ of these water samples (p -value = 0.03). This suggested that when PAC dosing concentration is higher than 50 mg L⁻¹, the removal of metaldehyde would be more effective when PAC was added in the water collected after 'static flocculation'. However, if the PAC dosing concentration was small (≤ 25 mg L⁻¹), the removal of metaldehyde would be more or less the same for every treatment stage; i.e. PAC can be dosed at any treatment stage. This finding agrees with Zhou *et al.* who suggested that a higher dosage of PAC achieved higher removal of DOC from water with the presence of flocs and Li *et al.* who found that there was higher removal of COD and lead ions from wastewater, using higher PAC dosage with the presence of flocs [208, 209]. In this case, higher dosage of PAC provides more adsorption sites for removing metaldehyde; therefore, a relatively more distinctive increase in the percentage removal of metaldehyde from the water collected after 'static flocculation' was observed at PAC dosing concentration higher than 50 mg L⁻¹.

Figure 5.10 demonstrates data fitted to the Freundlich and the Langmuir isotherm models for metaldehyde adsorbed onto PAC in the water collected after 'pre-ozone contactors' and after 'static flocculation'. As explained in Section 5.2.5, it was considered that adsorption of metaldehyde in the system was approaching equilibrium in 30 min; therefore, $C_{t-30min} = C_e$.

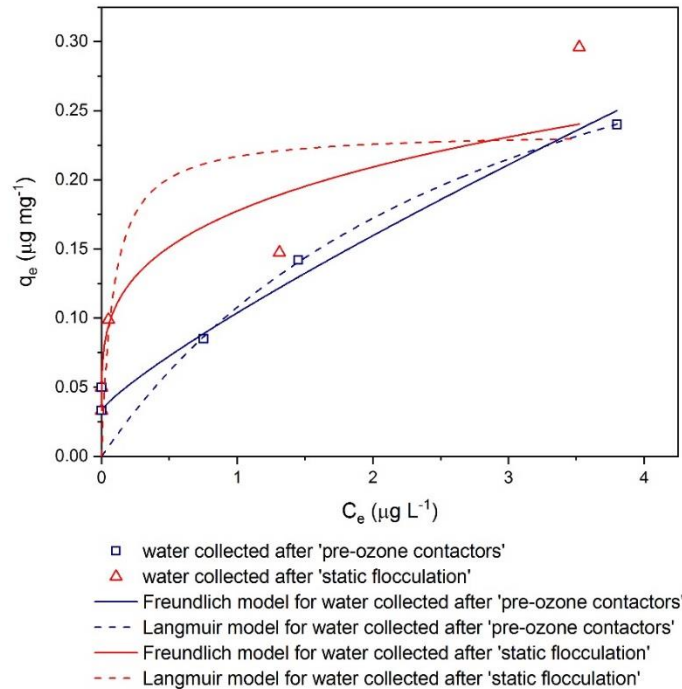


Figure 5.10 Metaldehyde adsorption equilibrium curve fitted to the Freundlich and the Langmuir isotherm models using the water collected after 'pre-ozone contactors' and after 'static flocculation' at WTWTW

For the experiment that used the water collected after 'pre-ozone contactors', data were well fitted to the Freundlich isotherm model using Equation 4.1 and Equation 4.2, with a R^2 value of 0.9898 (Figure 5.11). This fitting gives $1/n$ value of 0.63 ($n = 1.58$), indicating a physical adsorption process and a relatively low affinity between metaldehyde and PAC. K_F from this fitting was $0.11 (\mu\text{g mg}^{-1})/(\mu\text{g L}^{-1})^{1/n}$ obtained from the intercept. Similarly, as explained in Section 4.3.2.5, the Freundlich isotherm model is not completely suitable for fitting the experimental data. However, since it did provide information on the adsorption process, it cannot be firmly rejected.

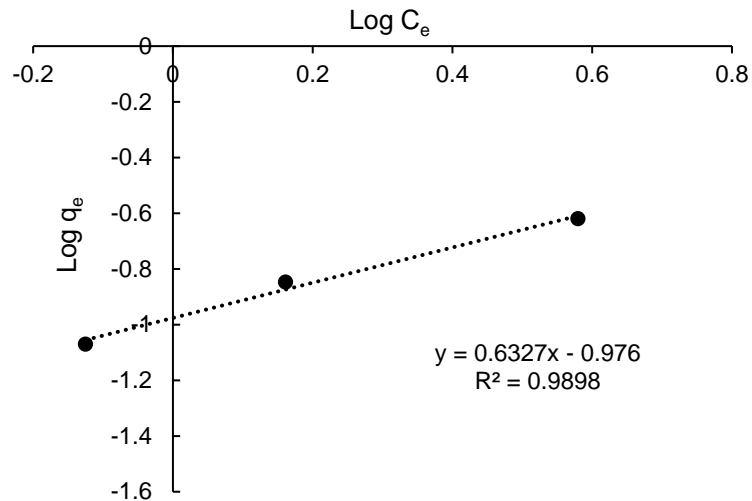


Figure 5.11 The Freundlich isotherm model fitting for the water collected after 'pre-ozone contactors' at WTWTW

The same data were not well fitted to the Langmuir isotherm model using Equation 4.3 and 4.4, with a R^2 value of 0.841 (Figure 5.12). From the Langmuir isotherm model fitting, the maximum adsorption capacity (q_m) is $0.25 \mu\text{g mg}^{-1}$, and the Langmuir constant (K_L) is $1.86 \text{ L } \mu\text{g}^{-1}$, suggesting a moderate adsorption capacity.

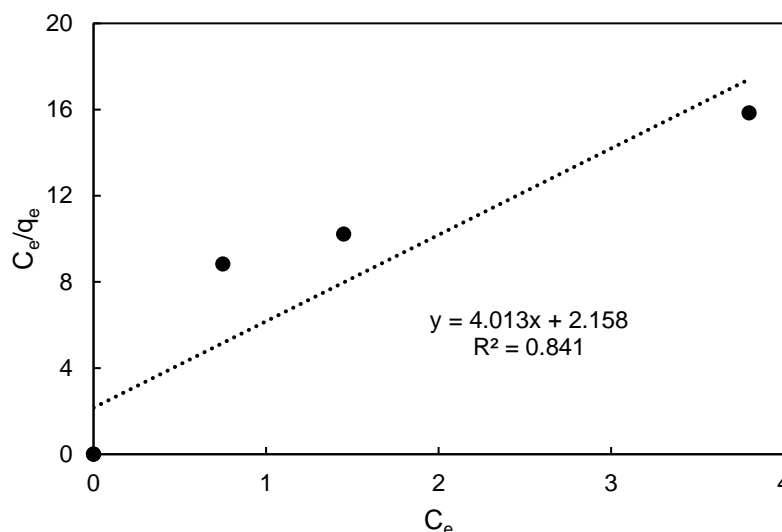


Figure 5.12 The Langmuir isotherm model fitting for the water collected after 'pre-ozone contactors' at WTWTW

For the experiment that used the water collected after 'static flocculation', data were not fitted well to both models. Figure 5.13 presents the Freundlich isotherm model fitting, with a R^2 value of 0.807. The Freundlich isotherm model gives $1/n$ value of 0.22 ($n = 4.47$) and K_F of $0.18 (\mu\text{g mg}^{-1})/(\mu\text{g L}^{-1})^{1/n}$. And this $1/n$ value indicates that adsorbent sites on PAC were more homogeneous [142], suggesting that the experimental data may fit better using an isotherm model for homogeneous adsorbents.

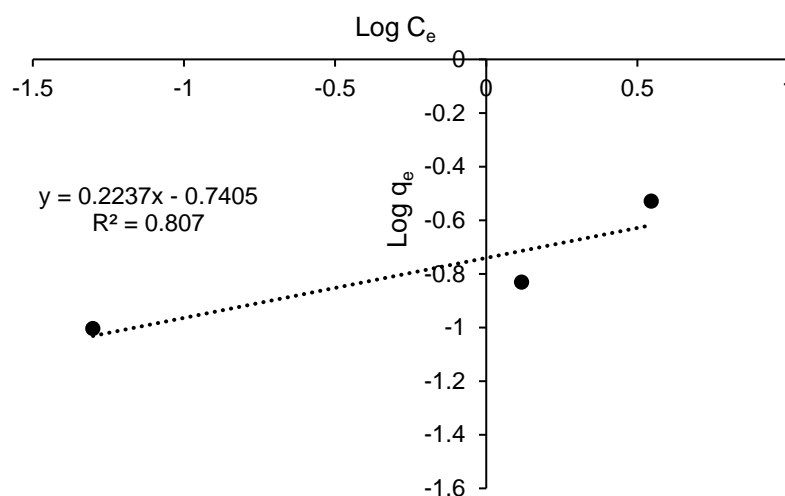


Figure 5.13 The Freundlich isotherm model fitting for the water collected after 'static flocculation' at WTWTW

The Langmuir isotherm model, which is valid for a homogeneous surface, may be relatively more suitable for analysing the experimental data, obtained using the water collected after 'static flocculation'. Data were slightly better fitted to the Langmuir isotherm model with a R^2 value of 0.8831 (Figure 5.14). The Langmuir isotherm model gives q_m of $0.29 \mu\text{g mg}^{-1}$ and K_L of $4.2 \text{ L } \mu\text{g}^{-1}$. This suggests that the maximum adsorption capacity of PAC for adsorbing metaldehyde ($5 \mu\text{g L}^{-1}$) from the water collected after 'static flocculation' is $0.29 \mu\text{g mg}^{-1}$, which is more than 100 times lower than the q_m (28.33 mg g^{-1}) obtained in Chapter 4 (using 1 mg L^{-1} metaldehyde working

solution in MilliQ water). This could be explained by the low initial concentrations of metaldehyde working solution used in this chapter and the presence of DOC in the adsorption system. It is suggested that the adsorption mechanisms of adsorbates and adsorbents depend on the initial concentrations of the adsorbates [210]. Table 4.4 presents all the parameters obtained from the adsorption isotherm study.

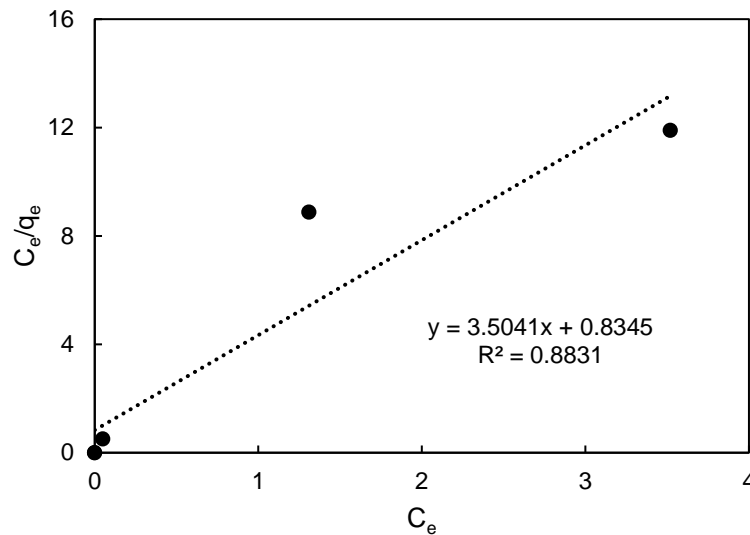


Figure 5.14 The Langmuir isotherm model fitting for the water collected after 'static flocculation' at WTWTW

Table 5.4 Summary of parameters obtained from the metaldehyde adsorption isotherm study using the water collected after ‘pre-ozone contactors’ and ‘static flocculation’

Water samples	Isotherm models	R ²	Parameters	
After ‘pre-ozone contactors’	Freundlich	0.9898	$1/n = 0.63$	$K_F = 0.11 (\mu\text{g mg}^{-1}) / (\mu\text{g L}^{-1})^{1/n}$
	Langmuir	0.841	$q_m = 0.25 \mu\text{g mg}^{-1}$	$K_L = 1.86 \text{ L } \mu\text{g}^{-1}$
After ‘static flocculation’	Freundlich	0.8225	$1/n = 0.22$	$K_F = 0.18 (\mu\text{g mg}^{-1}) / (\mu\text{g L}^{-1})^{1/n}$
	Langmuir	0.8827	$q_m = 0.29 \mu\text{g mg}^{-1}$	$K_L = 4.2 \text{ L } \mu\text{g}^{-1}$

Considering the potential application of PAC at WTWTW, the optimal location for dosing PAC found in this study is after ‘static flocculation’. This is not only because the highest removal of metaldehyde (98.4%) was found in the water sample taken after this treatment stage (Figure 5.8), but also because the majority of PAC in water can potentially be removed in the subsequent treatment stages of ‘CoCoDAF units’ and ‘GAC adsorbers’. However, dosing PAC after ‘static flocculation’ may affect the performance of ‘CoCoDAF units’, since a large amount of suspended solids would be present. If suspended PAC in water cannot be completely removed by the ‘CoCoDAF units’, it will then be filtered and retained at the ‘GAC adsorber’, which suggests that more frequent backwashing of the ‘GAC adsorber’ may be required. For example, as discussed in Section 5.3.3.1, the appropriate PAC dosing concentration to treat 600 mL of $5 \mu\text{g L}^{-1}$ metaldehyde solution was greater than or equal to 100 mg L^{-1} to ensure

the treated water would meet the EU and UK standard. Considering the output of WWTW (50 to 135 MLD), 5 to 13.5 tons of PAC may be needed to treat water with metaldehyde at a concentration of $5 \mu\text{g L}^{-1}$ every day. And this could have potential impacts on the 'CoCoDAF units' depending on their solid loading capacity, which is normally 4-15 kg of dry solids per h per m^2 [211]. Therefore, although the optimum dosing position of PAC for removing metaldehyde at WWTW was found to be after 'static flocculation' in this study, it is suggested by the researcher that separation of used PAC from the treated water at WWTW needs to be investigated in situ.

5.3.3.3 The effect of water quality on metaldehyde removal from different water samples

Water quality of the water samples, including pH, presence of different ions, and DOC, can affect the removal of organic pollutants by adsorption. For example, the removal of metaldehyde from MilliQ water onto PAC was slightly more effective under alkaline conditions, as discussed in Section 4.3.2.3. Moreover, according to Mukherjee *et al.*, the removal of phenol from water by three carbon materials including AC decreased with increasing concentrations of nitrate and chloride, due to the competition for adsorption sites between the ions and the adsorbate [212]. This suggests that the presence of ions in water samples may affect the adsorption of metaldehyde onto PAC. Additionally, Altmann *et al.* pointed out that PAC can adsorb DOC fractions, especially small fractions with low molecular weight [213]. Hence, the effect of water quality on metaldehyde removal was studied.

Removal of metaldehyde in the Regent's Park lake water, MilliQ water, and MilliQ water with HA were compared with the removal of metaldehyde in the water collected from different treatment stages at WWTW. Water characteristics without and after

PAC treatment of different water samples are presented in Figure 5.15 (two data points, $N = 2$). Raw data from the water characteristics analyses for these water samples without PAC treatment are presented in Table A.3.2, Appendix A.3; and raw data from the water characteristics analyses for these water samples after PAC treatment, are presented in Table A.3.3, Appendix A.3.

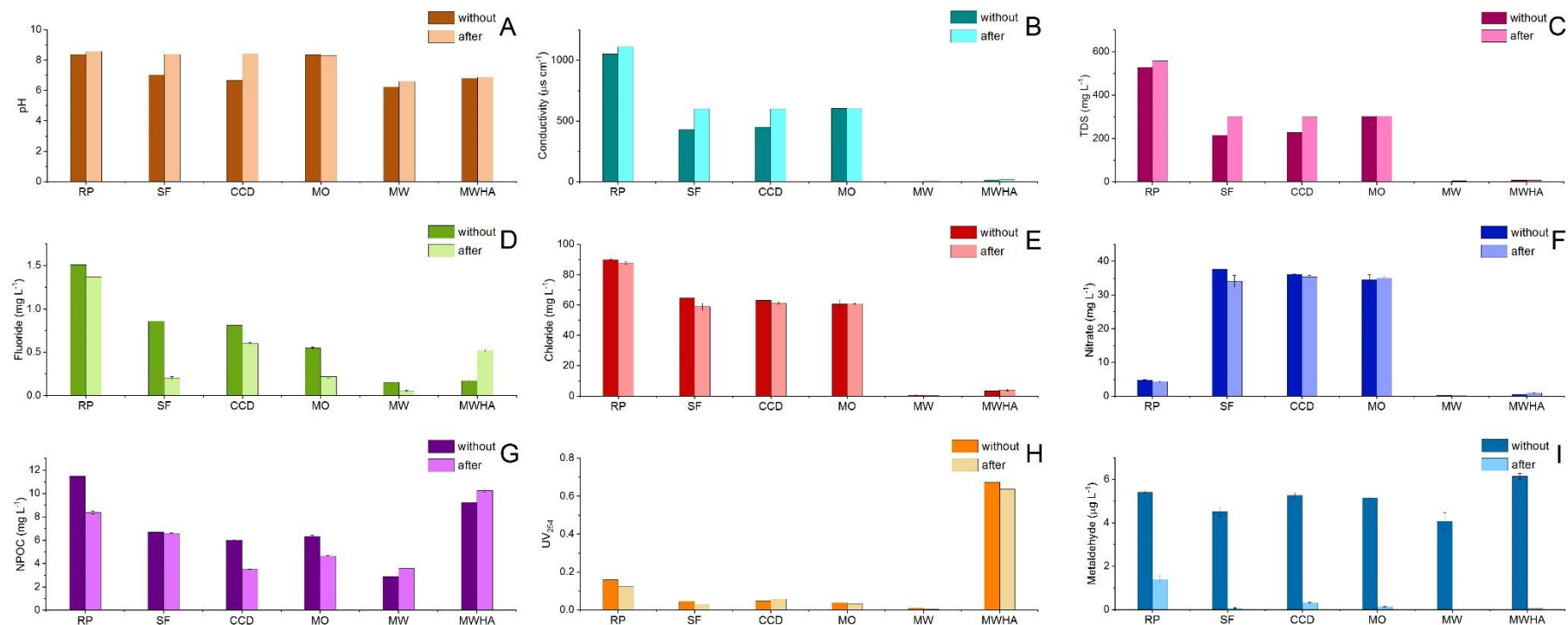


Figure 5.15 Comparison of water characteristics for different water samples without and after PAC treatment ($N = 2$ for **A**: pH value, **B**: conductivity, **C**: TDS, **D**: fluoride, **E**: chloride, **F**: nitrate, **G**: NPOC, **H**: UV_{254} ; $N = 3$ for **I**: concentration of metaldehyde; and **RP** = the water collected from the Regent's Park lake; **SF** = the water collected after 'static flocculation'; **CCD** = the water collected after 'CoCoDAF units'; **MO** = the water collected after 'main ozone contactors'; **MW** = MilliQ water; **MWHA** = MilliQ water with humic acid)

Metaldehyde was effectively removed from all water samples, suggesting that the adsorption of metaldehyde onto the PAC used in this study was not significantly affected by water quality, such as the presence of organic matter and negative ions. The presence of humic acid did not affect the removal of metaldehyde by the PAC as well, which agrees with the results in Chapter 4. Removal of metaldehyde from the water collected from the Regent's Park lake was the lowest (74.3%). The most distinctive characteristic of this water sample is that it has the highest NPOC of 11.47 mg L⁻¹ among all water samples, which is almost twice as high compared to the water samples collected at WTWTW (6.01 to 6.7 mg L⁻¹). However, the high NPOC in this water sample was expected because the Regent's Park lake is inhabited by aquatic animals. The PAC used in this study is characterized by abundant micropores and mesopores, which is favoured by adsorption of metaldehyde. This characteristic would also allow other organic compounds with small molecules to adsorb onto this PAC. In fact, Altmann *et al.* argued that small dissolved organic matter constituents are more effectively removed by adsorption onto PAC, compared to high molecular weight organics such as humic substances [213]. Therefore, the relatively lower removal of metaldehyde in the water collected from the Regent's Park lake, compared to other water samples, could result from its relatively high NPOC. This water sample possibly contains organic matters with smaller fractions than HA [213] and can adsorb onto PAC, as its NPOC decreased from 11.47 to 8.37 mg L⁻¹ after PAC treatment.

Conductivity, pH, and TDS increased for all water samples after PAC treatment due to the pH_{pzc} of PAC being 7.35. In fact, conductivity and TDS slightly increased after PAC treatment for almost all water samples. This may be explained by the fact that there are many inorganic impurities from the making of AC, such as salts of alkali and iron from coconut shells [214]. These impurities could detach from AC, dissolve in

water, and therefore increase the conductivity and TDS of the water samples. It is suggested by Song *et al.* and Cooney *et al.* that PAC can be washed with weak acid and deionized water to remove inorganic impurities prior to application [200, 215].

Negative ions including fluoride, chloride, and nitrate only slightly decreased for all water samples, as well as UV_{254} , suggesting there was adsorption of ions and dissolved NOM onto PAC. However, the removal was not significant, possibly because PAC was negatively charged in water and did not prefer adsorption of negative ions. The removal of NPOC in different water samples varied from 2 to 41.6%. And there was a significant difference in the NPOC level without and after PAC treatment for all water samples (p -value ≤ 0.05), except for the water collected after 'static flocculation'. It is worth noting that NPOC even increased in the metaldehyde solutions prepared using MilliQ water and MilliQ water with HA after PAC treatment. This suggests that the addition of PAC increased the DOC of the metaldehyde solutions prepared using MilliQ water. A control test of adding 50 mg L^{-1} of PAC into 600 mL of MilliQ water with constant stirring for 30 min was performed to confirm that NPOC increased from 0.16 to 1.09 mg L^{-1} . This was caused by the release of DOC from the surface of PAC into water, due to the high concentration gradient between PAC and MilliQ water. This can also explain that NPOC did not decrease significantly in the water collected after 'static flocculation' after PAC treatment. PAC adsorbed metaldehyde and DOC from the water collected after 'static flocculation', but in the meantime PAC itself was releasing DOC back to the water; hence, the concentration of DOC would be balanced out.

5.3.4 Adsorption mechanisms of metaldehyde onto PAC regarding different initial concentrations of metaldehyde working solutions

1 mg L⁻¹ was selected as the studied concentration of metaldehyde working solution in Chapter 4, and 5 µg L⁻¹ was selected as the studied concentration in this chapter. The results from Chapter 4 and the research of Li *et al.* showed that the adsorption capacity (q_m) of metaldehyde onto PAC was affected by the initial concentrations of metaldehyde working solutions [69]. Table 5.5 summarises the maximum adsorption capacity and the Langmuir constants obtained in Section 4.3.2.5 and in Section 5.3.3.2.

Table 5.5 Comparison of q_m and K_L regarding adsorption of metaldehyde onto PAC under different experimental conditions and using different water samples

Water sample	q_m (mg g ⁻¹)	K_L (L mg ⁻¹)	Experimental condition
MilliQ (Section 4.3.2.5)	28.33	88.25	5 to 500 mg of PAC into 500 mL of 1 mg L ⁻¹ metaldehyde solution for 2 h
After 'pre-ozone contactors' (Section 5.3.3.2)	0.25	1860	0.05 to 150 mg of PAC to 600 mL of 5 µg L ⁻¹ metaldehyde solution for 30 min
After 'static flocculation' (Section 5.3.3.2)	0.29	4180	5 to 150 mg of PAC to 600 mL of 5 µg L ⁻¹ metaldehyde solution for 30 min

From Table 5.5, q_m and K_L of metaldehyde adsorption by PAC varied significantly under different experimental conditions, with high initial concentration of metaldehyde working concentration at 1 mg L⁻¹ and low initial concentration of metaldehyde working concentration at 5 µg L⁻¹. Therefore, it suggests that the adsorption mechanisms of

metaldehyde onto PAC may be different for metaldehyde working solutions with different initial concentrations.

Hence, to investigate the effect of initial concentration on metaldehyde removal by PAC and to compare with the q_m and K_L demonstrated in Table 5.5, another set of experiments were performed. A set of 600 mL of metaldehyde working solutions was prepared using MilliQ water with different initial concentrations (1 to 1000 $\mu\text{g L}^{-1}$). 50 mg L^{-1} of PAC was added into each 600 mL of metaldehyde solution for a 30-min contact time. Figure 5.16 shows the effect of initial concentration on metaldehyde adsorption onto PAC in the single adsorption system.

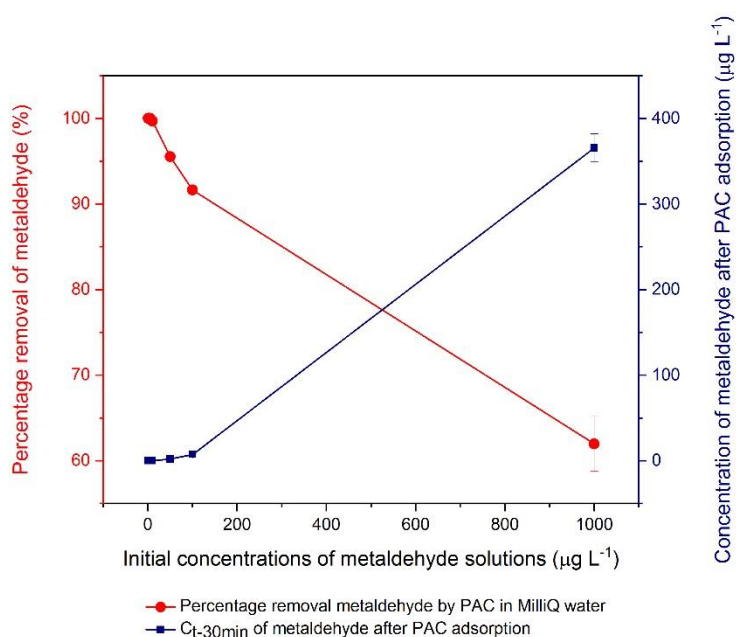


Figure 5.16 Effect of initial concentration on metaldehyde removal by PAC in the single adsorption system ($N = 3$, error bars showing SD)

Figure 5.16 shows that as initial concentration increased, the percentage removal of metaldehyde decreased. A similar finding was discussed by Gautam *et al.* in the removal of Alizarin Red S dye by mustard husk adsorbent; the removal of the dye decreased with increasing the initial concentration of the dye [210]. The EU and UK

standard of $0.1 \mu\text{g L}^{-1}$ can be met by adding 50 mg L^{-1} of PAC into 600 mL of metaldehyde working solution prepared using MilliQ water at concentrations $\leq 10 \mu\text{g L}^{-1}$ (Figure 5.16). And the standard can be met by adding 100 mg L^{-1} of PAC into 600 mL of $5 \mu\text{g L}^{-1}$ metaldehyde working solution prepared using the water collected after 'pre-ozone contactors' (Figure 5.7).

Adsorption isotherm studies were conducted as well. Figure 5.17 demonstrates data fitted to the Freundlich and the Langmuir isotherm models for metaldehyde adsorbed onto PAC in MilliQ water. As explained in Section 5.2.5, it was considered that adsorption of metaldehyde in the system was approaching equilibrium in 30 min; therefore, $C_{t-30\text{min}} = C_e$.

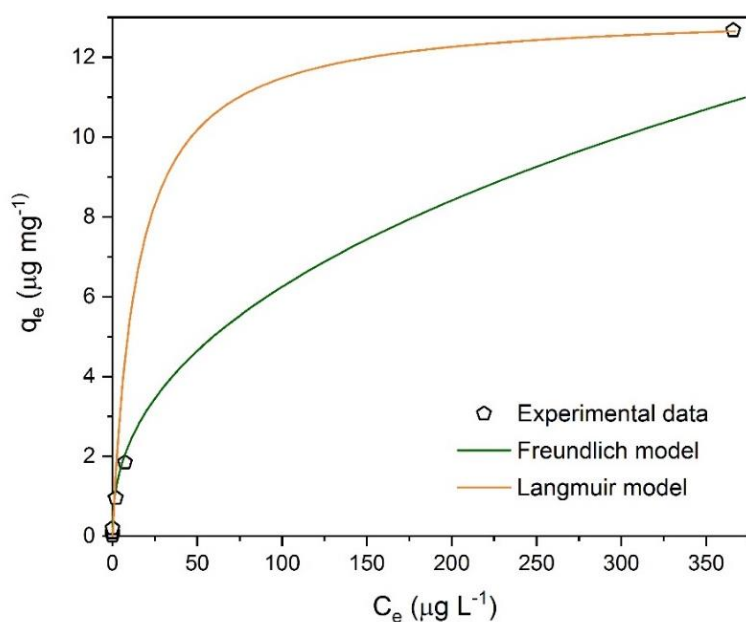


Figure 5.17 Metaldehyde adsorption equilibrium curve fitted to the Freundlich and the Langmuir isotherm models using MilliQ water

Data were quite well fitted to the Freundlich isotherm model using Equation 4.1 and Equation 4.2, with a R^2 value of 0.9894 (Figure 5.18). $1/n$ obtained from the Freundlich isotherm model is 0.43 ($n = 2.33$), suggesting relatively low affinity, similar to the value

obtained using the water collected after 'pre-ozone contactors'. This n value also suggests that the PAC used in the study is more homogeneous. K_F is $0.87 (\mu\text{g mg}^{-1})/(\mu\text{g L}^{-1})^{1/n}$, higher than that of the water collected after 'pre-ozone contactors'. However, this K_F is still considered low. K_F , as an indicator for adsorption capacity, should be around 2-3 $(\text{mg g}^{-1})/(\text{mg L}^{-1})^{1/n}$ to suggest effective adsorption [142]. K_F as low as 0.87 cannot explain the experiment results of effective removal of metaldehyde in MilliQ water. As discussed in Section 5.3.3.2, the Freundlich isotherm model is not completely suitable for explaining this adsorption mechanism but cannot be firmly rejected.

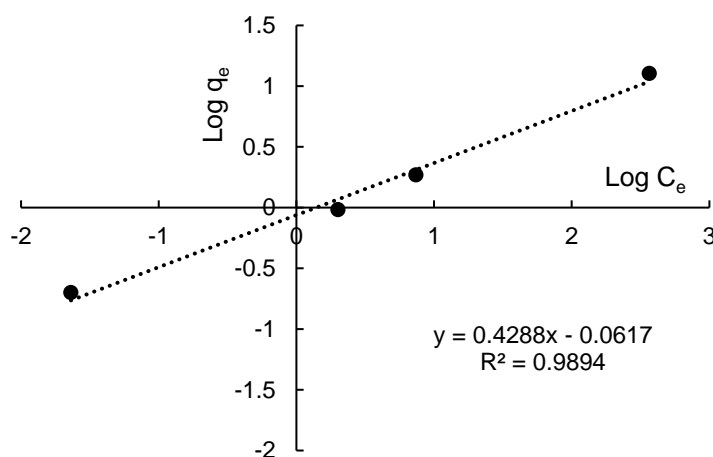


Figure 5.18 The Freundlich isotherm model fitting for MilliQ water

Data were quite well fitted to the Langmuir isotherm model using Equation 4.3 and Equation 4.4, with a R^2 value of 0.9857 (Figure 5.19). The maximum adsorption capacity (q_m) is $13.16 \mu\text{g mg}^{-1}$ and the Langmuir constant (K_L) is $0.07 \text{ L } \mu\text{g}^{-1}$. Although they are lower than the q_m (28.33 mg g^{-1}) and K_L (88.25 L mg^{-1}) obtained in Section 4.3.2.5, they do confirm the results of effective removal of metaldehyde. Hence, the Langmuir isotherm model may be a better model for analysing the adsorption of metaldehyde from MilliQ water onto PAC, with low initial concentrations.

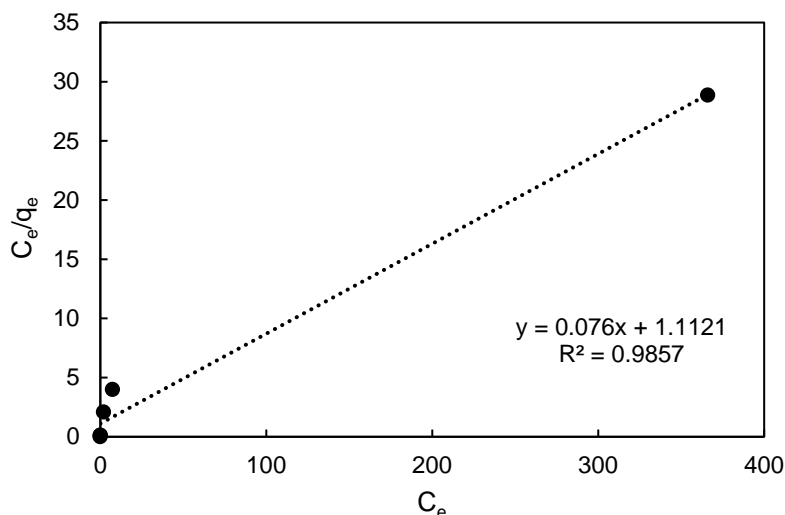


Figure 5.19 The Langmuir isotherm model fitting for MilliQ water

Parameters obtained from the adsorption isotherm studies are summarised in Table 5.6. The adsorption of metaldehyde by PAC is higher with higher initial concentrations of metaldehyde working solution. This behaviour may be explained by the low driving force for the mass transfer from the adsorbate to the adsorbent. The driving force is initiated by the initial concentration of the adsorbate [210]; therefore, the increase in the initial concentration would increase the driving force for the mass transfer due to the concentration gradient, and it would result in an enhanced adsorption of the adsorbate by the adsorbent. This was also confirmed by the study of Gautam *et al.*, which found that adsorption of metal ions increased with increasing initial metal ion concentrations [216].

Low adsorption of metaldehyde by PAC at low initial concentrations can be viewed from another aspect. Water molecules are considered significant in explaining the adsorption mechanisms of metaldehyde onto PAC. Low initial concentration of metaldehyde solution suggests more water molecules are present in the adsorption system. Ferino-Pérez *et al.* showed water behaves like an intermediary between AC

and metaldehyde and water molecules are competing with metaldehyde molecules for adsorption sites on PAC [42]. Busquets *et al.* also argued that there are possible competitive effects between metaldehyde and water molecules [30]. Therefore, less metaldehyde molecules would be adsorbed onto the surface of PAC if there are more water molecules present in the system.

Table 5.6 Parameters obtained from the metaldehyde adsorption isotherm study using MilliQ water

Isotherm models	R ²	Parameters	
Freundlich	0.9894	$1/n = 0.43$	$K_F = 0.87 (\mu\text{g mg}^{-1}) / (\mu\text{g L}^{-1})^{1/n}$
Langmuir	0.9857	$q_m = 13.16 \mu\text{g mg}^{-1}$	$K_L = 0.07 \text{ L } \mu\text{g}^{-1}$

5.3.5 Desorption of metaldehyde and regeneration of PAC

After the 30-min adsorption stage (described in Section 5.2.6), the concentrations of metaldehyde solutions reduced from 1.16 to 0.24 mg L⁻¹. Therefore, according to Equation 3.1, Equation 3.2, and Equation 3.3, q_e of the used PAC is 18.35 mg g⁻¹. Hence, the two sets of used PAC (30 mg) each had 550 μg of metaldehyde adsorbed on it. Table 5.7 shows the desorption of metaldehyde from these two sets of used PAC back to water.

Table 5.7 Detection of metaldehyde after dosing used PAC into MilliQ water

	$C_{\text{metaldehyde}}$ in water after dosing used PAC	$m_{\text{metaldehyde}}$ desorbed back to water
PAC dried at room temperature	79.07 ± 7.17 µg L ⁻¹	47.44 ± 4.3 µg
PAC dried in oven at 60 °C	6.41 ± 0.83 µg L ⁻¹	3.85 ± 0.5 µg

From Table 5.7, it suggests that a small amount of metaldehyde (8.6%) would desorb from used PAC back to water, due to the high concentration gradient of metaldehyde between MilliQ water and used PAC. In fact, desorption is very common for activated carbon and it is reported that desorption of metaldehyde from GAC back to water occurs, when the inlet concentration of metaldehyde decreases [74].

However, after heating the used PAC in the oven at 60 °C for 24 h, the amount of metaldehyde in MilliQ water (after dosing the used PAC) was 3.85 µg, which was only 0.7% of the total 550 µg metaldehyde adsorbed. It is significantly less than the used PAC dried at room temperature, suggesting that the majority of adsorbed metaldehyde on the used PAC may have been thermally degraded in the oven at 60 °C. Therefore, although there was desorption of metaldehyde from used PAC back to water, the degree of desorption was relatively small. Possible degradation of metaldehyde at 60 °C suggests that used PAC may potentially be regenerated at 60 °C. Therefore, it is recommended to further investigate the regeneration of used PAC by thermal treatments using a wide range of temperatures. In addition, it is suggested to repeat the tests using natural water, to investigate the effects of combined adsorption and desorption of metaldehyde onto/from PAC with the presence of other organic

compounds in natural water, and to investigate the regeneration of this used PAC at low temperatures. Analysis of the adsorption capacity of regenerated PAC for metaldehyde is recommended as well.

5.4 Summary

PAC could effectively remove metaldehyde from the water collected from the Regent's Park lake, the water collected from different treatment stages at Walton-on-Thames Water Treatment Works, and MilliQ water (with and without HA); giving q_m of 0.25 mg g⁻¹ for the water collected after 'pre-ozone contactors', and 0.29 mg g⁻¹ for the water collected after 'static flocculation', with the initial concentration of metaldehyde working solution at 5 µg L⁻¹. And q_m of 13.16 mg g⁻¹ was found for MilliQ water with a different range of initial concentrations of metaldehyde working solutions. The PAC dosing concentration to treat 600 mL of 5 µg L⁻¹ metaldehyde solution is suggested to be larger than or equal to 100 mg L⁻¹, to ensure the treated water to meet the EU and UK standard.

In the possible dosing points at WTWTW, the addition of PAC to the water collected after 'static flocculation' achieved the highest removal of metaldehyde (98.4%), highly likely due to the presence of flocs, which assists the adsorption of metaldehyde onto PAC. However, a full scale investigation at WTWTW is suggested to confirm the results. In this chapter, PAC effectively removed metaldehyde from different water samples, regardless of their water quality. This suggests that water quality did not significantly affect the removal of metaldehyde, under the studied experimental conditions. Furthermore, the increase in initial concentration of metaldehyde would promote the adsorption of metaldehyde onto PAC, due to high driving force for mass

transfer, which enhanced the adsorption of metaldehyde onto PAC. Therefore, q_m of PAC for metaldehyde would depend on the initial concentration of the metaldehyde working solution. This needs to be taken into account when PAC is used for treating metaldehyde in drinking water treatment plants; the dosing concentration of PAC needs to be adjusted, based on the concentration of metaldehyde detected in water via constant monitoring. It is also essential to monitor the desorption of metaldehyde from used PAC back to water during the treatment processes. This is helpful for identifying the specific time to replace the PAC that may have been exhausted and for considering the regeneration of used PAC, possibly at a low temperature.

Chapter 6. Removal of metaldehyde from aqueous solutions: an overall discussion

6.1 Overview of the experimental investigations

An overview of this thesis is demonstrated by Figure 6.1. This thesis provided a potentially feasible solution to the metaldehyde problem by undertaking three experimental investigations described in Chapter 3, Chapter 4, and Chapter 5.

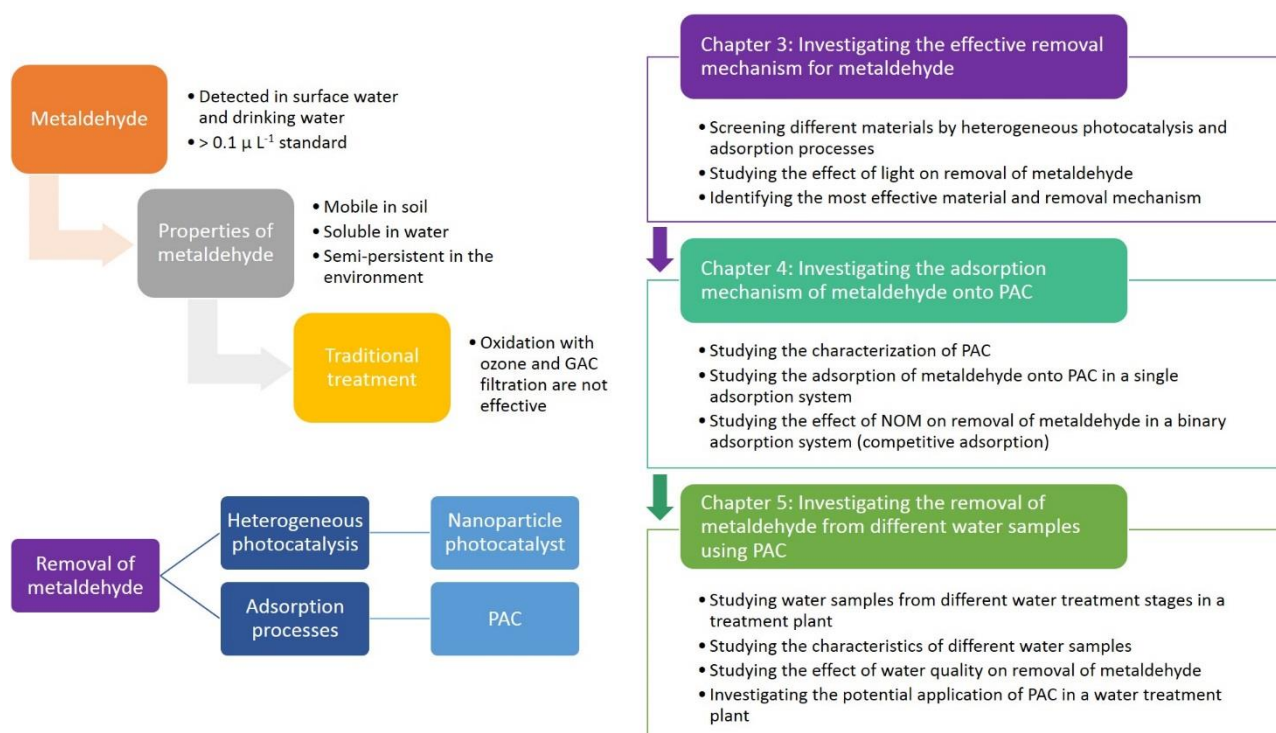


Figure 6.1 Overview of the thesis

Due to its physicochemical properties, metaldehyde is considered semi-persistent in the environment. And it cannot be effectively removed by traditional treatment methods used in drinking water treatment plants, including oxidation with ozone and GAC filtration. Two principles of common water treatment methods, oxidation and adsorption, were applied from different approaches to investigate the most effective

removal mechanism for metaldehyde, including heterogeneous photocatalysis using nanoparticle photocatalysts and adsorption processes using carbon materials. Chapter 3 compared the effectiveness of a variety of materials regarding the removal of metaldehyde from both approaches. It concluded that PAC was the most effective material studied in Chapter 3 for removing metaldehyde from MilliQ water. This conclusion does not necessarily suggest that heterogeneous photocatalysis is not effective for removing metaldehyde from water. It only implies that under the studied experimental condition, with the provided novel nanoparticle photocatalysts and commercial P25 TiO₂, the UV-C light intensity, the dosage of photocatalysts, and treatment time, heterogeneous photocatalysis was not effective for removing metaldehyde from water, especially in comparison with the effectiveness of PAC under the same experimental condition. Therefore, adsorption by PAC is considered as the preferred removal mechanism of metaldehyde. Chapter 3 also discussed the possible combination of adsorption and oxidation by incorporating UV-C light in the treatments of PAC/UV-C and GAC/UV-C. Adsorption kinetic of metaldehyde by PAC under UV-C light was studied to determine the adsorption equilibrium time and efficiency, since PAC/UV-C achieved the highest percentage removal of metaldehyde (81.4%). However, the combination of PAC and UV-C light did not significantly increase the percentage removal of metaldehyde, compared with PAC alone (76.8%). The energy consumption of this treatment, that applied the UV-C light (11 W and 240 V) to treat 500 mL solution for 2 h, was approximately 79.2 kJ (0.022 kWh). Scaling up to using UV-C light in drinking water treatment plants such as Walton-on-Thames Water Treatment Works (output of 50 to 135 MLD), the energy consumption could be substantial, approximating 528 kWh m⁻³. Since this thesis endeavoured to provide a feasible solution, it is therefore suggested by the researcher that the application of UV-

C light was not necessary in the rest of the experimental investigations. Chapter 3 delivered Objective (1) and Objective (4). Since PAC was found to be the most effective material for removing metaldehyde from MilliQ water in Chapter 3, the removal of metaldehyde from aqueous solutions by adsorption onto PAC became the focus of the rest of the thesis.

Chapter 4 closely studied the characteristics of PAC and described an experimental investigation of adsorption of metaldehyde onto PAC, with the presence of NOM. NOM was considered in Chapter 4 because metaldehyde enters surface water bodies via soil or directly, as discussed in Section 2.2.1; and NOM is often detected in surface water bodies; hence, they are often associated. Moreover, it is argued by many researchers that NOM molecules could affect the effectiveness of a number of treatment methods, as discussed in Section 4.1. Therefore, it is necessary to consider the effect of NOM on the adsorption of metaldehyde from water onto PAC, since this may potentially affect the treatment processes for metaldehyde in drinking water treatment plants. For example, if the removal of metaldehyde by PAC is significantly lowered by the presence of NOM, then it is necessary to remove NOM first, before dosing PAC to remove metaldehyde in drinking water treatment plants. HA was selected to represent NOM, since it contributes to 50-90% of organic matters in surface water [144]. In the single adsorption system, PAC can effectively remove metaldehyde from MilliQ water, especially under a more alkaline condition. On the other hand, PAC was not very effective for removing HA from MilliQ water, because the adsorption sites on the micropores of PAC may not be able to accommodate HA, due to its chemical structure. In the binary adsorption system, metaldehyde was effectively removed even with high concentrations of HA. Percentage removal of metaldehyde only decreased from 98.6 to 90.2%, with the concentration of HA

increased from 3 to 90 mg L⁻¹. Therefore, HA was not considered as an organic compound that would compete with metaldehyde for adsorption sites on PAC. Compared with HA, adsorption of metaldehyde onto PAC was favoured under the studied experimental condition. Chapter 4 delivered Objective (2) and Objective (4). Findings in Chapter 4 suggested that it may be possible to dose PAC in early treatment stages at drinking water treatment plants to remove metaldehyde, even with low quality influent. The advantage of dosing PAC at early treatment stage is that PAC can be subsequently separated from the treated water at later treatment stages such as DAF or filtration. These treatment stages can remove suspended solids from water, including used PAC. For example, during DAF, bubbles and PAC agglomerate can be effectively floated, collected, and skimmed off [217]. Moreover, researches showed that PAC can be effectively retained (> 99%) in a rapid filter with pumice as the filtration media [218, 219]. Therefore, based on the findings in Chapter 4, the experimental investigation described in Chapter 5 aimed to investigate the removal of metaldehyde by PAC in a more practical scenario.

Chapter 3 and Chapter 4 demonstrated that PAC was the most effective material studied so far for removing metaldehyde from MilliQ water. Hence, Chapter 5 investigated the removal of metaldehyde from different water samples with different water quality using PAC. This chapter aimed at providing a potentially practical solution to the metaldehyde problem. To investigate the removal of metaldehyde from water by adsorption onto PAC in a practical way, the studied concentration of metaldehyde was selected as 5 µg L⁻¹ to approximate the possible concentration of metaldehyde in surface water bodies that may feed the reservoirs of drinking water treatment plants. Different water samples were collected and spiked with metaldehyde, including natural surface water (pond water) collected from the Regent's Park lake and

partially treated water collected after different treatment stages at Walton-on-Thames Water Treatment Works. MilliQ water and MilliQ water spiked with HA were also used in Chapter 5 to compare with the pond water and partially treated water. All water samples were analysed for their water characteristics including pH, negative ions, DOC, turbidity, DO, and UV_{254} . Considering the practical dosing of PAC in drinking water treatment plants, PAC was added into aqueous solutions as slurry in Chapter 5. PAC dosing concentration equal to or higher than 100 mg L^{-1} could ensure the concentration of metaldehyde (in the partially treated water samples collected from WTWTW) to meet the EU and UK standard of $0.1 \text{ } \mu\text{g L}^{-1}$. For WTWTW, dosing PAC after 'static flocculation' achieved the highest percentage removal of metaldehyde (98.4%), suggesting that flocs may assist the adsorption of metaldehyde onto PAC. Moreover, water quality did not affect the removal of metaldehyde using PAC under the studied experimental condition, indicating that adsorption by PAC was indeed the favoured removal mechanism of metaldehyde. However, adsorption of metaldehyde by PAC would be lower if the initial concentration of metaldehyde is low; hence higher PAC dosage may be needed. In addition, desorption of metaldehyde from used PAC back to water can happen. This brings up the significance of monitoring the concentration of metaldehyde during the treatment stages at drinking water treatment plants. Used PAC need to be recycled and new PAC need to be dosed, to maintain the effective treatment for metaldehyde. Recycled PAC can potentially be regenerated at $60 \text{ } ^\circ\text{C}$, but further researches are needed to provide more information. Chapter 5 delivered Objective (3) and Objective (4). However, it is important to note that competitive adsorption onto PAC may happen at drinking water treatment plants, if there are micropollutants present in the water that share similar physicochemical properties with metaldehyde. Therefore, it is recommended by the researcher to

further investigate and identify compounds that may compete with metaldehyde for adsorption sites on PAC.

6.2 Adsorption mechanisms of metaldehyde from aqueous solutions onto PAC

Effective removal of metaldehyde from water by adsorption onto PAC largely resulted from the characteristics of the PAC used in this thesis, and the surface interactions among metaldehyde molecules, water molecules, and PAC. Table 6.1 summarises the adsorption kinetic and isotherm studies of the adsorption of metaldehyde onto PAC under different experimental conditions.

Table 6.1 Adsorption kinetic and isotherm studies of the PAC used for removing metaldehyde

PAC (purchased from)	Water sample	Experimental condition	Adsorption kinetic		Adsorption isotherm			
			k_1 (min^{-1})	k_2 ($\text{g mg}^{-1} \text{min}^{-1}$)	Freundlich $1/n$	Freundlich $K_F (\text{mg g}^{-1})/(\text{mg L}^{-1})^{1/n}$	Langmuir $q_m (\text{mg g}^{-1})$	Langmuir $K_L (\text{L mg}^{-1})$
BDH laboratory supplies	MilliQ (Chapter 3)	0.1 g of PAC into 500 mL of 5 mg L^{-1} metaldehyde solution for 2 h under UV-C light	3.71×10^{-2} ($R^2=0.7844$)	0.02 ($R^2=0.9994$)				
	MilliQ (Chapter 4)	0.05 g of PAC into 500 mL of 1 mg L^{-1} metaldehyde solutions for 2 h	0.05 ($R^2=0.6532$)	0.16 ($R^2=0.9999$)				
	MilliQ (Chapter 4)	5 to 500 mg of PAC into 500 mL of 1 mg L^{-1} metaldehyde solutions for 2 h			0.21 ($R^2=0.9966$)	31.59 ($R^2=0.9966$)	28.33 ($R^2=0.9994$)	88.25 ($R^2=0.9994$)
Sigma- Aldrich	After 'pre- ozone contactors' (Chapter 5)	0.05 to 150 mg of PAC into 600 mL of 5 $\mu\text{g L}^{-1}$ metaldehyde solutions for 30 min			0.63 ($R^2=0.9898$)	0.11 ($R^2=0.9898$)	0.25 ($R^2=0.841$)	1860 ($R^2=0.841$)
	After 'static flocculation' (Chapter 5)	5 to 150 mg of PAC into 600 mL of 5 $\mu\text{g L}^{-1}$ metaldehyde solution for 30 min			0.22 ($R^2=0.8225$)	0.18 ($R^2=0.8225$)	0.29 ($R^2=0.8831$)	4199 ($R^2=0.8831$)
	MilliQ (Chapter 5)	30 mg of PAC into 600 mL of 1 $\mu\text{g L}^{-1}$ to 1000 $\mu\text{g L}^{-1}$ metaldehyde solutions for 30 min			0.43 ($R^2=0.9894$)	0.87 ($R^2=0.9894$)	13.16 ($R^2=0.9857$)	70 ($R^2=0.9857$)

To be consistent throughout this thesis, it is ideal to use the same PAC in all experimental investigations. However, this was not possible, since BDH laboratory supplies stopped selling DARCO G60® PAC in 2017. Therefore, a second batch of PAC was purchased from Sigma-Aldrich and it was used in the experimental investigations in Chapter 4 and Chapter 5. Although both PAC bear the trademark of DARCO G60®, they have slightly different SSA. The SSA of the PAC purchased from BDH laboratory supplies was estimated to be 1037.89 m² g⁻¹, while the SSA of the PAC purchase from Sigma-Aldrich was measured to be 964.2 m² g⁻¹. However, they both have high SSA (compared to GAC) and similar PSD from the BET SSA analysis. Both are dominated by micropores with abundant mesopores, which justifies the effective removal of metaldehyde via the diffusion-controlled adsorption processes. The efficient removal of metaldehyde by PAC are also supported by fast/direct surface adsorption and promoted by the micropores and mesopores on the PAC, as discussed in Section 4.3.2.4 [30].

Adsorption kinetic studies suggest the pseudo-second order kinetic model is more suitable for the adsorption of metaldehyde from MilliQ water onto PAC under the studied experimental conditions in this thesis. The adsorption of metaldehyde onto PAC in the single adsorption system was very efficient, with k_2 around 0.02 g mg⁻¹ min⁻¹, compared with other researches, as discussed in Section 4.3.2.4. For example, the k_2 values obtained by Tao and Fletcher using amine functionalized silicas and ion exchange resin vary from 3.04×10⁻³ to 1.33×10⁻² g mg⁻¹ min⁻¹, which are lower than the one obtained in this thesis [220]. And k_2 obtained by Salvestrini *et al.* is 4.8×10⁻⁶ g μg⁻¹ h⁻¹ which is 288 times lower than the one obtained in this thesis [70].

Adsorption kinetics of metaldehyde were not studied in Chapter 5 because the contact time of each treatment stage is limited in drinking water treatment plants. A 30-min contact time for the adsorption experiments was selected because it fits the timescale of the contact time of most treatment stages at WTWTW. And the adsorption of metaldehyde onto PAC in MilliQ water plateaued in 30 min, while approaching equilibrium, as discussed in Section 4.3.2.2.

In terms of the adsorption isotherm studies, R^2 values suggested that both the Freundlich and Langmuir isotherm models can be well fitted to the experimental data. However, as discussed in Chapter 5, the K_F values obtained from the Freundlich isotherm model fittings are low, 0.11 to 0.87 ($\mu\text{g mg}^{-1}/(\mu\text{g L}^{-1})^{1/n}$), which cannot explain the effective adsorption of metaldehyde onto PAC observed during the experimental investigations. Moreover, the Freundlich isotherm model assumes heterogeneity of the adsorbent which does not apply in this thesis since the PAC used is generally homogeneous as shown in Section 4.3.1. This was confirmed by the low values of $1/n$ (indicator of heterogeneity) as well. On the other hand, the Langmuir isotherm model assumes a homogeneous adsorbent and that a monolayer of metaldehyde molecules will be adsorbed onto the surface of PAC; and these assumptions suit the adsorption systems investigated in this thesis. In addition, the parameters obtained from fitting the experimental data to the Langmuir isotherm model such as the maximum adsorption capacity (q_m) confirmed the effective adsorption of metaldehyde onto PAC. Therefore, the Langmuir isotherm is considered as a better model to explain the adsorption of metaldehyde onto PAC. However, q_m seems to be dependent on the initial concentration of metaldehyde working solution; higher initial concentrations of metaldehyde working solutions resulted in higher q_m . This was explained in Section

5.3.4, due to lower driving force for mass transfer and competition from water molecules for adsorption sites [30, 42, 210].

When compared with other adsorbents used by Tao and Fletcher, Busquets *et al.*, and Salvestrini *et al.* (Table 3.6 and Table 6.1), the q_m values of the PAC used in this thesis do not stand out [30, 32, 70, 141]. However, the high k_1 and k_2 values obtained in this thesis suggest efficient adsorption of metaldehyde onto PAC under the studied experimental conditions. Fast adsorption of metaldehyde onto PAC is beneficial due to the limited contact time of treatment stages at drinking water treatment plants, such as WTWTW (Figure 5.2). In combination with the possible regeneration of PAC at 60 °C, the removal of metaldehyde by adsorption onto PAC could be a fast and possibly economical treatment method.

6.3 Potential industrial application of PAC regarding removal of metaldehyde

From the findings of the three experimental investigations described in Chapter 3, Chapter 4, and Chapter 5, PAC may potentially be applied at drinking water treatment plants for removing metaldehyde from water. By constant monitoring of the concentration of metaldehyde in surface water bodies that feed the reservoir of the water treatment plant, appropriate amount of PAC can be dosed into the water at certain treatment stages as slurry; and PAC particles can be separated at later treatment stages such as DAF. More researches on recycling and regeneration of used PAC are needed. These researches can determine how many cycles PAC can be regenerated and re-used for removing metaldehyde before complete exhaustion.

It is possible that recycled PAC can be thermally regenerated at relatively low temperatures on-site and prepared as PAC slurry to be re-applied until exhaustion.

As discussed in Chapter 5, under the studied experimental condition, water quality did not affect the adsorption of metaldehyde onto PAC, suggesting that the dosing position of PAC can be adjusted depending on the installations of the specific water treatment plant. Researches and analyses for the specific water treatment plant are crucial to provide a customized design for applying PAC, considering the detected concentration of metaldehyde in the water source, the output of the water treatment plant, the contact time of each treatment stage, and the possible recycling and regeneration of used PAC. For instance, dosing PAC in the water collected after 'static flocculation' at WTWTW achieved the highest removal of metaldehyde under the studied experimental condition, while the dosing position and dosing concentration of PAC can differ for other drinking water treatment plants.

In fact, the application of PAC, especially dosing PAC as slurry in Chapter 5 is relatively more suitable and economical for drinking water treatment plants that already have treatment stages installed to remove suspended solids such as DAF, filtration, or sedimentation. For example, it is possible to dose PAC before 'CoCoDAF units' or 'GAC adsorbers' at WTWTW for removing metaldehyde and to separate used PAC from the treated water at 'CoCoDAF units' or 'GAC adsorbers'. And for drinking water treatment plants that do not have these treatment stages, additional installations are needed to separate PAC particles from the treated water or PAC needs to be immobilized during the treatment processes.

Lastly, the cost of applying PAC for metaldehyde removal at drinking water treatment plants needs to be considered. Taking WTWTW (output of 50 to 135 MLD) as an example, to ensure the EU and UK standard can be met, 5 to 13.5 tons of PAC may be needed to treat water with metaldehyde at a concentration of $5 \mu\text{g L}^{-1}$ every day. The PAC used in Chapter 5 was purchased from Sigma-Aldrich in June 2016. 250 g of PAC was purchased for the price of £24.40. Thus, the cost of applying this PAC to remove metaldehyde at WTWTW could be as high as £488000 to £1317600 every day. This may be a substantial additional expense for WTWTW, considering that 1 m^3 of water from Thames Water costs about 129.54 pence (£1.2954) [221], and 100 g of PAC (£9.76) would be needed to treat 1 m^3 of water. Therefore, real estimates should consider the cost of PAC supplied by industrial suppliers such as Chemvion and Eurocarb which may provide discounts for bulk orders. Also, treatment costs could be reduced if recycling/regeneration of used PAC is considered.

Chapter 7. Conclusions and future work

7.1 Findings and contributions of this thesis

Metaldehyde has been detected in surface water and drinking water in the UK, exceeding the EU and UK standard of $0.1 \mu\text{g L}^{-1}$. This thesis aimed at providing a feasible treatment method, that may potentially be applied drinking water treatment plants, to remove metaldehyde from water and meet the required standard. After reviewing the researches of the physicochemical properties and environmental fate of metaldehyde, detection methods of metaldehyde, and potential treatment methods of metaldehyde, this thesis chose to tackle the metaldehyde problem via heterogeneous photocatalysis and adsorption processes. This is because both approaches showed promising results of removing a variety of organic micropollutants from water including metaldehyde, as discussed in Chapter 2. However, many proposed treatment methods for removing metaldehyde from water are either time/energy-consuming or costly. They cannot be widely applied at an industrial scale. Hence, this thesis investigated the removal of metaldehyde from aqueous solutions by heterogeneous photocatalysis using nanoparticle photocatalysts and adsorption processes using carbon materials.

Regarding the novelty of this thesis and its contribution to knowledge, this thesis is the first research to discuss the removal of metaldehyde from water by adsorption onto PAC under UV-C light, to investigate the impact of HA on adsorption of metaldehyde onto PAC, and to investigate the removal of metaldehyde in water samples collected at different treatment stages at a water treatment plant by adsorption onto PAC. The experimental investigations described in Chapter 3, Chapter 4, and Chapter 5 have

been published in peer-reviewed journals: 'Environmental Science and Pollution Research', 'Royal Society of Chemistry: Advances', and 'Royal Society of Chemistry: Environmental Science: Water Research & Technology', respectively [69, 199, 222].

The main findings of this thesis are summarised as follows:

- Determination of metaldehyde in aqueous solutions by GC-MS via SPE

Metaldehyde in aqueous solutions including natural water, partially treated water, and MilliQ water can be detected and quantified by GC-MS with a LOD of $1.5 \mu\text{g L}^{-1}$ and a LOQ of $5 \mu\text{g L}^{-1}$. Using the modified SPE loading technique described in Chapter 5, metaldehyde can be concentrated 500 times, allowing it to be detected by GC-MS even at lower concentrations. Matrix extracted from natural water does not affect the detection of metaldehyde using this method. The recovery rates of metaldehyde were found within the acceptable range of 70 to 120% (with RSD < 20%) throughout the experimental investigations in this thesis, suggesting that this analytical method is valid.

- Investigation of the effectiveness of different materials regarding the removal of metaldehyde from MilliQ water using nanoparticle photocatalysts and carbon materials

The nanoparticle photocatalysts and carbon materials provided by NCL and C-MET are novel and it is the first time that they were tested for removing metaldehyde from water. All nanoparticle photocatalysts used in this thesis including C-40, C-80, $\text{TiO}_2\text{-G}$, ZnO-G , and commercially available P25 did not remove metaldehyde effectively (highest percentage removal < 6.4%) from MilliQ water under the studied experimental condition. Carbon materials including CPA,

CPAA, and GAC were not effective (highest percentage removal < 12.9%) in removing metaldehyde from MilliQ water. PAC (purchased from BDH laboratory supplies, used in Chapter 3) was found to be highly effective (76.8%) for removing metaldehyde, even without the application of UVC-light. The effective results may benefit from its SSA of $1037.89 \text{ m}^2 \text{ g}^{-1}$ and its prominent micropores, suggesting that adsorption by PAC is the preferred removal mechanism for metaldehyde under the studied experimental condition.

- Investigation of the effect of UV-C light on the removal of metaldehyde from MilliQ water using PAC (purchased from BDH laboratory supplies, used in Chapter 3) and GAC

PAC and GAC were selected for this experiment because PAC and GAC had the two highest percentage removal of metaldehyde in Section 3.3.2. This is the first time that the effect of UV-C light on adsorption of metaldehyde by PAC was studied. The possible combination of adsorption and oxidation was investigated by applying UV-C light in the adsorption system of PAC and GAC. Removal of metaldehyde was slightly improved by the addition of UV-C light, 4.6% for PAC/UV-C and 11.9% for GAC/UV-C. This indicated that the adsorption-oxidation system may work synergistically and improve the removal of micropollutants from water. Adsorption kinetic study of metaldehyde onto PAC under UV-C light was studied because it provided the highest percentage removal of metaldehyde. Data were better fitted to the pseudo-second order kinetic model, and $k_2 = 0.02 \text{ g mg}^{-1} \text{ min}^{-1}$ suggests fast adsorption of metaldehyde onto PAC.

- Characterizations of PAC (purchased from Sigma-Aldrich, used in Chapter 4 and Chapter 5)

Material characterization techniques, including SEM, BET SSA analysis, EDX, ATR-FTIR, and XPS, were used for analysing PAC. SSA of PAC was $962.4 \text{ m}^2 \text{ g}^{-1}$, with a total pore volume of $0.79 \text{ cm}^3 \text{ g}^{-1}$ ^{XIX}. Micropores and mesopores that dominate the PSD of PAC are indeed preferred by the adsorption of metaldehyde. EDX and ATR-FTIR analyses were not conclusive. Direct evidence of metaldehyde or HA adsorbed onto PAC cannot be observed. This is largely due to the limitations of the analytical methods. Due to the same limitation, XPS analysis showed only 1% oxygen increase (from metaldehyde) in metaldehyde loaded PAC.

- Adsorption of metaldehyde from MilliQ water onto PAC in the single adsorption system

This is the first time that the removal of metaldehyde by adsorption onto PAC was closely discussed in an experimental investigation. In the single adsorption system, adsorption of metaldehyde slightly favoured a more alkaline condition, as the percentage removal increased by 1.9%. Removal of metaldehyde (1 mg L^{-1}) from MilliQ (500 mL) water by adsorption onto PAC was highly effective, with 0.05 g PAC and a 2-h contact time. Concentration of metaldehyde plateaued around 30 min, approaching equilibrium. The adsorption of metaldehyde onto PAC under the studied experimental condition can be better explained by the pseudo-second order kinetic model. $k_2 = 0.16 \text{ g mg}^{-1} \text{ min}^{-1}$ suggested that intraparticle diffusion dominates the adsorption process, and the fast adsorption rate benefits from fast

^{XIX} For pores smaller than 315 nm in diameter, determined at 0.99388 relative pressure (P/P_0).

and direct surface adsorption. The adsorption isotherm study indicated that data were better fitted to the Langmuir isotherm model, giving $q_m = 28.33 \text{ mg g}^{-1}$ and $K_L = 88.25 \text{ L mg}^{-1}$; this confirmed the high affinity of metaldehyde molecules to adsorb onto PAC. However, q_m was affected by the initial concentration of metaldehyde working solution, as discussed in Section 5.3.4. $q_m = 13.16 \text{ } \mu\text{g mg}^{-1}$ was found by fitting data to the Langmuir isotherm model (30 mg of PAC was added into 600 mL of $1 \text{ } \mu\text{g L}^{-1}$ to $1000 \text{ } \mu\text{g L}^{-1}$ metaldehyde solution with a 30-min contact time). Due to low concentrations of metaldehyde, driving force for mass transfer is low and there are more water molecules competing with metaldehyde for adsorption sites on PAC.

- Adsorption of HA from MilliQ water onto PAC in the single adsorption system

In the single adsorption system, the removal of HA (30 mg L^{-1}) from MilliQ water (500 mL) by adsorption onto PAC was not as effective (50%) as metaldehyde, with 0.25 g PAC and a 30-day contact time. Adsorption of HA did not reach equilibrium in 30 days; hence, data were fitted to the pseudo-second order kinetic model, $k_2 = 4.23 \times 10^{-5} \text{ g mg}^{-1} \text{ min}^{-1}$. Adsorption of HA onto PAC tend to have two rates, hence the adsorption process can be best explained as diffusion-controlled.

- Removal of metaldehyde from MilliQ water onto PAC in the binary adsorption system (with presence of HA)

This is the first time that the effect of HA on adsorption of metaldehyde onto PAC was investigated. 500 mL of 1 mg L^{-1} metaldehyde can be effectively removed (90.2%) by 0.05 g of PAC with a 2-h contact time, even with a high concentration of HA (90 mg L^{-1}). This confirmed that HA was not competing with metaldehyde for

adsorption sites on PAC. 97.5% of metaldehyde was removed in the binary adsorption system (500 mL of 1 mg L⁻¹ metaldehyde and 30 mg L⁻¹ HA with a 2-h contact time). The PSD of the PAC used in this thesis is suitable for removing metaldehyde because of its abundant numbers of microspores and mesopores. Adsorption of metaldehyde onto PAC in the binary system was best fitted to the pseudo-second order kinetic model ($k_2 = 0.07 \text{ g mg}^{-1} \text{ min}^{-1}$). Adsorption of metaldehyde was slower with the presence of HA.

- Removal of metaldehyde from different water samples by adsorption onto PAC

This is the first time that the removal of metaldehyde was investigated by dosing PAC in water samples collected at different treatment stages of a water treatment plant. Metaldehyde in different water samples, including water collected from the Regent's Park lake, collected after the six different treatment stages at WTWTW, MilliQ water, and MilliQ water with HA, can be effectively removed (with lowest percentage removal of 74.3%), regardless of the water quality. This confirmed that PAC may potentially be applied for removing metaldehyde at drinking water treatment plants. PAC dosage $\geq 100 \text{ mg L}^{-1}$ for the water collected after 'pre-ozone contactors' at WTWTW would ensure the concentration of metaldehyde in water to be below $0.01 \text{ } \mu\text{g L}^{-1}$ (within the EU and UK standard of $0.1 \text{ } \mu\text{g L}^{-1}$) after PAC treatment. Among all the water samples collected from different treatment stages at WTWTW where PAC can potentially be applied, the highest removal of metaldehyde was found for dosing PAC in the water collected after 'static flocculation'. Data were better fitted to the Langmuir isotherm model with $q_m = 0.29 \text{ mg g}^{-1}$ and $K_L = 4.18 \text{ L } \mu\text{g}^{-1}$.

- Desorption of metaldehyde from used PAC back to water and low temperature thermal regeneration of used PAC

This is the first time that desorption of metaldehyde from used PAC back to water was studied. A small amount of metaldehyde (8.6%) would desorb from used PAC back to water, due to the high concentration gradient of metaldehyde between MilliQ water and used PAC. Desorption is quite common for AC; therefore, it is essential to monitor the concentration of metaldehyde in water and the usage of PAC. PAC needs to be recycled in time before desorption happens. Adsorbed metaldehyde on PAC may be thermally degraded at 60 °C. 0.7% instead of 8.6% of metaldehyde desorbed back to water, after used PAC was treated at 60 °C in the oven for 24 h.

7.2 Limitations and recommendations for future research

Due to the availability of materials and instruments, restrictions of laboratorial scale experiments, and limited timescale, it is inevitable that there are limitations of the experimental investigations in this thesis. They are listed below, together with recommendations for future research in related study areas.

- Application of nanoparticle photocatalysts for removing metaldehyde

The nanoparticle photocatalysts tested in Chapter 3 were not effective in removing metaldehyde from MilliQ water under the studied experimental condition. However, this could be limited by the light intensity of the UV-C light used, which was $35 \mu\text{mol m}^{-2} \text{s}^{-1}$, the dosing concentration of the photocatalysts which was 0.2 g L^{-1} , and the nature of the nanoparticle photocatalysts as discussed in Chapter 3. In fact, Reza

et al. suggested that degradation of dyes by applying TiO₂ photocatalysts under solar and UV light depends on a number of parameters, such as pH of solutions, dosing concentration of photocatalysts, initial concentrations of dyes, presence of oxidants, reaction temperature, and light intensity [223]. Therefore, the researcher suggests that future researches can vary and optimise the same parameters proposed by Reza *et al.* for degradation of metaldehyde by heterogeneous photocatalysts using nanoparticle photocatalysts [223].

- Degradation pathway of metaldehyde during heterogeneous photocatalysis

Since the removal of metaldehyde was not effective by heterogeneous photocatalysis using the nanoparticle photocatalysts tested in this thesis, the possible degradation products were not studied. However, it is worth investigating the degradation pathway of metaldehyde by heterogeneous photocatalysis and its degradation products during the process. It is suggested by the researcher that DOC should be measured as well, even when effective removal of metaldehyde is observed. This is because metaldehyde may not be detected by GC-MS after effective degradation, but its intermediate degradation products might still be present in water and they can be harmful. For instance, Sang *et al.* suggested that the photoinduced degradation by-products of acesulfame were more than 500 times more toxic than the parent compound [224].

- Combination of UV-C light and GAC for removing metaldehyde

As discussed in Chapter 3, incorporating UV-C for potential oxidation with adsorption using GAC for removing metaldehyde can be further investigated. The proposed adsorption-oxidation system may be effective for removing

micropollutants; for example, the removal efficiency of metaldehyde by GAC/UV-C can be further studied. An economic analysis to discuss the application of light source is recommended as well. For example, Kim *et al.* found more than 95% removal of HA by coupling adsorption and photocatalysis using TiO₂/Coconut Shell Powder Composite [160].

- Different activation methods of carbon powder

Different activation methods for activating carbon powder such as CPA can be investigated; for example, chemical activation methods using different acids including nitric acid, and physical activation methods using steam/vapour. Material characterizations of the carbon powder after activation are recommended, to determine their SSA and PSD after different activation methods. For instance, Bergna *et al.* suggested that different activation methods can affect the characterizations of AC including SSA and PSD [225].

- Effect of different PSD of PAC on removal of metaldehyde

PAC was the most effective material tested in this thesis for removing metaldehyde. According to the study of Busquets *et al.*, the adsorption capacity of adsorbents for metaldehyde is related to the PSD of adsorbents [30]. However, the PSD of the PAC used in this thesis was fixed and cannot confirm or support the conclusion of the research of Busquets *et al.*. Hence, the relationship between different PSD of PAC and removal of metaldehyde from natural water samples can be further investigated.

- Investigation of different fractions of HA and their impacts on the removal of metaldehyde by PAC

As mentioned in Chapter 4, HA is a distribution of molecules and it has different fractions which have different physicochemical properties, such as gray and brown HA. These fractions may affect the adsorption of metaldehyde onto PAC differently. Due to the availability of analytical instruments in this research, this aspect was not investigated. Therefore, it is recommended that nuclear magnetic resonance may be a better analytical method for characterizing HA and its fractions.

- Other organic pollutants in a multi-component adsorption system may compete with metaldehyde for adsorption onto PAC (possible competitive adsorption)

This thesis concluded that HA is not competing with metaldehyde for active adsorption sites on PAC under the studied experimental condition, due to the large and complex size of HA molecules and the PSD of the PAC used. However, there could be competitive adsorption in a multi-component adsorption system, if there are other organic micropollutants in the solution that share similar physicochemical properties with metaldehyde such as paraldehyde. They could compete with metaldehyde molecules for adsorption sites on PAC. It is recommended by the researcher to further investigate the possible competitive adsorption regarding the removal of metaldehyde by PAC in a multi-component adsorption system, and to determine the adsorption capacity of PAC. For example, Rolph *et al.* investigated the removal of metaldehyde together with a few potential competitive compounds including serine, leucine, and resorcinol [74]. Other potential competitive organic compounds such as paraldehyde are suggested to be investigated as well,

regarding the removal of metaldehyde from a multi-component adsorption system by adsorption onto PAC.

- Possible application of PAC for removing other organic micropollutants

As mentioned before, it is the combination of the physicochemical properties of metaldehyde and the characteristics of the PAC used in this thesis that resulted in the effective removal of metaldehyde. Hence, PAC may be used for removing other organic micropollutants that share similar properties with metaldehyde. It is suggested by the researcher to investigate the effectiveness and efficiency of PAC to remove other organic micropollutants.

- Surface interactions between metaldehyde molecules and PAC

There is more to study regarding the adsorption interaction mechanisms between the surface groups on PAC and metaldehyde. Ferino-Pérez *et al.* studied the interactions between metaldehyde and acidic surface groups of AC with changing pH conditions via modelling [42]. It could be beneficial to confirm their conclusions via experimental investigations.

- Impact of solid loading on treatment stages such as DAF, sedimentation and filtration

As discussed in Chapter 5, for drinking water treatment plants that have treatment stages to remove suspended solids, it is better to dose PAC before these stages, so that PAC can be separated from the treated water at these stages. However, dosing a large amount of PAC to remove metaldehyde and other pollutants from

water could have negative impacts on these stages. This needs to be further investigated before potential application of PAC at drinking water treatment plants.

- Desorption of metaldehyde from used PAC back to water and possible regeneration of used PAC

As suggested in Chapter 5, it is worth studying the combined desorption and adsorption processes of metaldehyde off-from/onto PAC, together with other organic pollutants in natural water, to provide insight regarding the suitable time to recycle used PAC and dose new PAC in the treatment system. Possible regeneration of used PAC needs to be studied as well. Treatment temperatures and methods can be varied to identify the most eco-friendly way for regenerating used PAC. The adsorption capacity of regenerated PAC also needs to be investigated, to determine how many cycles PAC can be used for removing metaldehyde before complete exhaustion. For instance, Li *et al.* stated that the regeneration of used PAC depends on the regeneration time and temperature, which affect the adsorption capacity of regenerated PAC [226].

- Economic analysis for application of PAC

An economic analysis for application of PAC in the water treatment industry regarding the cost could be beneficial to determine if PAC dosing can potentially be implemented in full-scale drinking water treatment plants.

References

1. Stamm, C., et al., *Chapter Four - Unravelling the Impacts of Micropollutants in Aquatic Ecosystems: Interdisciplinary Studies at the Interface of Large-Scale Ecology*, in *Advances in Ecological Research*, A.J. Dumbrell, R.L. Kordas, and G. Woodward, Editors. 2016, Academic Press. p. 183-223.
2. *Observatory monitoring framework – indicator data sheet*. 2012, UK Department for Environment, Food & Rural Affairs.
3. *Pharmaceuticals in Drinking-water*. 2011, World Health Organization.
4. Leung, H.W., et al., *Pharmaceuticals in tap water: human health risk assessment and proposed monitoring framework in China*. *Environmental Health Perspectives*, 2013. **121**(7): p. 839-846.
5. Kümmerer, K., *Pharmaceuticals in the Environment — Scope of the Book and Introduction*, in *Pharmaceuticals in the Environment: Sources, Fate, Effects and Risks*, K. Kümmerer, Editor. 2004, Springer Berlin Heidelberg: Berlin, Heidelberg. p. 3-11.
6. Kumar, A., B. Chang, and I. Xagorarakis, *Human health risk assessment of pharmaceuticals in water: issues and challenges ahead*. *International Journal of Environmental Research and Public Health*, 2010. **7**(11): p. 3929-53.
7. Jiang, J.-Q., *The role of coagulation in water treatment*. *Current Opinion in Chemical Engineering*, 2015. **8**: p. 36-44.
8. *Briefing paper on metaldehyde*. 2013, Water UK.
9. Li, J., Q. Zhou, and L.C. Campos, *The application of GAC sandwich slow sand filtration to remove pharmaceutical and personal care products*. *Science of the Total Environment*, 2018. **635**: p. 1182-1190.
10. Douglas, M.R. and J.F. Tooker, *Slug (Mollusca: Agriolimacidae, Arionidae) Ecology and Management in No-Till Field Crops, With an Emphasis on the mid-Atlantic Region*. *Journal of Integrated Pest Management*, 2012. **3**(1): p. C1-C9.
11. *The determination of metaldehyde in waters using chromatography with mass spectrometric detection* 2009, UK Environment Agency.
12. Castle, G.D., et al., *Review of the molluscicide metaldehyde in the environment*. *Environmental Science: Water Research & Technology*, 2017. **3**(3): p. 415-428.

13. *Conclusion on the peer review of the pesticide risk assessment of the active substance metaldehyde*. 2010, European Food Safety Authority. p. 1856.
14. Gupta, R.C., *CHAPTER 47 - Metaldehyde*, in *Veterinary Toxicology*, R.C. Gupta, Editor. 2007, Academic Press: Oxford. p. 518-521.
15. Margot, J., et al., *Treatment of micropollutants in municipal wastewater: ozone or powdered activated carbon?* *Science of the Total Environment*, 2013. **461-462**: p. 480-498.
16. Altmann, J., et al., *Combination of granular activated carbon adsorption and deep-bed filtration as a single advanced wastewater treatment step for organic micropollutant and phosphorus removal*. *Water Research*, 2016. **92**: p. 131-139.
17. Wu, D., et al., *Ozonation as an advanced oxidant in treatment of bamboo industry wastewater*. *Chemosphere*, 2012. **88**(9): p. 1108-1113.
18. Camel, V. and A. Bermond, *The use of ozone and associated oxidation processes in drinking water treatment*. *Water Research*, 1998. **32**(11): p. 3208-3222.
19. Narbaitz, R.M. and J. McEwen, *Electrochemical regeneration of field spent GAC from two water treatment plants*. *Water Research*, 2012. **46**(15): p. 4852-4860.
20. Bhatnagar, A., et al., *An overview of the modification methods of activated carbon for its water treatment applications*. *Chemical Engineering Journal*, 2013. **219**: p. 499-511.
21. Vilhunen, S. and M. Sillanpää, *Recent developments in photochemical and chemical AOPs in water treatment: a mini-review*. *Reviews in Environmental Science and Bio/Technology*, 2010. **9**(4): p. 323-330.
22. Ribeiro, A.R., et al., *An overview on the advanced oxidation processes applied for the treatment of water pollutants defined in the recently launched Directive 2013/39/EU*. *Environment International*, 2015. **75**: p. 33-51.
23. Deng, Y. and R. Zhao, *Advanced Oxidation Processes (AOPs) in Wastewater Treatment*. *Current Pollution Reports*, 2015. **1**(3): p. 167-176.
24. Pereira, V.J., et al., *UV Degradation Kinetics and Modeling of Pharmaceutical Compounds in Laboratory Grade and Surface Water via Direct and Indirect Photolysis at 254 nm*. *Environmental Science & Technology*, 2007. **41**(5): p. 1682-1688.

25. Vogna, D., et al., *Kinetic and chemical assessment of the UV/H₂O₂ treatment of antiepileptic drug carbamazepine*. *Chemosphere*, 2004. **54**(4): p. 497-505.
26. Klavarioti, M., D. Mantzavinos, and D. Kassinos, *Removal of residual pharmaceuticals from aqueous systems by advanced oxidation processes*. *Environment International*, 2009. **35**(2): p. 402-417.
27. Serrano, D., et al., *Removal of persistent pharmaceutical micropollutants from sewage by addition of PAC in a sequential membrane bioreactor*. *Water Research*, 2011. **45**(16): p. 5323-5333.
28. Chen, W., et al., *Arsenic removal by iron-modified activated carbon*. *Water Research*, 2007. **41**(9): p. 1851-1858.
29. Autin, O., et al., *Comparison of UV/H₂O₂ and UV/TiO₂ for the degradation of metaldehyde: Kinetics and the impact of background organics*. *Water Research*, 2012. **46**(17): p. 5655-5662.
30. Busquets, R., et al., *Phenolic carbon tailored for the removal of polar organic contaminants from water: a solution to the metaldehyde problem?* *Water Research*, 2014. **61**: p. 46-56.
31. Nabeerasool, M., et al., *Removal of Metaldehyde from Water Using a Novel Coupled Adsorption and Electrochemical Destruction Technique*. *Water*, 2015. **7**(6): p. 3057-3071.
32. Tao, B. and A. Fletcher, *Development of a novel dual-stage method for metaldehyde removal from water*. *Chemical Engineering Journal*, 2016. **284**: p. 741-749.
33. Matsui, Y., et al., *Effect of natural organic matter on powdered activated carbon adsorption of trace contaminants: characteristics and mechanism of competitive adsorption*. *Water Research*, 2003. **37**(18): p. 4413-4424.
34. Yoon, Y., et al., *HPLC-fluorescence detection and adsorption of bisphenol A, 17β-estradiol, and 17α-ethynyl estradiol on powdered activated carbon*. *Water Research*, 2003. **37**(14): p. 3530-3537.
35. *Restrictions on the use of metaldehyde to protect wildlife*. 2018, GOV.UK.
36. Bradbury, K. *Slug pellets ban lifted after legal challenge by manufacturer*. 10th August 2019 [6th April 2020]; Available from: <https://www.telegraph.co.uk/gardening/problem-solving/slug-pellets-ban-lifted-legal-challenge-manufacturer/>.

37. Calza, P., et al., *The photocatalytic process as a tool to identify metabolic products formed from dopant substances: the case of buspirone*. Journal of Pharmaceutical and Biomedical Analysis, 2004. **35**(1): p. 9-19.
38. Ali, I. and V.K. Gupta, *Advances in water treatment by adsorption technology*. Nature Protocols, 2006. **1**(6): p. 2661-2667.
39. Guo, Y. and E. Du, *The Effects of Thermal Regeneration Conditions and Inorganic Compounds on the Characteristics of Activated Carbon Used in Power Plant*. Energy Procedia, 2012. **17**: p. 444-449.
40. Joseph, L., et al., *Removal of bisphenol A and 17 α -ethinyl estradiol by combined coagulation and adsorption using carbon nanomaterials and powdered activated carbon*. Separation and Purification Technology, 2013. **107**: p. 37-47.
41. Li, Z., *Degradation of metaldehyde using powdered activated carbon and nanoparticle catalysts*, in *CEGE*. 2015, University College London.
42. Ferino-Pérez, A., et al., *Explaining the interactions between metaldehyde and acidic surface groups of activated carbon under different pH conditions*. Journal of Molecular Graphics and Modelling, 2019. **90**: p. 94-103.
43. *PPDB: Pesticide Properties DataBase*. 25th June 2019 [29th September 2019]; Available from: <http://sitem.herts.ac.uk/aeru/ppdb/en/Reports/446.htm>.
44. *U.S. National Library of Medicine Hazardous Substances Data Bank database*. 21st January 2010 [29th September 2019]; Available from: <https://toxnet.nlm.nih.gov/cgi-bin/sis/search/a?dbs+hsdb:@term+@DOCNO+1735>.
45. Voutsas, E., *Chapter 11 - Estimation of the Volatilization of Organic Chemicals from Soil*, in *Thermodynamics, Solubility and Environmental Issues*, T.M. Letcher, Editor. 2007, Elsevier: Amsterdam. p. 205-227.
46. Horwath, W., *Chapter 12 - Carbon Cycling: The Dynamics and Formation of Organic Matter*, in *Soil Microbiology, Ecology and Biochemistry (Fourth Edition)*, E.A. Paul, Editor. 2015, Academic Press: Boston. p. 339-382.
47. Luo, Y., et al., *A review on the occurrence of micropollutants in the aquatic environment and their fate and removal during wastewater treatment*. Science of the Total Environment, 2014. **473-474**: p. 619-641.
48. O'Sullivan, G. and D. Megson, *Chapter 1 - Brief Overview: Discovery, Regulation, Properties, and Fate of POPs*, in *Environmental Forensics for*

- Persistent Organic Pollutants*, G. O'Sullivan and C. Sandau, Editors. 2014, Elsevier: Amsterdam. p. 1-20.
49. Kay, P. and R. Grayson, *Using water industry data to assess the metaldehyde pollution problem*. *Water and Environment Journal*, 2014. **28**(3): p. 410-417.
50. Kar, D., *Chapter 8 - Methodologies of Different Types of Studies*, in *Epizootic Ulcerative Fish Disease Syndrome*, D. Kar, Editor. 2016, Academic Press. p. 187-221.
51. *The WHO Recommended Classification of Pesticides by Hazard and Guidelines to Classification 2009*. 2010, Stuttgart, Germany: World Health Organization.
52. Kamrin, M.A., *Pesticide Profiles: Toxicity, Environmental Impact, and Fate*. 1997, Boca Raton: CRC/Lewis Publishers.
53. Caloni, F., et al., *Chapter 3 - Epidemiology of Animal Poisonings in Europe*, in *Veterinary Toxicology (Third Edition)*, R.C. Gupta, Editor. 2018, Academic Press. p. 45-56.
54. Zoltani, C.K., *Chapter 14 - Cardiovascular Toxicity*, in *Veterinary Toxicology (Third Edition)*, R.C. Gupta, Editor. 2018, Academic Press. p. 227-238.
55. Dolder, L.K., *Metaldehyde toxicosis*. *Veterinary Medicine*, 2003: p. 213-215.
56. Gupta, P.K., *Chapter 4 - Epidemiology of Animal Poisonings in Asia*, in *Veterinary Toxicology (Third Edition)*, R.C. Gupta, Editor. 2018, Academic Press. p. 57-69.
57. Horgan, F.G., et al., *Responses by farmers to the apple snail invasion of Ecuador's rice fields and attitudes toward predatory snail kites*. *Crop Protection*, 2014. **62**: p. 135-143.
58. Moreau, P., T. Burgeot, and T. Renault, *In vivo effects of metaldehyde on Pacific oyster, Crassostrea gigas: comparing hemocyte parameters in two oyster families*. *Environmental Science and Pollution Research*, 2015. **22**(11): p. 8003-8009.
59. *EU Pesticides database*. 7th April 2016 [30th September 2019]; Available from: <https://ec.europa.eu/food/plant/pesticides/eu-pesticides-database/public/?event=activesubstance.detail&language=EN&selectedID=1556>.

60. *Pesticides - Drinking Water Inspectorate*. January 2010 [30th September 2019]; Available from: <http://dwi.defra.gov.uk/consumers/advice-leaflets/pesticides.pdf>.
61. Saad, A.M., S.W. Ismail, and F.A. Dahalan, *Metaldehyde Toxicity: A Brief on Three Different Perspectives*. Journal of Civil Engineering, Science and Technology, 2017. **8**(2): p. 108-114.
62. *The Drinking Water Inspectorate annual report drinking water 2015*. 2016 5th August 2016 1st October 2019]; Available from: <http://www.dwi.gov.uk/about/annual-report/index.htm>.
63. *Drinking Water Protected Areas (Surface Water)*. 28th June 2019 [1st October 2019]; Available from: <https://data.gov.uk/dataset/3d136e9a-78cf-4452-824d-39d715ba5b69/drinking-water-protected-areas-surface-water>.
64. *Drinking Water Protected Areas Safeguard Zones*. 3rd July 2019 [1st October 2019]; Available from: <http://apps.environment-agency.gov.uk/wiyby/141891.aspx>.
65. *Pesticides in the UK: The 2015 report on the impacts and sustainable use of pesticides*. 2015, The Pesticides Forum.
66. Rae, R.G., J.F. Robertson, and M.J. Wilson, *Optimization of biological (*Phasmarhabditis hermaphrodita*) and chemical (iron phosphate and metaldehyde) slug control*. Crop Protection, 2009. **28**(9): p. 765-773.
67. Kristo, M.J., *Chapter 21 - Nuclear Forensics*, in *Handbook of Radioactivity Analysis (Third Edition)*, M.F. L'Annunziata, Editor. 2012, Academic Press: Amsterdam. p. 1281-1304.
68. Mani, D., et al., *Chapter 3 - Organic Matter in Gas Shales: Origin, Evolution, and Characterization*, in *Shale Gas*, A.M. Dayal and D. Mani, Editors. 2017, Elsevier. p. 25-54.
69. Li, Z., et al., *Degradation of metaldehyde in water by nanoparticle catalysts and powdered activated carbon*. Environmental Science and Pollution Research, 2017. **24**(21): p. 17861-17873.
70. Salvestrini, S., et al., *Sorption of metaldehyde using granular activated carbon*. Journal of Water Reuse and Desalination, 2017. **7**(3): p. 280-287.
71. Tilvi, S., M.S. Majik, and K.S. Singh, *Chapter 8 - Mass Spectrometry for Determination of Bioactive Compounds*, in *Comprehensive Analytical*

- Chemistry*, T. Rocha-Santos and A.C. Duarte, Editors. 2014, Elsevier. p. 193-218.
72. Rahman, M., *Chapter 4 - Application of Computational Methods in Isolation of Plant Secondary Metabolites*, in *Computational Phytochemistry*, S.D. Sarker and L. Nahar, Editors. 2018, Elsevier. p. 107-139.
73. Crutchfield, C.A., et al., *Chapter 16 - Mass Spectrometry-Based Metabolomics of Yeast*, in *Methods in Enzymology*. 2010, Academic Press. p. 393-426.
74. Rolph, C.A., et al., *Metaldehyde removal from drinking water by adsorption onto filtration media: mechanisms and optimisation*. *Environmental Science: Water Research & Technology*, 2018. **4**(10): p. 1543-1552.
75. Li, C., et al., *Determination of Metaldehyde in Water by SPE and UPLC–MS–MS*. *Chromatographia*, 2010. **72**(9-10): p. 987-991.
76. A. Davey, T.H., J. Horn, J. Jönsson and R. Keirle, *Evidence Review of Catchment Strategies for Managing Metaldehyde Report Ref. No. 13/DW/14/7*. 2014, UK Water Industry Research Limited.
77. Brockett, J. *Promising results for metaldehyde detection trial*. 2017 [13th October 2019]; Available from: <https://wwtonline.co.uk/news/promising-results-for-metaldehyde-detection-trial#.Wlsb8n1y1dd>.
78. Raknes, K.L., *Ozone in Drinking Water Treatment: Process Design, Operation, and Optimization*. 2005, Denver: American Water Works Association.
79. Lawrence, J. and F.P. Cappelli, *Ozone in drinking water treatment: A review*. *Science of the Total Environment*, 1977. **7**(2): p. 99-108.
80. Andreozzi, R., et al., *Advanced oxidation processes (AOP) for water purification and recovery*. *Catalysis Today*, 1999. **53**(1): p. 51-59.
81. Glaze, W.H., *Drinking-water treatment with ozone*. *Environmental Science & Technology*, 1987. **21**(3): p. 224-230.
82. O'Shea, K.E. and D.D. Dionysiou, *Advanced Oxidation Processes for Water Treatment*. *The Journal of Physical Chemistry Letters*, 2012. **3**(15): p. 2112-2113.
83. Saritha, P., et al., *Comparison of various advanced oxidation processes for the degradation of 4-chloro-2 nitrophenol*. *Journal of Hazardous Materials*, 2007. **149**(3): p. 609-614.

84. Sanches, S., M.T. Barreto Crespo, and V.J. Pereira, *Drinking water treatment of priority pesticides using low pressure UV photolysis and advanced oxidation processes*. Water Research, 2010. **44**(6): p. 1809-1818.
85. Gan, Y., et al., *Photolysis of chloral hydrate in water with 254nm ultraviolet: Kinetics, influencing factors, mechanisms, and products*. Chemosphere, 2019. **218**: p. 104-109.
86. Song, W., V. Ravindran, and M. Pirbazari, *Process optimization using a kinetic model for the ultraviolet radiation-hydrogen peroxide decomposition of natural and synthetic organic compounds in groundwater*. Chemical Engineering Science, 2008. **63**(12): p. 3249-3270.
87. Z.K. Chowdhury, R.S.S., G.P. Westerhoff, B.J. Leto, K.O. Nowack, C.J. Corwin, *Activated Carbon: Solutions for Improving Water Quality*. 2013, Denver: American Water Works Association.
88. Ting Lee, C.-H.O., Radzali Othman and Fei-Yee Yeoh, *Activated carbon fiber - The hybrid of carbon fiber and activated carbon*. Reviews on Advanced Materials Science, 2014. **36**(2): p. 118-136.
89. Pollard, S.J.T., et al., *Low-cost adsorbents for waste and wastewater treatment: a review*. Science of the Total Environment, 1992. **116**(1): p. 31-52.
90. B. Averill, P.E., *General Chemistry: Principles, Patterns and Applications*. 2011, Washington, D.C.: Saylor Foundation.
91. Liu, X.W., W.W. Li, and H.Q. Yu, *Cathodic catalysts in bioelectrochemical systems for energy recovery from wastewater*. Chemical Society Reviews, 2014. **43**(22): p. 7718-7745.
92. Zhang, Y., et al., *Synthesis, Characterization, and Applications of ZnO Nanowires*. Journal of Nanomaterials, 2012. **2012**: p. 1-22.
93. Kim, J.K., et al., *Degradation of Humic Acid by Photocatalytic Reaction Using Nano-sized ZnO/Laponite Composite (NZLC)*. Water, Air, & Soil Pollution, 2013. **224**(11).
94. Doria, F.C., et al., *Removal of Metaldehyde Through Photocatalytic Reactions Using Nano-Sized Zinc Oxide Composites*. Water, Air, & Soil Pollution, 2013. **224**(2).
95. Khraisheh, M., et al., *Removal of Carbamazepine from Water by a Novel TiO₂-Coconut Shell Powder/UV Process: Composite Preparation and Photocatalytic Activity*. Environmental Engineering Science, 2013. **30**(9): p. 515-526.

96. McCullagh, C., et al., *The application of TiO₂ photocatalysis for disinfection of water contaminated with pathogenic micro-organisms: a review*. Research on Chemical Intermediates, 2007. **33**(3): p. 359-375.
97. Herrmann, J.M., C. Guillard, and P. Pichat, *Heterogeneous photocatalysis : an emerging technology for water treatment*. Catalysis Today, 1993. **17**(1): p. 7-20.
98. Kim, J., C.W. Lee, and W. Choi, *Platinized WO₃ as an Environmental Photocatalyst that Generates OH Radicals under Visible Light*. Environmental Science & Technology, 2010. **44**(17): p. 6849-6854.
99. Bae, E. and W. Choi, *Highly Enhanced Photoreductive Degradation of Perchlorinated Compounds on Dye-Sensitized Metal/TiO₂ under Visible Light*. Environmental Science & Technology, 2003. **37**(1): p. 147-152.
100. Hsieh, W.P., et al., *Enhance the photocatalytic activity for the degradation of organic contaminants in water by incorporating TiO₂ with zero-valent iron*. Science of the Total Environment, 2010. **408**(3): p. 672-679.
101. Li, G., et al., *Adsorption of cyclic organics generated during electrochemical oxidation of Orange II by activated carbon fibres and toxicity test*. Journal of Water Process Engineering, 2015. **7**: p. 21-26.
102. Xu, J., L. Wang, and Y. Zhu, *Decontamination of bisphenol A from aqueous solution by graphene adsorption*. Langmuir, 2012. **28**(22): p. 8418-8425.
103. Deng, X., et al., *The adsorption properties of Pb(II) and Cd(II) on functionalized graphene prepared by electrolysis method*. Journal of Hazardous Materials, 2010. **183**(1-3): p. 923-930.
104. Liu, T., et al., *Adsorption of methylene blue from aqueous solution by graphene*. Colloids Surf B Biointerfaces, 2012. **90**: p. 197-203.
105. Ali, I., et al., *Graphene based adsorbents for remediation of noxious pollutants from wastewater*. Environment International, 2019. **127**: p. 160-180.
106. Kaushik, B.K. and M.K. Majumder, *Carbon Nanotube Based VLSI Interconnects: Analysis and Design*. 2015, New Delhi: Springer.
107. Tofighy, M.A. and T. Mohammadi, *Adsorption of divalent heavy metal ions from water using carbon nanotube sheets*. Journal of Hazardous Materials, 2011. **185**(1): p. 140-147.

108. Li, Y.-H., et al., *Competitive adsorption of Pb²⁺, Cu²⁺ and Cd²⁺ ions from aqueous solutions by multiwalled carbon nanotubes*. Carbon, 2003. **41**(14): p. 2787-2792.
109. Eatemadi, A., et al., *Carbon nanotubes: properties, synthesis, purification, and medical applications*. Nanoscale Research Letters, 2014. **9**(1): p. 393.
110. Das, R., et al., *Carbon nanotube membranes for water purification: A bright future in water desalination*. Desalination, 2014. **336**: p. 97-109.
111. Tang, D., et al., *Adsorption of p-nitrophenol from aqueous solutions onto activated carbon fiber*. Journal of Hazardous Materials, 2007. **143**(1-2): p. 49-56.
112. Heijman, S.G.J. and R. Hopman, *Activated carbon filtration in drinking water production: model prediction and new concepts*. Colloids and Surfaces A: Physicochemical and Engineering Aspects, 1999. **151**(1): p. 303-310.
113. Park, S.-J. and Y.-S. Jang, *Preparation and characterization of activated carbon fibers supported with silver metal for antibacterial behavior*. Journal of Colloid and Interface Science, 2003. **261**(2): p. 238-243.
114. Fuertes, A.B., G. Marbán, and D.M. Nevskaja, *Adsorption of volatile organic compounds by means of activated carbon fibre-based monoliths*. Carbon, 2003. **41**(1): p. 87-96.
115. Ma, X., et al., *Preparation, Surface and Pore Structure of High Surface Area Activated Carbon Fibers from Bamboo by Steam Activation*. Materials (Basel), 2014. **7**(6): p. 4431-4441.
116. Woan, K., G. Pyrgiotakis, and W. Sigmund, *Photocatalytic Carbon-Nanotube-TiO₂Composites*. Advanced Materials, 2009. **21**(21): p. 2233-2239.
117. Asha, R.C., et al., *Livestock Wastewater Treatment in Batch and Continuous Photocatalytic Systems: Performance and Economic Analyses*. Water, Air, & Soil Pollution, 2015. **226**(5).
118. Subramani, A.K., et al., *Photocatalytic degradation of indigo carmine dye using TiO₂ impregnated activated carbon*. Bulletin of Materials Science, 2007. **30**(1): p. 37-41.
119. Yu, Y., et al., *Enhancement of adsorption and photocatalytic activity of TiO₂ by using carbon nanotubes for the treatment of azo dye*. Applied Catalysis B: Environmental, 2005. **61**(1-2): p. 1-11.

120. Wang, W., et al., *Visible light photodegradation of phenol on MWNT-TiO₂ composite catalysts prepared by a modified sol-gel method*. Journal of Molecular Catalysis A: Chemical, 2005. **235**(1-2): p. 194-199.
121. Tang, L.L., et al., *TAML/H₂O₂ Oxidative Degradation of Metaldehyde: Pursuing Better Water Treatment for the Most Persistent Pollutants*. Environmental Science & Technology, 2016. **50**(10): p. 5261-5268.
122. Nguyen, L.V., et al., *Graphene oxide-based degradation of metaldehyde: Effective oxidation through a modified Fenton's process*. Chemical Engineering Journal, 2017. **307**: p. 159-167.
123. Radjenovic A, M.G., *Adsorptive removal of Cr (VI) from aqueous solution by carbon black*. Journal of Chemical Technology and Metallurgy, 2015. **50**(1): p. 81-88.
124. Amidon, G.E., P.J. Meyer, and D.M. Mudie, *Chapter 10 - Particle, Powder, and Compact Characterization*, in *Developing Solid Oral Dosage Forms (Second Edition)*, Y. Qiu, et al., Editors. 2017, Academic Press: Boston. p. 271-293.
125. Ebnesajjad, S., *Chapter 4 - Surface and Material Characterization Techniques*, in *Surface Treatment of Materials for Adhesive Bonding (Second Edition)*, S. Ebnesajjad, Editor. 2014, William Andrew Publishing: Oxford. p. 39-75.
126. Amin, M.A., et al., *The inhibition of low carbon steel corrosion in hydrochloric acid solutions by succinic acid*. Electrochimica Acta, 2007. **52**(11): p. 3588-3600.
127. Mattox, D.M., *Chapter 2 - Substrate ("Real") Surfaces and Surface Modification*, in *Handbook of Physical Vapor Deposition (PVD) Processing (Second Edition)*, D.M. Mattox, Editor. 2010, William Andrew Publishing: Boston. p. 25-72.
128. Zhang, S., X.Y. Li, and J.P. Chen, *An XPS study for mechanisms of arsenate adsorption onto a magnetite-doped activated carbon fiber*. Journal of Colloid and Interface Science, 2010. **343**(1): p. 232-8.
129. Geng, H., D. Gupta, and C.-U. Ro, *Chapter 11 - Microscopic Single-Particle Analytical Methods for Aerosol Characterisation*, in *Comprehensive Analytical Chemistry*, P.B.C. Forbes, Editor. 2015, Elsevier. p. 331-366.
130. Dris, R., et al., *Chapter 3 - Microplastic Contamination in Freshwater Systems: Methodological Challenges, Occurrence and Sources*, in *Microplastic Contamination in Aquatic Environments*, E.Y. Zeng, Editor. 2018, Elsevier. p. 51-93.

131. Alawam, K., *Chapter Nine - Application of Proteomics in Diagnosis of ADHD, Schizophrenia, Major Depression, and Suicidal Behavior*, in *Advances in Protein Chemistry and Structural Biology*, R. Donev, Editor. 2014, Academic Press. p. 283-315.
132. Ahmed, M.H., et al., *Comparison between FTIR and XPS characterization of amino acid glycine adsorption onto diamond-like carbon (DLC) and silicon doped DLC*. *Applied Surface Science*, 2013. **273**: p. 507-514.
133. Athar, T., *Chapter 17 - Smart precursors for smart nanoparticles*, in *Emerging Nanotechnologies for Manufacturing (Second Edition)*, W. Ahmed and M.J. Jackson, Editors. 2015, William Andrew Publishing: Boston. p. 444-538.
134. Fu, F., L. Lin, and E. Xu, *4 - Functional pretreatments of natural raw materials*, in *Advanced High Strength Natural Fibre Composites in Construction*, M. Fan and F. Fu, Editors. 2017, Woodhead Publishing. p. 87-114.
135. Wu, F.-C., R.-L. Tseng, and C.-C. Hu, *Comparisons of pore properties and adsorption performance of KOH-activated and steam-activated carbons*. *Microporous and Mesoporous Materials*, 2005. **80**(1): p. 95-106.
136. Sposito, G., *On Points of Zero Charge*. *Environmental Science & Technology*, 1998. **32**(19): p. 2815-2819.
137. Carrales-Alvarado, D.H., et al., *Removal of the antibiotic metronidazole by adsorption on various carbon materials from aqueous phase*. *Journal of Colloid and Interface Science*, 2014. **436**: p. 276-85.
138. Chung, Y.-C. and C.-Y. Chen, *Degradation of azo dye reactive violet 5 by TiO₂ photocatalysis*. *Environmental Chemistry Letters*, 2009. **7**(4): p. 347-352.
139. Lin, Y., et al., *Study of benzylparaben photocatalytic degradation by TiO₂*. *Applied Catalysis B: Environmental*, 2011. **104**(3-4): p. 353-360.
140. Agrios, A.G. and P. Pichat, *State of the art and perspectives on materials and applications of photocatalysis over TiO₂*. *Journal of Applied Electrochemistry*, 2005. **35**(7): p. 655-663.
141. Tao, B. and A.J. Fletcher, *Metaldehyde removal from aqueous solution by adsorption and ion exchange mechanisms onto activated carbon and polymeric sorbents*. *Journal of Hazardous Materials*, 2013. **244-245**: p. 240-250.
142. Kumar, A., B. Prasad, and I.M. Mishra, *Adsorptive removal of acrylonitrile by commercial grade activated carbon: kinetics, equilibrium and thermodynamics*. *Journal of Hazardous Materials*, 2008. **152**(2): p. 589-600.

143. Ohno, T., et al., *Morphology of a TiO₂ Photocatalyst (Degussa, P-25) Consisting of Anatase and Rutile Crystalline Phases*. Journal of Catalysis, 2001. **203**(1): p. 82-86.
144. Wang, M., et al., *Adsorption of low concentration humic acid from water by palygorskite*. Applied Clay Science, 2012. **67-68**: p. 164-168.
145. Indrayanto, G., *Chapter Five - Validation of Chromatographic Methods of Analysis: Application for Drugs That Derived From Herbs*, in *Profiles of Drug Substances, Excipients and Related Methodology*, H.G. Brittain, Editor. 2018, Academic Press. p. 359-392.
146. Patnaik, P., *Handbook of Environmental Analysis: Chemical Pollutants in Air, Water, Soil, and Solid Wastes, Third Edition*. 2017: CRC Press.
147. *Guidance document on analytical quality control and validation procedures for pesticide residues analysis in food and feed*. 2013: European Commission Health & Consumer Protection Directorate.
148. Wang, X., *Chapter 3 - Lacustrine Shale Gas Reservoir in the Ordos Basin*, in *Lacustrine Shale Gas*, X. Wang, Editor. 2017, Gulf Professional Publishing. p. 93-178.
149. Chang, Q., *Chapter 10 - Surface of Solids*, in *Colloid and Interface Chemistry for Water Quality Control*, Q. Chang, Editor. 2016, Academic Press. p. 175-225.
150. Peter, L.M., *CHAPTER 1:Photoelectrochemistry: From Basic Principles to Photocatalysis*, in *Photocatalysis: Fundamentals and Perspectives*, Jenny Schneider, et al., Editors. 2016, Royal Society of Chemistry. p. 1-28.
151. Zhong, J., F. Chen, and J. Zhang, *Carbon-Deposited TiO₂: Synthesis, Characterization, and Visible Photocatalytic Performance*. The Journal of Physical Chemistry C, 2010. **114**(2): p. 933-939.
152. Chen, R., et al., *Preparation and characterization of activated carbons from tobacco stem by chemical activation*. Journal of the Air & Waste Management Association, 2017. **67**(6): p. 713-724.
153. Velasco, L.F., et al., *Photochemical behaviour of activated carbons under UV irradiation*. Carbon, 2012. **50**(1): p. 249-258.
154. Lagergren, S., *About the Theory of So-Called Adsorption of Soluble Substance*. Kungliga Svenska Vetenskapsakademiens Handlingar, 1898. **24**(4): p. 1-39.
155. Ho, Y.S. and G. McKay, *Pseudo-second order model for sorption processes*. Process Biochemistry, 1999. **34**(5): p. 451-465.

156. Plazinski, W., W. Rudzinski, and A. Plazinska, *Theoretical models of sorption kinetics including a surface reaction mechanism: a review*. Advances in Colloid and Interface Science, 2009. **152**(1-2): p. 2-13.
157. Suffet, I.H., *An Evaluation of Activated Carbon for Drinking Water Treatment: A National Academy of Science Report*. Journal (American Water Works Association), 1980. **72**(1): p. 41-50.
158. Xia, L., et al., *Chapter 1.8 - Antifouling Membranes for Bioelectrochemistry Applications*, in *Microbial Electrochemical Technology*, S.V. Mohan, S. Varjani, and A. Pandey, Editors. 2019, Elsevier. p. 195-224.
159. Darko, B., et al., *8 - Advances Made in Understanding the Interaction of Ferrate(VI) with Natural Organic Matter in Water*, in *Water Reclamation and Sustainability*, S. Ahuja, Editor. 2014, Elsevier: Boston. p. 183-197.
160. Kim, J.K., et al., *Synergistic Removal of Humic Acid in Water by Coupling Adsorption and Photocatalytic Degradation Using TiO₂/Coconut Shell Powder Composite*. Journal of Nanomaterials, 2016. **2016**: p. 1-10.
161. McCarthy, M.D. and D.A. Bronk, *Chapter 28 - Analytical Methods for the Study of Nitrogen*, in *Nitrogen in the Marine Environment (Second Edition)*, D.G. Capone, et al., Editors. 2008, Academic Press: San Diego. p. 1219-1275.
162. Radian, A. and Y. Mishael, *Effect of humic acid on pyrene removal from water by polycation-clay mineral composites and activated carbon*. Environmental Science & Technology, 2012. **46**(11): p. 6228-6235.
163. Zadaka, D., et al., *Atrazine removal from water by polycation-clay composites: effect of dissolved organic matter and comparison to activated carbon*. Water Research, 2009. **43**(3): p. 677-683.
164. Basumallick, S. and S. Santra, *Monitoring of ppm level humic acid in surface water using ZnO–chitosan nano-composite as fluorescence probe*. Applied Water Science, 2017. **7**(2): p. 1025-1031.
165. Gopal, K., et al., *Chlorination byproducts, their toxicodynamics and removal from drinking water*. Journal of Hazardous Materials, 2007. **140**(1-2): p. 1-6.
166. Morris, R.D., et al., *Chlorination, chlorination by-products, and cancer: a meta-analysis*. American journal of public health, 1992. **82**(7): p. 955-963.
167. Font-Ribera, L., et al., *Long-term exposure to trihalomethanes in drinking water and breast cancer in the Spanish multicase-control study on cancer (MCC-SPAIN)*. Environment International, 2018. **112**: p. 227-234.

168. Bleam, W., *Chapter 7 - Natural Organic Matter*, in *Soil and Environmental Chemistry (Second Edition)*, W. Bleam, Editor. 2017, Academic Press. p. 333-384.
169. de Melo, B.A., F.L. Motta, and M.H. Santana, *Humic acids: Structural properties and multiple functionalities for novel technological developments*. Materials Science and Engineering C, 2016. **62**: p. 967-74.
170. Han, L., et al., *Contaminant rejection in the presence of humic acid by membrane distillation for surface water treatment*. Journal of Membrane Science, 2017. **541**: p. 291-299.
171. Wang, Q., et al., *Effects and mechanism of humic acid on chromium(VI) removal by zero-valent iron (Fe⁰) nanoparticles*. Physics and Chemistry of the Earth, Parts A/B/C, 2011. **36**(9-11): p. 442-446.
172. Helal, A.A., G.A. Murad, and A.A. Helal, *Characterization of different humic materials by various analytical techniques*. Arabian Journal of Chemistry, 2011. **4**(1): p. 51-54.
173. Sooväli, L., et al., *Uncertainty sources in UV-Vis spectrophotometric measurement*. Accreditation and Quality Assurance, 2006. **11**(5): p. 246-255.
174. Liu, Z., et al., *Quantifying the concentration and penetration depth of long-lived RONS in plasma-activated water by UV absorption spectroscopy*. AIP Advances, 2019. **9**(1).
175. *Guidelines for the Validation of Chemical Methods in Food, Feed, Cosmetics, and Veterinary Products*. 2019.
176. Larason, T.C. and C.L. Cromer, *Sources of Error in UV Radiation Measurements*. Journal of research of the National Institute of Standards and Technology, 2001. **106**(4): p. 649-656.
177. Wassilkowska, A., et al., *An analysis of the elemental composition of micro-samples using EDS technique*. Technical Transactions: Chemistry, 2015.
178. Saleem, J., et al., *Production and applications of activated carbons as adsorbents from olive stones*. Biomass Conversion and Biorefinery, 2019. **9**(4): p. 775-802.
179. Zheng, X., et al., *Adsorption Properties of Granular Activated Carbon-Supported Titanium Dioxide Particles for Dyes and Copper Ions*. Scientific Reports, 2018. **8**(1): p. 6463.

180. Gupta, R.C., *Veterinary Toxicology: Basic and Clinical Principles*. 2012: Elsevier.
181. Fiol, N. and I. Villaescusa, *Determination of sorbent point zero charge: usefulness in sorption studies*. *Environmental Chemistry Letters*, 2008. **7**(1): p. 79-84.
182. Wong, Y.C., et al., *Pseudo-first-order kinetic studies of the sorption of acid dyes onto chitosan*. *Journal of Applied Polymer Science*, 2004. **92**(3): p. 1633-1645.
183. Li, P.H.Y., R.L. Bruce, and M.D. Hobday, *A pseudo first order rate model for the adsorption of an organic adsorbate in aqueous solution*. *Journal of Chemical Technology and Biotechnology* 1999. **74**(1): p. 55-59.
184. Han, X., et al., *Removal of methylene blue from aqueous solution using porous biochar obtained by KOH activation of peanut shell biochar*. *BioResources*, 2015. **10**(2): p. 2836-2849.
185. Liu, Q., et al., *Comparisons of two chelating adsorbents prepared by different ways for chromium(VI) adsorption from aqueous solution*. *Colloids and Surfaces A: Physicochemical and Engineering Aspects*, 2016. **511**: p. 8-16.
186. Plazinski, W., J. Dziuba, and W. Rudzinski, *Modeling of sorption kinetics: the pseudo-second order equation and the sorbate intraparticle diffusivity*. *Adsorption*, 2013. **19**(5): p. 1055-1064.
187. Febrianto, J., et al., *Equilibrium and kinetic studies in adsorption of heavy metals using biosorbent: a summary of recent studies*. *Journal of Hazardous Materials*, 2009. **162**(2-3): p. 616-45.
188. de Sá, A., et al., *8 - Polymeric materials for metal sorption from hydric resources*, in *Water Purification*, A.M. Grumezescu, Editor. 2017, Academic Press. p. 289-322.
189. Ajenifuja, E., J.A. Ajao, and E.O.B. Ajayi, *Adsorption isotherm studies of Cu (II) and Co (II) in high concentration aqueous solutions on photocatalytically modified diatomaceous ceramic adsorbents*. *Applied Water Science*, 2017. **7**(7): p. 3793-3801.
190. Mohammed, E.A., C. Naugler, and B.H. Far, *Chapter 32 - Emerging Business Intelligence Framework for a Clinical Laboratory Through Big Data Analytics*, in *Emerging Trends in Computational Biology, Bioinformatics, and Systems Biology*, Q.N. Tran and H. Arabnia, Editors. 2015, Morgan Kaufmann: Boston. p. 577-602.

191. Quesada-Peñate, I., et al., *Comparative adsorption of levodopa from aqueous solution on different activated carbons*. Chemical Engineering Journal, 2009. **152**(1): p. 183-188.
192. Akaike, H., *A New Look at the Statistical Model Identification*. IEEE Transactions on Automatic Control, 1974. **19**(6): p. 716-723.
193. Zhang, A., et al., *Mechanism of adsorption of humic acid by modified aged refuse*. RSC Advances, 2018. **8**(59): p. 33642-33651.
194. von Wandruszka, R., *Humic acids: Their detergent qualities and potential uses in pollution remediation*. Geochemical Transactions, 2000. **1**(1): p. 10.
195. Capasso, S., et al., *Sorption of humic acids on zeolitic tuffs*. Microporous and Mesoporous Materials, 2007. **105**(3): p. 324-328.
196. Kołodziej, A., et al., *Mechanism of adsorption of different humic acid fractions on mesoporous activated carbons with basic surface characteristics*. Adsorption, 2014. **20**(5-6): p. 667-675.
197. Baigorri, R., et al., *Complementary Multianalytical Approach To Study the Distinctive Structural Features of the Main Humic Fractions in Solution: Gray Humic Acid, Brown Humic Acid, and Fulvic Acid*. Journal of Agricultural and Food Chemistry, 2009. **57**(8): p. 3266-3272.
198. Singh, R., *Chapter 2 - Water and Membrane Treatment*, in *Membrane Technology and Engineering for Water Purification (Second Edition)*, R. Singh, Editor. 2015, Butterworth-Heinemann: Oxford. p. 81-178.
199. Li, Z., et al., *The impact of humic acid on metaldehyde adsorption onto powdered activated carbon in aqueous solution*. RSC Advances, 2019. **9**(1): p. 11-22.
200. Song, K.-Y., et al., *Coupling effect of 17 β -estradiol and natural organic matter on the performance of a PAC adsorption/membrane filtration hybrid system*. Desalination, 2009. **237**(1-3): p. 392-399.
201. Sakkayawong, N., P. Thiravetyan, and W. Nakbanpote, *Adsorption mechanism of synthetic reactive dye wastewater by chitosan*. Journal of Colloid and Interface Science, 2005. **286**(1): p. 36-42.
202. Boyatzis, S.C., G. Velivasaki, and E. Malea, *A study of the deterioration of aged parchment marked with laboratory iron gall inks using FTIR-ATR spectroscopy and micro hot table*. Heritage Science, 2016. **4**(1).

203. Anupam, K., et al., *Adsorptive removal of chromium (VI) from aqueous solution over powdered activated carbon: Optimisation through response surface methodology*. Chemical Engineering Journal, 2011. **173**(1): p. 135-143.
204. Hami, M.L., M.A. Al-Hashimi, and M.M. Al-Doori, *Effect of activated carbon on BOD and COD removal in a dissolved air flotation unit treating refinery wastewater*. Desalination, 2007. **216**(1-3): p. 116-122.
205. Serpa, A.L., I.A.H. Schneider, and J. Rubio, *Adsorption onto Fluidized Powdered Activated Carbon Flocs-PACF*. Environmental Science & Technology, 2005. **39**(3): p. 885-888.
206. Jiang, W., et al., *Removal of emerging contaminants by pre-mixed PACl and carbonaceous materials*. RSC Advances, 2015. **5**(45): p. 35461-35468.
207. Cook, D. and G. Newcombe, *Comparison and modeling of the adsorption of two microcystin analogues onto powdered activated carbon*. Environmental Technology, 2008. **29**(5): p. 525-34.
208. Zhou, Z., et al., *Coagulation efficiency and flocs characteristics of recycling sludge during treatment of low temperature and micro-polluted water*. Journal of Environmental Sciences, 2012. **24**(6): p. 1014-1020.
209. Li, W., et al., *Treatment of stabilized landfill leachate by the combined process of coagulation/flocculation and powder activated carbon adsorption*. Desalination, 2010. **264**(1-2): p. 56-62.
210. Gautam, R.K., A. Mudhoo, and M.C. Chattopadhyaya, *Kinetic, equilibrium, thermodynamic studies and spectroscopic analysis of Alizarin Red S removal by mustard husk*. Journal of Environmental Chemical Engineering, 2013. **1**(4): p. 1283-1291.
211. Ratnayaka, D.D., M.J. Brandt, and M. Johnson, *Twort's Water Supply*. 6 ed. 2009: Butterworth-Heinemann. 744.
212. Mukherjee, S., et al., *Removal of phenols from water environment by activated carbon, bagasse ash and wood charcoal*. Chemical Engineering Journal, 2007. **129**(1-3): p. 133-142.
213. Altmann, J., et al., *Direct comparison of ozonation and adsorption onto powdered activated carbon for micropollutant removal in advanced wastewater treatment*. Water Research, 2014. **55**: p. 185-93.

214. Kononova, M.A., et al., *Effect of inorganic compounds in the activated carbon phase and in solution on the adsorption of gold(I) cyanide complex*. Russian Journal of Applied Chemistry, 2009. **82**(2): p. 173-182.
215. Cooney, D.O., A. Nagerl, and A.L. Hines, *Solvent regeneration of activated carbon*. Water Research, 1983. **17**(4): p. 403-410.
216. Gautam, R.K., et al., *Biomass-derived biosorbents for metal ions sequestration: Adsorbent modification and activation methods and adsorbent regeneration*. Journal of Environmental Chemical Engineering, 2014. **2**(1): p. 239-259.
217. Roh, S.H., et al., *Simultaneous Removal of Algae and Their Secondary Algal Metabolites from Water by Hybrid System of DAF and PAC Adsorption*. Separation Science and Technology, 2008. **43**(1): p. 113-131.
218. Ruhl, A.S., et al., *Integrating Micro-Pollutant Removal by Powdered Activated Carbon into Deep Bed Filtration*. Water, Air, & Soil Pollution, 2014. **225**(3).
219. Altmann, J., et al., *How to dose powdered activated carbon in deep bed filtration for efficient micropollutant removal*. Water Research, 2015. **78**: p. 9-17.
220. Tao, B. and A.J. Fletcher, *Catalytic degradation and adsorption of metaldehyde from drinking water by functionalized mesoporous silicas and ion-exchange resin*. Separation and Purification Technology, 2014. **124**: p. 195-200.
221. *Household customer charges*. 2018 [3rd June 2020]; Available from: <https://www.thameswater.co.uk/-/media/Site-Content/Thames-Water/Your-Account/Billing-and-Payment/Our-charges/Our-charges-2018---2019.pdf>
222. Li, Z., et al., *Investigation of metaldehyde removal by powdered activated carbon from different water samples*. Environmental Science: Water Research & Technology, 2020.
223. Reza, K.M., A.S.W. Kurny, and F. Gulshan, *Parameters affecting the photocatalytic degradation of dyes using TiO₂: a review*. Applied Water Science, 2015. **7**(4): p. 1569-1578.
224. Sang, Z., et al., *Evaluating the environmental impact of artificial sweeteners: a study of their distributions, photodegradation and toxicities*. Water Research, 2014. **52**: p. 260-274.
225. Bergna, D., et al., *Effect of Some Process Parameters on the Main Properties of Activated Carbon Produced from Peat in a Lab-Scale Process*. Waste and Biomass Valorization, 2019.

226. Li, Y., et al., *Study on regeneration of waste powder activated carbon through pyrolysis and its adsorption capacity of phosphorus*. Scientific Reports, 2018. **8**(1): p. 778.

Appendix A.1 Supplementary information for Chapter 3

Figure A.1.1 presents the raw data from the BET SSA analysis for the PAC used in Chapter 3.

Quantachrome® ASiQwin™ - Automated Gas Sorption Data					
Acquisition and Reduction					
© 1994-2013, Quantachrome Instruments					
version 3.01					
Analysis		Report			
Operator:	ucl	Date:2017/08/23	Operator:	Date:2020/04/19	
Sample ID:	Act carbon q	Filename:	old PAC.qps		
Sample Desc:		Comment:			
Sample Weight:	0.09095 g	Instrument:	Autosorb iQ Station 2		
Outgas Time:	0.0 hrs	Outgas Temp.:	0 °C	CellType:	9mm w/o rod
Analysis gas:	Nitrogen	Non-ideality:	6.58e-05 1/Torr	VoidVol Remeasure:	off
Analysis Time:	12.43 hr:min	Bath temp.:	77.35 K	Warm Zone V:	12.4416 cc
Analysis Mode:	Standard				
VoidVol. Mode:	He Measure	Cold Zone V:	3.12657 cc		
Press	P0	Volume @ STP	Time	Tot	Equ
Torr	Torr	cc	min		
9.63311	764.47	21.3136	64.1	3	3
15.9601	764.52	22.2715	78.1	3	3
21.8983	764.23	22.9116	84.0	3	3
36.3693	764.40	24.0016	90.1	3	3
56.695	764.59	25.0285	95.9	3	3
74.7904	764.39	25.707	101.0	3	3
113.187	764.60	26.7823	106.8	3	3
154.574	764.13	27.6656	113.3	3	3
190.045	764.29	28.3018	118.7	3	3
227.999	764.45	28.9439	124.8	3	3
267.182	764.66	29.544	130.3	3	3
305.958	764.63	30.1127	136.0	3	3
344.142	764.55	30.6639	142.1	3	3
382.35	764.66	31.2267	148.1	3	3
420.113	764.29	31.8136	154.3	3	3
457.571	764.45	32.4385	160.6	3	3
494.338	764.17	33.1237	167.4	3	3
535.803	764.15	34.008	178.1	3	3
573.067	764.22	34.9487	184.8	3	3
608.693	764.20	36.0183	193.6	3	3
647.54	764.51	37.4425	204.2	3	3
686.112	764.36	39.245	216.8	3	3
725.754	764.58	41.9501	235.6	3	3
744.409	764.89	44.0932	258.6	3	3
760.367	764.49	48.3942	310.3	0	3
747.348	764.99	46.094	335.3	3	3
729.432	764.94	44.1674	351.3	3	3
688.071	764.01	41.5394	367.1	3	3
649.434	764.68	39.831	380.9	3	3
612.61	764.59	38.4752	391.2	3	3
572.343	764.93	37.1895	403.4	3	3
536.227	764.50	36.1939	412.6	3	3
496.993	764.71	35.2559	421.7	3	3
461.516	765.20	34.5529	428.0	3	3
418.68	765.20	33.7944	438.8	3	3
384.217	764.86	33.1261	447.8	3	3
343.182	765.09	31.0284	463.4	3	3
304.177	765.32	30.17	472.3	3	3
267.635	765.09	29.5969	478.0	3	3
229.54	765.33	29.0055	483.8	3	3
192.036	764.53	28.387	489.5	3	3
154.582	765.14	27.7036	495.1	3	3
113.734	765.16	26.8222	501.4	3	3
77.3078	765.01	25.7979	507.8	3	3
59.0904	764.93	25.1304	513.8	3	3
38.8451	764.93	24.1409	522.5	3	3
33.2962	765.30	23.792	527.1	3	3
14.5701	765.38	22.0535	542.7	3	3
7.55537	764.53	20.9203	561.2	3	3
3.82744	765.32	19.7713	593.4	3	3
0.768958	765.59	17.1539	763.7	3	3

Figure A.1.1 Data from the BET SSA analysis of the PAC used in Chapter 3

Table A.1.1 presents the five points selected in BET SSA analysis to calculate the SSA of the PAC used in Chapter 3.

Table A.1.1 Multi-point selected for BET SSA analysis of the PAC used in Chapter 3

Relative pressure (P/P_0)	Volume @ STP (cc g^{-1})	$1 / [W((P_0 / P) - 1)]$
2.08761E-02	225.0780	7.5793E-02
2.86539E-02	231.5474	1.0193E-01
4.75791E-02	242.5628	1.6478E-01
7.41507E-02	252.9405	2.5334E-01
9.78436E-02	259.7980	3.3401E-01

Figure A.1.2 presents the raw data from the BET SSA analysis for the GAC used in Chapter 3.

Quantachrome® ASiQwin™ - Automated Gas Sorption Data Acquisition and Reduction © 1994-2013, Quantachrome Instruments version 3.01						
Analysis			Report			
Operator:	ucl	Date:2017/08/04	Operator:	Date:2020/04/19		
Sample ID:	ac2--zhuojun	Filename:	ac20-zhuojun.qps			
Sample Desc:		Comment:	Autosorb IQ Station 1			
Sample Weight:	0.05205 g	Instrument:	0 °C			
Outgas Time:	0.0 hrs	Outgas Temp.:	6.58e-05 1/Torr			
Analysis gas:	Nitrogen	Non-ideality:	77.35 K			
Analysis Time:	12:24 hr:min	Bath temp.:	CellType: 12mm w/o rod			
Analysis Mode:	Standard	Cold Zone V:	VoidVol Remeasure: off			
VoidVol. Mode:	He Measure		Warm Zone V: 19.7426 cc			
Press	P0	Volume @ STP	Time	Tol	Equ	
Torr	Torr	cc	min			
7.64045	759.16	6.67655	84.6	3	3	
15.1649	759.12	7.11109	95.0	3	3	
22.1739	759.15	7.36665	99.4	3	3	
35.9083	759.30	7.73137	103.9	3	3	
54.722	759.43	8.10515	108.8	3	3	
74.3966	759.09	8.42622	114.0	3	3	
114.924	758.97	8.97704	119.9	3	3	
149.064	759.05	9.38724	125.0	3	3	
186.811	758.91	9.80982	130.6	3	3	
224.84	758.54	10.2209	136.0	3	3	
262.742	759.35	10.6203	141.6	3	3	
300.979	759.26	11.0177	147.2	3	3	
342.563	759.42	11.5566	156.6	3	3	
377.119	759.33	11.937	162.6	3	3	
419.361	759.20	12.4115	171.8	3	3	
452.767	759.12	12.8029	178.3	3	3	
494.363	759.36	13.3185	186.7	3	3	
532.437	758.63	13.841	196.0	3	3	
569.643	758.95	14.4196	205.9	3	3	
605.971	759.07	15.101	217.3	3	3	
645.639	759.29	16.0815	234.2	3	3	
681.897	759.40	17.6773	253.7	3	3	
718.09	759.10	20.4022	287.6	3	3	
737.292	758.92	22.6436	324.7	3	3	
755.382	759.46	26.1698	393.0	0	3	
741.243	759.22	25.4156	409.5	3	3	
723.454	759.29	24.1403	433.6	3	3	
685.746	759.79	21.4044	463.9	3	3	
648.665	760.02	19.4963	485.0	3	3	
607.283	759.94	17.9108	505.4	3	3	
568.415	759.75	16.7854	523.0	3	3	
532.519	759.59	15.9549	534.1	3	3	
493.894	760.17	15.1997	544.2	3	3	
454.771	759.83	14.5344	553.9	3	3	
420.77	759.96	14.0086	561.6	3	3	
381.92	760.30	13.5435	568.1	3	3	
343.005	759.82	12.2917	582.8	3	3	
303.416	759.24	11.5669	592.0	3	3	
267.699	759.90	11.1056	598.0	3	3	
229.67	759.91	10.6482	603.8	3	3	
191.62	759.91	10.186	609.6	3	3	
153.611	759.19	9.70953	615.3	3	3	
115.604	760.05	9.20363	620.7	3	3	
78.2566	759.76	8.65288	626.7	3	3	
59.7405	759.89	8.33889	633.5	3	3	
39.7765	759.30	7.93992	640.6	3	3	
31.0458	759.15	7.72768	646.3	3	3	
14.9493	759.15	7.19011	658.3	3	3	
7.38646	759.71	6.75222	674.1	3	3	
3.66741	759.41	6.3418	691.5	3	3	
0.761315	759.08	5.43822	744.7	3	3	

Figure A.1.2 Data from the BET SSA analysis of the GAC used in Chapter 3

Table A.1.2 presents the five points selected for BET SSA analysis to calculate the SSA of the GAC used in Chapter 3.

Table A.1.2 Multi-point selected for BET SSA analysis of the GAC used in Chapter 3

Relative pressure (P/P ₀)	Volume @ STP (cc g ⁻¹)	1 / [W((P ₀ / P) - 1)]
1.99769E-02	136.6204	1.1938E-01
2.92089E-02	141.5302	1.7009E-01
4.72910E-02	148.5374	2.6738E-01
7.20562E-02	155.7185	3.9899E-01
9.80073E-02	161.8871	5.3702E-01

Appendix A.2 Supplementary information for Chapter 4

Figure A.2.1 presents the raw data from the BET SSA analysis for the PAC used in Chapter 4.

Quantachrome® ASiQwin™ - Automated Gas Sorption Data					
Acquisition and Reduction					
© 1994-2013, Quantachrome Instruments					
version 3.01					
Analysis			Report		
Operator:	ucl	Date:2017/08/05	Operator:		Date:2020/04/19
Sample ID:	PAC	Filename:	pac-zhuojun.qps		
Sample Desc:		Comment:			
Sample Weight:	0.05769 g	Instrument:	Autosorb iQ Station 1		
Outgas Time:	0.0 hrs	Outgas Temp.:	0 °C		
Analysis gas:	Nitrogen	Non-ideality:	6.58e-05 1/Torr	CellType:	12mm w/o rod
Analysis Time:	12:56 hr:min	Bath temp.:	77.35 K		
Analysis Mode:	Standard			VoidVol Remeasure:	off
VoidVol. Mode:	He Measure	Cold Zone V:	3.06882 cc	Warm Zone V:	10.7393 cc
Press	P0	Volume @ STP	Time	Tot	Equ
Torr	Torr	cc	min		
7.64443	765.29	11.4191	93.3	3	3
15.5396	765.02	12.1044	107.4	3	3
20.9278	765.42	12.416	112.7	3	3
36.8962	765.48	13.0499	118.6	3	3
57.5978	765.07	13.5835	124.6	3	3
74.1389	764.71	13.9035	129.3	3	3
114.629	765.34	14.4845	134.8	3	3
155.584	765.16	14.9436	141.0	3	3
188.662	765.20	15.2822	145.9	3	3
226.901	765.14	15.6243	150.9	3	3
265.852	764.91	15.9545	156.6	3	3
303.808	764.87	16.2637	161.7	3	3
342.226	765.25	16.5725	167.2	3	3
380.371	765.03	16.8837	172.3	3	3
418.178	765.73	17.2044	177.5	3	3
456.629	765.61	17.5507	183.0	3	3
500.814	765.36	17.9894	191.7	3	3
532.752	765.09	18.3423	198.2	3	3
574.801	765.44	18.8751	206.1	3	3
611.597	765.94	19.4399	213.8	3	3
652.053	765.72	20.255	226.5	3	3
686.547	765.65	21.2757	238.0	3	3
725.145	765.74	23.6854	261.2	3	3
743.27	765.77	26.0501	290.9	3	3
760.839	765.52	29.5397	345.4	0	3
748.699	766.03	28.1217	368.9	3	3
730.248	765.88	26.2897	395.9	3	3
692.088	765.51	23.0717	418.1	3	3
650.478	765.88	21.4523	432.0	3	3
613.808	765.63	20.5934	442.0	3	3
576.216	766.07	19.9381	449.7	3	3
535.425	765.27	19.4493	457.8	3	3
495.78	765.50	18.9764	464.7	3	3
456.971	765.54	18.5693	472.8	3	3
423.523	765.93	18.2465	478.2	3	3
385.814	765.91	17.8909	484.4	3	3
345.044	765.88	16.9363	495.3	3	3
305.009	765.74	16.4432	501.9	3	3
270.221	766.04	16.1326	507.0	3	3
232.335	765.79	15.8022	511.9	3	3
194.369	766.03	15.4545	517.3	3	3
150.521	765.97	15.0146	523.0	3	3
112.421	765.76	14.5692	529.1	3	3
75.7412	765.83	14.025	535.4	3	3
59.4928	765.99	13.7126	540.5	3	3
38.001	765.89	13.1627	547.6	3	3
31.133	766.06	12.9278	552.6	3	3
14.8078	766.04	12.1126	565.9	3	3
7.68257	766.27	11.5238	585.7	3	3
3.71489	766.18	10.8715	624.9	3	3
0.759365	766.73	9.48471	776.6	3	3

Figure A.2.1 Data from the BET SSA analysis of the PAC used in Chapter 4

Table A.2.1 presents the five points selected in BET SSA analysis to calculate the SSA of the PAC used in Chapter 4.

Table A.2.1 Multi-point selected for BET SSA analysis of the PAC used in Chapter 4

Relative pressure (P/P₀)	Volume @ STP (cc g⁻¹)	1 / [W((P₀ / P) - 1)]
2.03127E-02	209.8185	7.9066E-02
2.73415E-02	215.2185	1.0450E-01
4.82003E-02	226.2077	1.7912E-01
7.52840E-02	235.4564	2.7665E-01
9.69509E-02	241.0040	3.5642E-01

Appendix A.3 Supplementary information for Chapter 5

Table A.3.1 presents the raw data from the water characteristics analyses for the water samples collected from the Regent's Park lake and after different treatment stages at WTWTW, without spiking metaldehyde.

Table A.3.2 presents the raw data from the water characteristics analyses for the water samples used Section 5.3.3.3, spiked with 5 $\mu\text{g L}^{-1}$ metaldehyde, without PAC treatment.

Table A.3.3 presents the raw data from the water characteristics analyses for the water samples used Section 5.3.3.3, spiked with 5 $\mu\text{g L}^{-1}$ metaldehyde, after the 30-min PAC treatment.

Table A.3.1 Characteristics of different water samples without spiking metaldehyde

Water samples (collected from)	pH	Conductivity and TDS ($\mu\text{s}/\text{cm}$; mg/L)	Fluoride (mg/L)	Chloride (mg/L)	Nitrate (mg/L)	NPOC (mg/L)	Turbidity (NTU)	Dissolved O ₂ (mg/L)	UV ₂₅₄ (cm ⁻¹)
The Regent's Park lake	8.75	1098; 551	1.5585	88.0492	4.5522	7.346	0.866	11.43	0.1619
	8.75	1098; 551	1.6063	90.3543	4.4773	7.339	0.867	11.48	0.1619
After 'pre-ozone contactors'	8.14	592; 297	0.1304	56.1827	30.7901	5.728	0.225	7.54	0.0772
	8.14	592; 297	0.1342	56.2482	30.8961	5.602	0.224	7.55	0.0772
After 'static flocculation'	6.32	617; 310	0.1201	57.1128	30.5679	3.802	0.441	7.25	0.0546
	6.32	617; 310	0.3345	56.539	30.6409	3.829	0.445	7.26	0.0546
After 'CoCoDAF units'	7.67	592; 298	0.1297	57.4569	31.149	4.001	0.107	7.27	0.0495
	7.67	592; 298	0.1352	56.4244	31.141	4.002	0.108	7.28	0.0495
After 'main ozone contactors'	7.64	592; 298	0.1368	57.1515	31.1665	3.731	0.083	7.96	0.0389
	7.64	592; 298	0.1437	56.6327	31.2487	3.511	0.084	7.94	0.0389
After 'GAC adsorbers'	7.43	601; 301	0.3546	57.396	31.4286	4.157	0.082	6.11	0.0298
	7.43	601; 301	0.1417	57.0418	31.5348	4.129	0.089	6.13	0.0298
After 'series of screens and a contact tank'	7.39	607; 305	0.3423	58.2469	31.639	3.048	0.102	6.79	0.028
	7.39	607; 305	0.1302	57.9494	31.496	2.949	0.103	6.80	0.028

Table A.3.2 Characteristics of different water samples spiked with 5 µg L⁻¹ metaldehyde without PAC treatment

Water samples (collected from)	pH	Conductivity and TDS (µs/cm; mg/L)	Fluoride (mg/L)	Chloride (mg/L)	Nitrate (mg/L)	NPOC (mg/L)	Dissolved O ₂ (mg/L)	UV ₂₅₄ (cm ⁻¹)
The Regent's Park lake	8.37	1051; 528	1.5084	89.7724	4.7471	13.13	10.30	0.1602
	8.37	1051; 528	1.5055	90.0091	4.8981	13.20	10.37	0.1602
After 'static flocculation'	7.04	429; 215	0.8567	64.5021	37.6415	6.570	11.55	0.0461
	7.04	429; 215	0.8678	64.6931	37.7308	6.831	11.58	0.0461
After 'CoCoDAF units'	6.66	452; 227	0.8096	62.8757	36.2496	6.017	11.57	0.048
	6.66	452; 227	0.801	63.2344	36.0847	6.001	11.66	0.048
After 'main ozone contactors'	8.35	603; 303	0.5415	58.1372	32.9556	6.269	11.80	0.0389
	8.35	603; 303	0.5658	63.4178	36.0807	6.423	11.77	0.0389
MilliQ water	6.24	2.19; 1.099	0.6234	1.044	0.3547	3.338	12.35	0.0094
	6.24	2.19; 1.099	0.1505	0.4591	0.2081	3.272	12.34	0.0094
MilliQ water with HA	6.80	16.50; 8.29	0.1795	3.3492	0.5749	10.61	12.32	0.6740
	6.80	16.50; 8.29	0.1576	3.4361	0.5717	10.62	12.35	0.6740

Table A.3.3 Characteristics of different water samples spiked with 5 µg L⁻¹ metaldehyde after the 30-min PAC treatments

Water samples (collected from)	pH	Conductivity and TDS (µs/cm; mg/L)	Fluoride (mg/L)	Chloride (mg/L)	Nitrate (mg/L)	NPOC (mg/L)	Dissolved O ₂ (mg/L)	UV ₂₅₄ (cm ⁻¹)
The Regent's Park lake	8.57	1111; 558	1.3696	86.9548	4.1661	9.450	11.65	0.1229
	8.57	1111; 558	1.3684	88.5297	4.3533	9.748	11.69	0.1229
After 'static flocculation'	8.39	599; 301	0.1772	56.4813	32.3031	7.596	11.86	0.0305
	8.39	599; 301	0.2223	61.5446	35.7902	7.484	11.90	0.0305
After 'CoCoDAF units'	8.41	600; 301	0.6162	60.611	35.0357	4.014	11.13	0.0573
	8.41	600; 301	0.591	61.9679	35.822	4.044	11.19	0.0573
After 'main ozone contactors'	8.31	601; 302	0.1992	60.6596	34.7852	5.367	11.73	0.0327
	8.31	601; 302	0.2465	61.2367	35.2653	5.348	11.76	0.0327
MilliQ water	6.60	7.84; 3.93	0.0418	0.4844	0.2825	4.159	11.80	0.0055
	6.60	7.84; 3.93	0.0623	0.4325	0.2833	4.090	11.85	0.0055
MilliQ water with HA	6.88	17.21; 8.65	0.5102	3.3737	0.759	11.59	12.14	0.6363
	6.88	17.21; 8.65	0.5247	4.6425	1.1317	11.92	12.19	0.6363